The Alpha and the Gamma of latency establishment: Deciphering early events after nuclear entry of herpesvirus genomes

by

Heidi Maria Meissner

Hamburg, April, 2022

The experimental work and preparation of this dissertation were performed at the Leibniz Institute for Experimental Virology (HPI) under supervision of Prof. Dr. Adam Grundhoff, Prof. Dr. Kay Grünewald and Assistant Prof. Dr. Jens Bosse between the 1st of April 2018 and the 1st of March 2022.

Contents

Nomenclature

Units

°C	degree Celsius
cm	centimeter
g	gravitiy
h	hour
kDa	kilodalton
M	molar
µg	microgram
µl	microliter
µm	micrometer
mA	milliampere
ml	milliliter
mm	millimeter
mmol	millimol
mM	millimolar
min	minute
ng	nanogram
nm	nanometer
pmol	picomol
rpm	rounds per minute
sec	second
V	volt

Acronyms

2A-DUB	2A-deubiquitinating enzyme
A	adenine
ac	acetylation
AEBP2	adipocyte enhancer-binding protein 2
ALT	alternative lengthening of telomers
AP	alkaline phosphatase
APS	ammonium persulfate
ASF-1	anti-silencing function protein 1

ATRX	α-thalassemia/mental retardation syndrome X-linked protein
BAC	bacterial artificial chromosome
BJ	immortalized human foreskin fibroblasts
bp	base pair
BSA	bovine serum albumin
c	canonical
C	cytosine
C1ORF43	chromosome 1 open reading frame 43
CaCl$_2$	calcium-chloride
CAF-1	chromatin assembly factor 1
CBP	chromatin binding domain
CBX	chromobox domain family protein
cGAS	cyclin GMP-AMP
ChIP	chromatin-immunoprecipitation
ChIP-seq	ChIP-sequencing
CLOCK	circadian locomotor output cycles kaput
CNS	central nervous system
CO$_2$	carbon dioxide
CPE	cytopathic effect
CpG	cytidine guanosine dinucleotide
CR2	complement receptor type 2
CRISPR	clustered regularly interspaced short palindromic repeats
Ct	cycle threshold
CuAAC	copper-catalyzed azide-alkyne cycloaddition
DAPI	4',6-diamidino-2-phenylindole
DAXX	death-associated protein 6
DC-SIGN	dendritic cell-specific intercellular adhesion molecule-3-grabbing non-integrin
dCas9	catalytically inactive Cas9
DEPC	diethylpyrocarbonate
DMEM	dulbecco's modified eagle's medium
DMSO	dimethylsulfoxide
DNA	deoxyribonucleic acid
DNMT	DNA methyltransferase
dNTP	desoxynucleosidtriphosphate
Dox	doxycyclin
DPBS	dulbecco's phosphate buffered saline
dpi	days post infection
dsDNA	double stranded DNA
DTT	dithiothreitol
E	early
EBV	Epstein-Barr virus

EdC	5-ethynyl-2'-deoxycytidine
EDTA	ethylendediamine tetra acetic acid
EED	embryonic ectoderm development
EGFP	enhanced green fluorescent protein
EGTA	ethylene glycol-bis-N'N'N'N'-tetracetic acid
EHV-1	equine herpesvirus-1
EHV-2	equine herpesvirus-2
En	enhancer
EP0	early protein 0
EphA2	ephrin receptor tyrosine kinase A2
EPOP	elongin BC and PRC2-associated protein
ER	endoplasmatic reticulum
ESC	embryonci stem cell
EZH	enhancer of zeste
FACS	fluoresncence activated cell sorting
FBS	fetal bovine serum
G	guanine
G-418	geneticin
GAPDH	glyceraldehyde-3-phosphate dehydrogenase
gDNA	genomic DNA
GFP	green fluorescent protein
H	Histidine
HAP1	near-haploid adherent fibroblast-like 1
HAT	histone acetyl transferase
HCF-1	host cell factor-1
HCl	Hydrochloric acid
HCMV	human cytomegalovirus
HDAC	histone deacetylase
HDF	human dermal fibroblasts
HEPES	4-(2-hydroxyethyl)-1-piperazineethanesulfonic acid
HFF	human forskin fibroblast
HHV6	human herpesvirus 6
HHV7	human herpesvirus 7
HIRA	histone regulator A
HIV	human immunodeficiency virus
HIV-1	human immunodeficiency virus-1
HOX	homeobox gene
HP1	heterochromatin protein 1
hpi	hours post infection
hpt	hours post transfection
HS	heperan sulfate

HSV	herpes-simplex viurs
HSV-1	herpes simplex viurs-1
HSV-2	herpes simplex viurs-2
HUSH	human silencing hub
HVS	herpesvirus samiri
ICP	infected cell protein
IE	immidiate early
IF	immunofluorescence
IFI16	Interferon gamma-inducible protein 16
IFN-α	interferon alpha
IP	immuno-precipitation
IRL	internal repreat long
IRS	internal repreat short
JARID	jumonji and (A+T)-rich interaction domain-containing protein 2
JMJD3	Jumonji domain-containing protein D3
K	Lysine
KAc	potassium acetate
Kap1	KRAB-associated protein 1
KBM-7	chronic myeloid leukemia (CML) derived
KCl	kalium-chloride
KDM	lysine-specific demethylase
KDM2B	lysine-specific demethylase 2B
KIF1A	kinesin family member 1A
KMT	lysine methyl-transferase
KOH	potassium hydroxide
KRAB	Krueppel-associated box
KSHV	Kaposi's Sarcoma-associated herpesviurs
L	late
LANA	latency associated nuclear antigen
LAT	latency associated transcript
LB	Lysogeny Broth
LiCl	Lithium-Chloride
lncRNA	long non-coding RNA
me	methylation
MgCl	magnesium-chloride
MgSO$_4$	magnesium-sulfate
MHC	major histocompatibility complex
min.pi	minutes post infection
miRNA	microRNA
miRNAs	microRNAs
MLL2	mixed-lineage leukemia protein 2

MnCl	mangan chloride
MOI	multiplicity of infection
MOPS	3-(N-morpholino)propanesulfonic acid
MPP8	M-phosphase protein 8
mRNA	messenger RNA
MYT	myelin transcription factor
NaCl	sodium-chloride
NB	nuclear body
nc	non-canonical
ncRNA	non-coding RNA
ND10	nuclear domain 10
NEC	nuclear egress complex
NHDF	normal human dermal fibroblasts
NP-40	nonident-P-40
Nrd1	X inactive specific transcript
NSD	nuclear receptor-binding SET domain-containing protein
NurD	nucleosome remodeling deacetylase
O$_2$	oxygen
Oct-1	octomer binding protein-1
OD	optical density
ORF	open reading frame
oriLyt	origin of lytic replication
p300	E1A binding protein 300
PAGE	polyacrylamide gel elecrophoresis
PALI	PRC2-associated LCOR isoform
PAN	polyadenylated nuclear
PcG	polycomb group
PCGF	Polycomb group RING finger
PCI	phenol-chloroform-isoamylalcohol
PCL	Polycomb-like
PCR	polymerase chain reaction
PEG	polyethylene glycol
PEI	polyethyleneimine
PEL	primary effusion lymphoma
pen/strep	penicillin streptomycin
PES	polyethersulfone
PFU	plaque forming unit
ph	phosphorylation
PI	IE180 transcomplementing PK15
PK15	porcine kindney epithelia
PML	promyelocytic leukemia

PRC	Polycomb repressive complexe
PRV	pseudorabies virus
PVDF	polyvinylidenfluorid
qPCR	qualitative real-time PCR
R	Arignine
RBBP	retinoblastoma-binding protein
RBCC	RING finger B-box and coiled-coil
RbCl$_2$	rubidium chloride
RBP-J$_\kappa$	recombination signal sequence-binding protein-J kappa
RC	replication compartment
RE	restriction
REST	RE1-Silencing Transcription factor
RING	really interesting new gene
RNA	ribonucleic acid
RNAi	RNA interference
RT	room temperature
RTA	replication and transcription activator
RYBP	YY1-binding protein
S	Serine
Scr	scramble
SD	standard deviation
SDS	sodiumdodecylsulfate
SDS-**PAGE**	sodium dodecyl sulfate polyacrylamide gel electrophoresis
Seb1	stress response element binding protein
SET	su(var) 3-9 enhancer of zeste and trithorax
SETD	SET domain
SETDB1	SET domain bifurcated histone lysine methyltransferase 1
sgRNA	single guide RNA
SIM	SUMO-interacting motif
siRNA	small interfering RNA
SOC	super optimal broth
SP100	nuclear antigen SP100
STING	stimulator of interferon genes
SUMO	small ubiquitin-related modifier
SUV39H	suppressor of variegation 3-9 homolog
SUV39H1/2	suppressor of variegation 3-9 homolog 1/2
SUZ12	suppressor of zeste 12
T	thymine
TAD	transcriptional activation domain
TAE	tris hydroxymethyl aminomethane acetic ethylenediamine tetra acetic acid
TASOR	Transgene activation suppressor protein

TBS-T	tris-buffered saline with Tween20
TE	tris ethylendediamine tetra acetic acid
TEMED	tetramethylethylenediamine
TET	ten-eleven translocation
TF	transcription factor
TG	trigeminal ganglia
Thr	Threonine
TLR	toll-like receptor
TR	terminal repeat region
Tris	tris hydroxymethyl aminomethan
TRL	terminal repreat long
TRS	terminal repreat short
U2OS	human bone osteosarcoma epithelial
ub	ubiquitination
UL	unique long
US	unique short
USP16	ubiquitin carboxyl-terminal hydrolase
UTX	ubiquitously transcribed tetratricopeptide repeat X-chromosome
vDNA	viral DNA
VHS	virion host shutoff protein
VIC	VP16 induced complex
VICE	virus-induced chaperone-enriched
VP	virion protein
VZV	varicella zoster virus
wt	wildtype
XBP-1	X-box binding protein 1
xCT	cysteine/glutamate transporter
XIST	X-inactive specific transcript
YAF	YY1-associated factor
ZNF	zinc-finger

List of Figures

List of Tables

Zusammenfassung

Herpesviren sind Krankheitserreger, die Menschen und Tiere infizieren können und gut an ihren Wirt angepasst sind. Eine Infektion mit Herpesviren führt zu einer lebenslangen Persistenz des Herpesvirus, mit der Möglichkeit zur Reaktivierung. Nach einer anfänglichen lytischen Replikationsphase gehen die meisten Herpesviren in Latenz. Während dieser latenten Phase werden nur wenige virale Gene transkribiert und die viralen Genome verbleiben in den infizierten Zellen, ohne vom Immunsystem eliminiert zu werden. Während der Latenz wird die herpesvirale Desoxyribonukleinsäure (DNS) durch epigenetische Modifikationen, d. h. DNS-Methylierung und posttranslationale repressive Histonmodifikationen, verändert. Eine kürzlich durchgeführte Studie zeigte, dass Polycomb repressive Komplexe (PRC) zu dem Cytidin-Guanosin-Dinukleotid (CpG)-reichen Genom des Gammaherpesvirus Kaposi-Sarkom-assoziiertes Herpesvirus (KSHV), über den nicht-kanonischen Rekrutierungsweg, gelangen. Dieser Mechanismus dient normalerweise dazu, CpG-Inseln der zellulären DNS, über die Erkennung von unmethylierten CpG-Motiven, zu reprimieren. Interessanterweise haben auch Alphaherpesviren wie Herpes-Simplex Virus-1 (HSV-1) einen sehr hohen Gehalt an CpG-Sequenzen. Frühere Ergebnisse unserer Gruppe deuten darauf hin, dass die PRC-vermittelte Repression ein Standardweg darstellen könnte, um CpG-reiche DNS zu reprimieren. Daher stellen wir die Hypothese auf, dass Herpesvirus-Genome mit hohem CpG-Gehalt diesen Weg generell nutzen, um Latenz zu etablieren.

Die hier vorgestellte Studie zielt daher darauf ab, diese Hypothese weiter zu validieren und auf andere Herpesvirusfamilien auszuweiten. Zu diesem Zweck wurde eine vergleichende Analyse zwischen KSHV und Mutanten der beiden Alphaherpesviren HSV-1 und Pseudorabies-Virus (PRV) durchgeführt. Die Mutanten der Alphaherpesviren sind, unter bestimmten Konditionen, nicht fähig lytisch zu replizieren.

Früh nach der Infektion wurden genomweite Chromatin-Analysen mittels Chromatin- Immunpräzipitation (ChIP)-Sequenzierung durchgeführt, um das Epigenom der Alphaherpesviren zu untersuchen. Darüber hinaus wurde, zu verschiedenen Zeitpunkten nach der Infektion, eine fluoreszenzbasierte Visualisierung, mittels bioorthogonaler Chemie, durchgeführt, um die räumliche und zeitliche Interaktion einzelner viraler Episomen mit verschiedenen Wirtsfaktoren zu verfolgen. Desweitern wurde ein Knock-down des Wirtsfaktors α-thalassemia/mental retardation syndrome X-linked protein (ATRX) mit anschließenden Infektionsexperimenten durchgeführt, um die Auswirkungen der Reduktion dieses Proteins auf die Reaktivierung des Herpesvirus zu untersuchen.

Die hier vorgestellten Daten zeigen, zum ersten Mal, den schnellen Erwerb der mit PRC-assoziierten, fakultativen Heterochromatin-Markierung H2AK119ub durch die hier verwendeten PRV und HSV-1

Mutanten. Interessanterweise erwarben beide Viren auch konstitutives Heterochromatin über H3K9me3. Eine weitere Analyse des zugrundeliegenden Mechanismus ergab, dass der Erwerb der verschiedenen Formen von Heterochromatin offenbar vom infizierten Zelltyp und damit sehr wahrscheinlich von verschiedenen Wirtsfaktoren abhängt. Insbesondere wurde nachgewiesen, dass der Wirtsfaktor ATRX, eine Komponente von promyelocytic leukemia-nuclear bodys (PML-NBs), eine Rolle bei der Etablierung eines stark unterdrückten Zustands des Virusgenoms spielt und die konstitutive Heterochromatinbildung beeinflussen könnte.

Die Ergebnisse dieser Dissertation deuten darauf hin, dass PRCs über den nicht-kanonischen-Rekrutierungsweg zu den Alphaherpesvirus-Genomen gelangen, ähnlich wie bei KSHV. Im Gegensatz zu latent replizierenden KSHV-Genomen haben die nicht-replizierenden Alphaherpesvirus-Genome kein H3K27me3 erworben. Da H3K27me3 bevorzugt auf replizierter DNA gebildet wird, könnte das Fehlen der DNA-Replikation in latenten Alphaherpesviren damit zusammenhängen, dass H3K27me3 auf diesen Genomen nicht nachgewiesen werden konnte. Daher könnte die Replikation von DNS eine wichtige Rolle beim Erwerb der verschiedenen Formen von Heterochromatin auf Herpesvirus-Genomen spielen.

Darüber hinaus lässt sich aus den hier vorgestellten Daten ein Latenz-Modell erstellen, in dem Alphaherpesviren zwei unterschiedlich reprimierte Subpopulationen bilden könnten. In diesem Modell führt die PRC-vermittelte Repression zur Etablierung authentischer latenter Alphaherpesvirus-Reservoirs mit der Fähigkeit zur Reaktivierung, während die PML-NB-vermittelte Repression zu einer permanenten Stilllegung und in sich teilenden Zellen sogar zur späteren Eliminierung des Virus führen könnte.

Zusammengenommen zeigen diese Ergebnisse einen neuen Aspekt der Heterochromatinisierung von Alphaherpesviren und verallgemeinern teilweise den PRC-vermittelten Repressionsmechanismus zwischen zwei Herpesvirus-Unterfamilien. Daher verbessert diese Studie das Verständnis der frühen Repression der herpesviralen DNS.

Abstract

Herpesviruses are pathogens that can infect humans and animals and are well adapted to their host. Primary infection with herpesviruses results in lifelong persistence of the herpesvirus, with the possibility of reactivation. After a first phase of lytic replication most herpesviruses enter a state known as latency. During latency, very few viral genes are transcribed and the genomes can remain in the infected cell without being eliminated by the immune system. During latency, the herpesviral deoxyribonucleic acid (DNA) is modified by epigenetic modifications, i.e. DNA methylation and posttranslational repressive histone modifications. A recent study showed that the cytidine guanosine dinucleotide-rich genome of the gammaherpesvirus Kaposi's Sarcoma-associated herpesviurs rapidly attracts Polycomb repressive complexes via the non-canonical (nc) recruitment pathway. This mechanism normally serves to silence CpG islands of cellular DNA via recognition of unmethylated CpG motifs. Interestingly, alphaherpesviruses such as herpes simplex viurs-1 also have a very high content of CpG sequences. Previous results from our group suggest that PRC-mediated repression may be a default pathway to repress CpG-rich viral DNA (vDNA). Therefore, we hypothesize that herpesviruses with high CpG content might generally exploit this pathway to support latency.

Therefore, the study presented here aims to further validate this hypothesis. To this end, a direct comparative analysis was performed between KSHV and lytic-cycle-deficient mutants of the alphaherpesviruses HSV-1 and pseudorabies virus, which also have a very high CpG content. Genome-wide chromatin analyses were performed by chromatin-immunoprecipitation-sequencing (ChIP-seq), early after infection, to elucidate the epigenome of the lytic-cycle-deficient alphaherpesviruses. Furthermore, a fluorescence-based visualization method, which makes use of bioorthogonal chemistry, was utilized to track the spatiotemporal interaction of individual viral episomes with host factors that might be involved in herpesvirus silencing. In addition, knock-down of the host factor ATRX was performed with subsequent infection experiments to investigate its impact on herpesvirus reactivation.

The data presented here show for the first time rapid acquisition of the PRC-associated facultative heterochromatin mark H2AK119ub by lytic-cycle-deficient PRV and HSV-1 genomes. Interestingly, both viruses also acquired constitutive heterochromatin, via H3K9me3. Further analysis of the underlying mechanism revealed that the acquisition of the different forms of heterochromatin appears to be dependent on the infected cell type and thus very likely on distinct host factors. In particular, evidence was provided that the host factor ATRX, a component of promyelocytic leukemia-nuclear bodys (PML-NBs), plays a role during the establishment of a tightly repressed condition of the virus genome and might influence constitutive heterochromatin formation.

These results suggest that alphaherpesvirus genomes, similar to KSHV, can attract PRCs via the ncPRC-recruitment pathway. Unlike latently replicating KSHV episomes, non-replicating alphaherpesvirus genomes did not acquire H3K27me3. Since H3K27me3 is preferentially formed on replicated DNA, the lack of vDNA replication in latent alphaherpesviruses may be related to the fact that H3K27me3 could not be detected on these genomes. Hence, vDNA replication may play an important role during the acquisition of the different forms of heterochromatin of herpesvirus genomes. Moreover, the data presented in this disseration suggest a model in which alphaherpesviruses might establish two differentially silenced subpopulations. In this model, PRC-mediated repression leads to the establishment of authentic alphaherpesvirus latent reservoirs with the ability to reactivate, whereas PML-NB-mediated repression can lead to permanent silencing and, in dividing cells, even to subsequent elimination of the virus.

Together, these results show a new aspect of alphaherpesvirus heterochromatinization and partly generalize the PRC-mediated repression mechanism among two herpesvirus subfamilies. Therefore, this study enhances the understanding of the early repression of incoming herpesviral DNA.

1 Introduction

Viruses are found in all living organisms, from bacteria, where they are called bacteriophages, to plants, animals and humans [1]. Some viruses are only shortly associated with their host, as an acute infection of such viruses can be cleared [2], whereas others can persist lifelong [3]. Due to their omnipresence and diverse effects on their hosts, viruses are subject to a broad variety of scientific research. One virus family that establishes lifelong association with their host is the family of *Herpesviridae* [3]. During productive, lytic infection, herpesviruses can cause various symptoms. Most of the time, herpesvirus genomes do not replicate lytically in immunocompetent individuals but are in a state known as latency. During latency, very few viral genes are transcribed and the genomes can remain in the infected cell without being eliminated by the immune system. The mechanisms leading to a latent infection, its maintenance and the ultimate reactivation are still not fully understood.

This work addresses the cellular mechanisms which lead to initial establishment and maturation of herpesvirus repression, early during infection. In particular, the establishment of repressive epigenetic modifications on the herpesviral genome was examined. This study focuses on the latent-state of alphaherpesviruses and compares its results with recent findings on latency establishment of gammaherpesviruses. Subsequently, this study aims to shed more light on common mechanisms leading to and maintaining herpesviruses' latency.

This chapter aims to summarize the current knowledge about herpesvirus infections, with special focus on latency. Furthermore, the background of cellular processes - believed to be involved in silencing of the herpesvirus genomes - will be explained. Since the here presented work mainly examined alpha- and gammaherpesviruses, the following chapters will consider especially these two herpesvirus subfamilies.

1.1 Herpesviruses

Herpesviruses are pathogens that can infect humans and animals and are well adapted to their host. Primary infection of immunocompetent hosts commonly leads to lifelong persistence of the herpesvirus, with the possibility of reactivation. [3] This infection strategy allowed herpesviruses to co-evolve with their hosts since the last 60-80 million years [4].

1.1.1 Taxonomy and epidemiology

The herpesvirus family has over 100 members, infecting a large variety of animal species [5]. Herpesviruses belong to the family of *Herpesviridae* and are divided into three subfamilies, alpha-, beta- and gammherpesviruses. This classification is based on common biological properties, sequence homologies and genome structure [4]. Among them, nine human herpesvirus species are known, as shown in Fig. 1.1 [6], since human herpesvirus 6 (HHV6) is divided into two subtypes, A and B [7, 8]. It is very likely that every human becomes infected with at least one of these herpesviruses during their life [9].
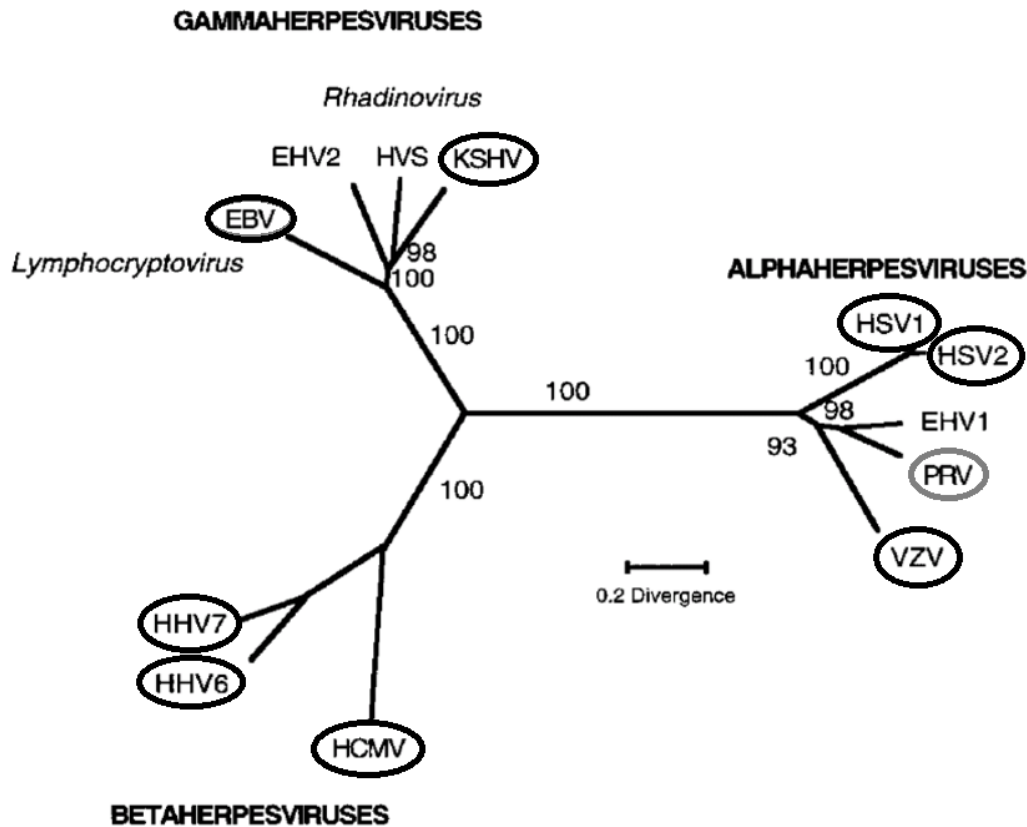
Figure 1.1: Herpesvirus Phylogenetic Tree. The herpesvirus subfamilies, alpha-, beta- and gammaherpesviruses. Nine human herpesviruses are distributed among the three families, highlighted with black circles. HSV-1 and -2 and varicella zoster virus (VZV) belong to the human alphaherpesviruses. Two very closely related animal alphaherpesviruses are PRV and equine herpesvirus-1 (EHV-1). PRV is highlighted by a gray circle, since this virus was investigated in the study presented here. human cytomegalovirus (HCMV), HHV6 and human herpesvirus 7 (HHV7) are characterized as betaherpesviruses, whereas KSHV and Epstein-Barr virus (EBV) belong to the family of gammaherpesviruses. Also in this group, two very closely related animal viruses exist, equine herpesvirus-2 (EHV-2) and herpesvirus samiri (HVS). The phylogenetic tree was modified from [6].

HSV-1, HSV-2 and varicella zoster virus (VZV) belong to the *Alphaherpesvirinae*. Alphaherpesviruses persist in peripheral neurons, mostly in the dorsal root ganglia or trigeminal ganglia [10–13]. HHV6A, HHV6B, HHV7 and human cytomegalovirus (HCMV) belong to the *Betaherpesvirinae*, while Epstein-Barr virus (EBV) and KSHV belong to the *Gammaherpesvirinae*. Beta- and gammaherpesviruses latently infect hematopoietic cells [14–18]. During primary infection, severe symptoms like mononucleosis, caused by EBV has been observed [19]. For immunocompromised patients, the persistent herpesvirus-infection can also cause tumor growth (e.g. KSHV and EBV) [20, 21] or organ damages (e.g. HCMV and HSV-1) [22], which ultimately can lead to death. Albeit being asymptomatic during latency, reactivation of a herpesvirus-infection may

cause symptoms like cold sores (HSV-1) or shingles (VZV) [23]. Recurrent events of reactivation from the latent state enables spreading of the virus to new hosts and maintenance of the infection. Reactivation of the virus can be triggered by various physiological and environmental stimuli [24–30].

Alphaherpesviruses. With some herpesviruses, even primary infections can lead to death, e.g. with PRV - a porcine alphaherpesvirus. The primary host of this virus is the common pig [31, 32]. While adult animals normally survive the infection, and become a reservoir of the latent virus, piglets and most other animals, that can also be infected with PRV, will die of this virus [31–35]. This phenomenon is caused by the neurodegenerative course of the disease, which gave PRV its name [36, 37]. In contrast, a primary infection with PRV of great apes and humans is mostly asymptomatic. Additionally, since no reservoir has been identified in these hosts, the infection is assumed to be cleared [35]. As most of the alphaherpesviruses, PRV also enters the host via infection of mucosal epithelia or cornea, through saliva of an infected animal [38, 39]. Similar to all alphaherpesviruses PRV also establishes a latent state in neurons, after a productive primary infection of epithelial cells. In neurons the viral genome persists as a non-integrated, circularized episome [10–13, 40, 41]. Although the two herpesviruses PRV and HSV-1 are very closely related [4], in contrast to PRV, HSV-1 specifically infects humans with a seroprevalence of about 67 % worldwide [42]. However, their life cycle, in the respective primary host, is very alike.

Betaherpesviruses. Betaherpesviruses are mostly shed through saliva, but HCMV has been also found in different bodily fluids, e.g. urine and blood [43, 44]. The subfamily of betaherpesviruses shows a relatively wide tropism and infects various immune cells. The different species among betaherpesviruses developed distinctive ways of latency. HHV6 for example was found to integrate its own genome into the host genome [45], whereas the life cycle of HCMV is cell dependent, establishing latency in an episomal state, e.g. in monocytes [46].

Gammaherpesviruses. Gammaherpesviruses are also shed mainly via saliva [47–49] and preserve their episomal genome through tethering to the host chromatin, allowing segregation to the daughter cells upon cell division [50–52]. While EBV is highly prevalent all over the world [53, 54], KSHV shows a distinct geographical pattern and is most abundant in sub-Saharan Africa [55, 56]. Symptoms of primary infection with EBV vary dependent on age [57], whereas KSHV primary infection is mostly asymptomatic. However, both viruses are linked to cancer, and therefore can be seen as oncoviruses [20, 21, 58].

1.1.2 Morphology and genome organization

Herpesvirus particles are 155 nanometer (nm) to 240 nm in diameter with a 125 nm large, icosahedral capsid [59, 60]. The capsid contains the linear, double stranded vDNA, varying between 120 kilo base pairs (kbp) and 230 kbp in length [61–63]. The HSV-1 genome is 152 kbp long and has a GC content of about 68 % [64]. The genome consists of two unique regions which are

named according to their length, the unique long (UL) and the unique short (US) region. The genome is flanked by two repeats, the terminal repreat long (TRL) and the terminal repreat short (TRS). The two regions, UL and US, are separated by the inverted repeats, the internal repreat long (IRL) and the internal repreat short (IRS). Furthermore, the genome termini contain direct repeats of a short sequence which is known as "a" sequence and is inverted in the internal part (a'). (Fig. 1.2e) [65]. This a sequence was found to mediate cleavage and packaging of the vDNA [66]. In Fig. 1.2 the genome organization of various herpesviruses is displayed, including HSV-1, PRV and KSHV. In contrast to the HSV-1 genome the repeats which flank the UL region of PRV are shorter and the a sequence was not described for this genome (Fig. 1.2d). The KSHV genome (Fig. 1.2b) harbors only one unique region and a large TR region, which consists of 35-40 repeats with each being 803 base pair (bp) long [67].

Within the capsid the HSV-1 genome shows a toroidal organisation [68]. The capsid is surrounded by a layer of viral proteins, the so called tegument. Upon infection, these proteins are released into the cytoplasm of the host cell and, subsequently, help evading the host immune system and enable the transport of the capsid to the nucleus [69]. The tegument is surrounded by a lipid envelope, which is acquired from the host cell membrane during release of the viral particle (described in more detail in Sec. 1.1.3.3). On top of this envelope, there are membrane-associated proteins called glycoproteins, which are essential for cell entry [70] (Fig. 1.2).
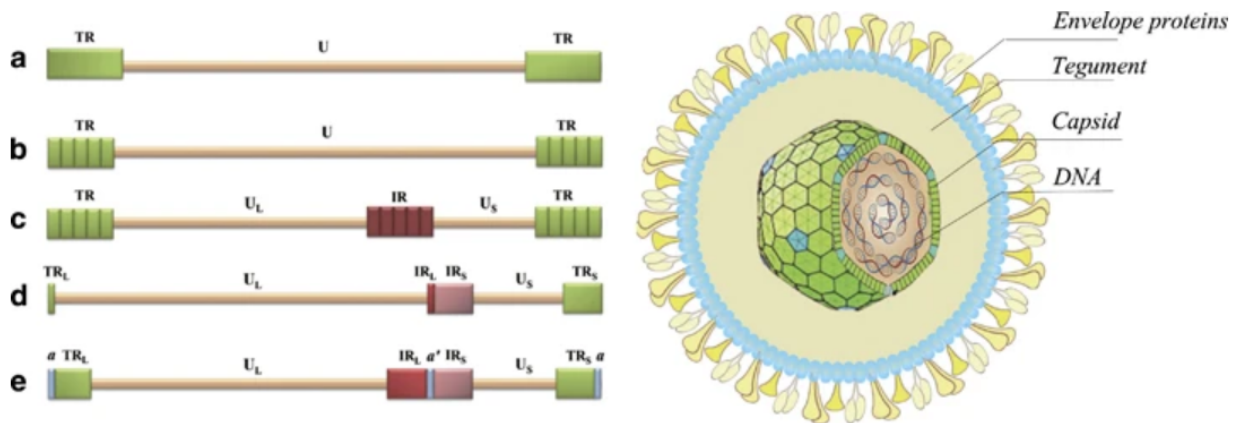
Figure 1.2: The herpesvirus virion consists of the envelope with glycoproteins, the tegument, the capsid and the vDNA. The genome organization differs slightly among the herpesviruses. (a) This type of genome only consists of a unique (U) region, flanked by direct terminal repeats (TR) and can be found in EHV-2. (b) This shows KSHV's genome organization, which also consists of a U region, flanked by several repetitive sequences, the TRs. (c) Here an the EBV genome structure is shown, which has several terminal repeat sequences and an internal direct repeat. Furthermore, the U region is divided into two parts the long (UL) and the short (US) part. (d) The here shown genome is a PRV genome, which is highly similar to HSV-1 genome depicted in (e) Both contain UL and US regions flanked by TRs and internal inverted repeats (IRs). However, in the HSV-1 genome a terminal direct repeat of approximately one hundred bps, known as "a" is unique for this genome and is inverted in the internal part. The graphical representation of the genome and virus particle originates from [71].

1.1.3 Life cycle and associated viral proteins

The herpesvirus life cycle is biphasic. In immunocompetent hosts the herpesvirus genomes are repressed and therefore exist in the latent phase of the infection. However, under certain stimuli, viral genomes can reactivate and enter the lytic phase of infection with subsequent progeny production.

1.1.3.1 Early infection

As soon as the virus particle reaches the cell surface the viral glycoproteins interact unspecifically with the cellular attachment factors heperan sulfate (HS) proteoglycans [72]. This interaction helps the virus particle to reach the specific surface receptors of the host cell. The glycoprotein gB and the heterodimer glycoproteins gH/gL together build the fusion machinery of all herpesviruses [73–78].

Specifics during alphaherpesvirus infection. During alphaherpesvirus infections, the glycoproteins (g) gD, gB and the gH/gL heterodimer mediate the fusion of the virus with the cell [73, 79–81]. When the membranes of host cell and virus particle are in close proximity, gD binds to its specific cellular receptors which are nectin-1 and -2, herpesvirus entry mediator (HVEM) and 3-O sulfated HS [82]. Upon receptor binding, gD changes its conformation and forms a complex together with gB and gH/gL [83–85]. The conformational changes of the viral glycoproteins move the cell and virus closer together. With the fusion of the viral envelope and cell membrane, tegument proteins and the nucleocapsid are released into the cytoplasm of the host cell [86] (Fig. 1.3). The viral capsids are then transported to the nucleus via dynein, which acts as a motorprotein on microtubules [87].

Specifics during gammaherpesvirus infection. During infection with the gammaherpesvirus KSHV, the protein K8.1 is needed for the initial attachment process. On endothelial cells, ephrin receptor tyrosine kinase A2 (EphA2) is used by gH/gL to internalize KSHV [77]. Furthermore, integrins, which are expressed by a variety of cells, are used by KSHV's gB as a cellular receptor [88]. Additionally, KSHV uses the cellular receptors cysteine/glutamate transporter (xCT) and dendritic cell-specific intercellular adhesion molecule-3-grabbing non-integrin (DC-SIGN) during its entry into the cell [89, 90]. KSHV then enters the host cell cytoplasm via endocytosis [91] (Fig. 1.3). Ultimately, the KSHV particle ends up in a low-pH vesicle, triggering fusion between the viral envelope and the vesicle membrane. This fusion allows the capsid to enter the cytoplasm where it is then transported through the cytoplasm, along microtubules, to the nucleus [92].

For both aforementioned herpesviruses, it was shown that as soon as the viral capsid reaches the nucleus, its DNA is injected, via the nuclear pore, and the released vDNA becomes circularized and chromatinized [93–96]. Subsequently, there either will be an active transcription and production of progeny or the viral episome will be repressed [97] (Fig. 1.3).

1.1.3.2 Latency

Latency establishment of the alphaherpesviruses HSV-1 and PRV. After a productive primary infection in non-neuronal cells, alphaherpesvirues access sensory free nerve endings and establish latency - as non-integrated, circularized episomes - in the nucleus of neurons [10–12, 98]. Virions arrive at their lifelong latent reservoir via retrograde transport through the axon [99–101]. The axon connects the cell body of a neuron to the axon termini. The capsid with inner tegument proteins is then transported to the cell body [101]. This is achieved by the viral

proteins virion protein (VP)1/2 (*UL36*), which mobilize the minus-end-directed motor protein dynein [102]. Through the long distance of the axon, capsid and tegument proteins are often separated from each other and arrive separately at the cell body [103]. Since the latter proteins are needed for (re)activation of transcription, their separation from the capsid is assumed to lead to fast latency establishment of the incoming viral genome. However, in commonly used *in vitro* systems for explant neurons, replication is induced upon *de novo* infection [104]. This phenomenon occurs most probably due to the missing axonal transport in the *in vitro* system [98, 105–107]. During latency, only a small part of the genome is still transcribed, i.e. the latency associated transcript (LAT) [108], which is a non-coding ribonucleic acid (RNA), whose exonic regions serves as precursor for microRNAs (miRNAs) [109]. The LAT-derived miRNAs help to repress viral lytic genes [109]. Moreover, the genes encoding LAT are antisense to the gene encoding infected cell protein (ICP)0 (*RL2*), ICP4 (*RS1*) and ICP34.5 (*RL2*). [110–113]. This may be related to latency maintenance and reactivation [113–115].

However, in some neurons, alphaherpesviruses replicate briefly upon primary infection [116]. This early replication phase is controlled by cells of the innate immune system, which results in a quiescent state of viral genomes, in all infected neurons, no later than 8 days post infection (dpi) [117]. Furthermore, interferon production upon primary infection is likely to influence latency establishment of alphaherpesviruses in neurons, by introducing an antiviral state. It has been shown, through explant neurons treated with interferon alpha (IFN-α), before infection with HSV-1 and PRV, that these viruses preferably established a quiescent state compared to viral genomes in untreated neurons [118]. Suzich et al. [119] observed augmented PML levels in neurons treated with interferon-alpha. Since PML is also known as an antiviral factor [120], this might be a possible explanation for the establishment of a quiescent state [119]. Differences in PML levels could therefore influence progression of the infection.

Since neurons do not divide, the loss of these cells cannot be compensated by new ones; thus, neurons aim to prevent cell death. However, it is known that during neurodegenerative diseases, neurons become apoptotic [121]. Furthermore, also virus infections can lead to neuronal-death mediated through the immune system [122, 123]. One mechanism how neurons can clear viral infections but promote their survival is by autophagy. Yet, HSV-1's neurovirulence factor, the infected cell protein 34.5 (ICP34.5) represses the autophagy pathway, by inactivating the host protein Beclin-1, which otherwise would recruit several other autophagy proteins [124].

Nevertheless, the immune system plays an important role in repressing viral gene expression and prevents reactivation, which is achieved by virus-specific CD8-positive T-cells [125–127]. These CD8-positive T-cells are found in close proximity to infected neurons [125–127] and release non-cytotoxic lytic granules, containing the protease granzyme B; this degrades the viral protein ICP4 [128], which is necessary for transcribing early and late genes [129–131]. Granzyme B activity normally leads to caspase activation, which ultimately would result in apoptosis [132]. However, LATs block caspase cleavage, which prevents cell death [133]. This mechanism shows that HSV-1 itself can prevent death of infected neurons to maintain the infection.

Additional to the control via the immune system, heterochromatinization of the viral genome

also leads to repression. So far it has been shown that HSV-1 acquires the repressive facultative heterochromatin modification H3K27me3, in latently infected neurons, after several dpi [95, 134]. Moreover, it is speculated that constitutive heterochromatin can be established on HSV-1 [135, 136] (Epigenetics will be further explained in Sec. 1.3).

Altogether, these mechanisms allow HSV-1 as well as PRV to latently persist in neurons. Furthermore, the non-dividing nature of neurons facilitates virus persistence, as there is no need to segregate virus into daughter cells.

Latency establishment of the gammaherpesviurs KSHV. Gammaherpesviruses establish latency in hematopoietic cells [17, 18], which in contrast to neurons are dividing cells. Furthermore, these viruses become repressed by default upon *de novo* infection [20, 137]. During latency of the gammaherpesvirus KSHV, there is expression of only a small subset of genes, i.e. v-FLIP, v-Cyclin, Kaposin, some viral miRNAs and latency associated nuclear antigen (LANA) [138–140]. All these gene products help the virus to maintain latency. However, LANA is the only protein which enables the virus genome to properly segregate to daughter cells during cell division, allowing the virus to persist in the host. LANA possesses a DNA binding capability via its N-terminus, thereby tethering the viral genome via its TR to the host chromatin. Furthermore, this viral protein has the ability to recruit the host replication machinery, leading to latent replication of the vDNA [141–143]. In addition, LANA is involved in repressing lytic activation of the virus by binding to the promoter region of the replication and transcription activator (RTA), which is needed for lytic reactivation, and therefore inhibiting its expression [144].

Similar to alphaherpesviruses, gammaherpesviruses also become chromatinized upon *de novo* infection [145]. Most of the KSHV genome is repressed by the facultative heterochromatin mark H3K27me3, between 24 hours post infection (hpi) to 48 hpi [93, 146]. Simultaneously, the activating histone mark H3K4me3 is established predominantly in regions expressed during latency, as well as on the promoter of the lytic transactivator RTA [93, 94, 147, 148]. Another epigenetic silencing mechanism is DNA methylation; however, KSHV genomes only acquire DNA methylation late during infection [93]. (Epigenetics will be further explained in Sec. 1.3).

In summary, a major difference during the latent state of alpha- and gammaherpesviruses is replication. While alphaherpesviruses establish latency in non-dividing cells and therefore need no replication to persist in the host, gammaherpesviruses establish their latent state in dividing cells. To overcome loss of the genomes by cell division, gammaherpesviruses tether their genome to the host genome and hijack the cellular replication machinery for to accomplish a licensed latent replication, once per cell cycle.

1.1.3.3 Lytic (re)activation and replication

Lytic replication of the alphaherpesviruses HSV-1 and PRV. Under certain stimuli, alphaherpesviruses can reactivate from their latent state in neurons. Among others, these stimuli can be exposure to stress or UV light as well as a microbial co-infection [24–27]. Upon reactiva-
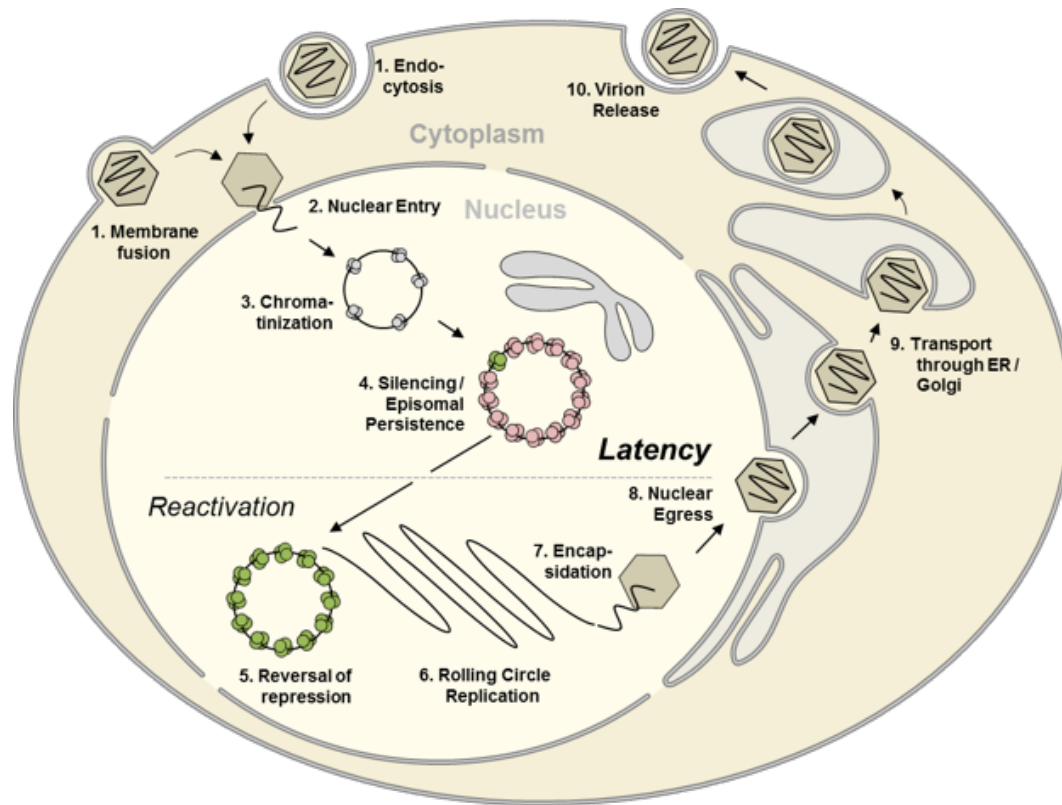
Figure 1.3: Herpesvirus Life Cycle. 1. Herpesvirus particles enter the cell either through membrane fusion or endocytosis. 2. After transport through the cytoplasm along microtubules the virions reach the nucleus and the viral DNA is injected through the nuclear pore. 3. Upon injection of the naked viral genome, it becomes circularized and chromatinized. 4. Histones will then be modified, leading either to a repressed state, where the genome can persist in the nucleus, or to viral replication. Replication can either occur shortly after infection or as an event called reactivation. 5. Reactivation happens after the episome was already silenced. 6. After activating marks are established all over the genome, the rolling circle amplification of the viral DNA starts and viral proteins are expressed. 7. Once capsids have formed, the naked viral genomes will be packaged into them. 8. Virions will then leave the nucleus through budding into the endoplasmatic reticulum (ER), followed by release into the cytoplasm where they acquire the tegument proteins and 9. are then transported through the Golgi. At this step they will their final envelope. 10. Ultimately, the vesicles - containing the mature virus particles - fuse with the plasma membrane and viral particles will be released into extracellular space. The graphical representation of the herpesvirus life cycle has been kindly provided by Adam Grundhoff (unpublished).

tion, the viral genome is transcribed and progeny is produced. This reactivation is important for spread to a new host. The establishment of lytic replication of alphaherpesviruses requires several proteins, which are independent of the infected cell type. An ordered transcription cascade characterizes the lytic replication cycle of these viruses and the transcribed genes can be categorized into three groups after their kinetics:

- immediate early (IE) genes, which prepare the host cell for viral replication e.g. by damage of antiviral proteins,

- early (E) genes, which are needed for replication of the virus, and

- late (L) genes, which mostly encode structural proteins, required for virion assembly of the virus. [149]

HSV-1 has six immidiate early (IE) gene products, which are the six infected cell proteins ICP0, ICP4, ICP22, US1.5, ICP27 and ICP47. [150]. Transcription of the IE genes is mediated by virion protein 16 (VP16), which is a component of the viral tegument [151]. Hence, during primary infection, this protein is present in the cytoplasm even before vDNA has entered the nucleus. The cytoplasmic protein, host cell factor-1 (HCF-1), acts together with VP16 and enables its transport into the nucleus. There, the two proteins interact with the transcription factor octomer

binding protein-1 (Oct-1). Both, VP16 and Oct-1, recognize the same target sequence, which lies in promoter regions of the viral IE genes. This so called VP16 induced complex (VIC) is then able to recruit various transcription factors through VP16's transcriptional activation domain (TAD) [152–154]. Additionally, VP16 can interfere with the virion host shutoff protein (VHS) to disrupt its normal function of degrading host and viral messenger RNA (mRNA) [155]. The viral protein ICP22, however, can counteract VP16's function by inhibiting IE gene transcription, leading to silencing of the viral genome [156]. This mechanism enables the maintenance of latency. Furthermore, when HSV-1 infects neurons, proteins like VP16 are frequently not passing the axons, which also leads to silencing of the viral genome [157]. Additionally, VP16 *de novo* synthesis is needed to allow normal rates of progeny production [158]. Albeit VP16 being defined as a late gene product, *UL48* - the gene from which VP16 is transcribed - shows a leaky-late kinetic, in latently infected neurons [158]. Upon certain reactivation stimuli, VP16 is expressed without the presence of any other viral protein. This leads to gene transcription of the viral IE genes and, ultimately, to lytic reactivation [158–160]. Nevertheless, other alphaherpesviruses were also able to reactivate from a latent state without the presence of VP16 [161–163]. Thus, VP16 is important for reactivation from latency and might increase viral yields, but is not solely necessary.

ICP0 is a really interesting new gene (RING)-finger E3-ubiquitin-ligase, which is expressed very early during primary infection [164]. This RING-finger is able to bind Zn^{2+}-ions, which enables the protein to interact with ubiquitin conjugating enzymes [164] and transactivates promoters of different viral genes [165–168]. ICP0 also has a nuclear domain 10 (ND10)-, also known as PML-NBs, localizing signal and is involved in degrading its components [169–172]. However, ICP0 is not essential for establishing a lytic infection [175], but only impairs virus production in most cell lines[176]. In many carcinoma cell lines the growth of a HSV-1ΔICP0 mutant is not impaired at all, but they seem to substitute for ICP0 [175, 177]. One example for this is the human bone osteosarcoma epithelial (U2OS) cell line [178]. Some theories about the permissiveness of this cell line have been discussed in literature, one is the absence of ATRX, a chromatin remodeller and antiviral host factor against vDNA [180]. ICP0 is also hypothesized to support eviction of repressive histone modifications on HSV-1 genomes during lytic replication [181].

The IE viral protein ICP4 is necessary for transcription of several viral early (E) and late (L) genes, as it binds to their promoters [129–131] and helps to recruit RNA Polymerase II, mediator components, replication proteins and transcription elongation factors [182]. Furthermore, chromatin remodelers are recruited to vDNA through ICP4 [183]. Additionally, the histone acetyltransferase circadian locomotor output cycles kaput (CLOCK) builds a complex with the viral proteins ICP4, ICP22 and ICP27 [183]. ICP27 is another IE gene product, which is necessary for viral replication and interacts with ICP8, the major vDNA binding protein [186, 187]. Their interaction seems to stimulate late gene transcription [188].

ICP22 is transcribed from the gene *US1*, which encodes a second protein, US1.5, a N-terminally truncated version of ICP22 [189]. In addition, ICP22 is required in some cell types to form a complex with ICP4 and ICP27 to allow efficient viral replication. This is the case in acute oral and neuronal replication [190, 191]. It is also required for the formation of the virus-induced chaperone-enriched (VICE) domains [192, 193], which contain multiple cellular chaperones, proteasomal

components, and ubiquitinated proteins [194, 195]. The VICE domains are required as protein quality control centers [196].

The sixth IE gene product, ICP47, has a protective role against CD8-positive T-cells by inhibiting the major histocompatibility complex (MHC) class I presentation pathway [197]. This feature leads to enhanced neurovirulence of HSV-1 *in vivo* [198].

Unlike HSV-1, PRV only needs one protein to start lytic replication and reactivation from latency; this is the protein IE180, which is also the only IE protein of PRV [123]. IE180 is the orthologue of HSV-1's ICP4 [199] and induces transcription of PRV's E genes [200]. As for VP16, *de novo* synthesis of IE180 is not required to start lytic replication [201]. To overcome the interferon-induced antiviral state during infection, the early protein 0 (EP0) - the orthologue of HSV-1's ICP0 - is necessary [202, 203]. However, EP0 is not sufficient to start lytic replication [203].

Lytic replication of the gammaherpesvirus KSHV. Essential and sufficient for replication of KSHV is the expression of the IE gene product RTA [204]. RTA together with its cellular co-activator recombination signal sequence-binding protein-J kappa (RBP-J$_\kappa$) induces several early and late viral genes, upon binding to RTA-responsive elements on the virus genome [205, 206]. Additionally, another IE gene product, K8, is important for transcription of the viral genome [207]. As already mentioned in Sec. 1.1.3.2, KSHV becomes repressed by default upon *de novo* infection [20, 137]. This happens via repressive epigenetic modifications on the viral genome [93, 94, 146, 208–210] Therefore, epigenetic modifying enzymes are needed to achieve an euchromatic state of the viral genome. During reactivation, the repressive mark H3K27me3 is erased by the lysine demethylases, ubiquitously transcribed tetratricopeptide repeat X-chromosome (UTX) and Jumonji domain-containing protein D3 (JMJD3), which both interact with the viral polyadenylated nuclear (PAN) long non-coding RNA (lncRNA) [211]. This RNA is highly abundant during lytic replication of KSHV and also interacts with mixed-lineage leukemia protein 2 (MLL2), an enzyme that methylates H3K4 [211]. Erasing H3K27me3 and catalyzing H3K4me3 ultimately leads to euchromatin formation and therefore to further gene expression.

Unlike latent replication, lytic replication is carried out by viral proteins, not the host replication machinery. KSHV's polymerase is transcribed from *ORF9*, with further proteins of the viral replication machinery being the polymerase processivity factor (ORF59), a primase and a primase-associated factor (ORF56 and ORF40/41, respectively), a helicase (ORF44) and a single stranded binding protein (ORF6) [212]. While genome amplification only occurs once per cell cycle and is restricted by the host replication machinery during the licensed latent replication, lytic replication is characterized by several amplifications of the viral genome through a rolling-circle mechanism (Fig. 1.3). KSHV episomes are decorated with two different histone modifications during latent infection [93, 94]. The bivalent chromatin state of KSHV allows fast reactivation from latency through stimuli like oxidative stress, hypoxia, or co-infection with human immunodeficiency virus-1 (HIV-1) [28–30]. Furthermore, under ER-stress, plasma-cell differentiation of primary effusion lymphoma (PEL) cells is induced, which reactivates KSHV via the transcription factor X-box binding protein 1 (XBP-1) [213–215].

1.1.3.4 Late replication, packaging and egress

During lytic infection the herpesviral genome is amplified in a special compartment in the nucleus, called replication compartment (RC) [216]. The constantly growing RC excludes host chromatin from the center of the nucleus to the edge. DNA concatemers are generated through rolling-circle amplification (Fig. 1.3), which subsequently are cleaved and transported to procapsids via the terminase complex [217].

During packaging of HSV-1 DNA the major capsid shell protein of HSV-1, VP5, interacts with the smallest capsid shell protein VP26 and - together with the triplex proteins VP19 and VP23 - forms the procapsid at the portal complex [218–221]. The terminase complex - which is made of the three viral proteins UL15, UL28, and UL33 - then binds to the portal of the procapsid, which leads to protease activation [222]. Subsequently, naked vDNA is cleaved and packaged into the capsid [222, 223]. The terminase complex then dissociates [223, 224] and the mature viral capsid, filled with vDNA, leaves the nucleus via budding. Specifically, the capsid buds into the inner nuclear membrane and then travels to the outer membrane, where it is released into the cytoplasm [225], which is all mediated by the nuclear egress complex (NEC) [226, 227]. The capsids are transported further through the cytoplasm, where the tegument proteins are located and acquired around the capsid [228, 229]. By budding into the Golgi, capsids undergo their secondary envelopment and acquire their final envelope, with glycoproteins [230, 231]. From here, vesicles with the mature virion are transported to the plasma membrane, where virus particles are released into extracellular space [232–234] (Fig. 1.3).

Alphaherpesvirus particles that are assembled in the cell body of a neuron, however, are transported to the site of primary infection by anterograde transport through the axon [99–101]. For an efficient anterograde transport, the viral proteins US9, gE and gI are necessary [99, 235–237]. US9 mediates the recruitment of the plus-end-directed kinesin-3 microtubule motor, the kinesin family member 1A (KIF1A), which is specific for neurons [238–241].

Furthermore, during lytic infection, viral episomes are associated with euchromatic histone modifications, e.g. H3K4me3, enabling replication of the virus [247] (Epigenetics will be further explained in Sec. 1.3). However, during viral progeny production, genomes are not chromatinized anymore, since they will be packaged into capsids as naive DNA. The detailed mechanisms underlying the switch from heterochromatinized episomes to euchromatinized episomes are still not known and need further investigation.

1.2 Epigenetics

After the herpesvirus life cycle has been discussed, this section will focus on the establishment and maintenance of epigenetic modifications. First the general cellular mechanisms will be explained, followed by describing the current knowledge of these modifications in the context with herpesviruses.

Epigenetic modifications are heritable and can be placed on the DNA directly, which is DNA methylation, or on histones, which are histone modifications. Epigenetic modifications alter chro-

matin accessibility, which can either lead to an open, actively transcribed chromatin, called euchromatin, or a closed, inaccessible, and therefore repressed, chromatin sate, called heterochromatin [248]. Chromatin is made of nucleosomes, which consists of four core histones that occur in duplicates [249]. Each nucleosome is wrapped with 147 bps of DNA [250]. Transcription of the canonical histones H2A, H2B, H3 and H4 is dependent on DNA replication [251, 252]. Non-canonical histones are constitutively expressed and are distinguished from their canonical form by only a few amino acids [253]. Histone H3, for example, has three variants, the canonical H3.1 and H3.2 and the non-canonical H3.3. The canonical H3 variants are expressed during S-Phase and are loaded via the histone chaperone chromatin assembly factor 1 (CAF-1) [254]. Another histone chaperone, the anti-silencing function protein 1 (ASF-1), helps CAF-1 to load H3.1 [255], majorly in heterochromatin regions [256]. The non-canonical variant H3.3 is expressed at any time of the cell cycle and therefore is incorporated without ongoing replication [257, 258]. H3.3 is mostly found at transcriptionally active genes and is deposited by the histone chaperone complex histone regulator A (HIRA) [259–261]. ASF-1 also helps HIRA to load H3.3 [262, 263]. Moreover, H3.3 replaces H3.1 and H3.2 in postmitotic cells, since without replication no canonical histones can be recruited [264, 265]. In addition to its localization at active regions in the genome, H3.3 was also found at constitutive heterochromatic regions, like telomers. Here it is loaded by a histone chaperone complex, consisting of death-associated protein 6 (DAXX) and ATRX [266, 267]. Furthermore, Jang et al. [268] demonstrated that H3.3 depletion destabilized heterochromatin structures at various sites at the genome, especially at telomers, centromers and pericentromeric regions. These properties highlight that H3.3 is necessary for genome integrity [268].

Changes in the epigenetic landscape are drivers for cellular differentiation, however, alterations in the balanced epigentic processes of an individual can lead to several diseases, including cancer [269]. In the following subchapters, the different epigenetic modifications and their establishment will be further explained. Among them, there will be a special focus on repressive histone modifications, since they are of particular interest for this study.

1.2.1 DNA methylation

DNA methylation occurs through enzymatic addition of a methyl group, from the donor S-adenosyl methionin to the fifth atom of the base cytosine. This process is catalyzed by DNA methyltransferases (DNMTs), and preferably occurs at CpGs [270–272]. There are two different DNA methylation processes to distinguish. One is *de novo* methylation - catalyzed by DNMT3A/B - and the other is maintenance from a hemi-methylated target site, e.g. after replication, or DNA repair - catalyzed by DNMT1 [271, 273].

DNA methylation was found to establish a closed chromatin state, excluding histone marks like H3K4me2/3 [274]. Furthermore, this epigenetic modification is important for other processes as well, such as the mammalian X-chromosome inactivation [275], specific gene silencing during embryonic development [276] or the genome stability through inactivation of repetitive elements like retrotransposons and satellites [277]. Furthermore, DNA methylation seems to play a role during host defense mechanisms, where it serves to inactivate foreign DNA, like that of DNA-

viruses [93, 278–280].

CpG dinucleotides are prone to be methylated, however, large regions in the genome with a high CpG densitiy - the so called CpG islands - are commonly hypomethylated [281]. CpG islands are defined as parts of the genome where at least 500 bps show C, G amounts of at least 55% [282]. Such CpG islands are mostly located in active gene promoters, e.g. those of housekeeping genes [283]. At these sites, it was shown that the presence of RNA polymerase II [284] or transcription factors [285] prevent DNA methylation.

Methylation is removed by the enzyme ten-eleven translocation (TET), converting 5-methylcytosine to its derivatives. These derivatives can be replaced by cytosine during cell division or actively by DNA repair mechanisms [286, 287]. Additionally, methylated cytosines are susceptible to deamination. The process of deamination of 5-methylcytosine, removes the amino group and, ultimately, converts Cs to thymines (Ts). This leads to under-representation of CpG in regions which used to be highly methylated, a phenomenon called CpG suppression [288].

1.2.2 Histone modifications

Similar to DNA methylation, histone modifications play an important role during the development of eukaryotes. Histone modifications are placed on the tails of all four histones; in general at the following amino acids: Arignine (R), Histidine (H), Threonine (Thr), Serine (S) and Lysine (K). The main modifications are methylation (me), acetylation (ac), ubiquitination (ub) and phosphorylation (ph). Each modification has an effect on how chromatin is compacted, which can either lead to transcriptional activation - where the DNA is more accessible - or repression - where DNA is tightly wrapped around histones.

Transcriptional activation. Examples for active histone modifications are trimethylation (me3) of the fourth lysine residue (K4) on histone H3 (H3K4me3), which can be mainly found at transcriptionally active promoters [289]. H3K4me3 is catalyzed by the histone methyltransferase su(var) 3-9 enhancer of zeste and trithorax domain 1A/B (SETD1A/B) and mono- and dimethylation are catalyzed by the lysine methyltransferases lysine methyl-transferase 2A - D (KMT2A-D), which is illustrated in Fig. 1.4. In addition, acetylation (ac) of lysine residue 27 on histone H3 (H3K27ac) is an active mark found not only at promoters but also at active enhancer regions [290]. This form of permissive chromatin is called euchromatin. Histone acetylation is established by the proteins E1A binding protein 300 (p300) and chromatin binding domain (CBP), which each contains a histone acetyl transferase (HAT) domain (Fig. 1.4) and removed by histone deacetylases (HDACs). H3K36me3 and H3K36me2, both belong to the activating chromatin modifications and can be established by several enzymes, e.g. nuclear receptor-binding SET domain-containing protein1-3 (NSD(1-3)) and SETD3 [291, 292] (Fig. 1.4). H3K36me2 is mainly found in gene bodies, whereas H3K36me2 is more diffusely distributed throughout the genome [293].

Transcriptional repression. Transcriptionally repressed chromatin is called heterochromatin, which has two subtypes. One is the so called facultative heterochromatin, whose hallmark
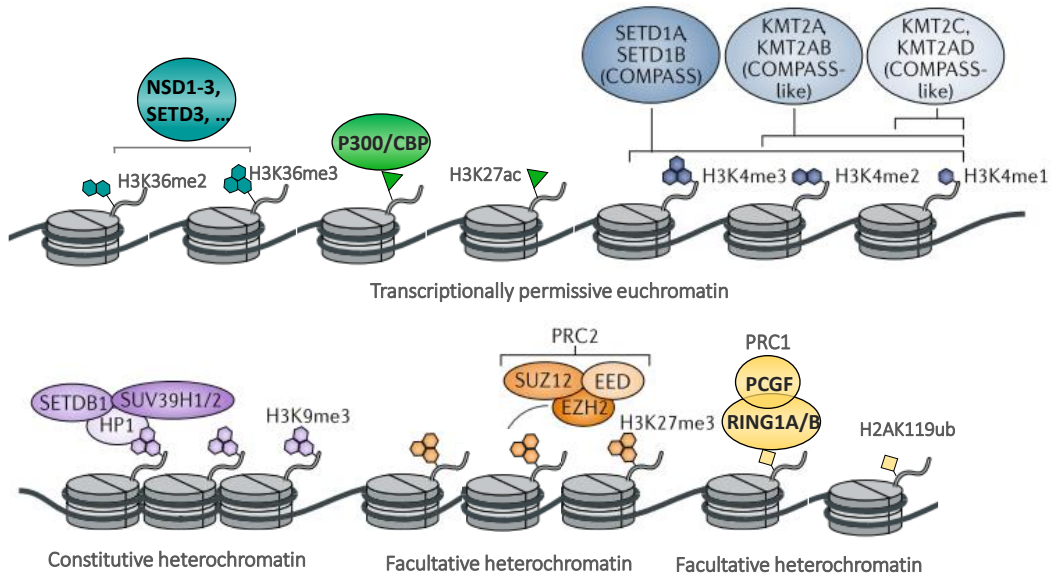
Figure 1.4: Histone modifications and their writers. Hallmarks of transcriptionally active euchromatin are H3K27ac and H3K4me3. Acetylation is set by P300/CPB, whereas trimethylation of H3K4 is established by the COMPASS proteins SETD1A and B, after mono- and dimethylation were acquired by the lysin methyltransferases and COMPASS-like proteins KMT2A to D. The tight repression of constitutive heterochromatin can be established by SETDB1 and SUV39H1/2. Subsequently, HP1 recognizes the acquired constitutive heterochromatin mark H3K9me3 and thus leads to its persistence. Facultative heterochromatin is established by the multiprotein complex PRC. H3K27me3 is established through PRC2 with its catalytic subunit EZH2, whereas H2AK119ub is established by PRC1 through its catalyzing subunit RING1A/B. The graphic originates from [294] and has been modified.

modifications are H3K27me3 and H2AK119ub. Both of these modifications are set by PRCs, which is illustrated in Fig.1.4. The other heterochromatin type is constitutive heterochromatin, with the hallmark H3K9me3, a rather permanent repressive mark, compared to H3K27me3 and H2AK119ub. This modification is established by the enzymes SET domain bifurcated histone lysine methyltransferase 1 (SETDB1) or suppressor of variegation 3-9 homolog 1/2 (SUV39H1/2), which is illustrated in Fig.1.4. Facultative and constitutive heterochromatin will be further explained in the next sections (Sec. 1.2.2.1 and Sec. 1.2.2.2).

1.2.2.1 Facultative heterochromatin

Facultative heterochromatin is established by polycomb group (PcG) protein complexes, called PRCs. PcG proteins are highly conserved and were first described in *drosophila melanogaster*. PRCs are multi-protein complexes, consisting of a core catalyzing unit, which sets the modification, and other subunits that, e.g. recognize specific histone modifications or guide the complex to distinct sequences [295, 296]. The two main PRCs and their paralogs are depicted in Fig. 1.5. The establishment of facultative heterochomatin is essential during embryonic development [297–299]. Hence, H3K27me3 and H2AK119ub can be found on cell type specific genes - e.g. during X-chromosome inactivation [300, 301] or on HOX-genes [302–305]. During differentiation, the H3K27me3 silenced genes can become easily activated again [304], since this modification as well as H2AK119ub, still allow transcription factors (TFs) to bind [306]. The activation of genes repressed by those modifications can be achieved through the formation of 3D loops. Here, enhancer (En)

regions will be brought in close proximity to the promoter of a gene, which subsequently will be activated by TF-binding [307–309].

In addition, repressive histone modifications can occur together with permissive histone modifications. This combination leads to a bivalent state, where transcription is repressed but can quickly be released under specific stimuli. In promoter regions of embryonic stem cells the combination of H3K27me3 and H3K4me3 has been demonstrated in several studies [306, 310–312].
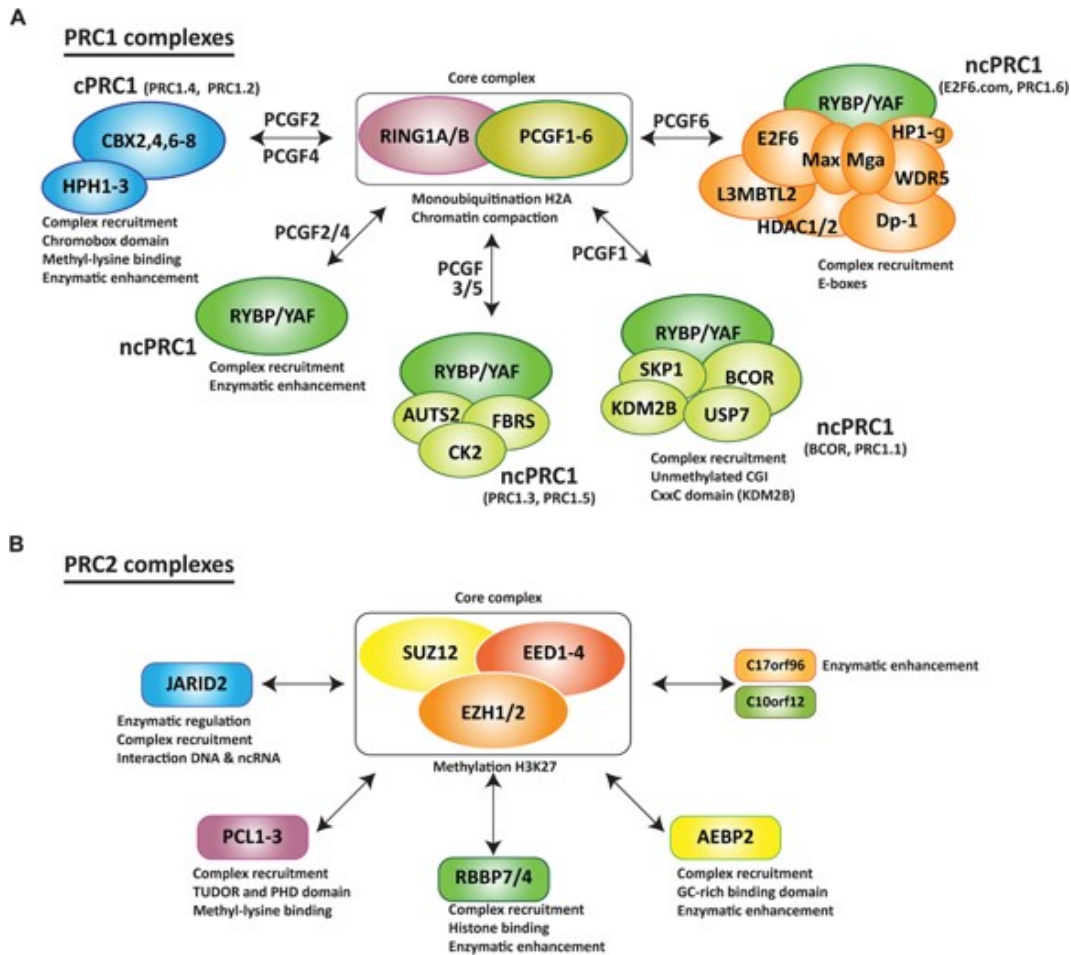
Figure 1.5: Polycomb repressive complexes and their function. (A) canonical (c) and non-canonical (nc) PRC1. RING1a/B and PCGF1-6 build the core complex of PRC1, which catalyze monoubiquitination of H2AK119. The six different forms are named after their PCGF protein 1-6. The cPRC1.2 and 1.4 contain PCGF2 and 4 respectively and are distinguished from the ncPRC1s by their chromobox domain family protein (CBX) proteins, which recognize H3K27me3. ncPRC1s contain YY1-binding protein (RYBP) or its homolog, YY1-associated factor (YAF), which bind to RING1B. (B) PRC2 catalyzes H3K27me3 via its subunit EZH1 or EZH2, which forms the core complex together with SUZ12 and EED1-4. The cPRC2.1 is recruited to unmethylated CpG islands via its Polycomb-like (PCL) proteins [313], which also has a H3K36me3 binding domain and demethylase function, whereas non-canonical PRC2.2 recognizes H2AK119ub by its subunit JARID [314]. Furthermore, PRC2 can be recruited to unmodified nucleosomes by the subunit RBBP7/4. The role of AEBP2 is not fully understood so far but has been shown to enhance the enzymatic activity of the protein complex. C17ORF96 better known as EPOP functions as a scaffold protein on PRC2.1 while C10ORF12, better known as PALI1 modulates catalytic activity and is also only found in PRC2.1. The graphical representation originates from [315].

Establishment of H2AK119ub by PRC1. H2AK119ub is a dynamic histone modification, which can be established and erased with high frequency [316]. Furthermore, H2A is the most abundant ubiquitinated protein in the nucleus of a mammalian cell, with about 5-15 % monoubiquitinated H2As [317].

PRC1s harbor a E3-ligase RING1A/B, which catalyzes monoubiquitination of H2AK119 [318]. Together with several PCGF proteins they form the core complex of all PRC1s. The six different

PCGFs determine the subtypes, ranging from PRC1.1 to PRC1.6. The c PRC1.2 and PRC1.4 contain PCGF2 and PCGF4, respectively and are distinguished from the ncPRCs1 by their CBX proteins [319]. In the canonical pathway H3K27me3 is acquired first and can be recognized by the CBX subunit of cPRC1 to ubiquitinate H2AK119 [319]. ncPRC1s contain RYBP or its homolog, YAF proteins, which bind to RING1B (Fig. 1.5A).

The ncPRC1.1 harbors a subunit that recognizes unmethylated CpG islands. This subunit is called lysine-specific demethylase 2B (KDM2B), which is specific for H3K36 [320, 321]. CpG-rich DNA can be found at the majority of mammalian promoters [283]. However, CpG islands are not the only polycomb target sites. PRC1.6 for example recognizes E- and T-box motifs, which can be found in germline-specific genes [322–324]. In the case of X-chromosome inactivation, PRC1 is targeted by the lncRNA X-inactive specific transcript (XIST) [325, 326].

In contrast to the cPRC silencing pathway, ncPRC1.1 first establishes H2AK119ub, which can be then recognized by the ncPRC2.2 subunits AEBP2 and JARID. PRC2.2 on the other hand sets the repressive mark H3K27me3, as shown in Fig. 1.6.

In the end both pathways result in a synergistic repression. Genes solely associated with ncPRC1 are still moderately expressed whereas cPRC1 association leads to strong gene repression [327].

H2AK119ub-specific deubiquitinases are ubiquitin carboxyl-terminal hydrolase (USP16) and 2A-deubiquitinating enzyme (2A-DUB) [299, 317, 328]. Deubiquitination processes are crucial for embryonci stem cell (ESC) gene expression and cell cycle progression [299, 317, 328, 329].
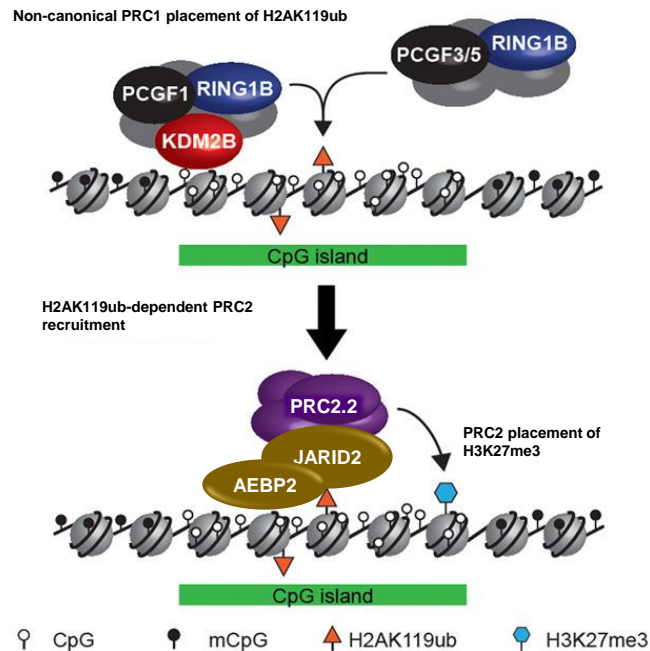
Figure 1.6: Non-canoical PRC recruitment. ncPRC1 recognizes unmethylated CpG islands via its subunit KDM2B and subsequently catalyzes monoubiquitination of H2AK119. This modification is recognized by the subunits AEBP2 and JARID2 of non-canonical PRC2, which sets H3K27me3. This graphical outline has been modified from [330].

Establishment of H3K27me3 by PRC2. PRC2 catalyzes H3K27me3 via its subunit EZH, which forms the core complex together with SUZ12 and embryonic ectoderm development 1-4 (EED1-4) (Fig. 1.5B). Expression of the two paralogs of EZH are cell dependent. While EZH1

occurs in adult and non-dividing cells, with only a minor methyltransferase activity, EZH2 can be found in dividing and embryonic cells [331].

The recruitment of PRC2 to DNA occurs through different subunits. The cPRC2.1 is recruited to unmethylated CpG islands via its PCL proteins [313], which harbor a H3K36me3 binding domain and demethylase function, whereas ncPRC2.2 recognizes H2AK119ub by its subunit JARID [314]. Histone demethylases, namely UTX and lysine-specific demethylase6B (KDM6B), are needed to remove the facultative heterochromatin modification H3K27me3 [332–335]. This leads to subsequent activation of the respective genes.

1.2.2.2 Constitutive heterochromatin

Constitutive heterochromatin is mostly found at repetitive elements, e.g. satellite DNA or transposons, which are located at telomers and centromers [336–340]. Its hallmark is H3K9me3, which can be recognized by other proteins, leading to a tight chromatin compaction [341]. Through this, the establishment of constitutive heterochromatin prevents gene expression and, additionally, recombination events between conserved regions in the genome [342]. This form of chromatin is hardly reversible and was even shown to favor consecutive DNA methylation [343, 344].

Establishment of H3K9me3.   The histone methyltransferase SETDB1 and the histone methyltransferase complex consisting of SUV39H1 and SUV39H2 are needed for H3K9me3 establishment [345]. Marina et al. [346] could show, that the lncRNA binding protein, stress response element binding protein (Seb1) is required for constitutive heterochromatin formation in *S.pombe*. Additionally, RNA interference (RNAi) was shown to be crucial for H3K9me3 *de novo* establishment in *S.pombe* [347–350]. This is initiated through transcription of centromeric repeat regions during S-phase. These transcripts are then processed to small interfering RNAs (siRNAs), which guide the cullin-dependent E3 ubiquitin ligase/histone H3-K9 methyltransferase complex (CLRC complex) to the repeat transcripts, which catalyzes H3K9me3. Therefore, transcription of heterochromatic regions seems to be necessary to recruit H3K9me3 writers [351–353].

Despite these first data about RNAi-mediated *de novo* H3K9me3 establishment, the initial mechanisms of enzyme recruitment to the specific genome locations are still not fully understood. However, for SETDB1 it was shown that this enzyme is recruited via the human silencing hub (HUSH) complex, which consists of the proteins Transgene activation suppressor protein (TASOR), M-phosphase protein 8 (MPP8) and Periphilin [354]. MPP8 can bind to H3K9me3 via its chromodomain [355]. Hence, this complex is assumed to maintain constitutive heterochromatin rather then initialize its establishment [354]. Furthermore, SETDB1 interacts with KRAB-associated protein 1 (Kap1), a co-repressor of the Krueppel-associated box (KRAB) domain zinc finger proteins, which recruits SETDB1 to specific loci that have to be silenced [356]. Kap1 also recruits HDACs and the nucleosome remodeling deacetylase (NurD) complex, which subsequently lead to the formation of a transcriptionally repressing environment [357, 358].

Additionally, the protein complex PML-NB harbors the histone methyltransferase SETDB1 and was found in association with telomers. There, together with its ligands DAXX and ATRX, the

complex incorporates H3.3 and establishes heterochromatin [359, 360]. SETDB1 is thought to execute PML-NB-mediated repression [361]. Although PML-NBs are a highly studied topic, the molecular mechanisms leading to PML-NB-mediated repression are still not fully understood.

However, this tight repressive modification can also be removed, which is catalyzed by members of the KDM4 family, to allow gene expression [362, 363].

Maintenance of H3K9me3 by HP1. H3K9me3 can be recognized by heterochromatin protein 1 (HP1), which stabilizes heterochromatic domains and mediates gene silencing [364–366]. Once HP1 oligomerizes, chromatin will be compacted [367]. In addition, several other histone methyltransferases can be recruited by HP1 [368].

HP1 was observed to induce phase separation and subsequently to create protected chromatin domains [369, 370]. However, it is highly debated whether constitutive heterochromatin can be defined as a phase separated compartment. Erdel et al. [371] recently suggested that it is more likely that constitutive heterochromain forms a collapsed and therefore hardly accessible state of chromatin, instead of a "real" phase. Nevertheless, stabilization through HP1 is crucial to serve genome integrity, by avoiding recombination events between the silenced repetitive elements and by preventing transcription of transposons.

1.3 Herpesviruses with epigenetic modifications

Epigenetic modifications seem to play an important role during host defense mechanisms, where they serve to inactivate foreign DNA, e.g. that of viruses [93, 278–280]. The chromatinization of naked, foreign DNA is needed to control its expression in the cell. The nucleocapsid DNA of herpesviruses is free of chromatin and therefore also of histones [372]. Hence, vDNA injected into the host nucleus is, at first, also not associated with histones [373, 374]. However, multiple ChIP experiments of infected cells have demonstrated that genomes of several herpesviruses become chromatinized shortly after injection [93, 135, 136, 210, 247].

Histone modifications during lytic infection. During lytic infection the genome of HSV-1 is decorated with euchromatic modifications, e.g. H3K4me3, which leads to active transcription [247]. Already two hours post infection with HSV-1, IE gene products can be detected. These genes are transcribed without the presence of *de novo* synthesized viral proteins but are induced by the viral transactivator and tegument protein VP16 (more information about VP16 can be found in Sec. 1.1.3). Herrera and Triezenberg [375] have shown that VP16 recruits chromatin modifying activators CBP and p300 to HSV-1 genomes, during lytic infection. Once the transcription has started, IE gene products are synthesized. The IE protein ICP0 was found to degrade PML-NBs, which were shown to colocalize with viral genomes very early during infection and are known to repress viral gene transcription. Furthermore, the same proteins were shown to interact with RE1-Silencing Transcription factor (REST)/coREST-HDAC repressor complex, thereby dissociating HDAC1 from vDNA [376, 377]. Additionally, ICP8 is hypothesized to recruit chromatin

remodeling complexes into RCs and onto newly synthesizes vDNA [378].

Upon reactivation of KSHV, H3K4me3 levels on the viral genome augment, whereas H3K27me3 levels decrease [94]. Rossetto and Pari [211] demonstrated that UTX and KDM6B but also the histone methyltransferase MLL2 interact with KSHV's lncRNA PAN. This interaction leads to demethylation of H3K27 and methylation of H3K4.

Histone modifications during latent infection. During latent infection of neurons, HSV-1 acquires facultative heterochromatin, several days post infection. First data indicate that infection of non-neuronal cells with lytic-cycle-deficient HSV-1 mutants leads to acquisition of constitutive heterochromatin, already 24 hpi. Genomes of the gammaherpesvirus KSHV by default become latent upon infection of most cells and are decorated with the repressive histone modifications H3K27me3 and H2AK119ub already 24 hpi to 48 hpi [93, 210].

Various host factors have been reported to play a role during the epigenetic regulation of herpesvirus infections. In recent literature, special focus has been on the establishment of repressive histone modifications on herpesviral DNA, which is depicted in Fig. 1.7. As this study also investigates the repressed state of herpesviruses, these host factors will be explained more detailed in the following sections.

1.3.1 PML-NB-mediated repression of herpesviruses

The PML protein. The PML protein has several isoforms, which are all generated from one gene. They only differ in their C-terminal region, while the N-terminal RING finger B-box and coiled-coil (RBCC)/tripartite motif is always the same [380, 381]. The highly conserved RBCC/tripartite motiv consists of three zinc-binding domains, one is a RING-finger, the other a coiled-coil region and the last one a B-box [382, 383]. This motif is found among several different cellular proteins and thus, characterizes a wide variety of functions. One of this functions is the elimination of missfolded proteins achieved through the E3 ubiquitin-ligase activity of the RING-domain [384]. Furthermore, PML proteins were found to be associated with the DNA-damage response, as DNA-damage sensors [385]. Additionally, these proteins directly bind to the tumor suppressor p53 and induces its expression [386, 387]. PML proteins can induce cell death upon different stimuli, whereas in absence of PML, cells can be resistant to apoptotic signals [388]. The absence of PML results in acute promyelocytic leukemia (APL) [389] and polyglutamine repeat neurodegenerative diseases [390]. In addition, Ishov et al. [391] discovered that the PML protein is the key organizer of a multi-protein complex formation, formally known as ND10 nuclear body - now referred to as PML-NB - which forms a matrix associated domain.

General characteristics of PML-NBs. The shell of a PML-NB consists of all nuclear isoforms of PML, which interact via their coiled-coil domain [392]. Additional proteins are recruited and a PML-NB is formed. The recruitment is achieved by sumoylation of its interaction partners, whereas PML itself has a SUMO-interacting motif (SIM). These complexes are 0.1 µm to 1.0 µm in diameter, belong to the nuclear matrix and are found in discrete foci all over the nucelus

[393]. Disruption of PML occurs under oxidative stress, causing the protein to conjugate by poly-SUMO2/3 chains. This results in the recruitment of a ubiquitin ligase, which polyubiquitinates the PML-NB components and leads to their degradation in proteasomes. The function of this protein complex is very diverse. On the one hand, PML-NBs are associated with activation of transcription [388, 393, 394]; on the other hand, it was shown that these complexes could also harbor repressive proteins, like DAXX and ATRX [395–397].

DAXX and ATRX. The protein ATRX forms a complex with DAXX. Together, they act as a histone chaperon, specific for the histone variant H3.3 [267]. With decreasing levels of PML caused by a knock-down of ATRX, Han et al. [398] could demonstrate that ATRX directly regulates PML expression. PML-NBs were found in association with telomers, where they - together with their ligands DAXX and ATRX - incorporate H3.3 and establish heterochromatin [360]. In general, PML-NBs can differ among each other, depending on cell type and cellular stress level. For example, interferon has been shown to be a trigger for PML-NB formation and growth of the complex, since expression levels of several PML-NB components are increased, upon interferon treatment [399].

PML-NBs' association with HSV-1 and PRV. A factor that can lead to interferon type I production is a virus infection of the cell [400]. Additionally, PML-NBs were found to be associated with the genomes of several DNA-viruses in the nucleus [169, 391, 401, 402]. However, some viruses - like HSV-1 - developed mechanisms to evade PML-mediated repression, to start replication. During the herpesvirus life cycle, activation [403] and repression [119, 404, 405] are associated with PML-NBs [406]. During infection with HSV-1wildtype (wt), the viral protein ICP0 degrades PML-NBs, enabling replication [171]. The recruitment of ICP0 is achieved by its SIM-like sequences, which bind to sumoylated PML [407]. Through the E3-ubiquitin-ligase activity of ICP0 proteins like PML can then be degraded by proteosomal degradation [164]. It was hypothesized that HSV-1 might exploit this mechanism to establish replication domains [406]. Already two hours post infection, the PML isoforms I-VI were shown to be degraded by ICP0 [171]. Moreover, the PML-NB component ATRX was shown to be actively degraded by ICP0 up on *de novo* infection of human fibroblasts [408].

However, early during infection, PML-NBs were also shown to associate with HSV-1 genomes, leading to decreased ICP0 expression [180, 405]. Although the entrapment by PML-NBs seems to be saturated - since infection with high multiplicity of infection (MOI) overcomes this repression - reintroduction of ICP0 leads to reactivation of the repressed genomes [135]. It is believed that this can occur since only a defined number of cellular repressors are in one cell, thus when all are occupied with viral genomes the remaining ones are not restricted and need no ICP0 to replicate anymore [175, 177]. HSV-1ΔICP0 null-mutants can efficiently replicate in ATRX knock-out cells compared to ATRX expressing cells [136]. Catez et al. [410] observed that, in neurons, PML-NBs entrapment of viral genomes reduces LAT expression. Furthermore, upon interferon treatment of neurons, prior to infection, PML levels increased and viral genomes were unable to reactivate [119]. Furthermore, it was reported that lytic-cycle-deficient HSV-1 genomes, associate with PML-

NBs shortly after infection and acquire H3K9me3, in human fibroblasts [135, 180]. In addition, Yu et al. [411] have recently shown that PRV colocalizes with PML, leading to suppressed gene transcription.

All these data demonstrate, that PML-NB-mediated repression seems to play a central role during silencing of alphaherpesvirus genomes.
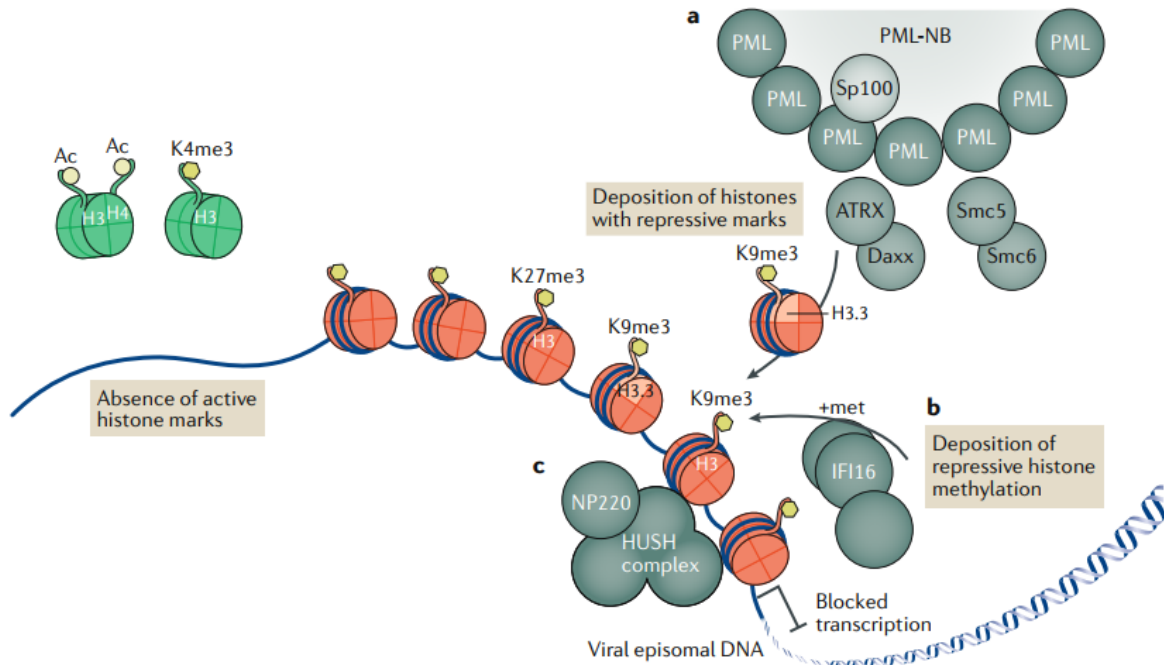
Figure 1.7: Epigenetic regulation of vDNA. Episomal vDNA becomes chromatinized and either activating or repressive histone modifications are set. H3K27ac, H3K9ac and H3K4me3 are activating marks, leading to an open form of chromatin, which is easily accessible for the replication machinery. H3K27me3 and H3K9me3 are hallmarks of repressed chromatin. H3K27me3 is established by PRC2, whereas several enzymes can establish H3K9me3. (a) During genome silencing H3K9me3 is established on H3.3, which is often found together with colocalization between viral genomes and PML-NBs. PML-NBs ahrbot the histon chaperone complex ATRX/DAXX (b) IFI16 was shown to colocalize with repressed herpesvirusgenomes and is also thought to mediate histone methylation. (c) The histonemethyltransferase SETDB1 can be recruited by the HUSH complex, which binds to H3K9me3. The graphical representation originates from [379].

PML-NBs' association with KSHV. In contrast to the above mentioned alphaherpesviruses, the gammaherpesvirus KSHV does not colocalize with PML [146]. Despite recent data suggesting colocalization of the viral protein LANA with DAXX [412], it was already demonstrated that depletion of DAXX does not interfere with latency establishment of KSHV [146]. Thus, PML-NB-mediated repression has no impact on latency establishment of KSHV.

The mechanisms leading to the difference between recognition of HSV-1 and PRV genomes by PML-NBs on one side and the absence of this recognition for KSHV on the other side have yet to be investigated.

1.3.2 PRC-mediated repression of herpesviruses

The PRCs are multi-protein complexes which catalyze the establishment of facultative heterochromatin. Detailed information of facultative heterochromatin and its establishment has been presented in Sec. 1.2.2.1.

PRCs' association with KSHV. Gene regulation of the gammaherpesvirus KSHV is highly dependent on histone modifications [93, 94]. In particular, most of the latent KSHV genome acquires facultative heterochromatin modifications already 24 hpi [93, 146, 210]. While H3K27me3 kept increasing to a certain point during the course of infection, H2AK119ub was highest in early stages of the infection [93, 146, 210]. Even though early heterochromatinization and silencing of KSHV by PRCs has been repeatedly described, the initial recruitment mechanisms are still poorly understood. Toth et al. [209] observed that LANA directly interacts with PRC2. Furthermore, LANA was shown to up-regulate EZH2 [413]. Besides, the high unmethylated CpG density of KSHV has also been demonstrated to play a pivotal role within the establishment of facultative heterochromatin [210]. The latter is supported by the description that the ncPRC1.1 can be directly recruited to highly CpG-dense regions via one of its subunits, which is KDM2B. KSHV, as well as HSV-1, are known to be highly CpG-rich and can be seen as one large CpG islands; thus they seem to be a proper target for this factor. Günther et al. [210] previously demonstrated that KDM2B is associated with KSHV genomes, very early during infection. From these results, it can be concluded that the ncPRC pathway - where H2AK119ub is established before H3K27me3 - plays a role during KSHV repression. However, further studies - including knock-outs of the catalytic subunit of PRC1 and its variants - need to be performed to determine a putative role of the ncPRC-mediated repression pathways during early infection of KSHV.

PRCs' association with HSV-1. Additionally, the alphaherpesvirus HSV-1 was reported to acquire the facultative heterochromatin modification H3K27me3 in latently infected neurons [95, 134, 414]. ChIP-qualitative real-time PCR (qPCR) showed that 14 dpi several lytic gene promoters of HSV-1 acquired this modification [95]. Furthermore, an association of SUZ12 and parts of the HSV-1 genome has been observed [95]. Moreover, Kwiatkowski, Thompson, and Bloom [414] found H3K27me3 together with H3K9me3 on HSV-1 genomes, in latently infected neurons at 28 dpi. Cliffe, Garber, and Knipe [134] compared a LAT-deficient HSV-1 to HSV-1wt infection, at 28 dpi, and observed reduced H3K27me3 levels, without LAT expression. Hence, LAT expression might promote establishment of facultative heterochromatin, facilitating repression and subsequently the latency establishment of the viral genome in neurons [134].

Although the importance of epigenetic regulation during the life cycle of different herpesviruses has been frequently reported, underlying recruitment mechanisms are still poorly understood. In particular, the different forms of heterochromatinization of the alphaherpesvirus HSV-1 shall be subject of future studies. Further understanding of how the two different forms of heterochromatin are acquired is a key step to understand the different outcomes of herpesvirus infections. Furthermore, data about a general mechanism among alphaherpesviruses, or even among different subfamilies, are still missing. From current literature, it can be assumed that central mechanisms - which determine the form of repressed chromatin - happen already early in infection. Therefore, this study aims to decipher molecular mechanisms of latency establishment early after nuclear entry of herpesvirus genomes in order to generalize previous findings.

2 Aim of the study

Herpesviruses can establish lifelong persistence in their host. This is achieved by silencing most of the viral genome. It has previously been shown that the CpG-rich gammaherpesvirus KSHV rapidly attracts PRCs, via the non-canonical recruitment, thereby being repressed through the histone modifications H2AK119ub and H3K27me3. These two modifications are hallmarks of the facultative heterochromatin, which represses transcription but can be erased relatively easily. A common feature of herpesviruses is to occasionally reactivate and produce progeny. Therefore, this metastable form of heterochromatin represents an ideal pathway for herpesviruses to acquire a form of latency from which they can escape. In the cellular context, the ncPRC-mediated repression serves to silence CpG islands via recognition of unmethylated CpG motifs. Interestingly, alphaherpesviruses, such as HSV-1, also exhibit very high CpG frequencies. In latently infected neurons, HSV-1 was shown to acquire the H3K27me3, whereas in fibroblasts there is evidence that HSV-1 acquires the constitutive heterochromatin modification H3K9me3.

The published data support the hypothesis that there are two mechanisms by which silencing of the herpesvirus genomes can be achieved, by establishment of facultative and by constitutive heterochromatin. However, the early recruitment mechanisms of repressive complexes and the decisive factors towards the different states of chromatinization and thus latency establishment are still under debate. Furthermore, there are only a few data on the epigenetic profile of HSV-1, with no available genome-wide data. Moreover, the connection between the epigenetic profile and the reactivation ability of herpesviruses is poorly understood. Hence, this study aimed to investigate whether PRC-mediated repression is a common feature among CpG-rich herpesviruses and how this way of silencing influences the ability of the virus to reactivate, in comparison to PML-NBs restriction and connect this to the epigenetic profile of the analyzed herpesviruses.

To answer this question, two closely related, lytic-replication-deficient alphaherpesvirus mutants, HSV-1*in1374* and PRVΔIE180, were used to assess the early chromatinization program of the vDNA. Usage of lytic-cycle-deficient mutants allowed to study early chromatinization independently of lytic reactivation - a state here called "quasi-latent" - in different cellular contexts. The "quasi-latent" state is defined by the absence of replication in non-neuronal cells, which do not represent the authentic latent reservoir of the used viruses. Furthermore, the used mutants allowed for reactivation, under certain conditions. Additionally, a bioorthogonal labeling system was adapted for PRV DNA, enabling the determination of host factors interacting with the viral genomes, early after nuclear entry. Furthermore, the ability of the virus to reactivate, after the successful acquisition of repressive chromatin, was investigated. Additionally, depletion and reintroduction of ATRX, in various cell lines, with subsequent infection experiments, should help to elucidate its influence on herpesvirus reactivation.

3 Results

Usage of lytic-cycle-deficient mutants of HSV-1 and PRV allowed to study early chromatinization independently of lytic reactivation *in vitro*, in non-neuronal cell lines, a state here called "quasi-latent". Such virus mutants were already generated by other groups, with the possibility to allow lytic replication under certain conditions.

For PRV lytic replication is entirely dependent on the IE gene IE180. Oyibo et al. [415] earlier generated a deletion mutant incapable of lytic reactivation, which is called PRVΔIE180. Trans-complementation of IE180, however, allows lytic induction and virus growth. The underlying model cell line for PRV infections is the porcine kindney epithelia (PK15) cell line. PK15 cells with an inducible IE180 gene were used for virus production, whereas PK15wt cells were used for investigating the epigenome and the colocalization with different host-factors during the "quasi-latent" state of PRVΔIE180. To this day, there is no knowledge about epigenetic marks on replication-deficient PRV.

Similar to PRV, there is a lytic-cycle-deficient mutant of human pathogenic HSV-1 available. This mutant is called HSV-1*in1374* and is characterized by loss of function mutations in the genes coding for the viral proteins VP16 and ICP0 [416, 417]. Additionally, it contains a temperature sensitive mutant of ICP4 [416, 417]. The temperature sensitivity of ICP4 enables the virus to replicate at a permissive temperature of 32 °C and to stay quiescent at a non-permissive temperature of 38.5 °C [416, 417]. The underlying model cell lines for *in vitro* HSV-1 infections are, besides neurons, human fibrolasts, which were used in the work presented here to investigate the epigenome and the reactivation ability during the "quasi-latent" state of HSV-1*in1374*, in different cellular contexts.

3.1 Lytic gene expression of PRVΔIE180 and HSV-1*in1374* is highly repressed

To verify the "quasi-latent" state of the infection system used, the absence of lytic gene expression in the virus mutants was examined by RNA-sequencing (RNA-seq). This was performed on PK15 cells infected with PRVΔIE180 and on immortalized human foreskin fibroblasts (BJ) cells infected with HSV-1*in1374* under non-permissive conditions. A detailed explanation about the methodology can be found in Sec. 6.3.2 and in Sec. 6.5.

As shown in the RNA-seq data of HSV-1*in1374* at 24 hpi (Fig. 3.1A), RNA of only a subset of viral genes could be detected with very low copy numbers, which is indicated by the low read counts on the Y-axis. Like the *LAT* region, where a small peak is visible, none of these genes is
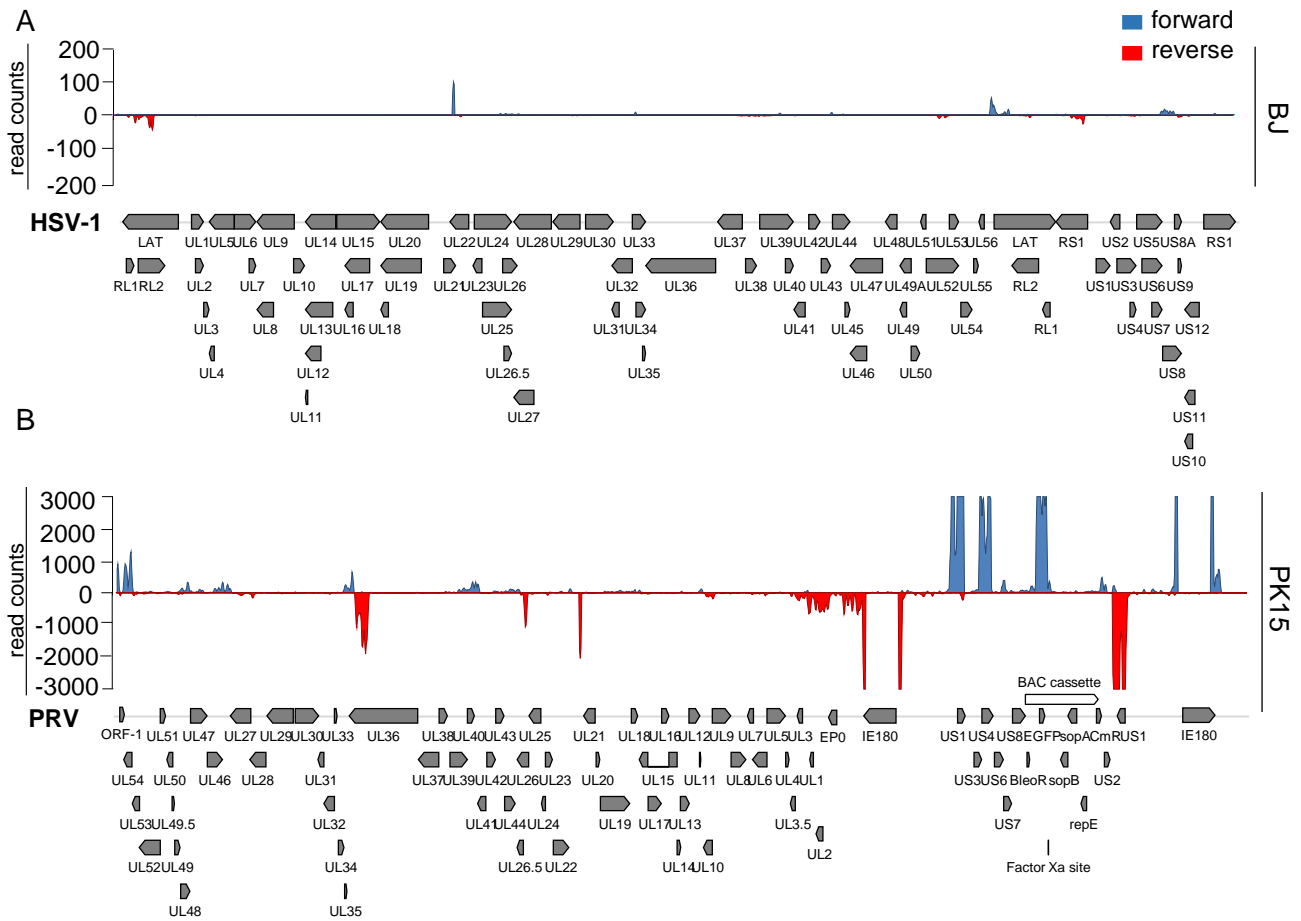
Figure 3.1: RNA-seq data of lytic-cycle-deficient HSV-1 or PRV. (A) RNA-seq analysis of BJ cells infected with HSV-1*in1374* at non-permissive temperature, 24 hpi, with MOI 10 (B) RNA-seq analysis of PK15 cells infected with PRVΔIE180, 24 hpi, with MOI 10. RNA-seq data were mapped to the respective viral genome using STAR. Reads were counted in 100 bp windows for forward (blue) and reverse (red) reads, respectively. Read counts across these windows are shown in the upper and lower panel, of the illustrated plots (Y-axis).

needed to initiate lytic replication. Another peak was detected at *UL21*, which transcribes for a tegument protein which facilitates cell-to-cell spread [418].

RNA-seq data of PRV-infected PK15 cells at 24 hpi, are shown in Fig. 3.1B. For PRVΔIE180 also only a few transcripts were detected. Some of the associated transcription levels were as high as the one coding for enhanced green fluorescent protein (EGFP), which is no part of the viral genome but only of the bacterial artificial chromosome (BAC)-cassette. Since the BAC-cassette has its own human promoter, the EGFP expression is unrelated to the viral gene expression. However, the human promoter located in the viral genome can contribute to transcription of other viral genes. The following viral genes were expressed:

- *US1*, which is an accessory regulator of viral gene expression [419, 420], responsible for the interaction with IE180 - if expressed.

- *US4*, which transcribes for glycoprotein G [421], which is also not needed for lytic replication.

- *UL36*, which is a tegument protein and important for virus envelopment, late during infection [422].

- *UL2*, which codes for the uracil-DNA glycosylase [123].

- *UL21*, which encodes a tegument protein.

- *ORF1*, whose function is still unknown [123].

To summarize, as none of these genes is capable of initiating viral lytic replication, these RNA-seq results ensure this work's investigation of repressed vDNA.

3.2 PRV∆IE180 acquires different types of heterochromatin

The PRV genome has a higher CpG content than that of KSHV. In addition, KSHV was shown to acquire repressive histone modifications via PRC. Thus, PRC-associated histone modifications were expected to be acquired by lytic-cycle-deficient PRV. To identify the epigenetic landscape of PRV∆IE180, PK15 cells were infected with the virus mutant with a MOI of 10 and ChIP experiments were performed at 24 hpi and 72 hpi (Fig. 3.2A). To investigate the presence of the different forms of heterochromatin H3K27me3, H2AK119ub and H3K9me3 were analyzed. To control for the absence of activating modifications of the viral genome H3K27ac and H3K36me2 were analyzed. Furthermore, another repressive epigenetic modification, DNA methylation, was analyzed. DNA methylation of the virus, at 72 hpi, was examined by MinION-sequencing (MinION-seq).

ChIP-seq of PRV∆IE180.   The infected cells were fixed at the corresponding time point post infection and, subsequently, ChIP was performed. A detailed explanation about the methodology can be found in Sec. 6.3.15 and Sec. 6.3.1.

ChIP-seq tracks of the respective histone modifications at 24 hpi are shown in Fig. 3.2B. The time point 24 hpi was picked to be displayed in a coverage plots, as an example for the pattern of the different histone modifications on the viral genome. However, both time points were used for quantification and statistical analysis, as shown in the box-plots in Fig. 3.2E-F. In Fig. 3.2B, the read coverage on the viral genome is shown for each modification. The higher the signal in the illustrated plot, the more vDNA was pulled down with the respective antibody. The input sample, where no antibody was added to the DNA, serves to quantify the efficiency of a pull-down relative to the initial sample quantity and is used to detect regionally different enrichment of a modification. The H3 sample is a control for the general nucleosome occupancy on the DNA and thus can be used as a reference for normalization, like the input. Hence, all signals above the levels for input and H3 can be assumed to be enrichment for the specific histone modification.

In stark contrast to KSHV, ChIP-seq of PRV-infected cells revealed that the PRV∆IE180 genomes did not acquire the PRC2-mediated facultative heterochromatin mark H3K27me3. However, it is decorated with the PRC1-mediated facultative heterochromatin mark H2AK119ub. The latter has also been found on KSHV [210]. Additionally, the presence of the ubiquitously present histone mark H3K36me2 was investigated, since this modification is actively erased by the ncPRC1.1 sub-unit KDM2B. H3K36me2 was not detected on the PRV∆IE180 genomes (Fig. 3.2B), supporting a model in which nc PRC1 recruitment via KDM2B is active on PRV∆IE180. In addition to the repressive mark H2AK119ub, the constitutive heterochromatin mark H3K9me3, which is less dy-
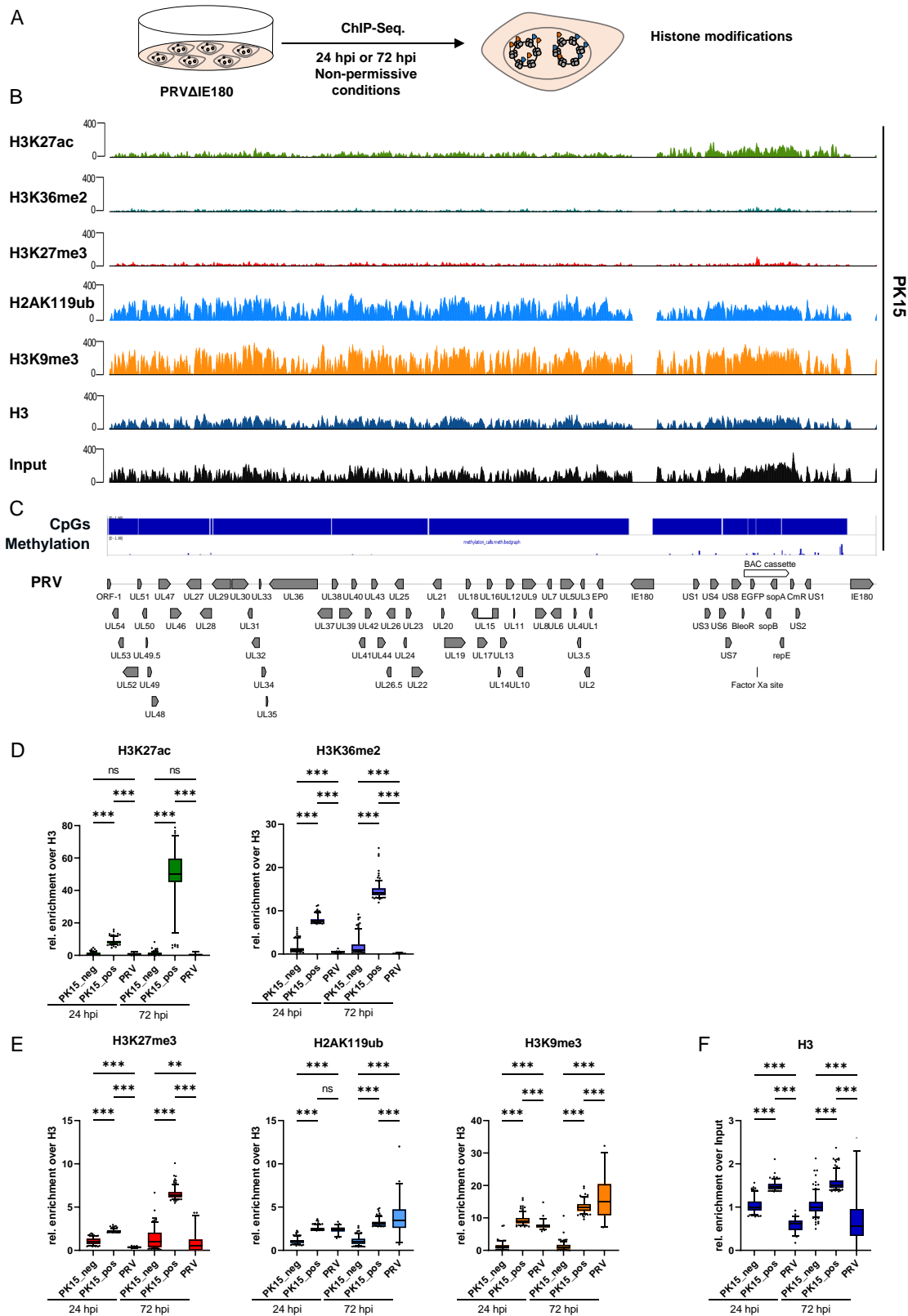
Figure 3.2: ChIP-seq analysis of PRVΔIE180 infected PK15 cells. (A) Experimental set-up to analyze histone modifications of the lytic-cycle-deficient PRV mutant. PK15 cells were infected with MOI 10 of PRVΔIE180. At two time points post infection - 24 hpi and 72 hpi - infected cells were fixed and ChIP was performed, followed by qPCR and sequencing. (B) The read coverage for H3K27ac-, H3K36me2-, H3K27me3-, H2AK119ub-, H3K9me3-, H3-pulldowns and input of PRV genomes in PK15 cells. Viral reads were mapped to the PRV genome by using Bowtie2. Depicted are total mapped read counts to the PRV genome. (C) The upper panel shows the total CpGs which could be analyzed through the obtained MinION reads, DNA methylation levels of PRVΔIE180 in the lower panel. (D - F) Box-whisker-plots with 5th – 95th percentile and median of average enrichment of the indicated antibody levels, in positive and negative regions of the cellular genome compared to the average enrichment on the PRV genome. For each antibody, 200 positive and negative regions were detected by EPIC2-peakcalling using a bin-size of 3 kbp. On the viral genome 2.5 kbp windows were used to calculate the enrichment. All the detected regions were normalized by H3 read counts and to the average of the negative control for each antibody. (F) The same was done for H3 levels, which were normalized to input. Furthermore, statistical testing was performed, using one-way ANOVA with subsequent Sidak's test. Significance levels are indicated by asterisks, which are displayed above the compared datasets, *p<0.033, **p<0.002, ***p<0.001. ChIP experiments were done in biological replicates; however, only one replicate was sequenced with the other being depicted as ChIP-qPCR in the supplement.

namic than facultative heterochromatin, was enriched across all the viral genome (Fig. 3.2B). In addition to repressive histone marks, the activating histone modification H3K27ac was analyzed, to control for the absence of an active state of the viral genome. H3K27ac was only detected in the BAC-cassette, confirming the just mentioned RNA-seq data, where PRVΔIE180 hardly transcribes any gene in this infection model.

Although the coverage data was normalized to total read counts, due to lacking enrichment patterns on the viral genome a statistical method, described previously by Günther et al. [210], was used. This method normalizes the ChIP-seq signals on the viral genomes to positive and negative control sites on the host genome for the respective modification. The box-plots in Fig. 3.2D - F show the quantified enrichment over H3 with respect to the host control regions, indicated as PK15pos and PK15neg. A more detailed explanation about the analytical methodology can be found in Sec. 6.5.

Different to most published data where histone marks are normalized to input, H3 levels were used in this study. H3 resembles a control for the general nucleosome occupancy on the DNA. In contrast to H3, the input harbors also unchromatinized DNA. Therefore, if not all of the viral genomes are chromatinized, which can be true especially early during infection, normalizing to input can lower the real enrichment levels of the respective histone modification.

Ultimately, the obtained results have been analyzed towards possible statistical significance. First the data were displayed in a box-plot and, subsequently, statistical testing was performed, using a one-way ANOVA with post-hoc Sidak's test. A more detailed explanation about the statistical methodology can be found in Sec. 6.7. The corresponding box-plots are shown in Fig. 3.2D - F, with the two time points directly compared to each other.

To analyze the general chromatinization state of the virus H3 levels on the viral genomes were caluclated. H3 levels were calculated by normalizing the specific signals to input, which is shown in Fig. 3.2F. The H3 levels on the viral genome were below 1 for both time points, indicating that not all episomes were chromatinized. This result justified the normalization to H3 instead of using the input.

For H3K9me3 and H2AK119ub, this comparison revealed that heterochromatinization remained constant over time, since both modifications were significantly enriched over the host negative control (Fig. 3.2 E). Furthermore, virus associated signals for H3K27ac, H3K36me2 and H3K27me3 entirely represent background, as judged by the respective negative controls (Fig. 3.2D and E).

The presented results in Fig. 3.2 represent one replicate. However, a second replicate was performed as ChIP-qPCR which, together with ChIP-qPCR data from the first replicate, can be found in the supplementary data (Fig. S1A - E). Performing a qPCR with the ChIP-samples is a good way to analyze the success of the experiment and to gain a first impression of whether the investigated modifications were present on the genome. However, unlike ChIP-seq data, which show information for the whole genome, ChIP-qPCR data only harbor information about some, selected, loci.

Both ChIP-qPCR experiment showed similar results (Fig. S1A - E) and these results were similar to the ChIP-seq data. Therefore, the qPCR of the second replicate can be considered as

independent verification of the data.

ChIP-seq of replication competent PRV.   In order to investigate the early onset of histone marks in a infection model with a replication-competent PRV, PK15 cells were infected with PRVwt with an MOI of 10. Cells were fixed at 3 hpi and subsequently ChIP-seq was performed. The obtained data were quantified and statistically analyzed, as described above, except for the normalization which was performed using input.
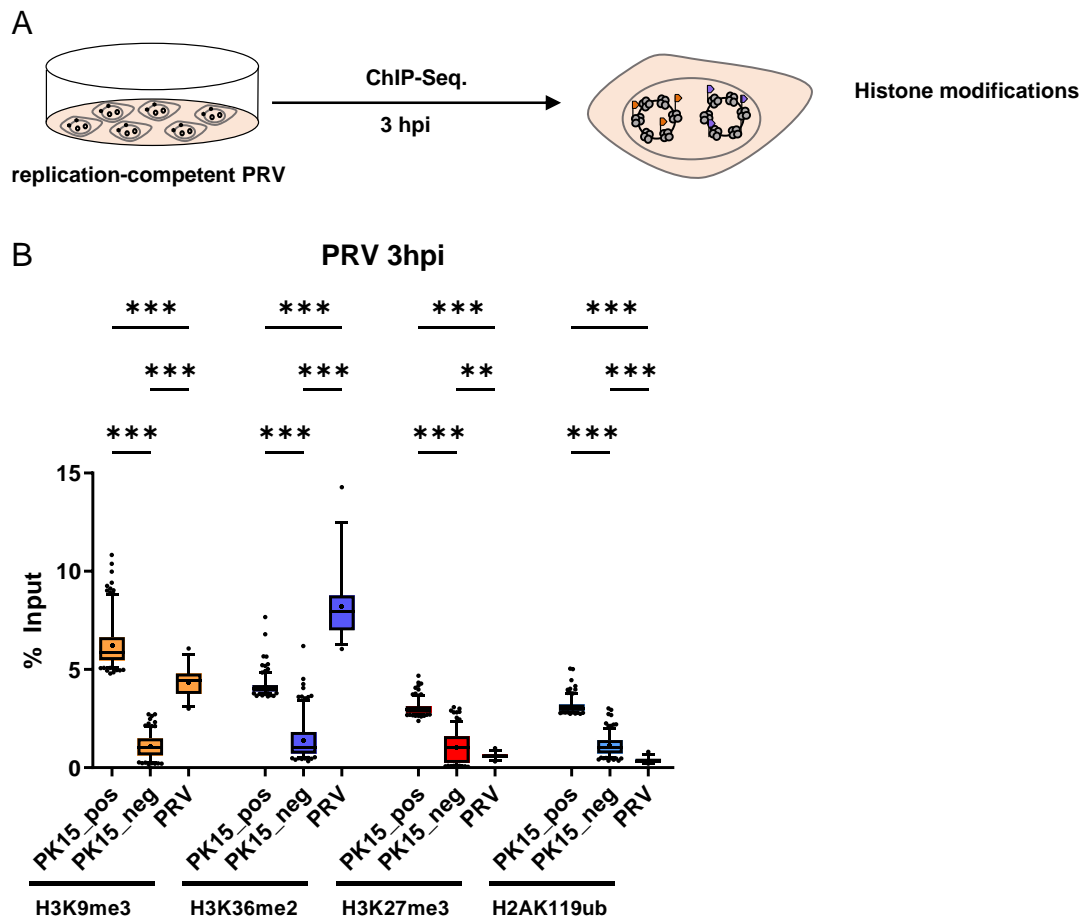
Figure 3.3: ChIP-seq analysis of PRV infected PK15 cells. (A) Experimental set-up to analyze histone modifications of the replication-competent PRV. PK15 cells were infected with MOI 10 of PRV. At 3 hpi infected cells were fixed and ChIP was performed, followed by sequencing. (B) Box-whisker-plots with 5th – 95th percentile and median of average enrichment of the indicated antibody levels, in positive and negative regions of the cellular genome compared to the average enrichment on the PRV genome. For each antibody, 200 positive and negative regions were detected by EPIC2-peakcalling, using a bin-size of 3 kbp. On the viral genome 2.5 kbp windows were used to calculate the enrichment. All the detected regions were normalized to input read counts and to the average of the negative control for each antibody. Furthermore, statistical testing was performed, using one-way ANOVA with subsequent Sidak's test. Significance levels are indicated by asterisks, which are displayed above the compared datasets, $*p<0.033$, $**p<0.002$, $***p<0.001$.

As shown in the box-plot of Fig. 3.3B, at 3 hpi, no H2AK119ub was acquired on the replication competent PRV. In addition, H3K27me3 levels on the viral genome were below the cellular negative control. However, H3K36me2 levels were significantly enriched over the negative control, on the viral genomes. The presence of this modification together with the absence of the two facultative heterochromatin marks argues for the absence of PRCs, on the viral genomes, at this time point. Since in this infection model the virus will start to replicate from approximately 4 hpi on, the absence of the repressive modifications was expected. However, another repressive histone

modification, H3K9me3, was detected on the viral genomes. This finding was unforeseen, since lytic replication was about to start shortly after the time point of fixation.

Taken together, the ChIP data revealed that lytic-cycle-deficient PRV genomes are able to acquire two different repressive histone modifications, i.e. H2AK119ub and H3K9me3. Furthermore, PRVwt did not acquire facultative heterochromatin marks, however, low levels of the constitutive heterochromatin mark, H3K9me3, could be detected.

DNA methylation has been shown to play an important role to distinguish cellular from foreign DNA [423]. DNA methylation was shown to be present on the viral genomes of EBV [424] and KSHV [93] in long-term-infected cells. However, it has previously been shown for KSHV that DNA methylation does not play a role in latency establishment [93]. Since DNA methylation is usually incompatible with ncPRC1 recruitment but not with constitutive heterochromatin [425–427], the methylation state of PRVΔIE180 was investigated. Since the above mentioned data demonstrated the presence of H3K9me3 on PRVΔIE180 genomes already 24 hpi, it was assumed to find this modification earlier on PRV than on KSHV. H3K9me3 was shown to correlate with DNA methylation. H3K9me3 was only found on KSHV in cancer cells harboring the virus and been infected for decades [94]. Hence, the DNA methylation state of PRVΔIE180-DNA was analyzed next.

DNA methylation of PRVΔIE180.   To investigate DNA methylation for PRV, the time point 72 hpi was chosen (Fig. 3.2C). At this time point high molecular genomic DNA was isolated from infected cells, to perform MinION-seq. The upper panel of Fig. 3.2C shows the total CpGs which could be analyzed through the obtained MinION reads. Almost the entire episome could be analyzed. However, virtually no DNA methylation was detectable, which is illustrated in the lower panel of Fig. 3.2C. Therefore, similar to KSHV-DNA methylation is very unlikely to play a role during early episome silencing and latency establishment.

In conclusion, two distinct constitutive heterochromatin modifications were detected on the lytic-cycle-deficent PRV genomes, however no methylation of the vDNA was observed. Since H3K9me3 and H2AK119ub establish two different forms of heterochromatin and are also not described to be found at identical regions of the cellular genome, it is highly unlikely that both histone marks are acquired on the same viral episome.

Together with the findings from the replication competent PRV the observed results hint towards a hypothesis where some alphaherpesvirus genomes acquire the tight repressive histone mark H3K9me3 even during a potential lytic infection and ultimately this subpopulation will not be able to replicate. Whereas the rest of the genomes acquires activating histone marks, like H3K36me2, during a lytic infection, which ultimately leads to progeny production. During a quiescent or latent infection the genomes that will not acquire H3K9me3 might be repressed through H2AK119ub.

To investigate whether there are two subpopulations of viral episomes, a tool was needed which could analyze single episomes, since ChIP data only display bulk information. A good method to study spatiotemporal dynamics of single episomes, interacting with different host factors, would

be an imaging system for vDNA.

3.3 Visualization of individual PRV episomes

To investigate whether there are two subpopulations of viral episomes, a visualization system for vDNA had to be established. Preferably, this should be a live-cell imaging system, as this has the advantage of tracking viral particles during infection. For KSHV-DNA, a live-cell imaging system has already been successfully established in the laboratory (T. Günther, unpublished). This system uses a clustered regularly interspaced short palindromic repeats (CRISPR)/Cas-based method. This requires a single guide RNA (sgRNA) against the viral genome. The technique for KSHV makes use of the viral TRs as targets for the sgRNA to allow amplification of the signal above the background. In the KSHV genome, the TRs are 801 bps long and there are 40 copies of each. Thus, enrichment of sgRNAs on the genome is possible. In contrast, the TRs in PRV are much shorter, so it was not certain whether there is sufficient spatial expansion for the system to work. Therefore, in parallel to the CRISPR/Cas based live-cell imaging technique, another live-cell imaging technique has been attempted to be established, as well as an alternative visualization system for vDNA, whereby the cells must be fixed. These three methods and the results obtained are described below.

A live-cell imaging approach to visualize PRV episomes via a CRISPR/Cas based technique. A system which enabled single episome visualization for KSHV was already established in the lab for, making use of a CRISPR/Cas9 based technique, which was published by Tanenbaum et al. [428]. This system uses a repetitive peptide array which the authors termed "SunTag". This peptide array is fused to a catalytically inactive Cas9 (dCas9) protein and recruits multiple copies of any protein that is fused to the respective antibody fragment.

For KSHV, a sgRNA, which binds to the TRs of the KSHV genome, was successfully used to recruit a dCas9. Furthermore, green fluorescent protein (GFP) fused to the respective antibody fragment, which could bind to the peptide array enabled the fluorescently labeling of incoming KSHV genomes (T. Günther, unpublished).

In an approach to establish this system for PRV, different sgRNAs against repetitive regions on the vDNA were used. Specifically, PK15 cells were stably transduced with the respective sgRNAs expression construct as well as the dCas9-"SunTag" and the scFv-GCN4-GFP expression constructs. Single cell clones were then screened by using a PRVwt infection to detect GFP-labeled RC, thereby verifying the successful labeling of vDNA. Subsequently, cell clones with the brightest signal for RCs were used for infection experiments and live-cell microscopy during the early phase of infection. To verify this method, a replication-competent PRV harboring an mCherry-tagged capsid was used. The capsid-tag allowed to track the virus particles early in infection. After several repetitions of the experiment, only replicating vDNA could be visualized by this approach. Shown as an example in Fig. 3.4A are infected cells at 1 hpi and at 15 hpi. At the later time point accumulation of the GFP signal was detected, in the form of a typically shaped alphaherpesvirus

acpRC [429, 430], filling almost the whole nucleus. However, no single incoming viral genomes could be detected, as shown for the early infection time point (Fig. 3.4A). One reason for the failure of this technique with single PRV genomes could be the small and few repetitive elements in the viral genome compared to KSHV. Therefore, not enough dCas9-"SunTag" was attached to the PRV genome to achieve sufficiently high signal amplification of the fluorophore relative to background fluorescence. Thus, this approach could be used for imaging in living cells to visualize replicating vDNA. However, for visualization of individual viral genomes, this approach requires structures similar to the TRs of KSHV to achieve sufficient signal amplification.

A live-cell imaging approach to visualize PRV episomes via the "ANCHOR" technology. Alternatively to the live-cell imaging approach described above, the recently published "ANCHOR" technology was employed to visualize viral genomes in living cells. The principle of the so-called "ANCHOR" technology, was adapted from a system found in bacteria, as part of the ParABS chromosome segregation machinery [431]. In its adapted form, the "ANCHOR" technology uses the 1 kbp large, highly repetitive, ANCH-sequence, to polymerize the OR-protein on it [432]. The ANCHOR technology has already been successfully used for other viruses, like HCMV, Adenovirus and human immunodeficiency virus (HIV) [433–435]. To visualize the process of the OR accumulation on the ANCH-sequence, the OR-protein was tagged with mCherry and stably transduced in PK15 cells. Additionally, the ANCH-sequence was incorporated into the vDNA by homologous recombination (a more detailed explanation of the methodology can be found in 6.6.3.2). As shown in Fig. 3.4B, at 1 hpi, only the capsid signal was visible but no ANCHOR-signal. Initially, this observation was attributed to the high background signal of the OR-mCherry construct. Thus, different sorting approaches with additional single-cell screening were used to reduce the high background signal. However, similar to the SunTag approach, again only replicating vDNA could be visualized late during infection, which is shown in Fig. 3.4.

A fixed-cell imaging approach to visualize PRV episomes via bioorthogonal labeling. With the primary objective to use the imaging system to investigate colocalization events between vDNA and host factors, another imaging approach was used, based on bioorthogonal labeling of vDNA. However, as this approach required cells to be fixed, it was no longer possible to follow a single virus genome during the course of an infection. In order to retain the possibility of investigating colocalization events between single episomes and host factors in a temporal manner, cells were fixed at different time points during the infection.

The bioorthogonal labeling method is based on the incorporation of a nucleotide analogue, here 5-ethynyl-2'-deoxycytidine (EdC), into replicating DNA, followed by addition of a fluorescently tagged azide-group, which covalently binds to the nucleotide analogue, via the so called click-chemistry. In this case, virus was produced in the presence of EdC and then harvested and concentrated to remove any of the residual EdC. A more detailed explanation of the method can be found in Sec. 6.6.2.

This method was used to incorporate EdC into either PRVΔIE180 or replication-competent PRV an GFP-tagged capsid. The underlying method was adapted from published data of HSV-1 [436]

and verified through colocalization between the capsid of the GFP-taged virus and the EdC-signal of the viral genome. As shown in Fig. 3.4C, replicating vDNA could be visualized during stock production with EdC, at 15 hpi. At this time point post infection GFP-signal accumulation in the form of a RC were observed. In addition, capsid and single genome dots were found in close proximity to each other, already 2 hpi (Fig. 3.4C).

After verification of the bioorthogonal labeling strategy, this method was further used for host-factor colocalization experiments.

Taken together, these results indicate that it was not possible to establish a live cell imaging approach for single viral episomes of PRV. This may be due to insufficient signal amplification over the background for a single viral episome. However, the successfully established bioorthogonal labeling approach of vDNA with fixed cells allowed further investigation of colocalization between host factors and PRV episomes.
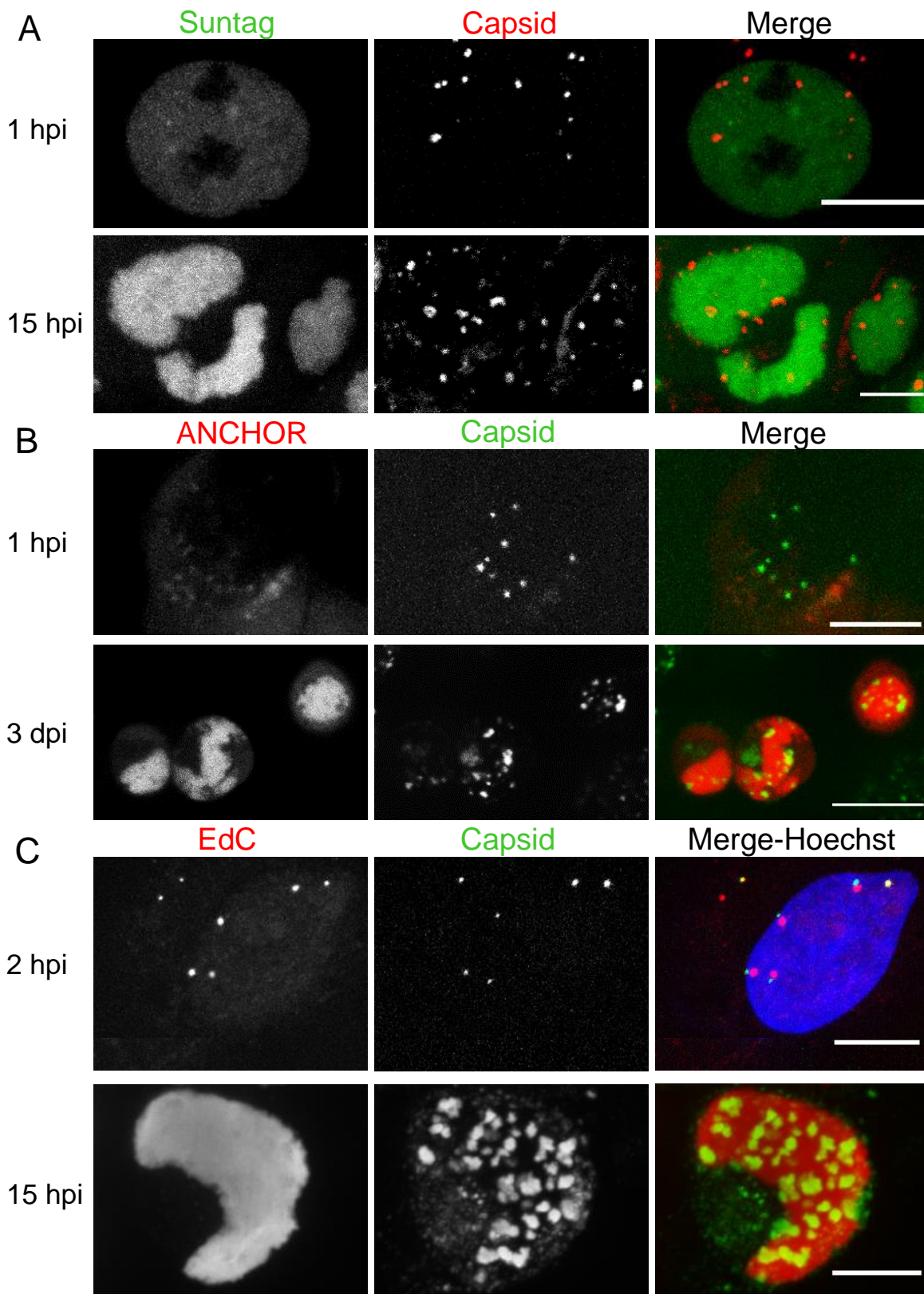
Figure 3.4: Different imaging approaches to visualize incoming vDNA into the nucleus. (A) The SunTag-System was applied to PRV by using a sgRNA against the virus and GFP as a fluorophor. To follow the infection, a PRV-mutant with a tagged capsid to mCherry was used. Imaging was done with a confocal fluorescence microscope with an incubation chamber from 1 hpi to 15 hpi. Only at late time points post infection, when replication was far advanced, replication compartments could be visualized by the SunTag-System. (B) The ANCHOR-technology was applied to PRV by using the OR protein tagged to mCherry and the ANCH-sequence incorporated into a PRV mutant with a tagged capsid to GFP. Imaging was done as explained above at different time points post infection. Visualization of vDNA was only possible after accumulation of DNA during replication, shown here at 3 dpi. (C) A Bioorthogonal labeling method was applied to PRV by using EdC as a nucleotide analogue during virus production. Using this method incoming genomes could be successfully visualized. The EdC signal was found in close proximity to the GFP-tagged capsid signal of PRV. As a control for incorporation during virus production with EdC, PRV producing cells were fed with EdC, fixed and stained 15 hpi. The EdC signal was highly enriched in the form of a RC. Images were done using a confocal fluorescence microscope. In all images representative areas for each cell type are shown as maximum intensity projections. Scale bars indicate 10 µm.

3.4 PRV episomes colocalize with host factors of two different repressive pathways

Colocalization events between lytic-cycle-deficient PRV∆IE180 with host factors were studied by applying the just described biorthogonal labeling together with different visualization techniques for the respective host proteins. The host factors of interest were either visualized by immunofluorescence (IF) or by cloning a fluorescent-tag on the respective host protein (Fig. 3.5A).

A fraction of PRV genomes colocalize with PML. Since for HSV-1 it is already known that vDNA colocalizes to PML-NBs [169–172] and this was recently also shown for PRVwt early in infection [411], a potential interaction between PML and PRV∆IE180 DNA was investigated. In order to do so, a PML-GFP construct was stably transduced into PK15 cells and GFP-positive cells were sorted prior to infection. The fluorescent tag was used because no commercial antibody against PML in porcine cells was available. Although the human and porcine PML proteins and their isoforms are very similar, the antibody against PML could not be detected in PK15 cells in our laboratory.

At different time points post infection, cells were fixed and, subsequently, biorthogonal labeling was performed. For the labeling of vDNA the Alexa Fluor 555 picolyl azide (ThermoFisher) was used, which was covalently bound to EdC. Additionally, the cells were stained with the DNA intercalating dye Hoechst33342, in order to identify the nucleus. The imaging process was conducted with a confocal laser-scanning microscope within the nucleus of infected PK15 cells (a more detailed description of the method can be found in Sec. 6.6.2)

Fig. 3.5B shows representative cells of this imaging at the indicated time point post infection, as maximum-intensity-projections. At 3 hpi, first colocalization events between PRV∆IE180-DNA and PML were visible, indicated by the white arrows in the respective merge-image (Fig. 3.5B). At later time points, ring-like structures, consisting of PML could be observed. These structures were found to enclose some of the viral particles (Fig. 3.5B, zoom). The colocalization events between the vDNA and PML were calculated in two independent experiments and are shown as bar-plots with the corresponding standard deviation (SD) (Fig. 3.5B). For the time point of 3 hpi, the SD between the experiments is not displayed, since it was less than one. The overall colocalization events increased over time, starting at about 11 % at 3 hpi, followed by 36 % at 6 hpi, to about 60 % at 24 hpi.

In conclusion, it could be shown that at 24 hpi colocalization levels between PML and PRV∆IE180 reached 60 %. The histone modification H3K9me3 is believed to occur upon PML-NBs-mediated silencing, as shown for telomers, since PML-NBs can harbor the H3K9-methyltransferase SETDB1. Thus, it is likely that the viral genomes colocalizing with PML-NBs acquire H3K9me3.

In addition to H3K9me3, the repressive histone mark H2AK119ub was found on the PRV∆IE180 genome 24 hpi (Sec. 3.2). In order to establish H2AK119ub, PRC1 has to associate with the viral genome. Since KDM2B - a subunit of the ncPRC1.1 complex - was already shown to associate with unmethylated CpG islands [437] and was recently found to be associated with KSHV genomes

[210], this protein was used for further colocalization studies.

A fraction of PRV genomes colocalize with KDM2B. After fixing the PRVΔIE180-infected cells, at 3 hpi and 6 hpi, labeling of the vDNA was performed and KDM2B was antibody-stained. Fig. 3.5C shows colocalization events between the PRVΔIE180-episomes and KDM2B. The sites of colocalization are indicated by the white arrows in the respective merge-image. The colocalization events between vDNA and KDM2B were quantified at two different time points post infection and the results are shown as bar-plot in Fig. 3.5C. Similar to PML, colocalization events between vDNA and the host protein increased over time. At 3 hpi about 10 % of the genomes colocalized with KDM2B, at 6 hpi 28 % of genomes colocalized with the host protein (Fig. 3.5C).

Taken together, the two host proteins PML and KDM2B were found to colocalize with PRV genomes. These host factors are associated with two different silencing complexes in the host cell. Furthermore, the two modifications have not been described to occur together on the same nucleosome. Therefore, these results support a model in which different cellular pathways and repressive complexes can act upon PRV genomes by yet unknown recruitment mechanisms. One pathway is by repression through PML and the other by repression through PRC1.

To examine whether this might be true not only for the porcine virus PRV but also for a human pathogenic virus a similar set of analyses was performed by using a lytic-cycle-deficient HSV-1 mutant. Moreover, since PK15 cells originate from pigs they are limited in terms of commercially available antibodies as well as siRNAs against different host proteins, which would enable further investigation of the host proteins. Therefore, by using a human alphaherpesvirus, human cell lines could be infected and subsequent experiments, including knock-down and knock-out studies of specific host factors were facilitated.
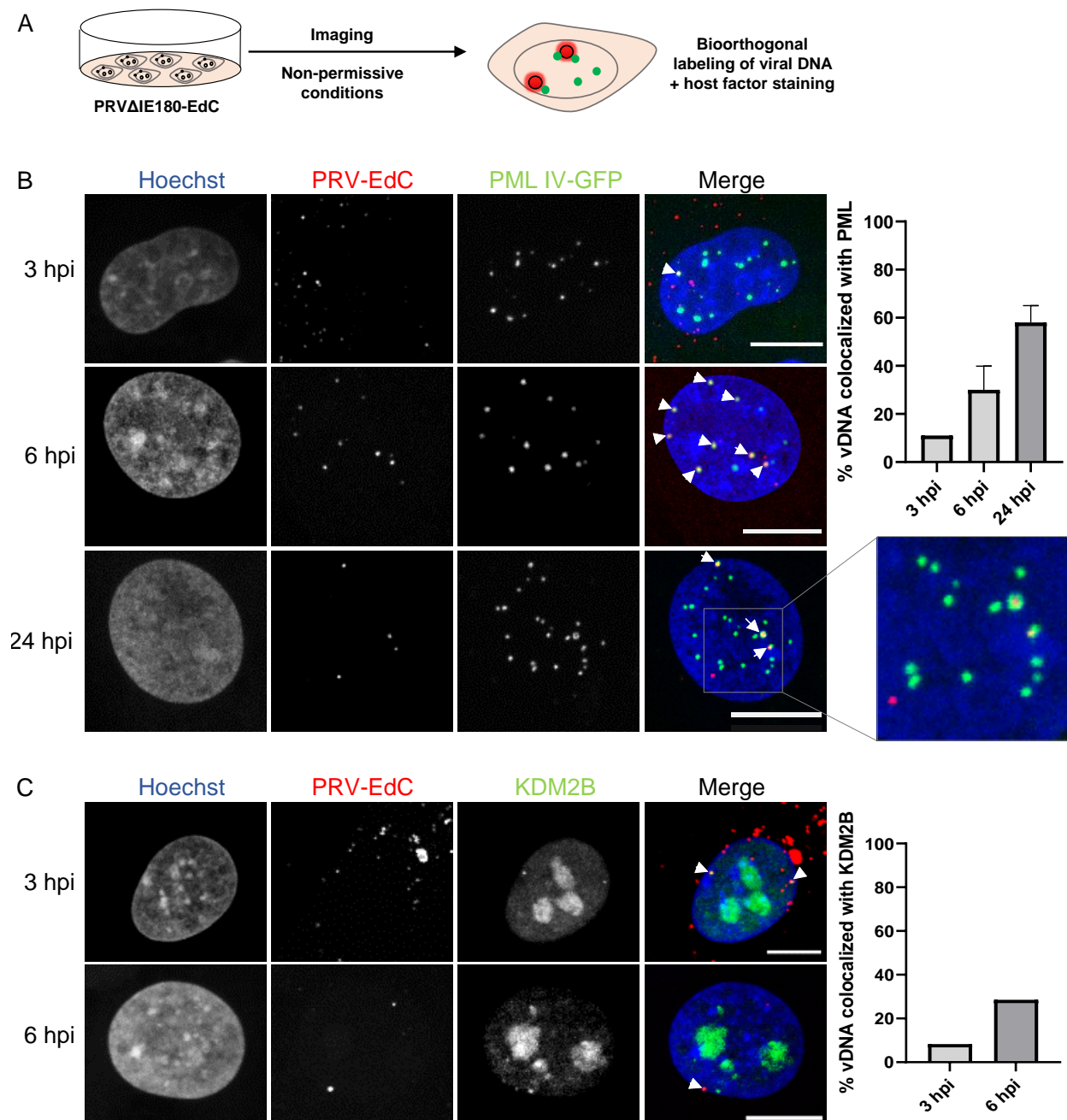
Figure 3.5: PRV colocalization with host factors. (A) Experimental set-up of the colocalization analysis between bioorthogonally labeled PRVΔIE180-EdC and fluorescently labeled host factors. PRVΔIE180-EdC was covalently linked to the Alexa Fluor 555 picolyl azide via the click-chemistry. At different time points post infection cells were fixed, stained and imaged. (B) Colocalization events between the vDNA and stably expressed PML IV-GFP in PK15 cells were imaged and a representative picture of each time point is shown as maximum-intensity-projection. Furthermore, colocalization events were calculated in two independent experiments and shown here as bar-plots with SD. For each experiment and time point between 26 and 50 cells were analyzed, with total genome numbers between 80 and 168. (C) Colocalization events between the vDNA and antibody-stained KDM2B, using a secondary Alexa Fluor 488 antibody in PK15 cells were imaged and a representative picture of each time point is shown as maximum-intensity-projection. Additionally, colocalization events between the vDNA and KDM2B were calculated in one experiment and shown here as bar-plots. For each time point between 31 and 58 cells were analyzed, with total genome numbers between 119 and 156. White arrows indicate colocalization events in the merged images. Hoechst33342 was added for nucleus staining. Scale bars indicate 10 μm.

3.5 Heterochromatinization of HSV-1*in1374* is cell dependent

HSV-1 is a human alphaherpesviurs and very closely related to PRV. For HSV-1 first available data indicates that the viral genome is decorated with H3K9me3 when human fibroblasts were infected

with an HSV-1 ICP0-null mutant [135]. However, in latently infected neurons, which resembles the natural reservoir of HSV-1, repression seems to be established by PRC2, since H3K27me3 was found on these genomes [95, 134]. Thus, different states of repressive heterochromatin can be acquired by HSV-1, depending e.g. on the cellular context.

For the experiments with HSV-1, the lytic-cycle-deficient HSV-1*in1374* was used. As described in the beginning of this chapter (Sec. 3), this virus mutant is characterized by loss of function mutations in the genes coding for the viral proteins VP16 and ICP0. Furthermore, it contains a temperature sensitive mutant of ICP4, with a replication inducing permissive temperature of 32 °C and a non-permissive temperature of 38.5 °C [416, 417]. The non-permissive condition was used to investigate the epigenetic profile of the quiescent and therefore a latency-like state of the HSV-1*in1374* genomes.

Although HSV-1*in1374* should be able to replicate at permissive conditions, not all cell types allowed virus production. In human dermal fibroblasts (HDF), for example, it was not possible to induce viral replication under the permissive temperature. This lack of virus production can most likely be attributed to the non-functional ICP0 in HSV-1*in1374*, which is not essential for virus replication but its mere absence has been shown to decrease viral yields [178]. To overcome this, U2OS cells were used for virus production of HSV-1*in1374*, since these cells were already known to support viral replication of HSV-1 ICP0-null mutants [178].

Considering the here observed, cell dependent, discrepancies in the virus' ability to replicate, differences in chromatinization of HSV-1*in1374* were suspected to be found when infecting the two cell lines U2OS and HDF. Therefore, chromatin states of HSV-1*in1374* were investigated in HDF as well as in U2OS cells, under non-permissive conditions (Fig. 3.6A).

ChIP-seq of HSV-1.   HDF and U2OS cells were infected with HSV-1*in1374* at MOI 10. Subsequently, ChIP was performed at 24 hpi (Fig. 3.6A). A detailed explanation about the methodology can be found in Sec. 6.3.15.

ChIP-seq tracks of the respective histone modifications at 24 hpi are shown in the coverage plots in Fig. 3.6B, in the indicated cell line. The viral reads for each modification were mapped to the HSV-1 genome, with input and H3 representing background controls, as described for the PRV data in Sec. 3.2.

Similar to PRV, in U2OS cells both diverging repressive histone marks were found on HSV-1*in1374* genomes. H2AK119ub was more abundant on the viral genome than H3K9me3 (Fig. 3.6C). Contrary to U2OS cells, in HDF cells only H3K9me3 was highly abundant, while PRC1-mediated ubiquitination of H2A was not detectable (Fig. 3.6B). Similar to PRV, H3K27me3 was not detected on HSV-1 genomes, which is shown for HDF cells in Fig. 3.6B and for U2OS cells in the supplementary Fig. S2.

As described above for PRV (Sec. 3.2), the enrichment of the respective histone modification on the viral genomes was calculated relative to the respective positive and negative regions for the modification on the host genome. The results of this comparison and the corresponding statistical analysis are shown in the box-plots in Fig. 3.6D and E.
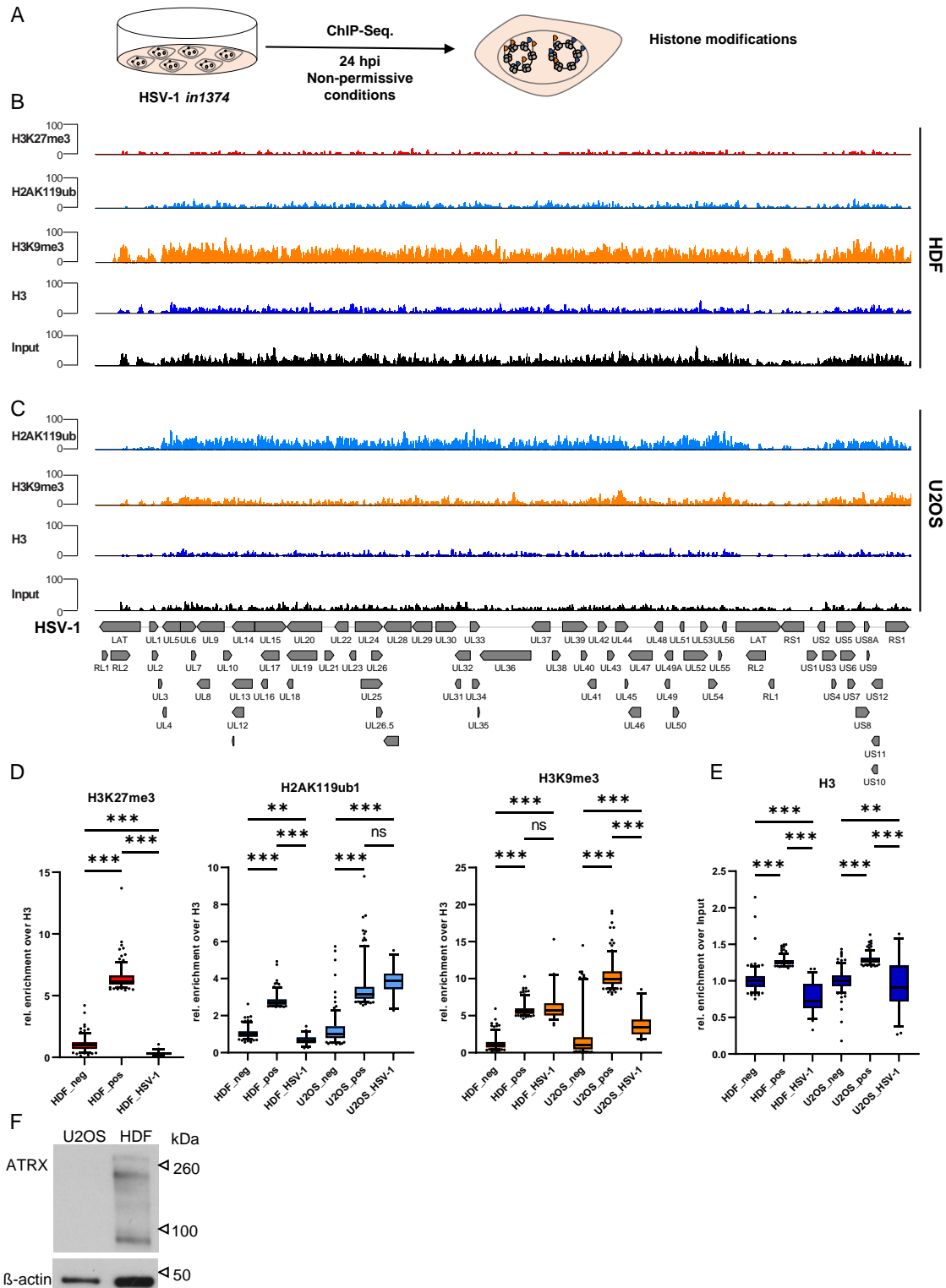
Figure 3.6: ChIP-seq analysis of HSV-1*in1374* infected HDF and U2OS cells. (A) Experimental set-up to analyze histone modifications of HSV-1*in1374*. HDF or U2OS cells were infected with MOI 10 of HSV-1*in1374*. At 24 hpi, infected cells were fixed and ChIP was performed. (B - C) Coverage plots are shown for H3K27me3, H2AK119ub, H3K9me3, H3 and input of HSV-1 genomes in HDF and U2OS cells, respectively. Viral reads were mapped to the HSV-1 genome, using Bowtie2. Depicted are total mapped read counts to the HSV-1 genome. (D - E) Box-whisker-plots with 5th – 95th percentile and median of average enrichment of the indicated antibody levels in positive and negative regions of the cellular genome, compared to the average enrichment on the HSV-1 genome. For each antibody, 200 positive and negative regions were detected by EPIC2-peakcalling, using 3kbp windows. On the viral genome, 2.5 kbp windows were used to calculate the enrichment. All the detected regions were normalized to H3 read counts and to the average of the negative control for each antibody. (E) The same quantification as in D was done for H3 levels, normalized to input. Furthermore, statistical testing was performed, using one-way ANOVA with subsequent Sidak's test. Significance levels are indicated by asterisks, which are displayed above the compared datasets, *p<0.033, **p<0.002, ***p<0.001. ChIP experiments were done in biological replicates; however, only one replicate was sequenced with the other being depicted as ChIP-qPCR in the supplement. (F) Immunoplot against ATRX and β-actin, of whole cell lysates of U2OS and HDF cells, respectively.

The quantification of the sequencing data revealed that H3K9me3 was highly enriched on the viral genome in HDFs, however, neither H2AK119ub nor H3K27me3 was detectable(Fig. 3.6D). In contrast to HDFs, H2AK119ub was highly enriched in U2OS cells (Fig. 3.6D). In addition, H3K9me3 was significantly enriched on HSV-1*in1374* in U2OS cells.

In summary, similar to lytic-cycle-deficient PRV, lytic-cycle-deficient HSV-1 was found to acquire constitutive as well as facultative heterochromatin. Furthermore, the respective levels are most likely dependent on the cellular context.

As for PRV, a second replicate of this experiment was performed, to confirm the above findings on the level of ChIP-qPCR and can be found together with the ChIP-qPCR data from the first replicate in the supplementary data (Fig. S2).

The ChIP-qPCR results were similar and consistent with ChIP-seq data with one exception. In the qPCR-data for HDFs the signal for H2AK119ub was higher than the respective negative control. This finding suggests that H2AK119ub would be present on the viral genome. However, H2AK119ub was not detected on the HSV-1 genome after sequencing. When comparing the signal for H2AK119ub to the positive control for H2AK119ub it is lower. Thus, for this modification it seems that the positive controls are more important to compare the enrichment. One possible explanation of the discrepancy, between the ChIP-seq and ChIP-qPCR result could be the fact that H2AK119ub is a highly dynamic and ubiquitously found mark on the cellular genome. Thus, when only using ChIP-qPCR as a analysis tool more human positive and negative controls should be used.

In the second replicate also H3K36me2 and H3K27ac were analyzed, similar to the sequenced replicate for PRV. Since both modifications were not detectable on the viral genome neither of the samples was sequenced.

In conclusion, different states of chromatin were acquired by lytic-cycle-deficient HSV-1 U2OS cells and HDFs. In U2OS cells two distinct heterochromatin marks were detected on the viral genomes; one a hallmark for constitutive heterochromatin and the other representing facultative heterochromatin. In contrast to this, in HDF cells only constitutive heterochromatin was observed on the viral genomes.

An important difference between both cell lines is the lack of the chromatin remodeler ATRX in U2OS cells, which is shown in the immunoblot against ATRX in Fig. 3.6F. In the U2OS cell lysate no ATRX was detected, while HDFs showed the specific band at 280 kDa. In addition, two more bands were detected in the HDF lysate, which can be assigned to the different isoforms of the protein.

Since ATRX together with DAXX acts as a H3.3 chaperone, this protein is important for *de novo* histone incorporation. Thus, total H3 levels were also examined on the viral genome. As shown in Fig. 3.6E, H3 levels were relatively similar. Therefore, although the chromatin remodeler ATRX is missing in U2OS cells, *de novo* acquisition of histones worked efficiently.

Considering U2OS cells being a tumor cell line, using the alternative lengthening of telomers (ALT) pathway to achieve unlimited proliferation, these cells might have acquired a mechanism

to overcome the absence of ATRX. This could be because another H3.3 chaperone, HIRA, is mediating the H3.3 incorporation in this case. To investigate the role of ATRX further, a knock-out and knock-down of this factor were established, in cells that regularly express ATRX.

3.6 Knock-out of ATRX affects chromatinization of HSV-1*in1374*

In order to investigate whether the mere absence of ATRX has an effect on chromatinization in general and the acquisition of a distinct form of heterochromatin specifically, an ATRX knock-out cell line was established.

The production of knock-out cell lines is often difficult. However, in haploid cell lines, such as near-haploid adherent fibroblast-like 1 (HAP1) cells, it has been shown that knock-outs can be generated more efficiently than in diploid cells such as HDFs. Thus, HAP1 cells, a near haploid cell line that is originated from a chronic myeloid leukemia (CML) derived (KBM-7) cell line, was used to generate a ATRX knock-out cell line. The knock-out has been accomplished through a CRISPR/Cas approach and the absence of the gene has been confirmed by polymerase chain reaction (PCR)-screening of several cell clones. A more detailed description of the methdology can be found in Sec. 6.2.8. Additionally, the absence of ATRX was detected by immunoblotting of a whole cell lysate of HAP1ΔATRX cells. As a control, a HAP1wt whole cell lysate was used (Fig. 3.7F). HAP1 cells showed only a faint band at about 280 kDa, however, a intense band at 100 kDa was detectable. Furthermore, three other faint bands were detected in between, which could be isoforms of ATRX. In contrast, the cell lysate of HAP1ΔATRX cells did not show any band, which confirmed the knock-out. When compared to the immunoblot before with HDFs and U2OS cells (Fig. 3.6F), two specific bands for ATRX were detected here (at 100 kDa and at 280 kDa), since another antibody was used here. Another antibody was used because the first one was limited in availability.

To identify the epigenome of the lytic-cycle-deficient HSV-1 mutant in this cell line, HAP1wt and HAP1ΔATRX cells were infected with HSV-1*in1374*, with an MOI of 10, for 24 hours (Fig. 3.7A). The subsequent ChIP experiments were performed as described above and in more detail in Sec. 6.3.15.

The coverage plots of each investigated histone modification were recorded for each respective cell line and are shown in Fig. 3.7B. Furthermore, these results have been analyzed statistically - as has been described for the ChIP-seq experiments above.

ChIP-seq of HSV-1*in1374* in HAP1 cells. This experiment revealed that only H3K9me3, and no PRC-mediated H2AK119ub, was acquired by the HSV-1*in1374* in HAP1wt cells. In contrast, on HSV-1*in1374* no histone modifications could be detected in HAP1ΔATRX cells (Fig. 3.7 A and B). Moreover, H3 was hardly detectable on the viral genomes in the absence of ATRX (Fig. 3.7E).

In contrast to the ChIP experiments before, the quantification of the obtained sequencing-data was
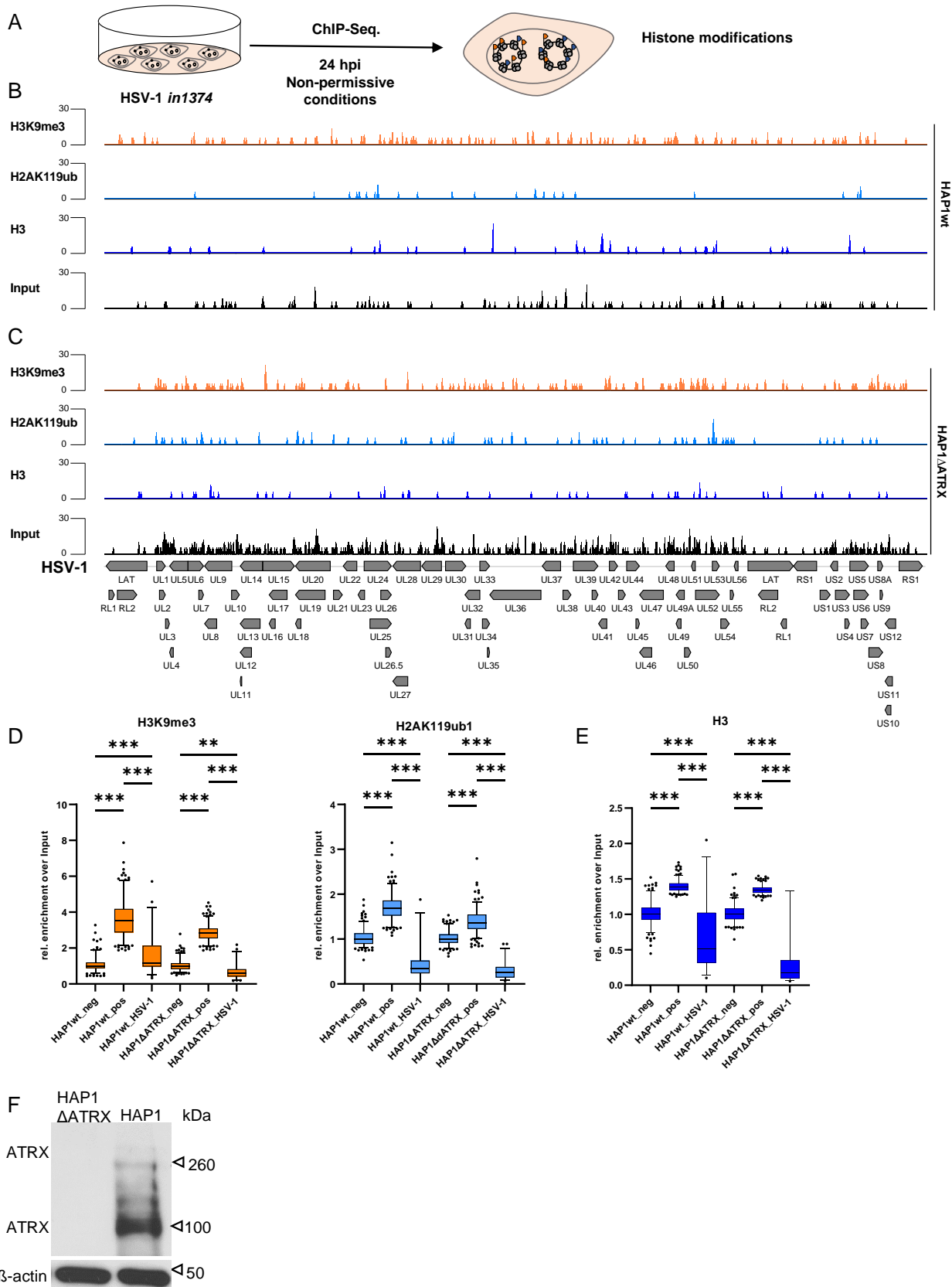
Figure 3.7: ChIP-seq analysis of HSV-1*in1374* epigenomes in HAP1wt and HAP1ΔATRX cells. (A) Experimental set-up to analyze histone modifications of the replication deficient HSV-1 mutant. HAP1wt and HAP1ΔATRX cells were infected with MOI 10 of HSV-1*in1374*, respectively. At 24 hpi, infected cells were fixed and ChIP was performed. Subsequently, qPCR and sequencing was performed. (B - C) Shown here are coverage plots of the viral epigenome in HAP1wt and HAP1ΔATRX cells. Viral reads were mapped to the HSV-1 genome by using Bowtie2. Depicted are total mapped read counts to the HSV-1 genome. (D -E) Box-whisker-plots with 5th – 95th percentile and median of average enrichment of the indicated antibody levels in positive and negative regions of the cellular genome, compared to the average enrichment on the HSV-1 genome. For each antibody, 200 positive and negative regions were detected by EPIC2-peakcalling, using 3kbp windows. On the viral genome 2.5 kbp windows were used to calculate the enrichment. All the detected regions were normalized to input read counts and to the average of the negative control for each antibody. Furthermore, statistical testing was performed, using one-way ANOVA with subsequent Sidak's test. Significance levels are indicated by asterisks, which are displayed above the compared datasets, *p<0.033, **p<0.002, ***p<0.001. ChIP experiments were done in biological replicates, however only one replicate was sequenced the other replicate is depicted as ChIP-qPCR in the supplement. (F) Immunoblot of HAP1 and HAP1ΔATRX cells against ATRX and βActin.

performed relative to input and not to H3. The quantified data further supported the results from the ChIP-seq tracks in Fig. 3.7A and B. H3K9me3 was significantly enriched over the negative control regions on the HSV-1 genome in HAP1wt cells, whereas this modification was significantly lower on the virus than on the cellular negative control in the absence of ATRX (Fig. 3.7D). Furthermore, H2AK119ub was not detected in any of the two cell lines (Fig. 3.7D).

Similar two the ChIP experiments before, a second replicate of this experiment was performed as ChIP-qPCR, which can be found together with the ChIP-qPCR data from the first replicate in the supplementary data, in Fig. S4A - D. Similar to PRVΔIE180 in PK15 cells and HSV-1*in1374* in HDFs and U2OS no H3K27me3, H3K27ac or H3K36me2 could be detected on HSV-1*in1374* in HAP1 and HAP1ΔATRX cells (Fig. S4A and B).

In conclusion, without ATRX, the viral genome incorporated less total H3 than in HAP1wt cells. Due to the low chromatinization levels no histone modifications could be detected on the viral genome, in the HAP1ΔATRX cells. However, in HAP1wt cells the histone modifications acquired by HSV-1 were similar to what was observed in HDF cells. Although ATRX is known as a chromatin remodeler, the here observed strong effect on chromatinization, due to the mere absence of this protein, was surprising.

To further examine the observed phenotype of the virus, depending on ATRX, the host factor was reintroduced into ATRX-depleted cells.

3.7 Introduction of ATRX affects chromatinization of the HSV-1*in1374* genomes

ATRX was reintroduced in a doxycyclin (Dox) inducible way, in U2OS and HAP1ΔATRX cells, to investigate the reversibility of the epigenetic phenotype. Therefore, a piggyBac vector system was used, containing inducible ATRX with a EGFP-tag (Fig. S3B) together with a transposase harboring vector to achieve stable integration od the construct into the cellular genome. The vector harbors a puromycin resistance cassette; thus, cells could be selected for the presence of the vector. Furthermore, ATRX expression could be induced by adding Dox. An inducible system was used since with such a system it was possible to compare an influence of the construct itself without the presence of the protein. A more detailed explanation about the about the methodology can be found in Sec. 6.2.9.

Overexpression of ATRX in HAP1ΔATRX cells. After two days of induction with Dox, the expression of the construct was confirmed by the presence of green-fluorescent cells, by microscopy. Induced and uninduced HAP1ΔATRX were then infected with MOI of 10, and a ChIP experiment was performed at 24 hpi. In the following, induced cells will be referred to as HAP1ΔATRX+Dox, whereas undinduced cells will be referred to as HAP1ΔATRX-Dox. As a positive control for H3K9me3 acquisition on the viral genome, infected HAP1wt cells were included in the experiment.

The ChIP-qPCR data are shown in Fig. 3.8A and B. Endogenous controls and viral genomic regions are separated through a vertical dashed line. As a cellular negative control region for heterochromatin on the human genome, C1ORF43 - an actively transcribed housekeeping gene - was used. ZNF268 and ZNF544 were used as a positive control for constitutive heterochromatin and HOXC12long as the corresponding counterpart for facultative heterochromatin. The level of the negative control for heterochromatin is indicated by the horizontal dashed line, which represents the background level. Similar to the experiment before, the H3-pulldown for the HAP1ΔATRX-Dox resulted in low DNA yields (data not shown). Hence, the qPCR data was normalized to input.
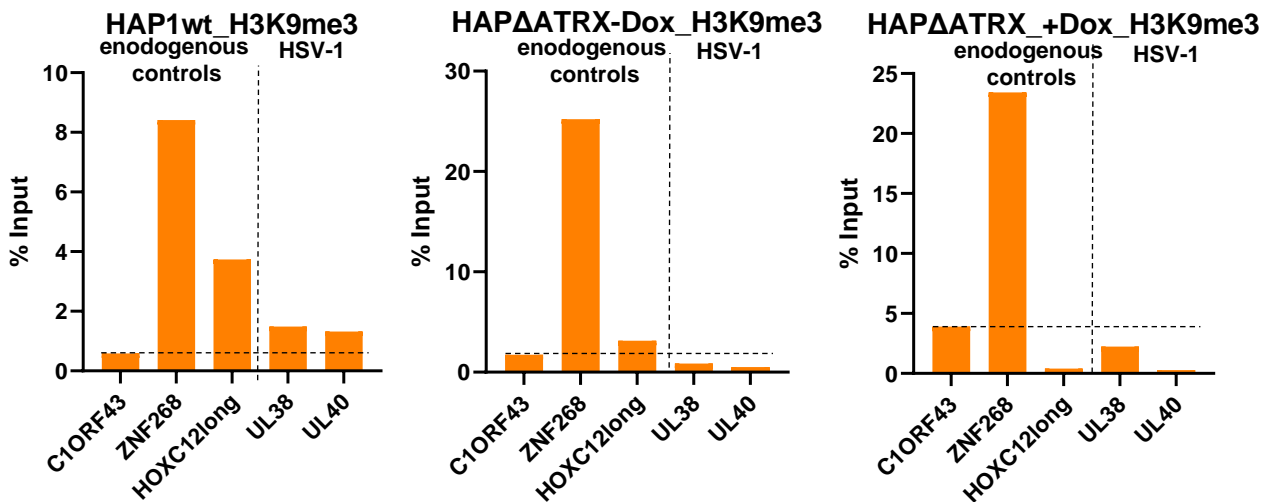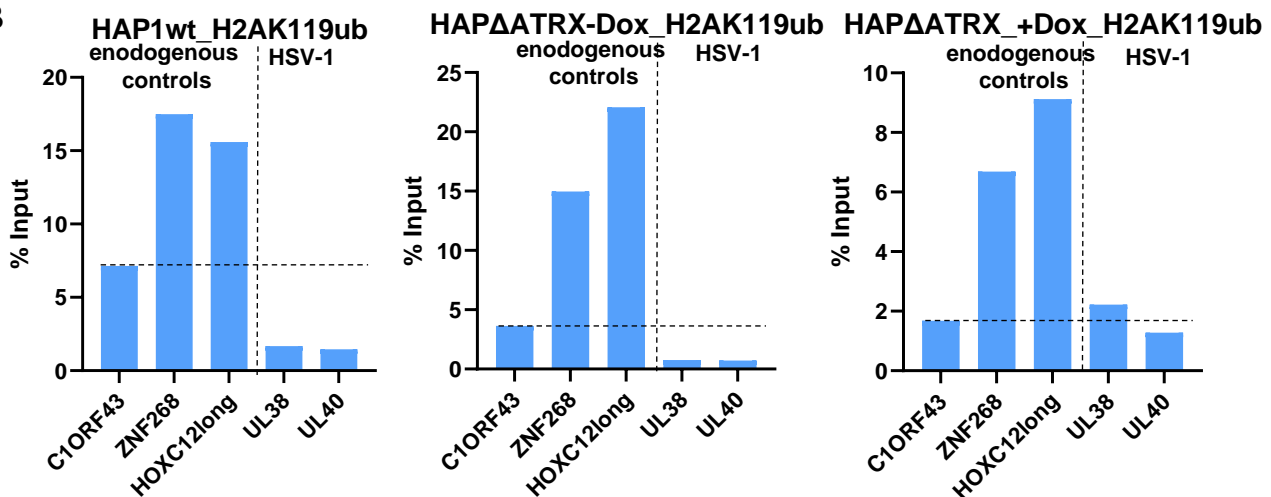
Figure 3.8: ChIP-qPCR results of HSV-1in1374 in HAP1wt, HAP1ΔATRX-Dox and HAP1ΔATRX+Dox, at 24 hpi and non-permissive conditions. (A) Bar-plots of H3K9me3 in the respective infected cell line, normalized to input (B) Bar-plots of H2AK119ub in the respective infected cell line, normalized to input. Threshold of the respective negative control is indicated by a horizontal dashed line. Endogenous controls and viral regions are separated by a vertical dashed line. As an endogenous negative region for heterochromatin C1ORF43 was used, as a positive control for endogenous H3K9me3 ZNF268 and ZNF544 were used and as a positive control for endogenous H2AK119ub HOXC12long was used. UL38 and UL40 are regions in the HSV-1 genome.

The result for HAP1wt cells is similar to the ChIP-seq experiment from above (Sec. 3.6). This can be seen as a replicate. While H3K9me3 levels of the two viral regions were higher than the negative control levels on cellular level (Fig. 3.8A), H2AK119ub levels were lower than the negative control (Fig. 3.8B).

In the ChIP-qPCR data of HAP1ΔATRX-Dox and in HAP1ΔATRX+Dox, H3K9me3 showed no enrichment over background on the viral loci in both. However in HAP1ΔATRX+Dox the signal for H2AK119ub on one of the viral loci was slightly higher than the negative cellular region. (Fig. 3.8A and B).

In summary, reintroduction of ATRX in HAP1ΔATRX did not lead to a reestablishment of the epigenetic modifications, when compared to HAP1wt cells. Moreover, although ATRX was tagged to EGFP the used cells were only selected with puromycin but not sorted according to their EGFP expression. Thus, it is likely that ATRX levels varied among the cells and it was also already observed that the expression of the construct could be silenced after several days in culture. Hence, cells should be sorted, upon induction, according to their expression levels of ATRX-EGFP. Therefore, U2OS cells were not only selected for the presence of the construct with puromycin but also sorted for EGFP-positive cells, via fluoresncence activated cell sorting (FACS) after two days of induction (Fig. 3.9A).

Overexpression of ATRX in U2OS cells. The overexpression of ATRX in U2OS cells resulted in 81.5 % GFP-positive cells, which is shown in the supplementary data in (Fig. S3A). FACS was performed 24 hours prior to infection and sorted cells were further induced to assure ATRX expression in all cells. In the following, these cells will be referred to as U2OSATRX+DOX. To exclude an effect due to the mere presence of the construct, selected but uninduced U2OS cells were included in the experiment. In the following, these cells will be referred to as U2OSATRX-DOX. The infected cells were harvested 24 hpi and a ChIP experiment was performed. As the H3 pulldown worked well for these cells, H3 was used to normalize the qPCR data. Furthermore, a second endogenous positive control region for H2AK119ub was included (HOXC13), since this modification is very dynamic.

The H3K9me3 levels on HSV-1*in1374* in U2OSATRX+DOX increased at some regions of the viral genome, compared to U2OSATRX-DOX cells (Fig. 3.9A). However, in both cell lines, H3K9me3 levels were above the negative control on all four analyzed viral loci.

In both cell lines all viral loci showed H2AK119ub levels above the negative control. However, in U2OSATRX+DOX cells, H2AK119ub levels slightly decreased, compared to U2OSATRX-DOX (Fig. 3.9B).

In summary, unlike the induced U2OS cells, not all induced HAP1ΔATRX cells expressed ATRX. Thus, the effect of the overexpressed protein might be not detectable in a the bulk experiment in the HAP1ΔATRX+ATRX cells. Therefore, this experiment should be repeated with selected and sorted cells.

Although the ChIP-qPCR data of the induced and uninduced U2OS cells supports a model in which ATRX, or other host factors recruited by ATRX, play a role in the repression of vDNA, through H3K9me3, a genome-wide analysis would give additional information and would enable a quantitative analysis. Thus, the ChIP samples will be sequenced in the future. Furthermore, the experiment should be performed in replicate.

The levels of ATRX expression in the used cell lines were compared by performing IF against the

A

B
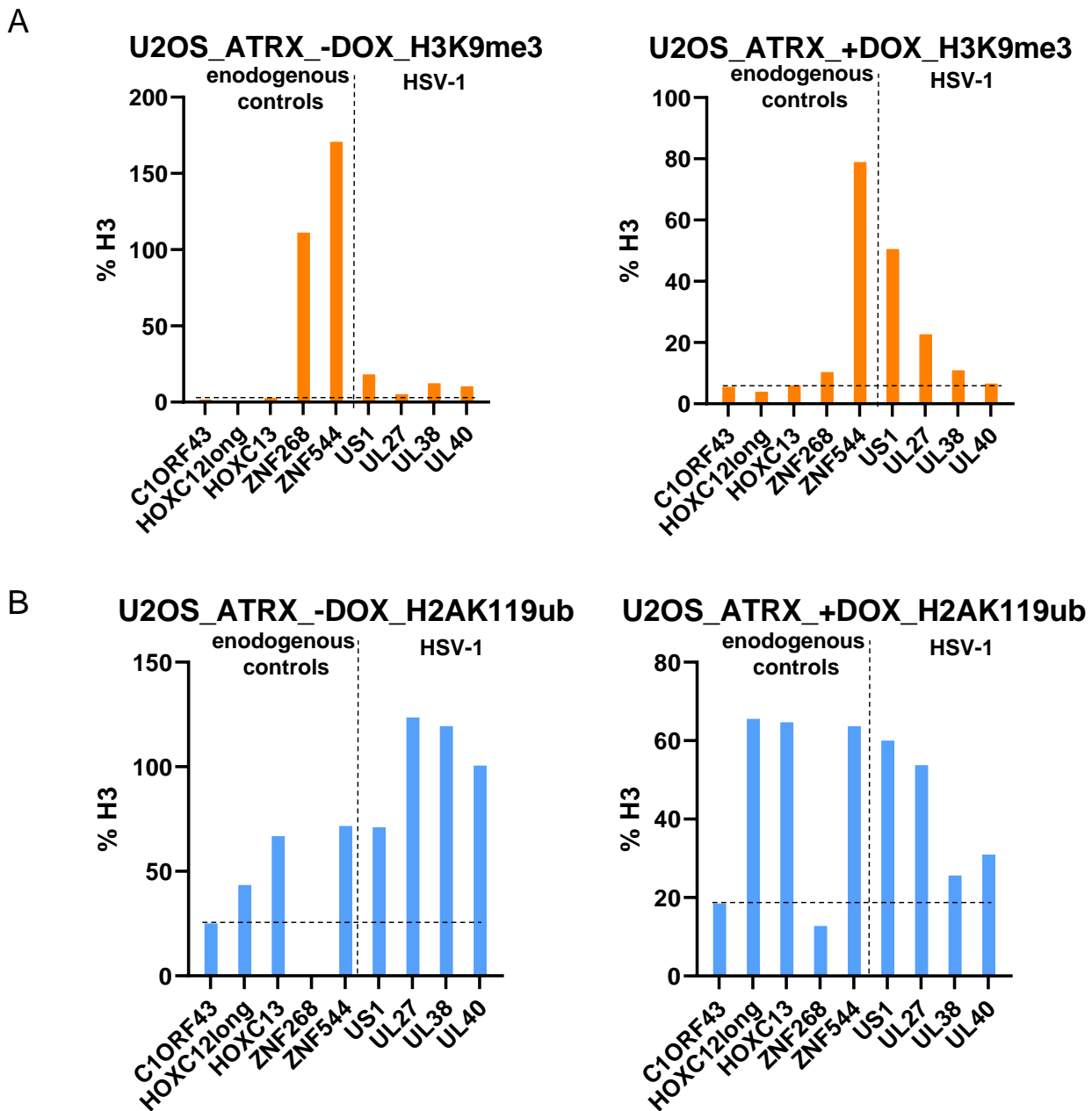
Figure 3.9: ChIP-qPCR results of U2OS cells transfected with the piggyBac ATRX-EGFP construct - induced and un-induced - infected with HSV1*in1374* at 24 hpi and non-permissive conditions. (A) Bar-plots of H3K9me3 in the respective infected cell line, normalized to H3 (B) Bar-plots of H2AK119ub in the respective infected cell line, normalized to H3. Threshold of the respective negative control is indicated by a horizontal dashed line. Endogenous controls and viral regions are separated by a vertical dashed line. As an endogenous negative region for heterochromatin C1ORF43 was used, as a positive control for endogenous H3K9me3 ZNF268 and ZNF544 were used and as a positive control for endogenous H2AK119ub, HOXC12long was used. US1, UL27, UL38 and UL40 are regions in the virus genome.

two proteins. Representative images of the experiment can be found in the supplementary data in Fig. S5. After qualitative analysis of the images, HDFs seemed to have the highest levels of ATRX. Even by overexpression of ATRX in U2OS cells such levels could not be reached. Since the HSV-1 genomes in HDF cells were only decorated with H3K9me3 (Sec. 3.5) and the cells showed high levels of ATRX, the effect of a ATRX depletion in this cell line was assumed to affect heterochromatinization of the virus. Therefore, the effect of an ATRX knock-down in HDF cells was investigated next.

3.8 Knock-down of ATRX in HDFs slightly affects heterochromatinizaion HSV-1*in1374* genomes

HDF cells were depleted of ATRX via siRNA transfection, using Viromer®BLUE as a transfection reagent (the detailed methodology can be found in Sec. 6.2.10). As a control for the mere effect of the transfection reagent, HDFs only treated with viromer were included in the experiment, which will be referred to as HDFviromer cells from here on. As a control for an siRNA in general, HDFs were transfected with a non-target siRNA, which will be referred to as HDFsiscramble (HDFsiScr) cells. Cells transfected with the target siRNA, will be referred to as HDFsiATRX, in the following. The successful knock-down of ATRX in HDF cells, was confirmed via immunoblotting and IF. Subsequently, the impact of ATRX on the viral chromatinization was investigated via ChIP.

Immunoblotting of ATRX depleted HDFs. For immunoblotting whole cell lysates of the HDFsiATRX cells were used, at different time points post transfection, as shown in Fig. 3.10A. As a positive control for ATRX expression, a whole cell lysate of HDFsiScr, was used. As a negative control for ATRX expression, a whole cell lysate of HAP1ΔATRX cells was included to the blot (Fig. 3.10A). The immunoblot was done independently of the ChIP experiment to confirm the knock-down beforehand. As shown in Fig. 3.10A, ATRX levels strongly decreased by 24 hours post transfection (hpt) and were stably depleted until 120 hpt. As observed before in HAP1 cells, when using this antibody in immunoblot (Fig. 3.7F), only one of the specific ATRX bands was visible, the one at around 100 kDa. This might be due difficulties with blotting high molecular weight protein bands.

Immunofluorescence of ATRX depleted HDFs. The knock-down of ATRX in cells that had been harvested for ChIP was analyzed by IF against ATRX. Subsequently, the amount of cells, showing ATRX-dots was counted. The results are depicted in the bar-plot in Fig. 3.10B. Only about 25 % of HDFsiATRX cells still showed ATRX-dots. In addition, no effect of siScr or the transfection reagent viromer itself on ATRX levels could be observed, since ATRX dots were detected in almost 100 % of the respective cells (Fig. 3.10B).

After the successful confirmation of the ATRX knock-down, ChIP-qPCR was performed with the infected cells. Similar to the knock-out of ATRX in HAP1 cells, the H3-pulldown of HDFsiATRX cells and unexpectedly also that of HDFsiScr cells resulted in low DNA yields. Hence, the qPCR data was normalized to input. The same loci as described above were used as endogenous controls, which were again separated from the viral loci by a vertical dashed line. The level of the cellular negative control, which represents the background level, is indicated by a horizontal dashed line.

H3K9me3 levels on HSV-1*in1374*. The ChIP-qPCR data for H3K9me3 are shown in Fig. 3.10C. The presence of H3K9me3 on the viral genome in HDFviromer cells, resembled the results from the ChIP-seq data of untreated HDF cells (Sec. 3.5). The knock-down of ATRX led to no detectable changes in H3K9me3 levels compared to HDFviromer cells. In contrast to this, HDFsiScr
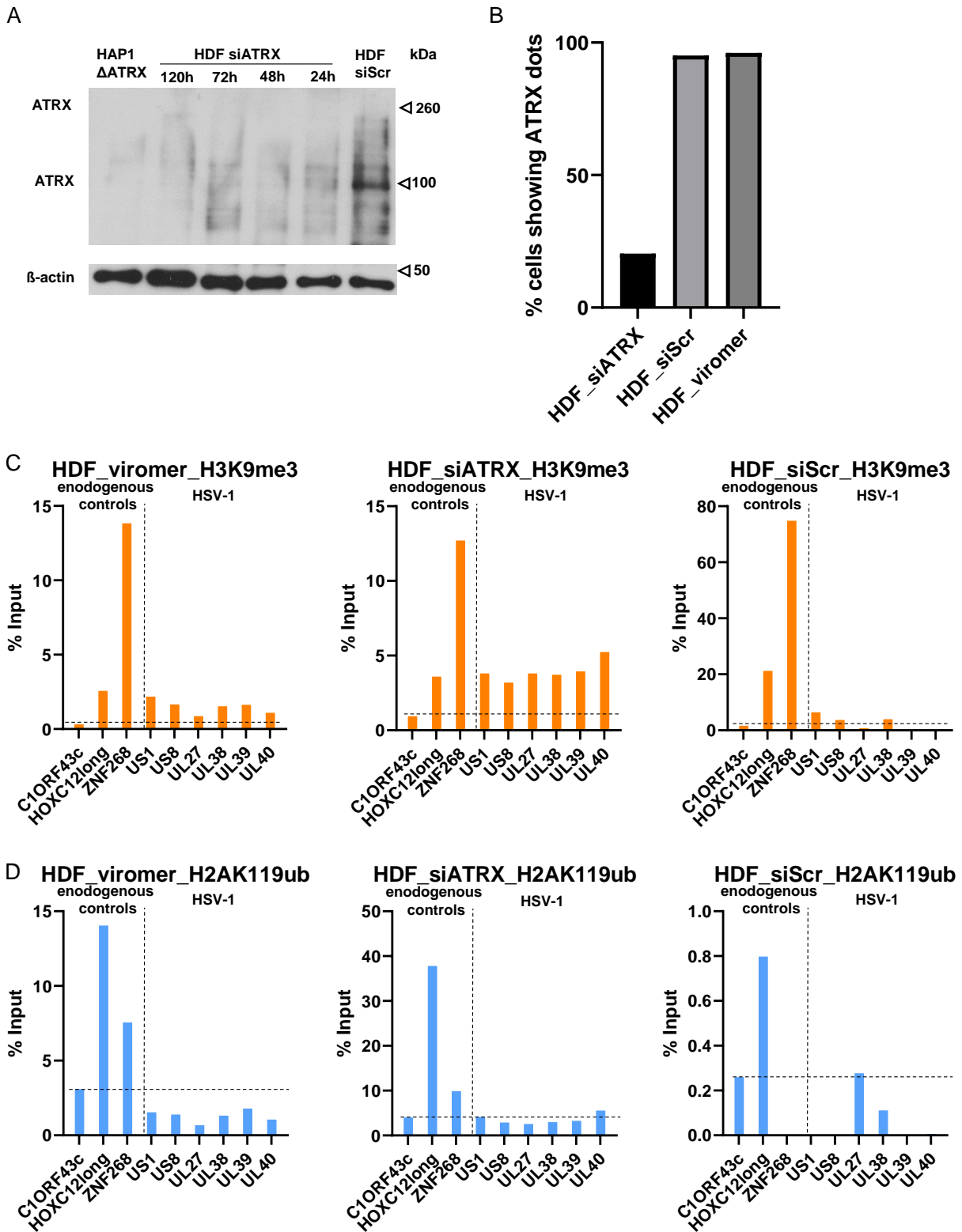
Figure 3.10: Verification of the ATRX knock-down and its efficiency and ChIP-qPCR results of HDF cells transfected with siRNA against ATRX or Scramble (Scr) or only with the transfection reagent viromer at 24 hpi and non-permissive conditions.(A) Immunoblot against ATRX and β-Actin of the indicated cells. HDF cells were incubated with siATRX between 24 and 120 hours post transfection, to analyze how long the knock-down lasts. HAP1ΔATRX were used as a negative control for ATRX, and HDF cells treated with siScr were used as positive control for ATRX expression. (B) Bar-plots of the percentage of cells showing detectable ATRX levels, via Immunofluorescence with subsequent microscopic-analysis. (C) Bar-plots of ChIP-qPCR results against H3K9me3 in the respective infected cell line, normalized to input (D) Bar-plots of ChIP-qPCR results against H2AK119ub in the respective infected cell line, normalized to input. Threshold of the respective negative control is indicated by a horizontal dashed line. Endogenous controls and viral regions are separated by a vertical dashed line. As an endogenous negative region for heterochromatin C1ORF43c was used, as a positive control for endogenous H3K9me3 ZNF268 was used and as a positive control for endogenous H2AK119ub HOXC12long was used. US1, US8 UL27, UL37, UL38 and UL40 are regions in the virus genome.

cells showed a decrease in H3K9me3 levels compared to HDFviromer cells and HDFsiATRX cells, which were even below the detection limit at three regions of the viral genome (UL27, UL39, UL40).

H2AK119ub levels on HSV-1*in1374*. The ChIP-qPCR data for H2AK119ub are shown in Fig. 3.10D. In HDFviromer cells, H2AK119ub levels on the HSV-1 genome were below the cellular negative control, which again resembled the data from HDFwt cells in the ChIP-seq experiment in Sec. 3.5. In HDFsiATRX cells, there was a slight increase in H2AK119ub levels at two viral regions (US1, UL40) which slightly exceeded the negative control (Fig. 3.10D). In HDFsiScr cells, the H2AK119ub level on one viral region (UL27) was slightly increased over the negative control. However, at four viral regions the H2AK119ub levels were below the detection threshold. Furthermore, the overall pulldown of this antibody was not as efficient as in the other two samples, as indicated by the Y-axis' magnitude (Fig. 3.10D). The enrichment over input for the endogenous positive control, HOXC12long, was around 0.8 %. In contrast, the same region in the HDFviromer cells was at 14 % and in HDFsiATRX cells at 38 %. Furthermore, H2AK119ub was not detectable at all on ZNF268, whereas in the other two samples the signal for H2AK119ub at this cellular locus exceeded the background level(Fig. 3.10D).

In conclusion, H3K9me3 was detected on the viral genomes in both, HDFviromer cells and HDFsiATRX cells. H2AK119ub levels were slightly increased on the virus in the HDFsiATRX cells, compared to the HDFviromer cells. Unexpectedly, HDFsiScr cells showed decreased levels of both histone modificathe whole-genomeme viral loci these were even undetectable. Since both siRNAs (ATRX and Scr) were bought from a company off-target effects were not to be expected. In fact, the HDFsiScr cells were supposed to be comparable to HDFviromer cells. Thus, this result is unforeseen. It has to be noted though that only a single replicate study has been performed and needs to be confirmed by further replicates. Moreover, to analyze the histone modifications on whole genome level, the samples will be sequenced in the future.

Although there was a strong decrease of ATRX in acHDFsiATRX cells, low levels of the protein were still detectable in the immunoblot, as well as in single cells during IF. Thus, the low ATRX levels might not lead to detectable chromatin changes in bulk. To investigate the effects of ATRX on a single cell level, an imaging system was designed and applied to the different wt cell lines, as well as the ATRX-modified cell lines.

3.9 HSV-1*in1374* is more prone to replicate in cells fully depleted of ATRX

The replication ability of HSV-1*in1374*, tested in dependence on ATRX, was analyzed by an imaging approach of the infected cells.

The different wt cell lines (HDF, U2OS and HAP1), as well as the ATRX-modified cell lines (HDF-siATRX, U2OS+ATRX and HAP1ΔATRX) were infected with HSV-1*in1374*, under permissive

or non-permissive conditions, and after a selected time, as described in the following, cells were fixed and IF was performed against the lytic viral protein ICP8, a common viral factor used for RC detection (Fig. 3.11A). With this system, cells that showed replication of the virus could be detected. Thus, differences in the ability of the virus to replicate and reactivate, depending on ATRX, could be analyzed. In the following, this experimental approach will be referred to as RC-formation assay.
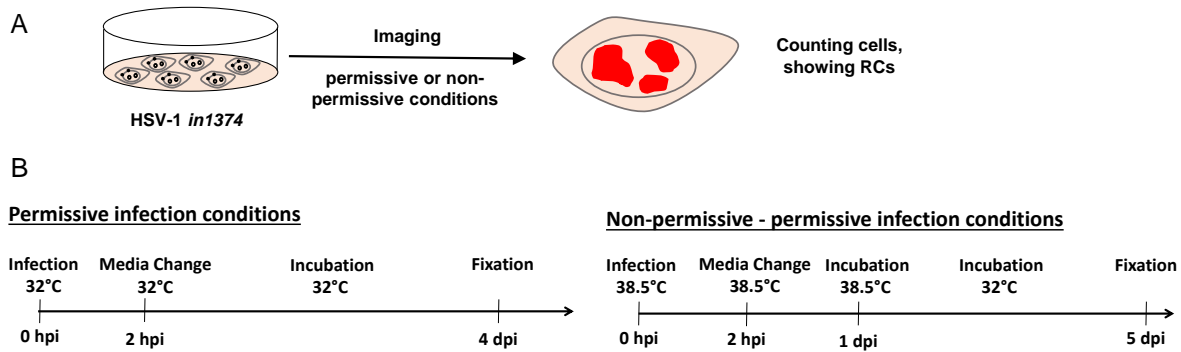
Figure 3.11: Experimental set-up of RC-formation assay during permissive and non-permissive - permissive HSV-1*in1374* infection. (B) Time line of the infection-scheme. Under permissive conditions, cells were infected with HSV-1*in1374* at MOI 1 and directly incubated at the permissive temperature of 32 °C. 2 hpi media was changed and cells were kept for 4 days at 32 °C. 4 dpi cells were fixed and immunostained with an ICP8 antibody. At non-permissive - permissive conditions, cells were infected with HSV-1*in1374* at MOI 1 and directly incubated at the non-permissive temperature of 38.5 °C. 2 hpi media was changed and cells were kept for one day at 38.5 °C. Infected cells were then shifted to 32 °C and incubated for another four days at the permissive temperature. After 5 dpi cells were fixed and immunostained with an ICP8 antibody.

Permissive infection conditions (direct replication). In order to investigate the ability of HSV-1*in1374* to directly replicate in the various cell lines, infection was performed under direct permissive conditions, at 32 °C, with a MOI of 1. The infected cells were incubated at the permissive temperature for four days. Afterwards, the cells were fixed and IF against ICP8 was performed (Fig. 3.11B). In the following, this infection condition will be referred to as permissive condition.

Non-permissive - permissive infection conditions (reactivation). To analyze the ability of the virus to reactivate after repressive histone marks were already established, the initial infection was performed under non-permissive conditions, at 38.5 °C, with an MOI of 1. At 24 hpi the cells were transferred to permissive conditions, at 32 °C and incubated for another four days. Subsequently, cells were fixed and IF was performed as described above (Fig. 3.11B). In the following, this infection condition will be referred to as non-permissive - permissive condition. Additionally, cells were stained with Hoechst33342 to be able to visualize the nuclei. Stained cells were imaged, using a confocal laser-scanning microscope. As a read-out, the percentage of cells which showed RCs was calculated (Fig. 3.11A).

Comparison of U2OS and HDF cells. First, the difference between viral replication of U2OS and HDF cells was investigated. Since the detected repressive histone modifications on the viral genome were different among the two cell types, it was hypothesized that these should affect

the ability for the virus to reactivate. Fig. 3.12A - D shows representative cells of each cell line and condition as maximum-intensity-projection. From these imaging data, the percentage of cells showing RCs was calculated in three independent experiments. At least 5.000 cells were analyzed for each cell line and each replicate. The results were illustrated as bar-plots with the corresponding SD in Fig. 3.12E - F. Additionally, statistical testing was performed using an unpaired t-test, indicated by the asterisks above the bars.

Under permissive conditions, about 40 % of the U2OS cells showed RCs, which was significantly more than in HDFs (Fig. 3.12A and E). In HDFs very few RCs were observed. Thus, spontaneous replication events can occur during permissive conditions, even in the presence of ATRX, however they are rare.

Under non-permissive - permissive conditions, replication was only observed in about 30 % of the U2OS cells (Fig. 3.12B and E). However, the difference between HDFs and U2OS cells was still significant, since under this condition no RCs could be detected in HDFs (3.12B and E).

In addition, the replication ability of the virus was compared, and statistically tested, among the same cell line under the different conditions (Fig. 3.12E). Although the difference between U2OS cells under non-permissive - permissive conditions was about one fourth less than in U2OS cells under direct permissive conditions, this difference was not significant (Fig. 3.12E). Most likely, this can be attributed to the relatively high SD among the three independent experiments.

During the primary incubation at non-permissive conditions no RCs at all were detected in HDFs. Although few cells, allowing replication under permissive conditions were observed, the difference between HDFs under the two conditions was not significant (Fig. 3.12E). This finding empathized how tight the epigenetic repression of the HSV-1 genomes is, once H3K9me3 is acquired.

In summary, viral replication was significantly facilitated in U2OS cells, compared to HDFs, under both conditions. By combining these findings with the ChIP-seq results of U2OS cells, it can be hypothesized that the presence of H2AK119ub or the absence of H3K9me3 might enhance the virus' ability to reactivate.

Comparison of HAP1 and HAP1ΔATRX cells. As ChIP data showed, HSV-1 acquired only H3K9me3 in HAP1wt cells, similar to HDF cells (Sec. 3.6). Thus, for HAP1wt cells it was expected that the amount of cells with RC-staining is comparable to the HDF counterparts. In contrast, in HAP1ΔATRX cells no chromatinization of the viral genome was detectable. It is yet unclear and worth investigating what specifically happens with the viral genomes in HAP1ΔATRX cells.

As depicted in the bar-plots in Fig. 3.12F, under permissive conditions, about 55 % of HAP1ΔATRX showed RCs, compared to only about 4 % in HAP1wt cells. This difference in RC occurrence is highly statistically significant - as indicated by the three stars in Fig. 3.12F.

In contrast, under non-permissive - permissive conditions, the difference between the two cell lines was insignificant (Fig. 3.12F). Similar to what was observed in HDF cells under non-permissive - permissive conditions, HAP1wt cells did not harbor any RCs (Fig. 3.12D and F).

Figure 3.12: RC formation staining and quantification during permissive and non-permissive - permissive HSV-1 *in1374* infection in different cell types. (A - D) Immunofluorescence of cells showing replication compartments and quantification of the data, under different conditions. Nuclei were stained with Hoechst and RCs were visualized by staining the viral protein ICP8. (E - F) Comparison of the two conditions, illustrated in bar-plots. Imaging was done with a confocal fluorescence microscope. Representative areas for each cell type are shown as maximum intensity projections. Scale bars indicate 20 µm. Quantification of the percentage of cells showing replication compartments are shown in bar-plots with SD, indicated above the bars. Data were collected and analyzed from three biological replicates and a minimum of 1500 cells, of each cell type. Statisitcal testing was performed using an unpaired t-test. Significance levels are indicated by asterisks, which are displayed above the compared datasets. *p<0.033, **p<0.002, ***p<0.001, ns = not significant.

However, comparing the RC occurrence in HAP1ΔATRX cells for these two conditions, a statistically significant decrease was observed under non-permissive - permissive conditions (Fig. 3.12F). The percentage of cells showing RC dropped from 55 % to about 6 %, respectively (Fig. 3.12F). This reduction indicates that there might be some silencing mechanism in HAP1ΔATRX cells, on the viral genome, that is hardly reversible. However, no repressive histone modification was observed in these cells, as shown before in Sec. 3.6.

Similar to HDFs, HAP1wt cells showed no significant difference in RC occurrence, under the two conditions (Fig. 3.12F).

In summary, the absence of ATRX facilitates viral replication in HAP1 cells. This phenomenon is similar to what was observed for U2OS cells when compared to HDF. Together with the epigenetic data, where HSV-1*in1374* acquired H3K9me3 in HAP1wt cells, these observations favor the hypothesis that the ability of the virus to reactivate is highly dependent on the chromatinization of the viral genome. Furthermore the acquisition of a rather tight repressive histone modification seems to be dependent on the presence of ATRX.

To further elucidate the influence of ATRX on the ability of the virus to reactivate, HDFsiATRX cells were used for the RC-formation assay.

Comparison of HDF and HDFsiATRX cells. The same experiment as described before was performed in HDFsiATRX cells and the control cells HDFsiScr and HDFviromer (Fig. 3.13). In addition to the ICP8 staining in red, ATRX was stained in green, to visualize the knock-down . Unlike in the above described experiments, more than two groups were compared to each other. Thus, the p-values were calculated using an ordinary one-way Anova with post hoc tukey's test, instead of a t-test.

In the images of Figs. 3.13A and B, ATRX was stained and visible in a typical dot like pattern in the nucleus, in HDFviromer cells and HDFsiScr cells. However, the majority of HDFsiATRX cells showed no ATRX dots. This observation confirms the results from the previously shown immunoblot (Fig. 3.10A) i.e. neither the transfection reagent itself nor siScr had an effect on ATRX levels.

The ChIP-qPCR data of these cells (Fig. 3.10), already showed a pattern of histone marks in HDFviromer cells as observed before in HDFwt cells. Thus, a result similar to what has been shown for HDFwt (Fig. 3.12) cells was expected.

Under permissive conditions no RCs were detected among the HDFviromer cells, as shown in the box-plot of Fig. 3.13A. This finding resembled the data for HDFs (Fig. 3.12A). In addition, under the same conditions 18 % of the HDFsiATRX cells showed RCs, in contrast to only 5 % in HDFsiScr cells (Fig. 3.13A). The difference in the amount of RCs of HDFsiATRX cells compared to the other two cell lines was statistical significant, indicated by the asterisk above the bars. Furthermore, HDFsiScr cells showed insignificantly higher levels of RCs, compared to HDFviromer cells (Fig. 3.13A). This observation led to the assumption that the siScr-pool has some off target effect on the cell, facilitating virus-replication, under permissive conditions, however these were not significant. In addition, the difference in the amount of cells showing RCs between HDFsiScr and HDFsiATRX was statistically significant (Fig. 3.13A). Thus, the effect of the siScrRNA on viral replication is significantly less than the actual ATRX knock-down.

Remarkably, under non-permissive - permissive conditions no RCs at all were detected, independent of the treatment; thus, no bar-plot is displayed here (Fig. 3.13B).

In conclusion, replication of HSV-1*in1374* could be only detected under permissive conditions. In contrast to this, under non-permissive - permissive conditions no replication events were observed. Thus, reactivation from a repressed state of the viral genomes was not possible, even with the ATRX knock-down. When comparing this finding with the respective ChIP data of these cells

(Sec. 3.8), H3K9me3 is likely leading to a strong block of lytic reactivation and replication. Thus, the acquisition of this modification may represent a dead-end for the virus.
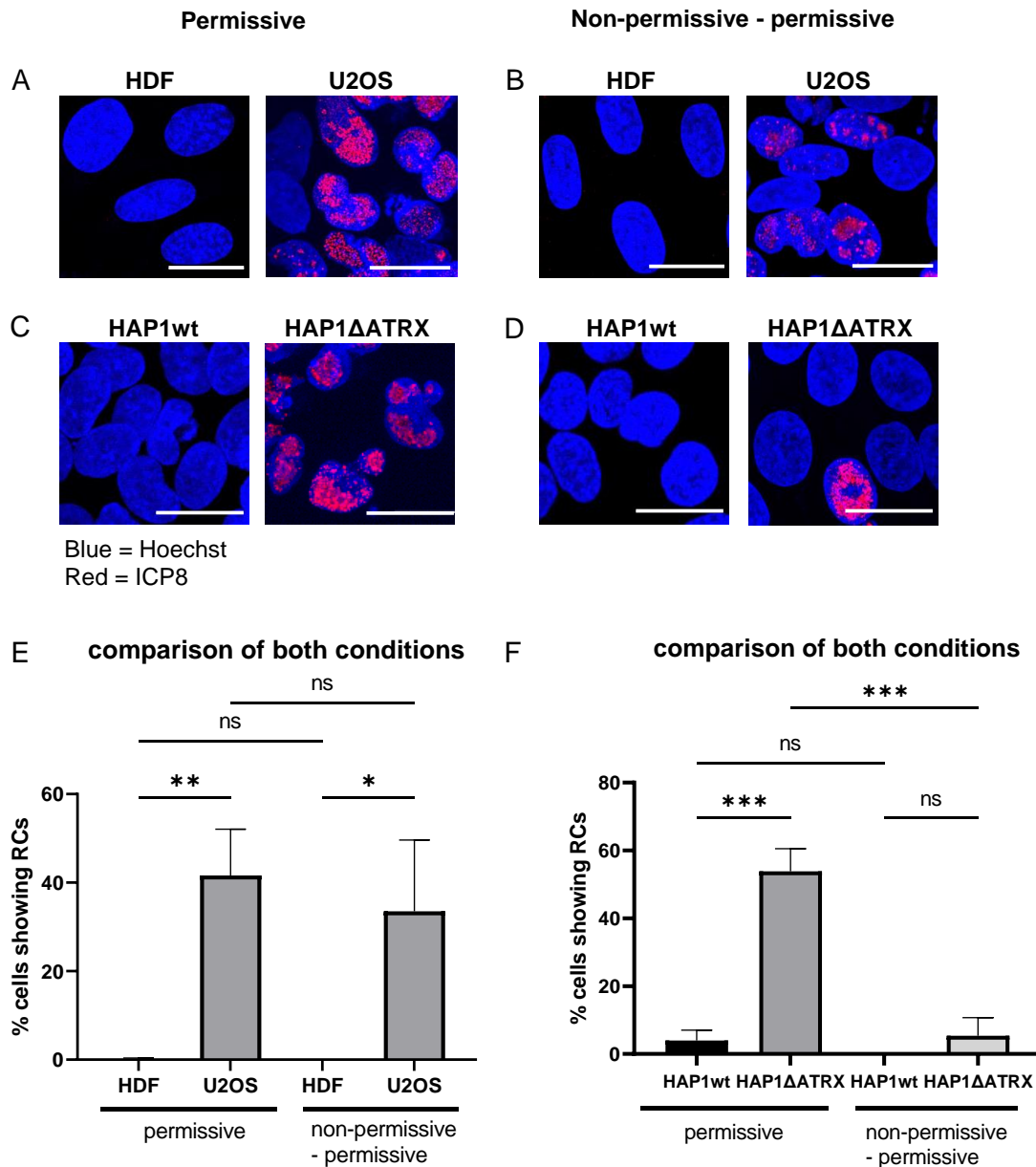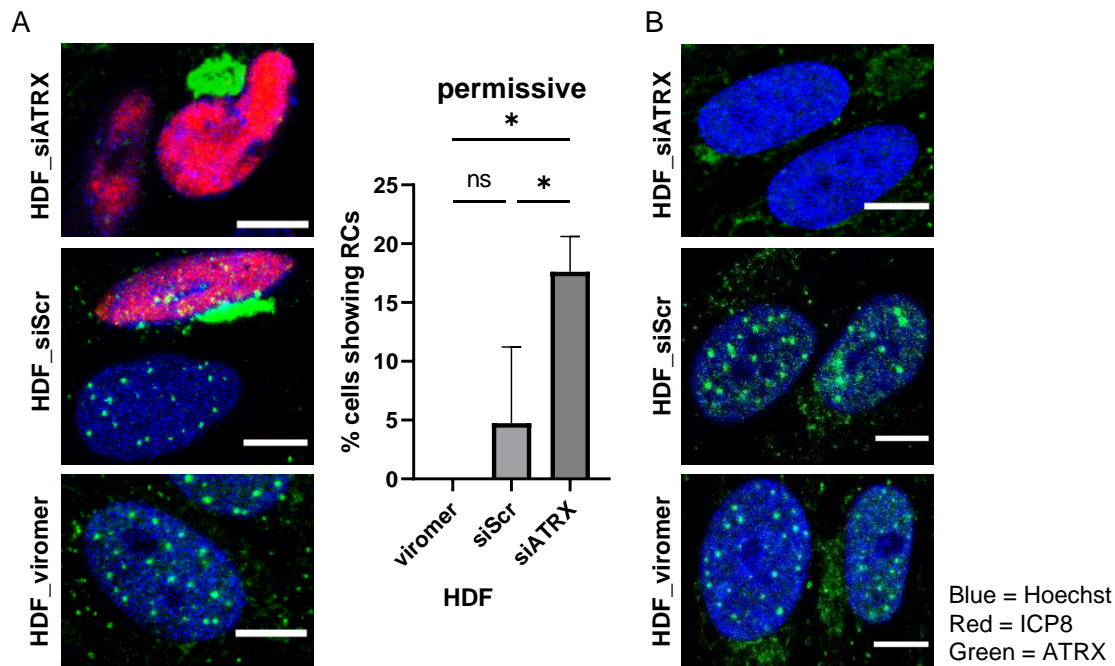

Figure 3.13: RC formation staining and quantification of RCs during permissive and non-permissive - permissive HSV-1*in1374* infection in HDFsiATRX, HDSsiScr and HDFviromer cells. (A) Immunofluorescence of HDFs transfected with siRNA against ATRX or Scr or only with the transfection reagent viromer in infected cells at permissive conditions. (B) The same as in (A) but under non-permissive - permissive conditions. Nuclei were stained with Hoechst33342, RCs were visualized, using an antibody against the viral protein ICP8 and a secondary antibody with a red fluorophor. ATRX was stained with an anti-ATRX antibody and a secondary Alexa Fluor 488 antibody. Imaging was done with a confocal fluorescence microscope. Representative areas for each cell-type are shown as maximum intensity projections. Scale bars indicate 10 μm. Quantification of the percentage of cells showing replication compartments are displayed as bar-plots with SD. Data were collected and analyzed from three biological replicates and a minimum of 500 cells, of each cell type. Statistical testing was done, using ordinary one-way Anova with post hoc tukey's test. Significance levels are indicated by asterisks, which are displayed above the compared datasets, *p<0.033, **p<0.002, ***p<0.001, ns = not significant.

3.10 Introduction of ATRX in U2OS cells lowers the viral replication ability

The RC-formation assay was additionally performed in U2OS cells with ATRX overexpression. Like the previous experiment, an additional antibody was used to stain ATRX, in green (Fig. 3.14A and B). Again, this experiment was done in triplicate, using a minimum of 1500 cells of each cell type and the p-values were calculated by using an unpaired t-test.

As illustrated in the images of Fig 3.14A and B, U2OSATRX+DOX cells showed high amounts of greenfluorescent cells, with even individual ATRX dots. This confirmed the presence of ATRX in those cells. In U2OSATRX-DOX cells no such greenfluorescent signals were detected. Moreover, In both cell types as well as in HDF cells, stained with the ATRX antibody (Fig. 3.13), a higher background signal in the green channel was observed upon infection (Fig. 3.14A and B). This could be due to rearrangement of the cell, since they are already apoptotic, leading to unspecific binding of the ATRX antibody.

As indicated by the ChIP-qPCR data before (Fig. 3.9) in U2OSATRX-DOX cells, HSV-1*in1374*
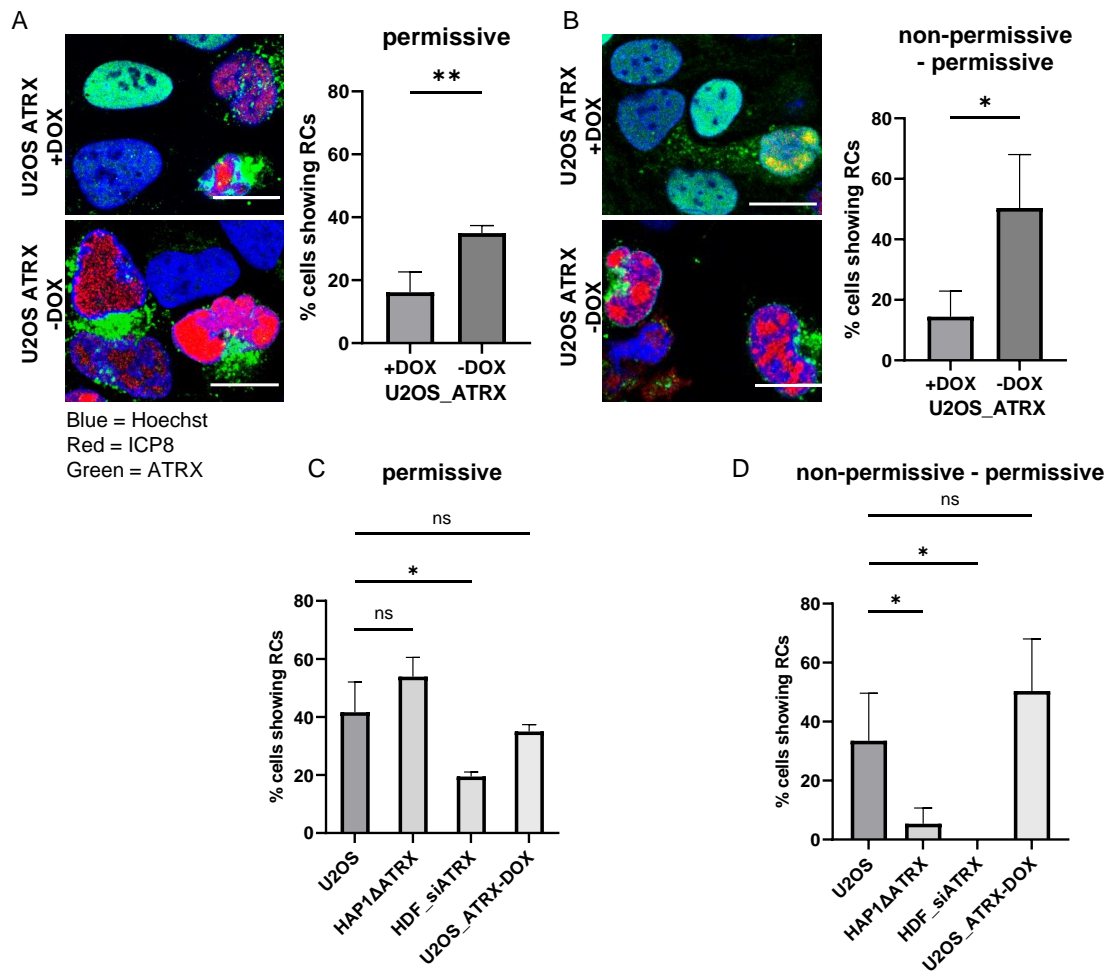
Figure 3.14: RC formation staining and quantification of replication compartments during permissive and non-permissive - permissive, HSV-1*in1374* infection, in different cell types. (A) Immunofluorescence of U2OS cells induced or un-induced with Dox for ATRX production under permissive and (B) non-permissive - permissive conditions. Nuclei were stained with Hoechst, replication compartments were visualized, using an antibody against the viral protein ICP8 and a secondary Alexa Fluor 555 antibody, ATRX was stained with an anti-ATRX-antibody and a secondary Alexa Fluor 488 antibody. Imaging was done with a confocal fluorescence microscope. Representative areas for each cell type are shown as maximum intensity projections. Scale bars indicate 20 µm. Quantification of the percentage of cells showing replication compartments are displayed as bar-plots with SD. Data were collected and analyzed from three biological replicates and a minimum of 500 cells, of each cell type. Statistical testing was done, using unpaired t-test. Significance levels are indicated by asterisks, which are displayed above the compared datasets, *p<0.033, **p<0.002, ***p<0.001. (D -E) Differences of the ability to replicate of HSV-1*in1374*, between the different cell lines depleted of ATRX are shown as bar-plots with SD. Data were collected and analyzed from three biological replicates and a minimum of 500 cells, of each cell type, were analyzed. Statistical testing was done, using ordinary one-way Anova with post hoc tukey's test. Significance levels are indicated by asterisks, which are displayed above the compared datasets, *p<0.033, **p<0.002, ***p<0.001, ns = not significant.

showed a similar epigenetic profile as in U2OS cells. Hence, also a similar outcome in the RC-formation assay was expected. In contrast, U2OSATRX+DOX cells, showed slightly higher levels of H3K9me3 and decreased levels of H2AK119ub; thus, fewer U2OSATRX+DOX cells were expected to show RCs.

Cells supporting viral replication could be observed in uninduced and in induced U2OSATRX cells, under both conditions. However, the amounts of cells showing RCs differed between the two conditions.

Under direct permissive conditions, about 18 % of the U2OSATRX+DOX cells showed RCs, compared to 35 % of the U2OSATRX-DOX cells. The difference could be confirmed statistically significant, indicated by the asterisks above the bars (Fig. 3.14A).

Under non-permissive - permissive conditions, about 15 % of the U2OSATRX+DOX cells showed RCs, compared to 50 % of U2OSATRX-DOX cells. Although the p-value calculated under the latter condition was slightly higher than under permissive conditions the difference between induced and uninduced cells was still statistically significant (Fig. 3.14B). The higher p-value could result from the higher SD between the individual replicates in the latter experiment.

In summary, overexpression of ATRX resulted in decreased RC formation. These results further indicate that ATRX is an important factor for establishing a tight repressed viral genome and its absence facilitates virus replication.

In addtion, differences in the replication ability of the virus mutant between the different ATRX-deficient cell lines (U2OS, HAPΔATRX, HDFsiATRX, U2OSATRX-DOX) were statistically tested (Fig. 3.14 C and D). Since more than two groups should be compared to each other, a one-way Anova test with post hoc tukey's test was performed. The corresponding data was illustrated as bar-plots and is shown in Fig. 3.14C and D.

As a result the difference in RC occurrence between U2OS cells and U2OSATRX-DOX cells was statistically insignificant, under both conditions (Fig. 3.14C and D). Subsequently, it can be concluded that the construct itself had no effect on replication ability of the virus.

Furthermore, there was no statistical significant difference between U2OS cells and HAP1ΔATRX cells under permissive conditions (Fig. 3.14C). In contrast, under non-permissive - permissive conditions a statistical significant difference for the two cell lines was observed (Fig. 3.14D). This result indicated that there has to be a tight repressive mechanism on the viral genomes in HAP1ΔATRX cells, since viral reactivation seems to be much more difficult in this cell line. However, as described above, none of the investigated histone modifications were detected on HSV-1*in1374* genomes in the HAP1ΔATRX cells.

As a final observation, HDFsiATRX cells showed a statistical significant difference for either condition, compared to U2OS cells (Fig. 3.14C and D). This result was expected for non-permissive - permissive conditions, since there was no detectable RCs in HDFsiATRX cells and, furthermore, H3K9me3 levels on the viral genome were similar to HDFviromer cells and HDFwt cells. However, under permissive conditions the viral replication ability was significantly increased in HDFsiATRX compared to HDFviromer cells. Hence, the significant difference between U2OS and HDFsiATRX cells under these conditions was surprising. Nevertheless, this indicates that ATRX levels play an important role in silencing the herpesvirus genomes.

The observations made in this study suggest that the presence of ATRX is involved in mediating strong vDNA suppression, which is likely achieved by higher recruitment of H3K9me3. Although downregulation or overexpression of ATRX strongly affects the reactivation ability of HSV-1*in1374*, the effect on heterochromatinization appears to be rather modest. In contrast to viral genomes that acquired H3K9me3, the virus could still be reactivated after the establishment of the PRC-mediated repressive histone modification H2AK119ub.

4 Discussion

This study aimed to decipher molecular mechanisms of latency establishment of alphaherpesvirus genomes, early after nuclear entry. The ultimate goal was to generalize previous findings for the gammaherpesvirus KSHV with new results for the two investigated alphaherpesviruses.

Up to this point, acquisition of heterochromatin on PRV genomes has not been investigated. However, it was demonstrated that the closely related alphaherpesvirus HSV-1 acquires the facultative heterochromatin modification H3K27me3, in neurons. Additionally, preliminary data observed this modification on two viral promoters of a HSV-1 ICP0-null mutant, in non-neuronal cells. Furthermore, H3K9me3 was detected on lytic-cycle-deficient HSV-1 genomes in human fibroblasts, however, this observation is limited to a few selected viral loci. Additionally, it is only poorly understood what molecular mechanism lead to the recruitment of host factors establishing these modifications.

This study showed for the first time that alphaherpesviruses are able to acquire H2AK119ub - a facultative heterochromatin modification established by the ncPRC1.1. Moreover, H3K9me3 and H2AK119ub were found to decorate the whole viral genome of two different alphaherpesviruses - PRV and HSV-1 - which indicates that the observed mechanism is a common feature among this herpesvirus subfamily. At least in part, the acquisition of the respective modification seemed to be dependent on the host factor ATRX. Furthermore, from the data presented here, it can be hypothesized that the two different forms of heterochromatin - constitutive and facultative - have an effect on the ability of the virus to reactivate. In addition, evidence of the establishment of two differently repressed virus subpopulations, within one cell type, was found. Besides, the here presented data demonstrated a partly similar silencing mechanism between two herpesvirus subfamilies, alpha- and gammaherpesviruses.

4.1 Constitutive heterochromatin leads to tightly repressed alphaherpesvirus genomes

H3K9me3 is the hallmark of constitutive heterochromatin, resembling a very tight form of chromatin. This repressive heterochromatin form is not easily reverted and was shown to favor DNA methylation later on [343, 344].

4.1.1 Acquisition of H3K9me3 on HSV-1*in1374* seems to restrict reactivation

For the first time, the data presented here show that the entire genome of HSV-1*in1374* is covered with H3K9me3 (Fig. 3.6). Unlike a previous ChIP-qPCR study of HSV-1*in1374* [135], the data of this dissertation enabled a whole-genome analysis by performing ChIP-seq.

The establishment of H3K9me3, on the alphaherpesviral genomes, was detected in three different non-neuronal cell lines, already at 24 hpi. In HDF and HAP1 cells, no further epigenetic modification was detected (Secs. 3.5 and 3.6). Therefore, acquisition of H3K9me3 seems to be the default early repression mechanism in these cells. Furthermore, in the cell lines where H3K9me3 was the only repressive histone modification found, a 24 h incubation time at non-permissive conditions lead to a reactivation inability of the lytic-cycle-deficient HSV-1 genomes when shifting the infected cells to the permissive temperature (Fig. 3.12). Therefore, it can be assumed that, in those cells, most viral genomes are tightly repressed already shortly after entering the nucleus. However, under direct permissive conditions a few cells showed productive replication (Fig. 3.12). This finding supports recently published data, where it was shown, for infected non-neuronal cells, that viral progeny is only produced from a minority of HSV-1 genomes [438–440].

4.1.2 PRVΔIE180 genomes colocalize with PML and acquire H3K9me3 but no DNA methylation

With this study, the acquisition of H3K9me3 by lytic-cycle-deficient PRV genomes has been shown for the first time (Fig. 3.2). As for lytic-cycle-deficient HSV-1, this modification was established along the whole genome. The observed acquisition of H3K9me3 on both lytic-cycle-deficient alphaherpesvirus genomes suggests that H3K9me3 is a common mechanism of early repression among alphaherpesviruses.

As mentioned above H3K9me3 was shown to favor DNA methylation later on [343, 344]. Furthermore, previous literature demonstrated that DNA methylation can be found on KSHV genomes in long-term infected cells. Thus, DNA methylation on PRVΔIE180 was investigated, but could not be detected at the analyzed time point (Fig. 3.2C). It has to be noted though that the loss of alphaherpesvirus episomes after several rounds of cell division may have been a limiting factor in this experimental set-up. Unlike the cells used here, the authentic reservoir, which are neurons, do not divide. Hence, it might be that the alphaherpesvirus genomes could acquire DNA methylation in neurons over a long period of time. However, DNA methylation has been already investigated in latently infected neurons with HSV-1, where this epigentic modification was excluded as a silencing mechanism [441]. With these data it can be excluded that DNA methylation leads to the establishment of a repressed alphaherpesvirus genome in the investigated infection-model, but H3K9me3 seems to play an important role in the early silencing of alphaherpesvirus genomes.

It is still not fully understood how the enzymes which establish H3K9me3 are directed to the respective genome regions. The multi-protein complex, PML-NB can harbor the H3K9-methylase, SETDB1 [361] and is known to associate with HSV-1 genomes in quiescent infection models [135].

Thus, PML-NBs might be involved in the establishment of H3K9me3.

The data presented here demonstrate that about 60 % of the lytic-cycle-deficient PRV genomes colocalize with PML (Fig. 3.5). The latter observation is consistent with recently published data showing that PML and PRV colocalize [411]. However, the mentioned study was performed with a replication-competent virus and the colocalization frequency between viral genomes and PML was not quantified.

For replication-competent HSV-1 it was recently demonstrated that treatment of neurons with IFN-α leads to elevated levels of PML expression, which ultimately result in a decrease of viral reactivation [119]. This suggests that highly restrictive repression of vDNA is dependent on the abundance of PML. Indeed, Lukashchuk and Everett [409] showed that PML-NB levels vary among different cell lines. One of their investigated cell lines was U2OS, where they found relatively low levels of PML. This was connected to permissiveness of a HSV-1 ICP0-null mutant [409]. Similar to their study, higher abundance of PML in HDF compared to U2OS cells - observed through IF against PML (Fig. S5) - has also been demonstrated in this dissertation. Therefore, if PML levels are low, which might also result from the missing PML-NB-component ATRX in U2OS cells, viral lytic replication might be facilitated. Furthermore, in U2OS cells hardly any colocalization between PML and vDNA was observed by Alandijany et al. [180].

Therefore, it can be speculated that the cellular background, and thus most likely the abundance of certain host factors, directly influences the repression of alphaherpesviruses. From the studies mentioned above and the data presented here, it can be hypothesized that high PML levels favor the establishment of highly repressed viral genomes, probably through the acquisition of H3K9me3. However, an unanswered question that remains is what happens to viral genomes that do not colocalize with PML.

Interestingly, it has been shown that PML does not colocalize with KSHV-DNA [146]. Furthermore, KSHV genomes acquire H3K9me3 only in long-term infected cells [93, 94], thus, this modification is not involved in the establishment of repression of KSHV genomes [93, 146, 210]. For KSHV, silencing is mediated via PRC and KSHV genomes were observed to colocalize with the host factor KDM2B - a subunit of ncPRC1.1[210].

4.2 Acquisition of facultative heterochromatin seems to facilitate reactivation

The establishment of facultative heterochromatin, especially through H3K27me3, is essential during embryonic development [297, 298]. H3K27me3-silenced genes can become easily activated again [304], which is in contrast to the more permanently silenced genes via H3K9me3.

4.2.1 PRVΔIE180 colocalize with KDM2B and acquires H2AK119ub

This dissertation demonstrated not only colocalization between PML and a subset of PRVΔIE180 genomes, but also between a subset of PRVΔIE180 genomes and KDM2B (Fig. 3.5). This

observation suggests that lytic-cycle-deficient PRV genomes might also be repressed by PRC. This finding is consistent with the ChIP-seq data showing that PRV∆IE180 acquired not only H3K9me3 but also the PRC-mediated repressive histone modification H2AK119ub (Fig. 3.2).

4.2.2 HSV-1*in1374* genomes acquire H2AK119ub in a cell-dependent manner

Matching the observations from Alandijany et al. [180], who detected only few colocalization events between PML and vDNA in U2OS cells, the here presented data showed only low levels of H3K9me3 but high levels of H2AK119ub on lytic-cycle-deficient HSV-1 genomes in U2OS cells (Fig. 3.6). U2OS cells express less PML compared to other cell types like HDFs. Furthermore, they are lacking the chromatin remodeler ATRX, a component of PML-NBs. This deficiency might explain why in contrast to HDFs the facultative histone modification H2AK119ub is found on the viral genomes, in addition to H3K9me3.

Together the acquired epigenetic data of lytic-cycle-deficient PRV and HSV-1 show that PRC-mediated repression can act on alphaherpesvirus genomes, in non-neuronal cells. Furthermore, the RC-formation assay showed that viral genomes are more prone to reactivate in U2OS cells compared to HDFs (Fig. 3.12). When combining these results it can by hypothesized that viral genomes which acquire H2AK119ub are more prone to reactivate than viral genomes that acquired H3K9me3.

4.2.3 Reintroduction of ATRX in U2OS cells leads to a decrease in replication and reactivation

Overexpression of ATRX in U2OS cells led to a significant reduction of reactivation from the repressed state (Fig. 3.13) and viral genomes in those cells showed an increase in H3K9me3 and a decrease in H2AK119ub levels (Fig. 3.9).

This result is consistent with the hypothesis that viral episomes which acquire facultative heterochromatin are more susceptible to reactivate, whereas constitutive heterochromatin is more difficult to remove, making genomes that are repressed by H3K9me3 more unlikely to reactivate. However, to support this result, ChIP-seq of samples should be performed, as qPCR limits the analysis to a few selected loci. In addition, a second replicate of the ChIP experiment should be performed to confirm the observed phenomenon.

4.2.4 Knock-down of ATRX leads to a higher replication ability under permissive conditions

In contrast to the phenomenon observed in U2OS cells, the change in the epigenetic profile of HSV-1*in1374* was only minor when ATRX was depleted in HDFs. H3K9me3 was detected on the viral genomes in HDFviromer and HDFsiATRX cells (Fig. 3.10).

For the HDFviromer cells, this result was expected and demonstrates that the transfection reagent does not impact heterochromatinization, as the virus behaves similarly in HDFwt cells (Fig. 3.6). However, for the confirmed knock-down of ATRX in HDFs this result was surprising since H3K9me3 levels were reduced in U2OS cells. However, the enrichment for H2AK119ub on the HSV-1*in1374* genomes in HDFsiATRX exceeded background level at one viral region (Fig. 3.10). This suggests that upon ATRX depletion some viral genomes might acquire H2AK119ub, which is in contrast to HDFs and HDFviromer cells, where H2AK119ub was not detected on the viral genomes (Fig. 3.6 and Fig. 3.10).

Interestingly, HSV-1*in1374* showed significant higher levels of reactivation ability in HDFsiATRX cells, compared to HDFviromer cells under permissive conditions (Fig. 3.13). In this set-up the repressive histone marks were not established, since genomes were allowed to directly replicate. This observation is similar to the result from HAP1ΔATRX cells (Fig. 3.12). Therefore, it can be assumed that ATRX depletion facilitates virus replication when genomes are able to directly replicate.

Under non-permissive - permissive conditions infected HDFsiATRX cells showed no RCs. Thus, if ATRX levels were reduced but not completely degraded, the amount of protein remaining might be sufficient to cause strong suppression of most viral genomes, which is consistent with the detected H3K9me3 on these viral genomes.

From the acquired data it can be concluded that while the knock-down of ATRX in HDFs had only a modest effect on the viral genome chromatinization under non-permissive - permissive conditions, the ability for lytic replication was significantly increased under permissive conditions. When the infected cells were transferred to permissive conditions, the genomes were probably already tightly repressed by PML-NBs. Since HSV-1*in1374* does not express functional ICP0, which would be needed to degrade ATRX and PML, the viral genomes cannot overcome PML-NBs-mediated restriction. Hence, it can be assumed that even low levels of ATRX are enough to establish tightly repressed virus genomes under non-permissive conditions. However, under permissive conditions with only low ATRX levels subset of genomes is able to start replication, because there is no sufficient restriction mechanism. However, since PML levels hardly change upon ATRX knock-down, and the effect of ATRX is rather modest, PML alone might be more important for H3K9me3 establishment than ATRX.

In conclusion, the here presented data could show that ATRX is involved in tight repression of the viral genomes. However, ATRX seems to be non-essentially involved in the mechanism of the formation of constitutive heterochromatin, which can be probably taken over by other proteins or PML-NBs/ATRX-mediated repression is not necessarily associated with H3K9me3.

4.2.5 Knock-out of ATRX in HAP1 cells results in a general defect of chromatinization

In contrast to HDFsiATRX cells, in HAP1ΔATRX cells neither H3K9me3 nor H2AK119ub was detected on viral genomes. Furthermore, chromatinization of the viral genomes, in the latter

cells, was generally impaired (Fig. S4). Strikingly, reintroduction of ATRX to those cells did not lead to increased chromatinization levels. However, this phenomenon might have resulted from selected cells that did not longer express the ATRX construct. Thus, the results from this experiment should be treated with caution. However, it could also be that the vDNA is just degraded without chromatinization in those cells. This would lead to degraded vDNA which could then be detected as a signal in ChIP input samples. To investigate this further, HAP1 and HAP1ΔATRX should be infected with KSHV and chromatinization should be compared. Since KSHV is not associated with PML-NBs, but only becomes repressed by PRCs [146], ATRX depletion should not influence its heterochromatinization. An observed change would hint towards a general chromatinization impairment in the HAP1ΔATRX cells. If KSHV's chromatinization would be different in HAP1ΔATRX compared to HAP1 cells, the observed phenomenon could not be exclusively connected to the absence of ATRX.

4.3　Alphaherpesviruses appear to form two different silenced subpopulations

Since H3K9me3 and H2AK119ub establish two distinct forms of heterochromatin - consitutive and facultative heterochromatin - and do not coexit at the same regions on the cellular genome, it is unlikely that both marks are established on the same viral episome. Therefore, it can be assumed that there might be two subpopulations, acquiring different forms of heterochromatin.

An easily reversible repression, like it is established by facultative heterochromatin would support the herpesvirus life cycle, since genomes can reactivate from their latent state. This means they have to erase the repressive modification and instead acquire activating marks. This would be much easier from factulative heterochromatin than from constitutive heterochtomatin. Nevertheless, it is hypothesized that some genomes never reactivate [443], which would support a scenario of two subpopulations where H3K9me3 could be a "dead-end" to the virus. Moreover, the colocalization experiment between PRVΔIE180 genomes and the host factors PML and KDM2B further support this hypothesis, although no parallel colocalization experiment could be performed due to problems with the KDM2B antibody. Thus, a validation of this hypothesis is lacking an should be performed in the future.

Cliffe, Coen, and Knipe [95] showed that lytic gene promoters acquired H3K27me3 at 14 dpi and also demonstrated association between SUZ12 and parts of HSV-1. A few years earlier, the same group showed increasing levels of H3K9me2 on vDNA, from 5 dpi to 15 dpi, in latently infected neurons [444]. Furthermore, they observed an increase in vDNA, until 3 dpi, which afterwards dropped rapidly, highlighting the ongoing viral replication in the beginning of an HSV-1 infection [444].

Bringing these two findings together, it seems that progeny production of a *de novo* infection at 3 dpi is followed by H3K9me2-induced silencing at 5 dpi. Ultimately, only at 14 dpi H3K27me3 could be detected. Thus, there is first evidence that two distinct virus populations could exist in latently infected neurons:

- one population tightly silenced by H3K9me2 early during infection via PML-NBs, maybe dependent on interferon levels in the respective neuron,

- whereas the other population could be already decorated with H2AK119ub, which had not been analyzed yet, and will be later restricted via H3K27me3, by PRC2.

Such a mechanism would be in partial agreement with the genome-wide data shown here, where very early during lytic infection, H3K9me3 was detected on replication-competent PRV genomes (Fig. 3.3). In this early infection state, H3K36me2 was still prevalent and neither H2AK119ub nor H3K27me3 were established. This indicated that PRC is not present on the PRV genome that early during lytic infection. PRC might even never be recruited during lytic infection, since either genomes are already silenced by H3K9me3 and thus entrapped by PML-NBs, i.e. they are not accessible, or genomes will start to replicate and subsequently, acquire activating histone modifications. This finding adds more evidence to the hypothesis that two viral subpopulations could be established during alphaherpesvirus infections.

The results of this dissertation could show that PML-NB-mediated repression seems to be the major silencing pathway in human fibroblasts, with H3K9me3 being the only repressive modification on the viral genomes, which is in agreement with recently published data from Cohen et al. [135]. In addition, the PML-NB component ATRX seems to be important for a tight repression of vDNA. Furthermore, the high percentage of colocalization events between PRVΔIE180 genomes and PML together with the epigenetic profile, with H3K9me3 being highly enriched on the viral genomes, suggests a connection between the colocalization of PML and H3K9me3. However, the presence of H2AK119ub and the colocalization of KDM2B with a subset of PRVΔIE180 genomes, in the same cell type, indicates that an alternative repression mechanism, via acquisition of facultative heterochromatin, exists. Nevertheless, further investigations are required in order to be able to fully understand the molecular mechanisms which govern establishment and maintenance of herpesviruses latency.

4.4 DNA replication might balance the two states of heterochromatin establishment

The histones H3.1 and H3.2 are incorporated into the cellular genome in a strictly replication-depended manner, whereas H3.3 can be also incorporated into nucleosomes without ongoing replication [258]. As a result, histone variants change during the progress of a lytic viral infection. Very early during infection, the histone variant H3.3 is incorporated into the viral chromatin by default but becomes replaced by H3.1 upon replication initiation [447]. The histone variants are deposited onto DNA by distinct histone chaperones. For H3.1 and H3.2 this histone chaperone is CAF-1 [254, 259]. H3.3 is deposited by the histone chaperone complexes ATRX/DAXX and HIRA [261].

Since both H3.3 chaperone complexes, HIRA and ATRX/DAXX, were found to colocalize with vDNA, it was hypothesized that H3.3 would also be found in association with HSV-1 genomes.

Cohen et al. [135] showed that DNA of a lytic-cycle-deficient HSV-1 mutant almost exclusively colocalized with H3.3. Furthermore, ChIP-qPCR-data of this study showed that H3K9me3 is established on H3.3. By depleting ATRX, DAXX or HIRA they observed decreased colocalization of vDNA with PML, although PML levels were similar to untreated cells. A phenomenon that was also observed in this dissertation upon ATRX depletion (Fig. S5. The absence of PML alone significantly affected H3.3 levels on HSV-1 genomes. When depleting PML, colocalization between HSV-1 DNA and ATRX and DAXX was significantly decreased, whereas colocalization between viral genomes and HIRA was unaffected. This finding suggests that H3.3 deposition is associated with PML-NBs which harbor ATRX/DAXX. Furthermore, they could show that viral genomes can reactivate from the PML-NB-repressed state only if ICP0 is reintroduced [135].

The data presented in this dissertation could extend the findings from Cohen et al. [135] to a genome-wide level on two different alphaherpesviruses. Furthermore, another repressive histone modification, H2AK119ub, was detected, showing that PRC1 is associated with replication-deficient alphaherpesvirus genomes.

The establishment of H3K27me3 requires active DNA replication, since it was shown that H3K27me3 can only be (re)established after mitosis [448]. Only then H3.3 is exchanged by H3.1, which can be modified by PRC2, as H3.3 was shown to be a poor PRC2 target [449, 450]. Furthermore, H3K27-monomethyltransferases were observed to be specific for H3.1 [451]. Thus, although PRC2 might be recruited to the alphaherpesvirus genomes, via the nc PRC-repression pathway, the complex is probably unable to perform methylation of H3K27 on the non-replicating genome.

In contrast to alphaherpesviruses, the gammaherpesvirus KSHV undergoes licensed latent replication, which leads to H3.1 deposition onto the vDNA during latency and, subsequently, to silencing via H3K27me3. Therefore, it is rather unlikely that H3K27me3 can be established on HSV-1 genomes. However, just recently H3K27me3 was detected on two viral promoters in a non-neuronal cell line [136]. In addition, other studies were able to observe H3K27me3 on HSV-1, in latently infected neurons [134, 414] - and even its interaction with SUZ12 [95]. Thus, there might be a currently unknown distinction between neuronal and non-neuronal cells that can lead to H3K27me3 acquisition on latent HSV-1 genomes. Hence, for neurons, the exact molecular mechanism of how PRC2 should be recruited to the viral non-replicating alphaherpesvirus genomes is still an open question. Therefore, it would be of interest to investigate the histone variations that are deposited onto alphaherpesviruses DNA in neurons.

Given the two distinct heterochromatin modifications detected here in lytic-cycle-deficient HSV-1 and PRV together with the data on the host factors PML and KDM2B, relevant new insights into how alphaherpesviruses establish latency were gained. Overall, the data presented here not only shed more light on the early heterochromatinization of alphaherpesviruses but also raises exciting new questions. These should help to design further experiments aimed at investigating the link between histone modifications and the ability of alphaherpesviruses to reactivate, as well as investigating additional potential host factors that may be involved in the early repression process.

4.5 Proposed model of balancing epigenetic repression on herpesviral DNA

Summing up, this study proposes that PRC-mediated repression leads to the establishment of authentic alphaherpesvirus latency reservoirs with the ability to reactivate, while PML-NB-mediated repression may result in permanent silencing and, in dividing cells, even lead to subsequent elimination of the virus (Fig. 4.1A). Hence, this study proposes a model of two differently silenced alphaherpesvirus subpopulations.

In contrast to KSHV, alphaherpesviruses acquire distinct heterochromatin states, which may depend on the cellular background. For KSHV, the unmethylated CpG-rich vDNA becomes repressed by PRC, whereas for PRV there seems to be some kind of balance between PRC- and PML-NB-mediated repression, early in infection. For HSV-1, the results presented here revealed that ATRX plays a role in tightly repressing its genomes. Therefore, ATRX levels might influence the balance between the two different repressive histone modifications (Fig. 4.1B). However, knock-down of ATRX was not sufficient to abolish H3K9me3, even in U2OS cells in which ATRX is completely depleted. The overexpression of ATRX in U2OS cells resulted in a modest increase in H3K9me3, and modest decrease in H2AK119ub levels. Thus, it seems that ATRX is not the essential host factor influencing the repression of alphaherpesviruses. Therefore, further studies are needed to investigate additional host factors involved in H3K9me3 deposition on vDNA. Furthermore, additional single-genome experiments should be performed to conclusively prove the proposed model of the co-existence of two viral subpopulations.
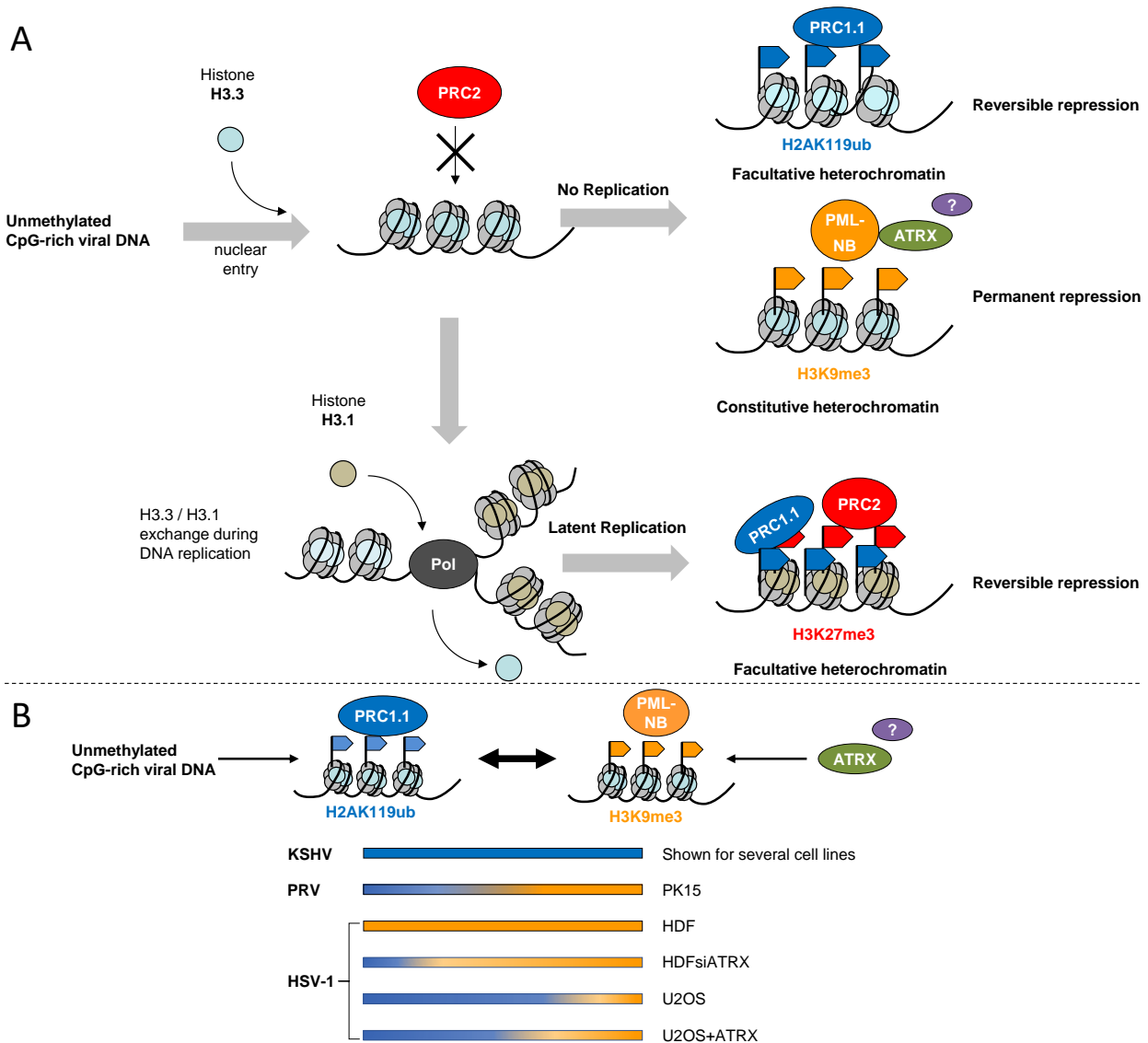
Figure 4.1: Proposed Model of balancing epigenetic repression on herpesviral DNA. (A) Proposed mechanism of how and why CpG-rich vDNA can be silenced by different host factors. The exchange of H3.3 by H3.1 during KSHV's licensed latent replication might be the driver for PRC2-mediated repression of KSHV. In contrast, the non-replicating alphaherpesvirus genomes seem to be poor targets of PRC2 since histone H3.3 is not exchanged. Thus, in the "quasi-latent" infection system studied here, alphaherpesvirus genomes only acquired the PRC1.1-mediated repressive histone modification H2AK119ub to acquire a repressed state that can be easily revised, while another part of the alphaherpesvirus genomes acquired H3K9me3 as more permanent repression. (B) Graphical summary of the findings of the work presented here, compared to currently published data of our group about KSHV. In contrast to KSHV, lytic-cycle-deficient PRV and HSV-1 acquire H3K9me3 and H2AK119ub. However, the acquisition of these modifications seems to be dependent on the cellular background. One host factor that might influence the balance between the two modifications is ATRX. In HDFs only H3K9me3 was detected on the viral genome, however, a knock-down of ATRX in those cells enabled the acquisition of H2AK119ub. Nevertheless, H3K9me3 seemed still to be the dominant histone modification on the viral genomes in the knock-down cell line. Overexpression of ATRX in U2OS cells shifted the balance from a high occupancy of H2AK119ub to slightly more H3K9me3 in those cells.

5 Conclusion and Outlook

The work of this dissertation aimed to decipher early events of herpesvirus infection, after entry into the nucleus. As a basis for this, recently published data from our group suggested that PRC-mediated repression may represent a default pathway that silences CpG-rich vDNA. Thus, we hypothesize that herpesviruses with high CpG content may generally exploit this pathway to support latency establishment. Investigating this hypothesis was the subject of the work presented here.

In conclusion, the data of this dissertation showed a new aspect of alphaherpesvirus silencing with the histone modification H2AK119ub on two different lytic-cycle-deficient alphaherpesviruses. With this finding, the present work was able to generalize parts of the PRC-mediated repression mechanism between two herpesvirus subfamilies, dependent on the cellular background. Moreover, this is the first study describing repressive histone modifications on lytic-cycle-deficient PRV genomes. Therefore, the work of this dissertation contributes to a better understanding of the epigenetic regulatory processes which lead to the establishment of early repression of incoming herpesviral DNA. The observed cell-dependent establishment of distinct heterochromatin states on alphaherpesvirus genomes seems to be partly influenced by ATRX, a component of PML-NBs. However, the effects of its downregulation or overexpression were rather modest. Thus, the investigation of additional host factors involved in establishment of constitutive heterochromatin via H3K9me3 should be a focus of future studies.

One such host factor could be PML, since it is the scaffold protein of PML-NBs and its absence was shown to influence H3.3 levels on HSV-1 genomes. It would be interesting to investigate the state of viral chromatin when PML itself is depleted. If the absence of PML were to lead to the absence of H3K9me3 and viral genomes acquire H2AK119ub instead, it could be proclaimed that PRC-mediated repression is impaired by the presence of PML. Another host-factor described to be involved in early sensing of vDNA is Interferon gamma-inducible protein 16 (IFI16) [136, 452, 453]. Moreover, IFI16 and PML were shown to have restrictive functions for the viral genome but are distinct from each other [180, 452]. Therefore, it would be of interest to study the epigenetic landscape of alphaherpesviruses in relation to IFI16.

Furthermore, this study proposes the existence of two alphaherpesviral subpopulations. One being suppressed by PRC, leading to the establishment of true alphaherpesvirus latent reservoirs with the ability to reactivate, and the other being suppressed by components of PML-NBs, leading to permanent silencing of the virus. However, the existence of the two subpopulations needs to be further proven by single-genome investigations. Parallel colocalization studies of individual alphaherpesvirus genomes, each colocalizing with components of only one of the two protein

complexes, PRCs or PML-NB, would support the observations made in this work.

Another interesting question remaining from this study is how H3K27me3 is established on HSV-1 genomes in neurons, as shown by several publications [95, 134, 136]. Especially the presence of H2AK119ub and histones of latent HSV-1 genomes, in infected neurons, should be investigated, since this would help to understand whether there might be a histone variant exchange. Additionally, it should be further analyzed whether two virus subpopulations can be found in such an infection system. So far the H3K9me2 and H3K27me3 were reported to be both found on HSV-1 genomes, in latently infected neurons of mice [444]. Interestingly, when neurons were first explanted and then infected, PML-association with viral genomes was only observed when treated with IFN-α, before infection [119]. However, no epigenetic analysis on the viral genomes in this infections was performed. Epigenetic data of HSV-1 in infected neurons are still lacking and based on the study by Suzich et al. [119], explant-neurons seem to be a suitable and highly interesting model system to be used for this.

According to the model postulated here, H3K9me3 together with PML-NB association could lead to the elimination of herpesvirus genomes, in dividing cells. Therefore, it would be interesting to investigate whether this silencing pathway can be enforced in other herpesviruses and whether this leads to the elimination of viral genomes. For this purpose, a system could be used that allows to recruit e.g. individual components from PML-NBs to herpesviruses such as KSHV, which was not found to be associated with PML-NBs. Such a system would allow to investigate whether the respective host factors affect heterochromatinization and virus genome maintenance. Such a system is currently being established in our laboratory and could thus answer this question in the future.

6 Material and Methods

6.1 Material

6.1.1 Chemicals and consumables

Table 6.1: List of media used for cell culture

Name	Supplier
Fetal bovine serum (FBS)	Gibco
Dulbeccos's modified eagle's medium (DMEM)	Gibco
OptiMEM-I	Gibco
Medium199	Gibco

Table 6.2: List of chemicals used for cell culture

Name	Supplier
Dimethylsulfoxide (DMSO)	Sigma-Aldrich
Trypsin-EDTA	Thermo Fisher Scientific
4-(2-hydroxyethyl)-1-piperazineethanesulfonic acid (HEPES)	Thermo Fisher Scientific
Sodium-Pyruvate	Thermo Fisher Scientific
Dulbecco's phosphate buffered saline (DPBS)	Merck
Polybrene	Sigma-Aldrich
Lipofectamin2000	Thermo Fisher Scientific
	Continued on next page

Name	Supplier
Polyethylenimine (PEI)	Thermo Fisher Scientific
TransIT®-LT1	Mirus
EdC	Sigma-Aldrich
SensiMix™ SYBR	Meridian Bioscience (Bioline)

Table 6.3: List of antibiotics used for cell culture

Name	Supplier
Penicillin/Streptomycin (pen/strep)	Sigma-Aldrich
Doxycyclin (Dox)	Thermo Fisher Scientific
Zeocin	Thermo Fisher Scientific
Puromycin	Thermo Fisher Scientific
Hygromycin	Thermo Fisher Scientific

6.1.2 Cells

The following cells were used in this study.

Table 6.4: List of cells used in this study

Name	Description	Supplier
PK15	Pig epithilial kindney cells	A gift from the lab of Lynn Enquist
PI	Pig epithilial kindney cells with Dox inducible IE180 construct	A gift from the lab of Lynn Enquist, constructed by [415]
U2OS	Osteosarcoma cells	A gift from the lab of Thomas Dobner
		Continued on next page

Name	Description	Supplier
BJ	hTert immortalized human foreskin fibroblasts, tranfected with the pGRN145 hTERT-expressing plasmid (ATCC MBA-141), constructed by [454]	ATCC (CRL-4001™)
HDF	Human Dermal Fibroblasts	Lonza (CC-2509)
LentiX 293T	subclone of the transformed human embryonic kidney cell line HEK293	Clontech (Cat No. 632180)

6.1.3 Viruses

The following viruses were used in this study.

Table 6.5: List of viruses used in this study

Name	Description	Supplier
PRV960	Pseudorabies Virus with a mCherry tag at VP26	A gift from the lab of Lynn Enquist, constructed by Jens Bosse
PRV943c	Pseudorabies Virus with a GFP tag at VP26	A gift from the lab of Lynn Enquist, constructed by Jens Bosse
PRV943c-EdC	Pseudorabies Virus with a GFP tag at VP26 and EdC incorporation to perform click-chemistry	EdC-incorporation by Heidi Meissner
PRV128	replication deficient Pseudorabies Virus without IE180	A gift from the lab of Lynn Enquist, constructed by [415]
		Continued on next page

Name	Description	Supplier
PRV128-EdC	replication deficient Pseudorabies Virus without IE180 and EdC incorporation to perform click-chemistry	EdC incorporation by Heidi Meissner
HSV-1 VP26-mCherry	Human Herpes Virus-1 with VP26-mCherry tag	A gift from the lab of Beate Sodeik, [455, 456]
HSV-1*in1374*	replication deficient Human Herpes Virus-1 with temperature sensitive ICP4, permissive at 32 °C, deletion in ICP0 and insertion in VP16	Gift from Roger Everett

6.1.4 Bacteria

All experiments were done using one bacterium

Table 6.6: Bacteria used in this study

Name	Description	Supplier
Escherichia coli DH5α	F– Θ80lacZΔM15 Δ(lacZYA-argF) U169 recA1 endA1hsdR17 (rK–, mK+) phoA supE44 λ– thi-1 gyrA96 relA1	Thermo Fisher Scientific

6.1.5 Medium for bacteria

Medium for bacteria contained the following components.

Table 6.7: List of medium for bacteria culture used in this study

Reagent	Ingredients	Supplier
Lysogeny Broth (LB) medium	1 % Trypone 0.5 % Yeast extract 0.5 % sodium-chloride (NaCl)	Roth
Lysogeny Broth (LB) agar	1 % Trypone 0.5 % Yeast extract 0.5 % NaCl 15 g/L Agar-Agar	Roth
Super Optimal Broth (SOC) medium	2 % Trypone 0.5 % Yeast extract 0.5 % NaCl 10 mM NaCl 2.5 mM kalium-chloride (KCl) 10 mM magnesium-chloride (MgCl) 10 mM magnesium-sulfate (MgSO$_4$) 20 mM Glucose	Thermo Fisher Scientific

6.1.6 Oligonucleotides

All oligonucleotidese were designed with the web-based primer-designing tool primer-blast, from NCBI. All oligonucleotides were ordered from eurofins genomics.

Table 6.8: List of conventional PCR primers used in this study

Name	Sequence
PRVΔIE180-Bleo homology_fw	ATCAGCGCGGTCCAGGACCAGGTG
PRVΔIE180-Bleo homology_rv	AATTCCCACTCCTTTCAAGACCTAGA
ANCH_1kb fragment_overlap PRVΔIE180_Bleo_fw	TCTAGGTCTTGAAAG-GAGTGGGAATTCGTCACTTTG-GCAGGATCT
ANCH_short fragment_overlap PRV128_Bleo_fw	TCTAGGTCTTGAAAGGAGTGGGAAT TCTTTCAACGTTGAAACAAGAGAGC
SFFV promotor-Hygro_fw	TGAAAGACCCCACCTGTAGGTTTG

Name	Sequence
ANCH_1kb fragment_overlap SFFV-promotor_rv	CAAACCTACAGGTGGGGTCTTTCAT-GCCAAGCTCGGCATGATCACCTCAGT
ANCH_short fragment_overlap SFFV-promotor_rv	CAAACCTACAGGTGGGGTCTTTCATT TTCAACGTTGAAAATCGGGAGATCC
PRVΔIE180-WPRE_homology_rv	AAGTCCCGGAAAGGAGCTGACAG
PRVΔIE180-WPRE_homology_fw	TCTAGAGATTACATCAAGCTTATC
Hygro_rv_ overlap WPRE	GATAAGCTTGATGTAATCTCTAGACT ATTCCTTTGCCCTCGGACGAGTG
EM7 fw	CATCGGCATAGTATATCGGCATAGT
ANCH long fw	CGTCACTTTGGCAGGATCT
Hygro rv	CTATTCCTTTGCCCTCGGACGAGTG
ANCH short fw	CTTTCAACGTTGAAACAAGAGAGC
EM7/Bleo rv.2	CCCACTCCTTTCAAGACCTAGA
EM/Bleo short_ rv overhang	GTCCTGCTCCTCGGCCACGAAGTGA-GATCCTGCCAAAGTGACG
RE_WPRE_overhang	GCGGCCGCTGTCAAGAATATTAAC-GAAGTCCCGGAAAGGAGCTG
RE_EM7_overhang	CTCGAGAGCGTTAATATTCTTGAT-CATCGGCATAGTATATCGGC
IE180_fw	CTTATAAGCGCGGTCTCCATC
IE180 _rv	GGTTCAGAAAATACAGCACAAAC
EGFP_left_overhang_fw.2	GTGGTGCCCATCCTGGTC
EGFP_right_overhang_fw.2	CTCGTCCATGCCGAGAG
IE180_SbfI_kozak_fw	CCTGCAGGGCCACCATGGCCGAC-GATCTCTTTG

Name	Sequence
IE180_V5_NheI_rv	GCTAGCGGTTCCGTAGAATCGAGAC-CGAGGAGAGGGTTAGGGATAGGCT-TACCGTCAGCGGAGCAGCAGGTAG
NdeI_Hygro-homology_SceI_Kana_fw	CATATGCGCGATTGCTGATCCCCATG TGTATCACTGGCAAACTGTGATGGA CGACTAGGGATAACAGGGTAATCGA TTTATTCAACAAAGC
NdeI_Kana_rv	CATATGGCCAGTGTTACAACCAAT-TAAC
WPRE_96bp_rv	GCGTAAAAGGAGCAACATAGTTAAG
EM7_107bp_fw	GACTGACACGTGCTACGAGG
EM7_shorter-homology_fw_2	AGGACTGACACGTGCTACGA
WPRE_shoerterhomology_rv_2	GCAGCGTATCCACATAGCGT
10bp_NdeI_Hygro-homology_SceI_Kana_fw	GCGTGATTTCATATGCGCGA
10bp_NdeI_Hygro-homology_SceI_Kana_rv	CAATCGCGCCATATGGCCAGT
IE180_primer_fw	ATGGCCGACGATCTCTTTG
IE180_primer_rv	TCAGCGGAGCAGCAGGTAG
BamHI_Kozak_Blast_fw	CGCCCGGATCCGCCACCATGGC-CAAGCCTTTGTCTC
EcoRI_Blast_rv	CCGGAATTCTTAGCCCTCC
BamHI_Kozak_Neo_fw	CGCCCGGATCCGCCAC-CATGGGCAGCGCCATCGAGC
EcoRI_Neo_rv	CCGGAATTCTCAGAAGAACTCG
fw_sgRNA1+2_PRV128	GTGCGTGTCATCGTGGTCG
rv_sgRNA1+2_PRV128	AAAGATGCGCTTGTTTGGCA
fw_sgRNA3_PRV128	CGGCAGGATCTCTCTGCATC

Name	Sequence
rv_sgRNA3_PRV128	CTCGTCTCTCGGGCGTTTTT
fw_sgRNA3_PRV128_2	CAACTCTCTCGTCTCTCGGG
rv_sgRNA3_PRV128_2	CTGAGCCCGGCAAGGTATAA
fw_sgRNA4_PRV128	GGATGTGTGGTCCGACGAAG
rv_sgRNA4_PRV128	AAGTGCGAACGCCGAAAAT
fw_sgRNA5_PRV128	GTCGCGTCCGAGTTTAGCTT
rv_sgRNA5_PRV128	GAGAGTTGAGGTTCGAGCGG
fw_sgRNA1+2_PRV128	GCCCCGTGTGTGGAAATA
fw_sgRNA4_PRV128	AAGAACATTTTCACCCGCGCT
rv_sgRNA4_PRV128	CCGTCCCGTCGAATCCA
fw_sgRNA3_PRV128	CTCGAACCCGACGCGCCC
rv_sgRNA3_PRV128	GTTTATTGAGGGCACAACAGAG
HSV-1_US8_fw	CATGGACGTCGTCTGGTTGA
HSV-1_US8_rv	CGGAGCCGTTGGTGATAAGA
HSV-1_UL39_fw	GATCATCGACGGAGACGTGG
HSV-1_UL39_rv	CATGTAGTGCCCGCCAAAAC

Table 6.9: List of primers used for qPCR in this study

Name	Sequence
ss_MYT1_fw	GATGGCTTGTGGAAGAGCCT
ss_MYT1_rv	AGTGAAAGAGCACGGAAGGG
ss_GAPDH_fw	AGCTGAGGTCCAGCTGACTA
ss_GAPDH_rv	TAAGCCTTCTACCCCTGCCT
ss_RPLP0_fw	TAAATCTGCAGCAACTTGCCTCT

Continued on next page

Name	Sequence
ss_RPLP0_rv	TGTATCCATCTTTGGGGAAGTCTG
prv_US8_fw	ACGTTCGACCTGATGCCG
prv_US8_rv	CGTAGTACCAGTCCAGCGTG
prv_US8/9_fw	GTGACGAATGGGCCCAACTA
prv_US8/9_rv	CTCCCGGTATTTAAGCGGGG
prv_UL54_fw	GAGGTGCAGGCGATTGTAGC
prv_UL54_rv	GACCTCGAAGAAGGGCACG
prv_US4_fw	GATGGAGTACGCCCTCGTGA
prv_US4_rv	CGAGCACGACGATGTACAGG
rv_UL27_fw	CACACCACCAACGACACCTA
prv_UL27_rv	TCCTCGACGATGCAGTTGAC
hs_C1ORF43c_fw	AGTGGGTGGAGAATGCAGAC
hs_C1ORF43c_rv	GAGATTACCCCACCCCATTC
hs_HOXC12long_fw	AAAGCTTCCCACTGCAAAGA
hs_HOXC12long_rv	AAATCTGGGGGCGAACTACT
hs_ZNF268_fw	AATGCATTTCCACACTGCAA
hs_ZNF268_rv	AAAGAGGTTGCTGCCAAGAC
ss_MYT1_fw	GGCTTCTTAGGCAGGAGACC
ss_MYT1_rv	AAGACAGACGCTCACATGGC
ss_ZNF312_ss_1_fw	TTCTTCCTCTGGGAGAGTCCT
ss_ZNF312_ss_1_rv	AAGACCTGGAGAAACCGAAGG
ss_GAPDH_fw	GTAAAGTCGCGAGTAGCCGA
ss_GAPDH_rv	GTGCACATTGGCAGAACCAG
hsv_UL38_fw	GGCTGCGAACCATCTTGTTG
hsv_UL38_rv	CCTGTTGGCGCAGTTTCAG

Name	Sequence
hsv_UL39_fw	CAGACGTTTGACTTTGGGCG
hsv_UL39_rv	TGTAGCGTGCTGTCGATCAT
hsv_UL40_fw	GTGATATGCCGGGTCACGAT
hsv_UL40_rv	GGCCTGTGGACTCTTCTGAA
hsv_US8_fw	ATGGACGTCGTCTGGTTGAG
hsv_US8_rv	GCTGCGGGTGATACAGACAC

6.1.7 Buffers

Table 6.10: Composition of transformation buffers to produce chemically competent bacteria

Reagent	Ingredients	pH
Transformation buffer I	100 mM $RbCl_2$ 30 mM potassium acetate (KAc) 10 mM $CaCl_2$ 50 mM $MnCl_2$ 15 % (v/v) glycerol acetic acid	5.8
Transformation buffer II	10 mM $RbCl_2$ 10 mM MOPS 75 mM $CaCl_2$ 15 % (v/v) glycerol	-

Table 6.11: Buffers used for agarose gel electrophoresis

Reagent	Ingredients	pH
50x TAE	2 M Tris-HCl 50 mM EDTA 5 % (v/v) acetic acid	8.0

Table 6.12: Buffers for SDS-PAGE and Western Blot

Reagent	Ingredients	pH
Resolving Gel	375 mM Tris-HCl 10 % Acrylamide 0.01 % TEMED 0.1 % Ammonium persulfate 0.1 % SDS	8.8
Stacking Gel	125 mM Tris-HCl 4 % Acrylamide 0.3 % SDS	6.8
High Salt Buffer	50 mM Tris-HCl 300 mM NaCl 0.5 % Triton-X-100 0.1 % SDS	8.0
Nuclear Extraction Buffer	50 mM Tris-HCl 150 mM NaCl 0.5 % nonident-P-40 (NP-40)	8.0
Protein Extraction Buffer	5 mM Hepes 1.5 mM $MgCl_2$ 300 mM NaCl 0,5 mM DTT	8.0
5X Sample Loading Buffer	200 mM Tris-HCl 12 % (w/v) SDS 40 % (v/v) Glycerol 5 % (v/v) beta-Mercaptoethanol 0.004 % Bromphenolblue	8.0
1X Running Buffer	25 mM Tris-HCl 3.5 mM SDS 192 mM Glycin	8.3
10X TBS-T Buffer	100 mM Tris-HCl 1.5 mM NaCl 1 % Tween	8.0
Buffer C	25 mM Tris-HCl 25 mM Aminohexanoic Acid 10 % Methanol	9.4

Reagent	Ingredients	pH
Buffer B	25 mM Tris-HCl 10 % Methanol	10.4
Buffer A	300 mM Tris-HCl 10 % Methanol	10.4

Table 6.13: ChIP buffer compositions

Reagent	Ingredients	pH
ChIP-Buffer I	50 mM Hepes-KOH 140 mM NaCl 50 mM EDTA 10 % Glycerol 0.5 % NP-40 0.25 % Triton X-100	8.0
ChIP-Buffer II	10 mM Tris-HCl 200 mM NaCl 1 mM EDTA 0.5 mM EGTA	8.0
ChIP-Buffer III	50 mM Tris-HCl 10 mM EDTA 1 % SDS	8.0
ChIP Dilution-Buffer	16,7 mM Tris-HCl 1.2 mM EDTA 0.01 % SDS 167 mM NaCl 1.1 % Triton X-100	8.0
ChIP Elution-Buffer I	50 mM Tris-HCl 10 mM EDTA 1 % SDS	8.0
ChIP Low-Salt-Buffer	20 mM Tris-HCl 150 mM NaCl 2 mM EDTA 1 % Triton X-100 0.1 % SDS	8.0

Continued on next page

Reagent	Ingredients	pH
ChIP High-Salt-Buffer	20 mM Tris-HCl 500 mM NaCl 2 mM EDTA 1 % Triton X-100 0.1 % SDS	8.0
ChIP LiCl-Buffer	10 mM Tris-HCl 250 mM LiCl 1 mM EDTA 1 % NP-40 1 % Na-Deoxycholate	8.0
ChIP TE-Buffer	10 mM Tris-HCl 1 mM EDTA	8.0
ChIP CaCl$_2$-Buffer	10 mM Tris-HCl 300 mM CaCl$_2$	8.0

6.1.8 Antibodies

Table 6.14: List of primary antibodies used in this study

Name	Description	Supplier
anti-VP5	anti-HSV-1 + HSV-2 ICP5 major capsid protein antibody, mouse monoclonal	Abcam
anti ICP8	anti-HSV-1 ICP8 antibody, mouse monoclonal	Santa Cruz
anti KDM2B	anti-JHDM1B (KDM2B) antibody, rabbit polyclonal	Merck Millipore
anti PML	anti-PML (PG-M3), mouse monoclonal	Santa Cruz
anti ATRX	anti-ATRX antibody, rabbit polyclonal	Abcam
anti ATRX	anti-ATRX antibody, clone f39, mouse polyclonal	A gift from the lab of Thomas Dobner
		Continued on next page

Name	Description	Supplier
anti H3K9me3	anti-trimethyl-histone H3 (Lys9) antibody, rabbit polyclonal	Active Motiv
anti H3K27me3	anti-methyl-histone H3 (Lys27) (C36B11), rabbit monoclonal	Cell Signaling
anti H3K27ac	anti-histone H3 (acetyl K27) antibody, rabbit polyclonal	Abcam
anti H3K4me3	anti-trimethyl-histone H3 (Lys4) antibody, clone MC315, rabbit monoclonal	Merck Millipore
anti H3K36me2	anti-dimethyl-histone H3 (Lys36), rabbit polyclonal	Merck Millipore
anti H2AK119ub1	anti-ubiquityl-histone H2A (Lys119), rabbit monoclonal	Cell Signaling
anti H3	anti-histone H3 (pan H3) antibody, rabbit polyclonal	Abcam
anti H3.3	anti-histone H3.3 antibody, rabbit polyclonal	Merck Millipore

Table 6.15: List of secondary antibodies used in this study

Name	Description	Supplier
Alexa-488	goat anti-rabbit IgG (H+L) cross adsorbed Alexa Fluor 488-conjugated secondary antibody, polyclonal	Invitrogen
Alexa-555	goat anti-rabbit IgG (H+L) cross adsorbed Alexa Fluor 555-conjugated secondary antibody, polyclonal	Invitrogen

6.1.9 Plasmids

Table 6.16: List of plasmids used in this study

Name	Description	Supplier
Lenti VSV env R861	used for the production of infectious lentivirus containing supernatants, expressing the envelope protein	Addgene
Lenti gag-pol	used for the production of infectious lentivirus containing supernatant, expressing the group-antigen and the polymerase	Addgene
Lenti rev	used for the production of infectious lentivirus containing supernatant, expressing the rev-responsive element	Addgene
ANCHOR	A vector containing the ANCH and OR sequence	A gift from the lab of Kerstin Bystricky
LeGo-sgRNAs	LeGo vector containing sgRNA against PRV genome	Designed by Thomas Günther
px458-Cas9-GFP-gRNA-hATRX	Vector with Cas9, sgRNA against ATRX and GFP expression	Designed by Simon Weißmann
PiggyBac pTet-ON hsATRX	PiggyBac backbone containing inducible ATRX-EGFP expression cassette	backbone from Sanger Plasmid Repository, constructed for ATRX overexpression purpose by Simon Weißmann
PiggyBac Transposase pCMV hyPBase	PiggyBac helper plasmid, expressing the transposase for efficient integration	Sanger Plasmid Repository

6.1.10 siRNAs

Table 6.17: List of siRNAs used in this study

Name	Description	Supplier
siATRX	ON-TARGETplus siRNA reagent ATRX, smartpool	Horizon/Dharmacon
siScr	ON-TARGETplus non-targeting siRNA	Horizon/Dharmacon

6.1.11 Kits

Table 6.18: List of kits used in this study

Name	Supplier
Zymo Gelextraction	Zymo
Mini-prep	Qiagen
Maxi-prep	Qiagen
DNA clean and concentrator	Zymo
Gibson Assembly	NEB
Mycoplasm Detection	Merck
Molecular Probes Click-iT Plus Alexa Fluor 555 Picolyl Azide Toolkit	Thermo Fisher Scientific

6.1.12 Devices

Table 6.19: List of devices used in this study

Name	Supplier
Nikon Spinning Disk	Nikon
Nikon A1	Nikon
Gel-Doc	BD Biosciences
Rotorgene	Qiagen
PCR-cycler	NEB
Nano-Drop 1000	Thermo Fisher Scientific
Incubator	Heracell
Thermomixer	Thermo Fisher Scientific
	Continued on next page

Name	Supplier
Waterbath	Heraeus
Sterile Bench	Heracell
Centrifuge	Eppendorf
NextSeq	Illumina

6.1.13 Software

The following software products have been used for this work.

Table 6.20: List of software used in this study

Name	License	Used For
CLC	Commercial	Cloning
SnapGene	Commercial	Cloning
Imaris	Commercial	Image Analysis
Fiji	Free	Image Analysis
GaphPad Prism	Commercial	Statistics
Adobe	Commercial	Image Processing
Microsoft Office	Commercial	Creation of Figures
QuPath	Free	Image Analysis
LaTeX	Free	Documentation

6.2 Methods in cell biology

6.2.1 Cell culture

All cell lines were maintained in 10 centimeter (cm) or 15 cm dishes or T75 flasks. In general the medium was composed of DMEM supplemented with 10 % FBS, which will be from here on called culture medium. For selection different antibiotics were added, which can be found in Sec. 6.3. BJ cells were maintained in a medium containing DMEM and Medium199 in a ration 1:1, supplemented with 20 % FBS and 2 % Sodium-Pyruvat. All cells were passaged when reaching about 90 % confluence by adding 2.5 ml of Trypsin and incubation at 37°C until cells detached. To stop the enzymatic reaction, three times the amount of culture medium was added and cells were spitted according to their growth behavior 1:5, 1:10 or 1:20. Cell counting was done by using a Neubauer cell chamber. When freezing cells, these were trypsinized as mentioned before and then centrifuged at 300 g for 5 min. The supernatant was discarded and the cell pellet was resuspended in an appropriate volume of culture medium. Aliquots of 1 ml containing between $1 \cdot 10^6$ and $5 \cdot 10^6$

cells were frozen in cryotubes, which were placed in Mr. Frosty™ (Thermo Fisher) cell freezing containers for three days. The cell freezing containers were filled with propanol, to slow down the cooling process and avoid cell damage. For short term storage the cells were kept at –80°C and transferred to liquid nitrogen after a few weeks for long time storage. Cells were thawed shortly in a 37°C waterbath, then mixed with 9 ml of pre-warmed culture medium and plated into a T75 flask. All Cells were incubated at 37 °C with 80 % relative humidity, 5 % CO_2 and 20 % O_2. While handling the cells a laminar flow hood was used.

6.2.2 Mycoplasma test

To test cells for mycoplasmic contamination the LookOut® Mycoplasma PCR Detection Kit (Merck) was used, according to the manufacturer's protocol.

6.2.3 PRV production and titration

The PRVΔIE180 mutant was grown on IE180 transcomplementing PK15 (PI) cells, in culture medium. PI cells were selected for the doxycyclin-inducible IE180 clones in the presence of 500 µg/ml geneticin (G-418). PI cells were grown in a 10 cm dish until they reached 80 % confluence. Two hours before infection 10 µg/ml Dox was added to a total volume of 5 ml culture medium. Cells were infected with a MOI of 0.1 for one hour at 37°C. The inoculum was aspirated and 10 ml culture medium, supplemented with 10 µg/ml Dox, were added to the cells. As soon as the cells experienced 100 % cytopathic effect (CPE) (after two to three days), cells were scraped off the plate and together with medium centrifuged at 300 g for 3 min, to get rid of cells and cell debris. The supernatant was split into 1 ml aliquots and stored at –80 °C.

For the titration of PRVΔIE180 $5 \cdot 10^6$ PI cells were plated into each well of a 6-well plate, in the presence of 10 µg/ml Dox. When they reached confluence a series dilution of one aliquot of the virus stock was made in culture medium containing 10 µg/ml Dox, starting from 10^{-2} to 10^{-7}. The medium was aspirated of each well, and 250 µl of each dilution was added into one well. This was incubated for one hour at 37°C and rocked every 15 min. In the meantime 10 µg/mL Dox was added to 1.5 % methocel in 1x DMEM and incubated at 37 °C. One hour after incubation 2 ml of methocel were added to each well. The plate was then incubated at 37 °C for three to four days, until plaques were visible. To determine the virus titer, plaques of two dilutions were counted, multiplied by four and by the dilution factor to determine the plaque forming unit (PFU) per ml.

The other PRV mutants used in this study were able to lytically replicate in PK15wt cells. Thus, virus production and titration was performed as described for PRVΔIE180, except for using PK15wt cells without adding Dox.

6.2.4 HSV-1 production and titration

The HSV-1*in1374* mutant was grown on U2OS cells in culture medium. U2OS cells were grown in a 10 cm dish until they reached 80 % confluence. One day prior to infection they were incubated

at 32 °C, the permissive temperature of the virus mutant. Cells were infected with a MOI of 0.1 for two hours at 32 °C. The inoculum was aspirated and 10 ml pre-warmed culture medium was added to the cells. As soon as the cells experienced 100 % CPE (after four to five days), cells were scraped off the plate and together with medium centrifuged at 300 g for 5 min. The supernatant was split into 1 ml aliquots and the cell pellet was resuspended in 1 ml culture medium and freeze-thawed three times. Cells were centrifuged at 300 g for 3 min to get rid of cells and cell debris and the supernatant was added to the aliquots. Virus supernatant was frozen and stored at –80°C. For the titration $5 \cdot 10^6$ U2OS cells were plated into each well of a 6-well plate. When they reached confluence the next day a series dilution of one aliquot of the virus stock was made in culture medium, starting from 10^{-1} to 10^{-6}. The medium was aspirated of each well, and 250 µl of each dilution was added into one well. This was incubated for two hours at 32 °C and rocked every 15 min. In the meantime 1.5 % methocel in 1x DMEM was pre-warmed to 32 °C and after the incubation time 2 ml of methocel were added in each well. The plate was then incubated at 32 °C for four to seven to ten days, until plaques were visible. To determine the virus titer, plaques of two dilutions were counted, multiplied by four and by the dilution factor to determine the PFU per ml.

6.2.5 Methylcellulose production

To produce 1.5 % methocel in 1 x DMEM 3 % weight/volume solution of methocel in water was made. When all the powder was solubilized, the solution was autoclaved. Since after autoclaving methocel will form a solid with water around, it has to be stirred over night at 4 °C. Meanwhile 2x DMEM was prepared by dissolving the appropriate amount of DMEM powder (Fisher cat SH30003.03) in water. This solution was then filter-sterilized. After the methocel solution has become homogenous again 2 x DMEM was added to 3 % methocel in a ratio 1:1. 7.5 % Sodium Bicarbonate and 5 % FBS were added. Everything was mixed well and stored at 4 °C.

6.2.6 Non-permissive viral infections

The respective target cells were counted and plated into dishes or well-plates, 24 h prior to infection. Subsequently, cells were infected with the desired MOI and incubated for one hour at 37 °C when using PRV or for two hours at 38.5 °C when using HSV-1*in1374*. Afterwards the inoculum was aspirated and fresh, pre-warmed culture medium was added. Infected cells were further incubated at 37 °C for PRV and 38.5 °C for HSV-1*in1374*.

6.2.7 Transfection of vDNA for the PRV master stock production

For transfection of nucleocapsid vDNA, PK15 or PI cells were plated in 6-well plates and incubated at 37 °C until they reached 80 % confluence. PI cells were used when producing the IE180-null mutant; thus, cells were incubated with 10 µg/ml Dox 24 hours prior to transduction. 2.5 µg nucleocapsid DNA of PRV were mixed with Opti-MEM to reach a volume of 250 µl. In parallel 20 µl of Lipofectamin2000 were mixed with 230 µl of Opti-MEM. Each mixture was incubated for

5 min at room temperature (RT), then both solutions were combined and incubated for another 20 min at RT. Meanwhile medium was aspirated from the cells and 1 ml of fresh, pre-warmed culture medium was added to each well, since antibiotics can decrease the transfection efficiency. Then the mixed solution was carefully pipetted in drops onto the cells and they were incubated over night at 37 °C. The supernatant was then aspirated and 2 ml of fresh, pre-warmed culture medium were added to each well. During production of the IE180-null mutant 10 µg/ml Dox were added. When cells showed 100 % CPE they were scraped off the plate and together with the supernatant frozen at -80°C. This master virus stock was then titered and used for working stock productions of the designated virus as described in section 6.2.3.

6.2.8 Establishment of an ATRX knock-out in HAP1 cells

The laboratory work for the establishment of an ATRX-ko HAP1 cell line was performed by a masterstudent in our lab, Armin Günther. In order to generate a complete ko of ATRX a CRISPR/Cas9-based approach was used. For this two different sgRNAs were designed, one at the 5'-end and the other at the 3'-end of the gene. These sgRNAs were cloned into a vector expressing Cas9 and GFP. Single cells were sorted and each clonal population was screened via PCR for the absence of ATRX. This could be achieved by using two primer pairs, one located inside the ATRX-gene and the other one flanking the ATRX-locus. Cell clones with successful ATRX-deletion should only show a small band since the gene was excised, while in cell clones still harboring the gene, amplification via the primer pair which binds inside the gene body would take place. After the screening via PCR the respective cell clones were controlled for the absence of ATRX expression via immunoplotting. Afterwards, the cell clone which did neither show the respective ATRX-PCR fragment nor ATRX protein levels was used for further experiments.

6.2.9 Transfection of piggyBac vector constructs

For the transfection with the piggyBac vector constructs two different transfection reagents were used, depending on the cell type which should be transfected. HAP1 cells were transfected with TransIT®-LT1 transfection reagent, while U2OS cells were transfected using Lipofectamine2000. For HAP1ΔATRX cell-transfection, 250.000 cells were plated in one 6-Well and transfection was perform immediately after seeding the cells. 2 µg PB transposase vector + 2 µg PB construct vector + 4 µl transfection reagent were added to 250 µl Opti-MEM. This was mixed and incubated for 30 min at RT. Then the Opti-MEM-mix was added to the cells. Cells were incubated for 24 h at 37 °C. Afterwards the medium was changed and selection was started with 1 µg/ml puromycin. For U2OS cells 250.000 cells were plated in one 6-Well and incubated over night at 37°C. The next day 9 µl Lipofectamin2000 were diluted in 100 µl Opti-MEM. In parallel 2 µg PB construct vector and 2 µg PB Transposase vector were mixed with 150 µl Opti-MEM. Each mixture was incubated for 5 min at RT, then both solutions were combined and incubated for another 20 min at RT. Meanwhile, medium was aspirated from the cells and 1 ml of fresh, pre-warmed culture medium was added to each well, since antibiotics can decrease the transfection efficiency. The

mixed solution was then carefully pipetted in drops onto the cells and they were incubated over night at 37 °C. The next day the supernatant was aspirated and 2 ml of fresh, pre-warmed culture medium were added to each well, containing the selection antibiotic puromycin (1 µg/ml).

U2OS and HAP1ΔATRX cells were transfected with this piggyBac vector together with a transposase vector, which enables integration into the genomic DNA and thus stable expression of the construct. Cells were selected for one to two weeks with puromycin, afterwards cells were induced with 1 µg/ml of Dox.

6.2.10 Transfection of siRNA

For transfection with siRNAs 10.000 or 125.000 HDF cells were plated into an 8-well IBIDI or a 6-well plate, respectively and incubated at 37 °C over night. The next day cells were transfected with a total of 7 pmol or 28 pmol, respectively and 0.25 µl or 1 µl viromer blue transfection, reagent diluted in 10x viromer blue reaction buffer. The siRNA - viromer blue mixture was incubated at RT for 15 min. Meanwhile, the medium on cells was exchanged and 225 µl or 900 µl of fresh, pre-warmed culture medium was added to each well, respectively. Then the mixed solution was carefully pipetted in drops onto the cells and they were incubated for four hours at 37 °C. The supernatant was then aspirated and 250 µl or 1 ml of fresh, pre-warmed culture medium were added to each well. Transfected cells were further incubated for 48 h at 37 °C, since at this time point the targeted protein was already highly downregulated. Afterwards, infection experiments were performed with HSV-1*in1374*.

6.2.11 Lentivirus production and transduction

For the production of lentiviral particles, lenti-XTM 293T cells were used. $5 \cdot 10^6$ cells were seeded into a 10 cm dish, one day prior to infection. For transfection of the cells, 10 µg of the lentiviral construct was mixed with 1 ml Opti-MEM and with the packaging plasmids (10 µg phCMV-gag-pol, 5 µg phCMV-rev, 2 µg phCMV-VSV-G env). 270 µl polyethyleneimine (PEI) were added to the mixture. Afterwards, the solution was incubated for 30 min at RT. The media of the lenti-XTM 293T cells was aspirated and 6 ml Opti-MEM were added. The transfection mix was then added to the cells. and 8 h post transfection the media was changed to culture medium. The supernatant was harvested, two to three days after transfection. Subsequently, the supernatant was filtered through a 0.22 µm polyethersulfone (PES)-membrane (Merck Millipore), and frozen in 2 ml aliquots, at -80 °C.

Target cells were transduced with different dilutions of lentivirus supernatants. Starting from 1:2, 1:5, 1:10 and 1:100 diluted in culture medium. For better transduction efficiency Polybren was added in a dilution 1:1000. After 8 h medium was changed with culture medium and cells were grown for two to three days until they were plated in 10 cm dishes and if possible selection was started. If the lentivirus construct expressed a fluorescent protein cells were sorted by FACS. For this cells were grown until they reached complete confluence in a 10 cm dish, then harvested and sorted according to 6.2.12

6.2.12 Preparation of cells for FACS

Cells were trypsinized and resuspended in culture medium as described in 6.2.1. Then cells were pelleted in 15 ml falcons for 5 min at 300 g and resuspended according to cell number in 250 µl to 500 µl of FACS-buffer, containing 2 % FBS in DPBS. Cells were then pipetted through a filter into FACS-tubes. After sorting, cells were collected in 5 ml of culture medium supplemented with 1 % pen/strep, since the possibility of contaminating cells is quite high during sorting. Cells were then plated into 10 cm dishes and treated with the pen/strep supplemented culture medium for two to three passages.

6.3 Methods in molecular biology and biochemistry

6.3.1 Genomic DNA extraction

Cells were infected as described in 6.2.6. Cells were incubated at the specific temperature for 24 h or 48 h. Then they were trypsinized, centrifuged at 300 g for 5 min, washed one time with DPBS, centrifuged again and resuspended in 1 ml to 2 ml of lysis buffer. Proteinase K was added and cells were incubated at 37 °C for 24 h. 500 µl of the viscous cell-solution were carefully pipetted into a Phase-Lock tube for Phenol-Chlorofrom extraction, with one time phenol-chloroform-isoamylalcohol (PCI) and one time Chloroform. The viscous upper phase was carefully pipetted into a 50 ml falcon and precipitated with NaCl and 100 % ice-cold ethanol for 10 min on ice. Then the DNA was either rolled up on a glass hook, washed three times in 70 % ethanol and air-dried on the glass hook or pelleted at 2000 g for 15 min at 4 °C and then washed three times with 500 µl 70 % ethanol and air-dried in the falcon. Deionized water was then added to the DNA and solubilized at 4 °C for at least 24 h. After the pellet was solubilized, the DNA concentration and quality was measured with a spectrophotometer (Nanodrop-1000). When quality or concentration was low it was dialyzed using dialysis tubes and eluted in the appropriate volume of deionized water. The extracted high-molecular DNA was further used for minion-sequencing.

6.3.2 RNA extraction

For RNA extraction $1 \cdot 10^6$ to $5 \cdot 10^6$ cells were harvested, washed with DPBS and lysed in 500 µl Trizol, by pipetting up and down several times. At this step cells could be frozen at -80 °C. To continue with RNA-isolation 100 µl chloroform were added, the solution was vortexed and incubated on ice for 10 min. The sample was then centrifuged at 12.000 g for 15 min at 4 °C. Afterwards, the organic and aqueous phase should be separated. The aqueous phase contains the RNA and was therefore transferred into a new tube, whereas the organic phase contains proteins and DNA and was discarded. The RNA containing phase was then precipitated by mixing with 80 % of the transferred volume of isopropanol and incubated on ice for 30 min. The sample was then centrifuged at 20.000 g for 5 min at 4 °C to pellet the RNA. The pellet was washed with 75 % ice-cold ethanol, centrifuged as before and ethanol was discarded carefully. Afterwards, the pellet

was air-dried for max. 10 min at RT. Depending on the cell number, the pellet was resuspended in 20 - 50 µl of diethylpyrocarbonate (DEPC) treated water. RNA-concentration and quality was determined by using a spectrophotometer (Nanodrop-1000).

6.3.3 Cell preparation for immunoblotting

Cells were trypsinized and centrifuged for 3 min at 600 g. The cell pellet was washed with DPBS two times. Afterwards the pellet was resuspended either in high salt buffer or nuclear extraction buffer (see Tab. 6.12). During nuclear extraction, the cell pellet was carefully resuspended in nuclear extraction buffer and then nuclei were spinned down at 20.000 g for 1 min at 4 °C. Afterwards, nuclei were resuspended in protein extraction buffer (see Tab. 6.12) and sonification was performed for five cycles at high intensity. Proteinconcentration was then measrued, using bradford assay. Afterwards, 4x loading-buffer was added to the sample and incubated for 10 min at 95 °C. 20-40 µg protein were loaded onto the gel.

6.3.4 SDS-PAGE and immunoblot

The SDS-Gel was placed into the Biorad gel-device. The device was filled with 1x running buffer (6.12) and applied for 90 min at 150 V. To transfer the proteins from the gel to a carrier membrane the gel was blotted onto a methanol-activated polyvinylidenfluorid (PVDF) membrane via a semi-dry method. In order to do this, the gel and the membrane were placed amongst filter papers soaked into different buffers (6.12) and amplied to a electric field at 115 mA for 75 min. Afterwards the membrane was blocked in 5 % milk in tris-buffered saline with Tween20 (TBS-T) for 30 - 60 min, to inhibit unspecific binding of the antibodies. The membrane was incubated with the first antibody diluted in 5 % milk in TBS-T over night at 4 °C. After washing the membrane three times for 5 min with TBS-T, the second antibody was incubated for 1 h at RT. Again the membrane was washed three times with TBS-T. After incubation with luminol reagent (Santa Cruz) for 1 min at RT the membrane was developed. This process is based on the oxidation of luminol in the developer solution through horseradish peroxidase. Ultimately, the luminesense is captured on a X-ray film.

6.3.5 Conventional PCR

Conventional PCR was first described as a method to amplify specific DNA fragments by annealing oligonucleotides to a template DNA and amplifying this template region through polymerases [457]. Here, this *in vitro* technique was used to amplify DNA fragments for cloning and screening bacterial colonies. Depending on fragment length and GC-content different polymerases and thermocycler programs where used, which can be found in table 6.22 and 6.21.

After the PCR, the amplified fragments were loaded onto a gel to check for the right product and quality. For colony-PCR this technique was used to screen for clones with the right insert. After cloning, plasmids were digested and the success of a cloning-experiment was proven by the

right digest pattern in the gel. For ChIP, 10 µl of the input sample was loaded onto the gel, to determine the proper fragmentation of the chromatin.

Table 6.21: PCR reaction mix for one reaction with a total volume of 20 µl

Reagent	Amount
10x PCR buffer	2 µl
dNTPs	0.5 µl
Primer reverse	1 µl
Primer forward	1 µl
Polymerase	0.25 µl
Template gDNA	100 ng
DEPC treated water	add to 20 µl

Table 6.22: PCR thermocycle conditions

Cycles	Temperature in °C	Time
1	95	2 min
30	95	20 sec
	58 - 64	15 sec
	72	15 - 60 sec
1	72	3 min
1	4	hold

6.3.6 Agarose gel electrophoresis

Depending on the fragment length different agarose concentrations were used, ranging from 0.5 % to 2 % (w/v). To prepare the gel, an appropriate amount of agarose was mixed with the specific volume of TAE-buffer and shortly boiled in a microwave. After cooling down, but before getting viscous, ethidiumbromide was added in a dilution 1:20.000. The gel was then poured into a gel chamber and samples were mixed with 10x FastDigest Green Buffer (Thermo Fisher) and loaded onto the gel together with the GeneRuler DNA-ladder-mix (Thermo Fisher). Gels were run, depending on their purpose, at between 70 V and 110 V, 400 mA and 30 min to 2 h. Afterwards, the gel was illuminated with UV-light and a photo was taken using a GelDoc (In Genious) for documentation.

6.3.7 Purification of DNA fragments from an agarose gel

To purify PCR products for cloning, the specific bands were cut from an agarose gel with a scalpel while illuminated with UV-light. Afterwards the DNA fragments were purified using the Zymoclean Gel DNA Recovery Kit (Zymo Research), according to the manufacturer's protocol.

6.3.8 Production of chemically-competent bacteria

The Rubidium-Chloride method was used to produce chemically competent bacteria (*E.coli*, DH5α). For this, an overnight culture, grown at 37 °C, was diluted 1:100 in LB-medium. This dilution was further grown at 37 °C until the exponential growth phase was reached, at an optical density (OD) between 0.5 and 0.6. Bacteria were then chilled on ice for 15 min and pelleted at 5000 g for 5 min and at 4 °C. After resuspending the pellet in 150 ml cold tranformation buffer I (Tab. 6.10). The solution was incubated on ice for 90 min. Another centrifugation step was performed as described above and the pellet was resuspended in 30 ml cold transformation buffer II (Tab. 6.10). Aliquots of the now chemically competent bacteria were frozen in liquid nitrogen and kept at -80°C.

6.3.9 Bacterial transformation

Competent bacteria were thawed on ice and 50 µl of bacteria were mixed with either 1 ng of plasmid-DNA or 10 µl of a ligation product (6.3.12) and incubated for 20 min on ice. Chemically competent bacteria were transformed by heat shock at 42 °C for 30 sec and afterwards incubated 2 min on ice. 950 µl SOC medium was then added to the bacteria and they were incubated for 1 h at 37 °C. The bacteria samples were plated on LB-agar supplemented with selecting antibiotics and incubated over night at 37 °C.

6.3.10 DNA-isolation from bacteria

To purify bacterial DNA different kits were used (see Tab. 6.18). For cultures up to 5 ml a Mini-Prep Kit (Qiagen) was used. For cultures up to 100 ml a Midi-Kit was used (Qiagen) and for bigger cultures a Maxi-Prep Kit (Qiagen) was used.

6.3.11 Restriction digestion of DNA

Cloning DNA fragments into vectors was performed by cutting the vector, using specific restriction sites. These restrictions sites were added during PCR to the DNA fragments that should be inserted into the vector. Restriction digestion was further used to test for successful cloning, which was analyzed by an agarose gel. For restriction digestion either 200 ng of a DNA fragment or 1 µg of a plasmid vector were mixed with 1 µl of a FastDigest restriction enzyme (Thermo Fisher) together with 10x FastDigest Buffer (Thermo Fisher) and incubated at 37 °C for 60 min. When using a plasmid vector for ligation, the respective vector was treated with alkaline phosphatase (AP) after restriction (RE)-digestion.

6.3.12 DNA ligation

For the ligation, the vector and the insert were mixed at a molar ration of 1:3 together with T4-DNA-ligase and 10x T4-Buffer (Thermo Fisher). This was incubated at 16 °C over night. To

test whether the ligation reaction was successful the ligase-product was loaded onto an agarose gel and analyzed as described in 6.3.6.

6.3.13 Gibson assembly

Gibson Assembly was used to combine several short DNA-fragments with overlapping sequences. Four fragments should be assembled for cloning the ANCH-sequence with adjacent PRV homologies and an antibiotic-resistance cassette. Each fragment was amplified with an overlapping sequences to its future adjacent fragment by conventional PCR and then mixed in equimolar ratios together with the Gibson Assembly Master-Mix (NEB) according to manufacturer's protocol.

6.3.14 Sanger sequencing

All cloned plasmids were sequenced by sanger sequencing, after successful RE-digestion. This was performed by the TubeSeq-Service from Eurofins.

6.3.15 ChIP

ChIP-Experiments were performed based on the protocol published by Günther et al. [458]. Cells were harvested and fixed with 1 % formaldehyde for 10 min at RT, then quenched for 5 min with $1/10^{th}$ the volume 1.25 M glycine and pelleted at 200 g for 3 min. The pellet was washed once with cold PBS and cells were again pelleted at 200 g for 3 min at 4 °C. The cell pellet was resuspended in ChIP buffer I (Tab. 6.13) and incubated for 10 min at 4 °C while rotating. Nuclei were pelleted by centrifugation at 2000 g for 5 min at 4 °C. The pellet was resuspended in ChIP Buffer II (Tab. 6.13) and treated the same as before. This pellet was then vigorously resuspended in ChIP buffer III (Tab. 6.13) by pipetting up and down at least 30 times. The volume of ChIP buffer III should be calculated to end up with chromatin of $1 \cdot 10^6$ per 100 µl. The suspension was then sheared using a Biorupter^{TM} (Diagenode) for 15 cycles (30 sec "on" and 30 sec "off") at highest intensity at 4 °C, which should result in fragments between 100 to 500 bp. Afterwards, $1/10_{th}$ of the sample volume of a 10 % Triton X-100 solution was added and mixed. To get rid of cellular debris, the sample was centrifuged at 20,000 g for 10 min at 4 °C. The supernatant was transferred in a new tube and $1/4^{th}$ of the amount needed for one immuno-precipitation (IP) ($1 \cdot 10^6$ cells) was used as an input sample and frozen at -20 °C. The residual chromatin was pre-cleared with pre-washed magnetic beads for 30 min at 4 °C, to reduce unspecific binding. Supernatant was transferred to a new tube and for each IP chromatin of $1 \cdot 10^6$ cells was diluted 1:10 in dilution buffer (Tab. 6.13) and the appropriate amount of antibody was added. To achieve sufficient binding of the antibody to its epitope(s) the antibody-chromatin-mix was rotated over night at 4 °C. Meanwhile, 50 µl of the magnetic beads for each IP were washed with dilution buffer and blocked over night at 4 °C with bovine serum albumin (BSA). The next day blocked beads were washed with dilution buffer and resuspended in their original volume. 50 µl of blocked beads were added to each antibody-chromatin-mix and incubated at a rotating wheel for 1 h at 4 °C. Afterwards the samples were put in a magnetic stand. When all beads were settled they were

washed once with low-salt-, high-salt-, LiCl-buffer and two times with tris ethylendediamine tetra acetic acid (TE)-buffer. The supernatant was discarded and beads were resuspended in 210 µl of ChIP elution buffer (Tab. 6.13) and incubated at 65 °C for 30 min. After incubation samples were shortly centrifuged and put on a magnetic stand, 200 µl of the eluted chromatin was transferred to a new tube. Meanwhile, the frozen input sample was thawed on ice and ChIP elution buffer was added to end up with 200 µl total volume. 8 µl of 5 M NaCl were added to each sample and the input. All samples were incubated over night at 65 °C at 1000 rpm. The next day 200 µl TE buffer and 3 µl RNaseA (10 mg/ml) were added and incubated for 2 h at 37 °C, to degrade RNA. Then 7 µl CaCl$_2$ and 4 µl Proteinase K (20 mg/ml) were added and incubated for 1 h at 55 °C, to degrade protein. Afterwards, samples were transferred to Phase-Lock-tubes and two rounds of PCI extraction with an additional round of chloroform extraction were performed with centrifugation steps at 18,000 g for 4 min at 4 °C. The upper phase, which contains DNA, was transferred to a new 1.5 ml tube and DNA was precipitated by adding 24 µl of NaCl, 3 µl glycine and 1055 µl ice-cold 100 % ethanol. Samples were mixed by vortexing and incubated at -80 °C for at least 3 h. Samples were centrifuged at 20,000 g for 15 min at 4 °C, washed with 70 % ethanol and centrifuged again at 20,000 g for 15 min at 4 °C. The supernatant was carefully removed and the pellet was air-dried at 37 °C. Each pellet was resuspended in 55 µl elution buffer (Qiagen) and incubated at 37 °C to facilitate the pellet to go in solution. Afterwards, 10 µl of the input sample were loaded onto a 1.5 % agarose gel to check for correct fragmentation of the chromatin. ChIP samples were then analyzed by qPCR and normalized to input or H3. Ultimately, samples were sequenced by illumina sequencing.

6.3.16 qPCR

As described before (6.3.5) PCR amplifies target DNA fragments. With qPCR the amount of these PCR-products can be measured in real-time. To achieve this the fluorescent dye SYBR-Green (Thermo Fisher), which binds double stranded DNA (dsDNA) and therefore labels each new fragment during amplification, was used in this study. The dye amplified PCR-products are detected when reaching a certain threshold of fluorescence intensity over background. The first cycle number at which a sample reaches this threshold is called cycle threshold (Ct) and used for concentration calculation, since the relative fluorescence intensity is directly proportional to the number of amplified dsDNA fragments. To calculate the Ct-values standard curves of the respective primer pair were generated by running a dilution series of a known sample containing the target sequence for each primer pair. With such a standard curve the fluorescence threshold was set, from which Ct-values could be determined. Standard curves also give information about the specificity of the primer pair, which was only used when one specific product was produced with an efficiency of at least 80 %. To control for amplification of only one product, melting curves were included into each run, where the samples are gradually heated from 65 °C to 95 °C and the fluorescence intensity was measured. If there was only one specific product amplified the melting curve should only have one sharp peak, since the melting temperature should be always the same. With this method specificity of the primers and quality of the sample can be elucidated,

since primer dimer, contamination or unspecific products would give a secondary peak. Samples without template were included as a control for contamination. In this study, qPCR was mainly used to analyze and evaluate ChIP experiments. Cycler-conditions can be found in Tab. 6.24 and composition of a SYBR-Green Master-Mix in Tab. 6.23. Sequences of the used primer pairs can be found in Tab. 6.9.

Table 6.23: qPCR reaction mix with a total volume of 10 µl

Reagent	Amount
SensiMix SYBR (Bioline)	5 µl
Primer reverse (10 µM)	0.3 µl
Primer forward (10 µM)	0.3 µl
Template gDNA	1.5 µl
DEPC treated water	2.9 µl

Table 6.24: qPCR cycler conditions

Cycles	Temperature in °C	Time
1	95	10 min
	95	15 sec
40	57	30 sec
	72	20 sec
1	4	hold

6.4 Sequencing

6.4.1 ChIP-sequencing

Library preparation of the ChIP-samples, generated as described in 6.3.15, was performed by using the Nextflex ChIP-seq Library Prep Kit (Bio Scientific), according to the manufacturer's instructions. The mean library size and quality were examined on a Bioanalyzer with the High Sensitivity DNA Kit (Agilent). Subsequently, the libraries were sequenced on a NextSeq 500 with an intended sequencing depth of 20 mio reads.

6.4.2 MinION-sequencing

The MinION-sequencing experiment performed by using the Rapid Sequencing Kit (SQK-RAD004). 400 ng of genomic DNA (gDNA) were loaded. For sequencing the oxford-nanopore sequencer was used with a GridION. Sequencing was performed for 72 h, on the flow cell: FAP06212.

6.4.3 RNA-sequencing

RNA was isolated from infected and uninfected cells as previously described (Sec. 6.3.2). The RNA quality was measured on a Bioanalyzer with the RNA Nano Kit (Agilent). Then polyadenylated RNA was enriched, using the NEBNext Poly(A) Magnetic Isolation Module (New England Biolabs). Samples were then processed to library preparation, using the NEXTflexTM Rapid Directional qRNA-Seq Kit (Bioo Scientific) according to the manufacturer's instructions. Finally, single-read sequencing was performed, with a read length of 75 bp, on a NextSeq 500 platform with an intended sequencing depth of 20 mio reads.

6.5 Bioinformatical analysis

6.5.1 Bioinformatical analysis of ChIP-sequencing

Single end reads were first quality filtered and then used for subsequent analysis. By using Bowtie2, a program for aligning DNA sequence reads to genomes [459], these reads were aligned to the respective viral and host reference genomes. Viral genomes used in this study were: PRV (NC006151) and HSV-1 (NC001806). Host genomes used in this study were the following: human genome (hg38) and pig genome (ss11). To exclude multi mapping reads the option -m was used. Other then this, standard settings for Bowtie2 were applied. Visualization of ChIP-seq tracks was done with the software EaSeq [460, 461].

6.5.2 Bioinformatical analysis of RNA-sequencing

Mapping of RNA-seq data was performed by STAR, a program which aligns spliced transcripts to a reference [462]. Quality filtered paired end reads were aligned to the following reference genomes: human genome (hg38) and pig genome (ss11) and HSV-1 (NC001806) and PRV (NC006151). Trancriptional profiles of HSV-1$in1374$ and PRV were generated by using IGVTools [463]. First the viral genome was divided in areas containing 100 bp. Then the count function of IGVTools was used to analyze the coverage in the defined areas. Furthermore, forward and reverse reads were analyzed individually. Coverage-plots were, subsequently, generated from the acquired data with Microsoft Excel (Excel-script generated by Adam Grundhoff, unpublished).

6.6 Methods in microscopy

For Imaging either the Nikon Spinning Disk confocal microscope with a Nikon Ti2 frame using a 100x magnification or the Nikon A1 confocal microscope with a Nikon Ti2 frame using a 60x magnification. Images were analyzed using the software Imaris (BitPlane, South Windsor, CT, USA) or Fiji [464].

6.6.1 Immunofluoresence

For IF, cells were counted and the appropriate cell number (about 40,000 cells) was plated either in 8-Well IBIDI slides or in 24-Well plates onto a coverslip, one day prior to the IF. Cells were fixed with 4 % Formaldehyde for 15 min at 37 °C then permeabilized with 2 % Triton-X for 15 min at RT and blocked for 15 min with 3 % BSA at RT. The primary antibody was diluted according to manufacturer's suggestion in 3 % BSA. 200 µl of the antibody-dilution were added to the fixed cells. The primary antibody was incubated over night at 4 °C. Cells were washed three times for 5 min with DPBS. The secondary antibody was diluted 1:1000 in 3 % BSA and incubated on the cells for one h at RT. Cells were again washed three times for 5 min with DPBS. Hoechst33342 was added 1:2000 when performed in IBIDI dishes. when performed on coverslips, these were mounted with mounting solution supplemented with 4',6-diamidino-2-phenylindole (DAPI) on glass slides.

6.6.2 Fluorescent bioorthogonal labeling of vDNA by click-chemistry

Bioorthogonal labeling of vDNA was performed by the so called click-chemistry (Click-iT kit from Thermo Fisher Scientific) or azide-alkyne cycloaddition, catalyzed by copper (CuAAC). This was performed to visualize vDNA in the nucleus for microscopy. First a PRV stock was produced in presence of EdC (Sigma-Aldrich) and then harvested and concentrated to get rid of residual EdC. Concentration of the viral stock was performed by using the polyethylene glycol (PEG)-based LentiX-concentrator from Takara. The viral supernatant was incubated together with the LentiX-concentrator solution, as proposed by the manufacturer. Then the supernatant was centrifuged for 45 min, at 1500 g and 4 °C. The remaining pellet was diluted in one tenth of the volume, to achieve a 10-fold concentration. The pellet was incubated over night at 4 °C, to fully solubilize the virus-pellet. The virus stock was stored at -80 °C, titered as described in Sec. 6.2.3 and used for subsequent experiments. The method was adapted from published data of HSV-1 [436]

All the experiments were performed in 8-Well IBIDI slides. Before infection cells were plated in each well reaching 70 % confluence on the day of infection. Infected cells were fixed with 4 % Formaldehyde for 15 min at 37 °C then permeabilized with 2 % Triton-X for 20 min at RT and blocked for 15 min with 3 % BSA at RT. 500 µl of total Click-iT Master-Mix were prepared as shown in Tab. 6.25. It is highly important to mix these components in the exact same order as listed here. Also Copper-Protectant and Copper-Sulfate should be mixed before adding them to the 1x Click-iT Buffer.

All components were mixed by pipetting until the dye was homogeneously distributed in the solution. Each well was incubated with 125 µl of the reaction mix for 30 min, at RT in the dark and then washed 3 times with PBS. In the end Hoechst33342 was added 1:2000. Samples were stored at 4 °C, in the dark.

Table 6.25: Click-iT reaction mix with a total volume of 500 μl

Reagent	Amount
DEPC treated water	396 μl
10x Click-iT Buffer	44 μl
Copper Protectant	7 μl
CuSo4	13 μl
Alexa fluorohpor picolylazide	1.2 μl
Reaction Additive	50 μl

6.6.3 Live cell imaging approaches

6.6.3.1 SunTag-System

The SunTag-System is based on the CRISPR/Cas technology [428]. The used dCas9 is tagged to an epitope tail with binding sites for GFP. sgRNAs were designed, which specifically bind to repetitive regions in the PRV genome to recruit several dCas9 molecules to the viral genome. Then the sgRNAs together with GFP and dCas9 were stably transduced into PK15 cells. Subsequently, single cell clones were screened by PRVwt infection and RC formation. From this the most promising clones were used for infection experiments and live-cell microscopy, during the early phase of infection. By using a PRV mutant with a mCherry tagged capsid, the infection could be observed under a confocal laser-scanning microscope, with an incubation chamber for live-cell imaging.

6.6.3.2 ANCHOR-System

The "ANCHOR" technology uses a 1 kbp large, highly repetitive sequence, called ANCH, to polymerize the protein OR on it. To visualize the process of the OR accumulation on the ANCH-sequence the OR protein was tagged to mCherry and stably transduced in PK15 cells. Additionally, the ANCH-sequence was incorporated into the vDNA by homologous recombination of the virus with the ANCH fragment, on which homologous arms to the PRV genome were added. Homologous recombination is a phenomenon that is described to happen commonly during alpha-herpesvirus infection. By transfecting the nucleocapsid DNA of PRV together with the ANCH-sequence, containing homologoues sequence-elements to PRV, the vDNA should incorporate the ANCH-sequence, while replicating. To achieve a "pure" virus population, with viral genomes solely harboring the ANCH-sequence, five rounds of plaque-picking were performed. For this the virus supernatant from the transfection experiment was harvested and a plaque-assay, as described in Sec. 6.2.3, was performed. After two to three dpi, three pre-plaques, which showed high mCherry signal were picked. These three plaques were diluted in culture medium and subsequently new plaque-assays from these dilutions were performed. This was done five times in a row. After the fifth plaque-pick, the picked plaques were again diluted in growth medium and frozen at -80 °C.

From these dilutions virus stocks were produced, as described in Sec. 6.2.3.

6.6.4 Microscopic data analysis

The percentage of cells showing viral RCs was quantified using the software QuPath [465]. First maximum-intensity projections of all acquired images were generated using Fiji [464]. Then, these 2D images were loaded into the QuPath software. With QuPath nuclei were identified; subsequently nuclei which harbor RCs were detected, since these were stained with an anti-ICP8 antibody. The precentage of cells showing a RC compared to the total amount of nuclei was calculated for each image by the software. The results were exported as a table format and further analyzed in Excel and GraphPad Prism.

6.7 Statistical analysis

6.7.1 Statistics for ChIP-sequencing

The relative enrichment of histone modifications on the viral genomes was calculated relative to the respective host genomes. First the 200 most significantly enriched regions for the respective modification on the host genome, compared to their input samples or H3 samples, were calculated. For this the program SICER/EPIC2 [466] was used. These regions were used as host positive regions (host pos). To describe the general background of each experiment host negative regions (host neg) had to be generated. This was done by applying the program bedtools with the command bedtools shuffle, which randomly permutes genomic locations of a distinct feature file. For this the 200 most significant regions were used as a feature file. Afterwards, a random selection of genomic locations with the same size distribution as displayed in the feature file was generated and at the same time the positive regions were excluded. Furthermore, regions with less than 10 reads were excluded. This aims to prevent selection of regions which could not be mapped later on. Additionally, ENCODE Blacklists were used to identify and subsequently remove genomic regions which are known to be problematic during analyzing genomics data, like repetitive regions [467]. Since some of the analyzed histone modifications are known to accumulate over long regions in the host genome the viral genomes were segmented into 5 kbp regions, to mirror such regions. FeatureCounts, a function assigning mapped reads to a genomic feature [468], was applied to count reads within the positive, negative and viral regions. The detected regions were then normalized to input or H3 read count ratio and to the average of the negative control for the respective histone modification. This resulted in a set of values which together display the relative enrichment signal of each histone modification over the general ChIP background. These values were transferred to GraphPad Prism where box-whisker-plots with 5th-95th percentile and median of the average enrichment were generated. This was done for each modification, of the host positive and negative and viral regions. Statistical significance was calculated in GraphPad Prism, using one-way ANOVA with subsequent Sidak's test to compare every mean to every other mean. Significance levels are indicated by asterisks, which are displayed above the compared datasets.

ChIP experiments were done in biological replicates, however only one replicate was sequenced the other replicate is depicted as ChIP-qPCR in the supplementary data.

6.7.2 Statistics for microscopic data

The average of the percentage of RCs-positive cells was calculated for each analyzed cell line and each experiment separately. Average numbers were then transferred to GraphPad Prism where bar-plots were generated, SD was calculated from the average number of the individual experiments and displayed above each bar. Finally, statistical testing was performed by using GraphPad Prism's analysis function. Significance was calculated by one-way ANOVA or unpaired t-test, depending on the number of samples which should be compared, and displayed above the compared bars by asterisks. Each experiment was done in triplicate and microscopic images of a minimum of 500 cells, per experiment, were acquired.

Supplementary Data
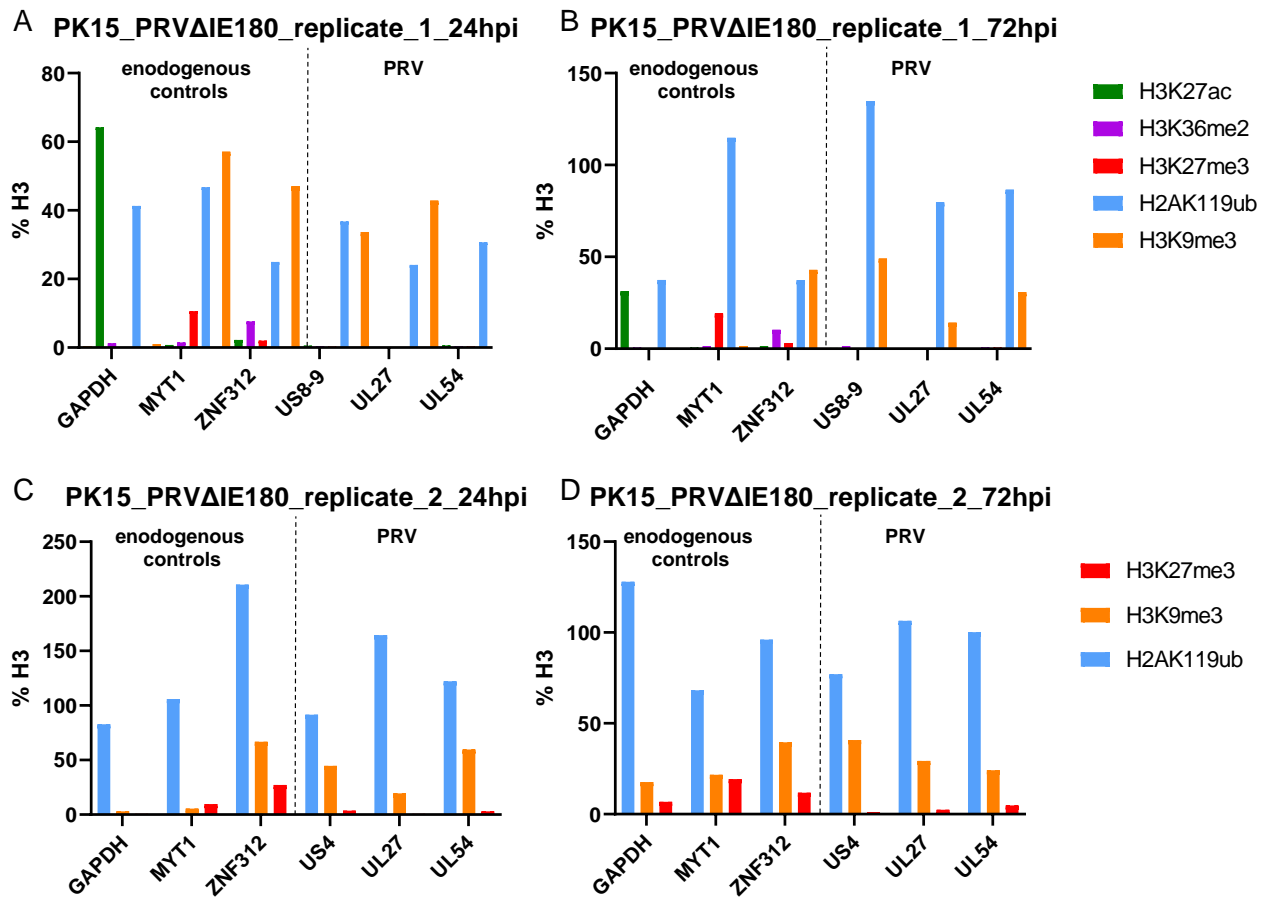
Figure S1: ChIP-qPCR results of PK15 cells infected with PRVΔIE180 at 24 hpi and 72 hpi. Control regions of the host genome that show constant presence or absence of the respective modifications are necessary to decide about an enrichment of the specific modification on the viral genome. GAPDH - an actively transcribed housekeeping gene - was used as a cellular negative control region for heterochromatin on the pig genome. As a positive control for constitutive heterochromatin on the pig genome ZNF312 was used, while as a positive control for facultative heterochromatin MYT1 was used. US4, UL27 and UL54 represent the viral genome. The vertical dashed line separates the endogenous controls from the viral loci. Only the signals for the two repressive marks H3K9me3 and H2AK119ub were above the background signal, on the selected viral regions. In all bar-plots, H3K27me3 levels on the viral loci were below the GAPDH signal. Additionally, H3K27ac levels on the viral genomes were also below the enrichment of the respective negative controls ZNF312 and MYT1. The same was observed for H3K36me2. Therefore, the ChIP-qPCR data showed similar results, when compared to the ChIP-seq data.
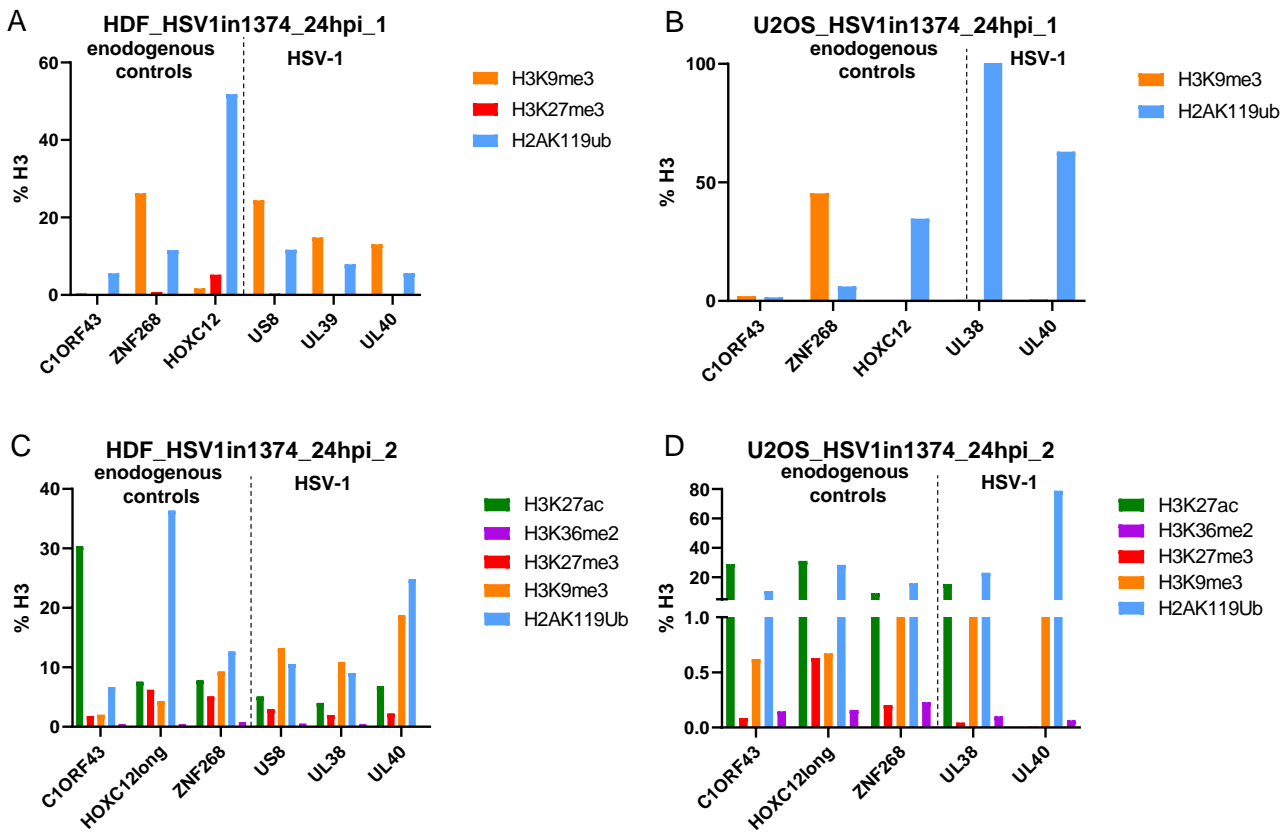
Figure S2: ChIP-qPCR results of HSV-1*in1374* infected HDF and U2OS cells 24 hpi. As a cellular negative control region for heterochromatin on the human genome, C1ORF43 - an actively transcribed housekeeping gene - was used. ZNF268 was used as a positive control for constitutive heterochromatin and HOXC12long as the corresponding counterpart for facultative heterochromatin. The vertical dashed line separates the endogenous controls from the viral loci, i.e. US8, UL38 and UL40. In U2OS cells, the repressive histone marks H3K9me3 and H2AK119ub showed higher signals on the virus genome than the negative control region, indicating the presence of these modification on the viral genome. Furthermore, H2AK119ub signals were higher above background than H3K9me3 signals. This observation corresponds with the sequencing-data in the U2OS cells which were just described. For HDFs, this ratio was inverted, with H3K9me3 signals exceeding H2AK119ub.
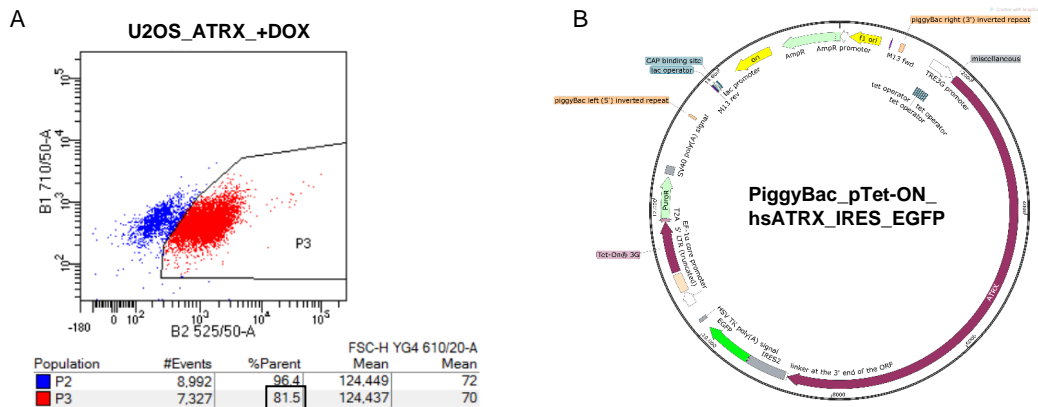
Figure S3: (A) FACS-sorting of cells expressing EGFP after induction with doxycyclin. P3 resembles the EGFP-positive cell population. (B) PiggyBac vector harboring the ATRX-EGFP construct with a doxycyclin inducible Tet-ON promoter and a puromycin resistance-cassette.
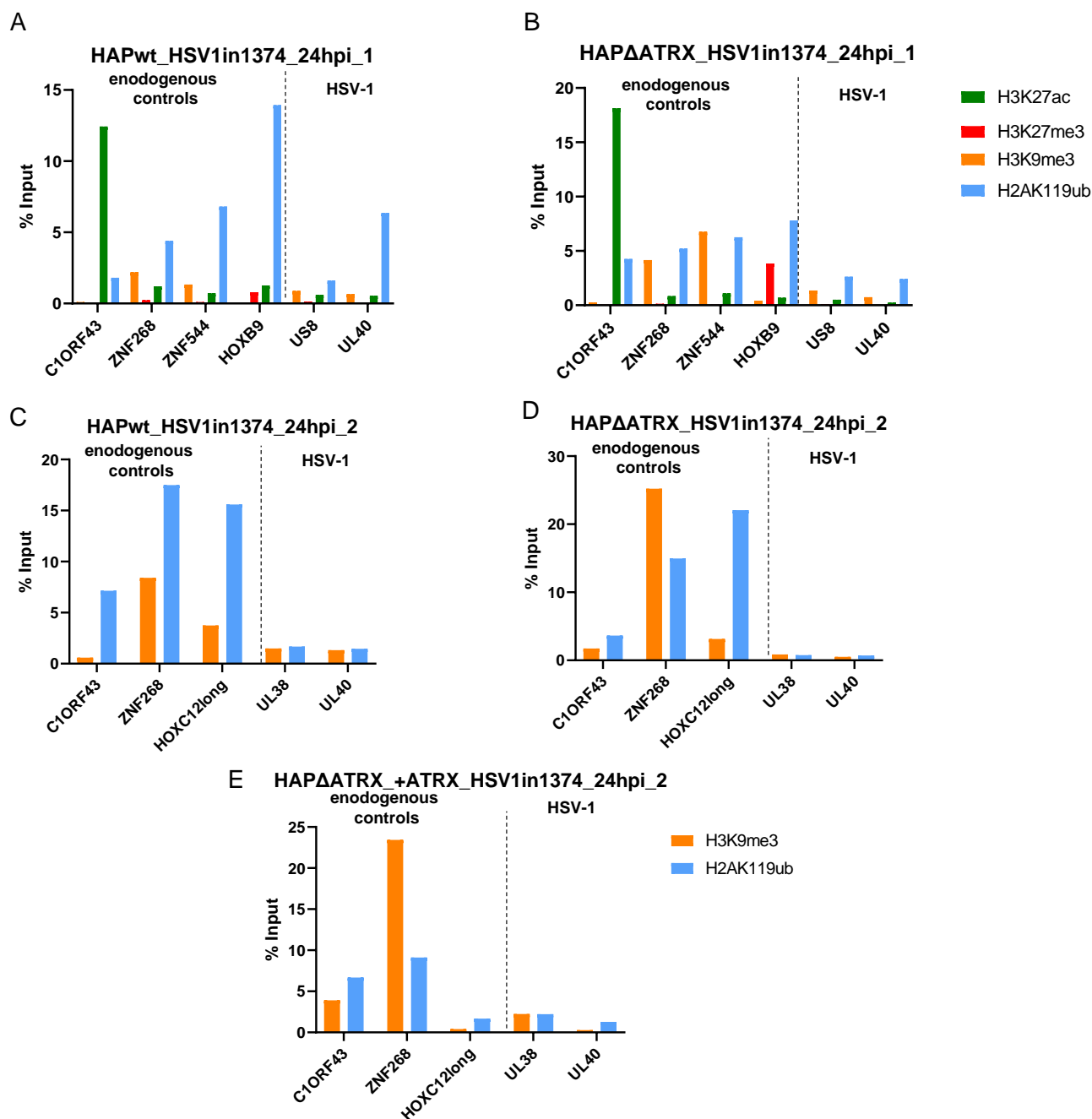
Figure S4: ChIP-qPCR results of HAP1 cells infected with HSV-1in1374 24 hpi. As a cellular negative control region for heterochromatin on the human genome C1ORF43 was used. ZNF268 and ZNF544 were used as a positive control for constitutive heterochromatin and HOXB9 or HOXC12long as the corresponding counterpart for facultative heterochromatin. The vertical dashed line separates the endogenous controls from the viral loci, i.e. US8, UL40 and UL38. Moreover, similar to lytic-cycle-deficient PRV and HSV-1 genomes in the other investigated cell lines, HSV-1 did not acquire H3K27me3 in the two HAP1 cell lines. In the first replicate the enrichment of H2AK119ub was higher than the negative control for this modification, on one viral loci (UL40), in HAP1wt cells. However, this phenomenon was neither observed in the sequencing-data nor in the second replicate. In the first replicate H3K9me3 levels, on the viral genomes, were above the negative control (C1ORF43), in both cell lines, while in the second replicate this was only observed in HAP1wt cells. In addition, after sequencing of the first replicate neither H3K9me3 nor H2AK119ub was detected on the viral genomes in HAP1ΔATRX cells.
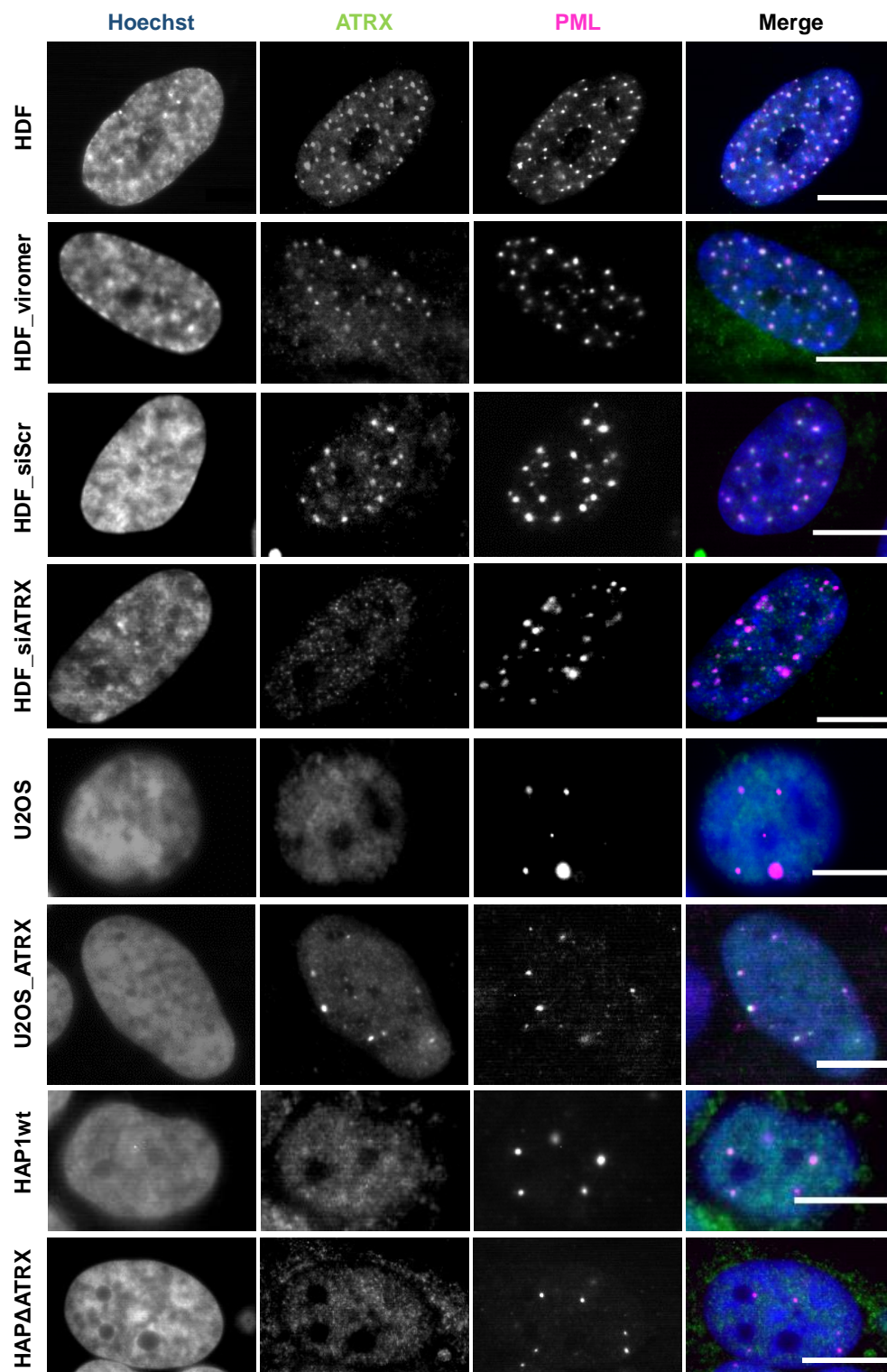
Figure S5: PML-expression in different cell lines was visualized via IF against PML. The nucleus was stained with Hoechst33342. ATRX was visualized by IF with a secondary green-fluorescent antibody, while PML was visualized by IF using a secondary red-fluorescent antibody. Overlapping of the ATRX and PML signals are shown in the merge image. Scale bar indicates 10 µm.

Bibliography

[1]   A. G. Cobián Güemes et al. "Viruses as Winners in the Game of Life." In: *annurev-virology* 3 (2016), pp. 197–214. ISSN: 23270578. DOI: 10.1146/ANNUREV-VIROLOGY-100114-054952.

[2]   L. F. Ludwig-Begall, A. Mauroy, and E. Thiry. "Noroviruses—The State of the Art, Nearly Fifty Years after Their Initial Discovery." In: *Viruses* 13.8 (2021). ISSN: 19994915. DOI: 10.3390/V13081541.

[3]   J. I. Cohen. "Herpesvirus latency." In: *The Journal of Clinical Investigation* 130.7 (2020), pp. 3361–3369. ISSN: 0021-9738. DOI: 10.1172/JCI136225.

[4]   D. J. McGeoch et al. "Molecular phylogeny and evolutionary timescale for the family of mammalian herpesviruses." In: *Journal of molecular biology* 247.3 (1995), pp. 443–458. ISSN: 0022-2836. DOI: 10.1006/JMBI.1995.0152.

[5]   A. J. Davison. "Overview of classification." In: *Human Herpesviruses: Biology, Therapy, and Immunoprophylaxis* (2007), pp. 3–9. DOI: 10.1017/CBO9780511545313.002.

[6]   P. S. Moore et al. "Primary characterization of a herpesvirus agent associated with Kaposi's sarcomae." In: *Journal of virology* 70.1 (1996), pp. 549–558. ISSN: 0022-538X. DOI: 10.1128/jvi.70.1.549-558.1996.

[7]   E. C. Schirmer et al. "Differentiation between two distinct classes of viruses now classified as human herpesvirus 6." In: *Proceedings of the National Academy of Sciences of the United States of America* 88.13 (1991), pp. 5922–5926. ISSN: 0027-8424. DOI: 10.1073/PNAS.88.13.5922.

[8]   P. J. Walker et al. "Changes to virus taxonomy and to the International Code of Virus Classification and Nomenclature ratified by the International Committee on Taxonomy of Viruses (2021)." In: *Archives of Virology* 166.9 (2021), pp. 2633–2648. ISSN: 14328798. DOI: 10.1007/S00705-021-05156-1.

[9]   H. W. Virgin, E. J. Wherry, and R. Ahmed. "Redefining Chronic Viral Infection." In: *Cell* 138.1 (2009), pp. 30–50. ISSN: 0092-8674. DOI: 10.1016/J.CELL.2009.06.036.

[10] J. R. Baringer and P. Swoveland. "Recovery of herpes-simplex virus from human trigeminal ganglions." In: *The New England journal of medicine* 288.13 (1973), pp. 648–650. ISSN: 0028-4793. DOI: 10.1056/NEJM197303292881303.

[11] W. B. BIAs et al. "Herpesvirus hominis: Isolation from Human Trigeminal Ganglion." In: *Science* 178.4058 (1972), pp. 306–307. ISSN: 00368075. DOI: 10.1126/SCIENCE.178.4058.306.

[12]   M. L. Cook, V. B. Bastone, and J. G. Stevens. "Evidence that Neurons Harbor Latent
        Herpes Simplex Virus." In: *Infection and Immunity* 9.5 (1974), pp. 946–951. ISSN: 00199567.
        DOI: `10.1128/IAI.9.5.946-951.1974`.

[13]   D. H. Gilden et al. "Detection of varicella-zoster virus nucleic acid in neurons of normal
        human thoracic ganglia." In: *Annals of Neurology* 22.3 (1987), pp. 377–380. ISSN: 1531-8249.
        DOI: `10.1002/ANA.410220315`.

[14]   K. Kondo, H. Kaneshima, and E. S. Mocarski. "Human cytomegalovirus latent infection of
        granulocyte-macrophage progenitors." In: *Proceedings of the National Academy of Sciences*
        91.25 (1994), pp. 11879–11883. ISSN: 0027-8424. DOI: `10.1073/PNAS.91.25.11879`.

[15]   C. Soderberg-Naucler, K. N. Fish, and J. A. Nelson. "Reactivation of Latent Human Cy-
        tomegalovirus by Allogeneic Stimulation of Blood Cells from Healthy Donors." In: *Cell* 91.1
        (1997), pp. 119–126. ISSN: 0092-8674. DOI: `10.1016/S0092-8674(01)80014-3`.

[16]   E. J. Minton et al. "Human cytomegalovirus infection of the monocyte/macrophage lineage
        in bone marrow." In: *Journal of Virology* 68.6 (1994), pp. 4017–4021. ISSN: 0022-538X. DOI:
        `10.1128/JVI.68.6.4017-4021.1994`.

[17]   W. Kempf et al. "CD68+ cells of monocyte/macrophage lineage in the environment of
        AIDS-associated and classic-sporadic Kaposi sarcoma are singly or doubly infected with
        human herpesviruses 7 and 6B." In: *Proceedings of the National Academy of Sciences* 94.14
        (1997), pp. 7600–7605. ISSN: 0027-8424. DOI: `10.1073/PNAS.94.14.7600`.

[18]   P. K. Pattengale, R. W. Smith, and P. Gerber. "Selective transformation of B lymphocytes
        by E.B. virus." In: *Lancet (London, England)* 2.7820 (1973), pp. 93–94. ISSN: 0140-6736.
        DOI: `10.1016/S0140-6736(73)93286-8`.

[19]   J. C. Niederman et al. "Infectious Mononucleosis: Clinical Manifestations in Relation to
        EB Virus Antibodies." In: *JAMA* 203.3 (1968), pp. 205–209. ISSN: 0098-7484. DOI: `10.
        1001/JAMA.1968.03140030037009`.

[20]   E. Cesarman et al. "Kaposi's sarcoma-associated herpesvirus-like DNA sequences in AIDS-
        related body-cavity-based lymphomas." In: *The New England journal of medicine* 332.18
        (1995), pp. 1186–1191. ISSN: 0028-4793. DOI: `10.1056/NEJM199505043321802`.

[21]   J. Soulier et al. "Kaposi's Sarcoma-Associated Herpesvirus-Like DNA Sequences in Multi-
        centric Castleman's Disease." In: *Blood* 86.4 (1995), pp. 1276–1280. ISSN: 0006-4971. DOI:
        `10.1182/BLOOD.V86.4.1276.BLOODJOURNAL8641276`.

[22]   W. Britt. "Manifestations of Human Cytomegalovirus Infection: Proposed Mechanisms
        of Acute and Chronic Disease." In: *Current Topics in Microbiology and Immunology* 325
        (2008), pp. 417–470. ISSN: 0070217X. DOI: `10.1007/978-3-540-77349-8_23`.

[23]   P. D. L Crombie mD and b. R. Edgar Hope-Simpson MRcs. "The Nature of Herpes Zoster: A
        Long-Term Study and a New Hypothesis:" in: *http://dx.doi.org/10.1177/003591576505800106*
        58.1 (1964), pp. 9–20. ISSN: 01410768. DOI: `10.1177/003591576505800106`.

[24] Y. Chida and X. Mao. "Does psychosocial stress predict symptomatic herpes simplex virus recurrence? A meta-analytic investigation on prospective studies." In: *Brain, Behavior, and Immunity* 23.7 (2009), pp. 917–925. ISSN: 0889-1591. DOI: 10.1016/J.BBI.2009.04.009.

[25] L. El Hayderi et al. "Herpes simplex virus reactivation and dental procedures." In: *Clinical Oral Investigations* 17.8 (2013), pp. 1961–1964. ISSN: 14326981. DOI: 10.1007/S00784-013-0986-3/TABLES/1.

[26] D. A. Padgett et al. "Social stress and the reactivation of latent herpes simplex virus type 1." In: *Proceedings of the National Academy of Sciences* 95.12 (1998), pp. 7231–7235. ISSN: 0027-8424. DOI: 10.1073/PNAS.95.12.7231.

[27] B. Roizman and R. J. Whitley. "An Inquiry into the Molecular Basis of HSV Latency and Reactivation." In: *http://dx.doi.org/10.1146/annurev-micro-092412-155654* 67 (2013), pp. 355–374. ISSN: 00664227. DOI: 10.1146/ANNUREV-MICRO-092412-155654.

[28] F. Ye et al. "Reactive oxygen species hydrogen peroxide mediates Kaposi's sarcoma-associated herpesvirus reactivation from latency." In: *PLoS pathogens* 7.5 (2011). ISSN: 1553-7374. DOI: 10.1371/JOURNAL.PPAT.1002054.

[29] D. A. Davis et al. "Hypoxia induces lytic replication of Kaposi sarcoma-associated herpesvirus." In: *Blood* 97.10 (2001), pp. 3244–3250. ISSN: 0006-4971. DOI: 10.1182/BLOOD.V97.10.3244.

[30] V. Varthakavi et al. "Human immunodeficiency virus type-1 activates lytic cycle replication of Kaposi's sarcoma-associated herpesvirus through induction of KSHV Rta." In: *Virology* 297.2 (2002), pp. 270–280. ISSN: 0042-6822. DOI: 10.1006/VIRO.2002.1434.

[31] S. J. McCullough and D. Todd. "Subclinical Aujeszky's disease virus infection in a pig herd and the characterisation of the strain of virus isolated." In: *The Veterinary record* 122.4 (1988), pp. 77–81. ISSN: 0042-4900. DOI: 10.1136/VR.122.4.77.

[32] M. Pensaert. "Virus infections of porcines." In: (1989). DOI: 10.3/JQUERY-UI.JS.

[33] W. J. Elford and I. A. Galloway. "The Size of the Virus of Aujeszky's Disease ("Pseudorabies", "Infectious Bulbar Paralysis", "Mad-itch") by Ultrafiltration Analysis." In: *The Journal of hygiene* 36.4 (1936), pp. 536–539. ISSN: 0022-1724. DOI: 10.1017/S0022172400043886.

[34] M. Köhler and W. Köhler. "Zentralblatt für Bakteriologie–100 years ago Aladár aujeszky detects a 'new' disease–or: it was the cow and not the sow." In: *International journal of medical microbiology : IJMM* 292.7-8 (2003), pp. 423–427. ISSN: 1438-4221. DOI: 10.1078/1438-4221-00233.

[35] J. Sehl and J. P. Teifke. "Comparative Pathology of Pseudorabies in Different Naturally and Experimentally Infected Species—A Review." In: *Pathogens 2020, Vol. 9, Page 633* 9.8 (2020), p. 633. ISSN: 20760817. DOI: 10.3390/PATHOGENS9080633.

[36]   E. E. Brittle, A. E. Reynolds, and L. W. Enquist. "Two modes of pseudorabies virus neuroinvasion and lethality in mice." In: *Journal of virology* 78.23 (2004), pp. 12951–12963. ISSN: 0022-538X. DOI: 10.1128/JVI.78.23.12951-12963.2004.

[37]   E. Wyssmann. *Nochmals zur Frage des Vorkommens der Aujeszky'schen...* 1942.

[38]   R. R. Gillespie et al. "Infection of pigs by Aujeszky's disease virus via the breath of intranasally inoculated pigs." In: *Research in Veterinary Science* 68.3 (2000), pp. 217–222. ISSN: 0034-5288. DOI: 10.1053/RVSC.1999.0364.

[39]   R. R. Gillespie, M. A. Hill, and C. L. Kanitz. "Infection of pigs by aerosols of Aujeszky's disease virus and their shedding of the virus." In: *Research in Veterinary Science* 60.3 (1996), pp. 228–233. ISSN: 0034-5288. DOI: 10.1016/S0034-5288(96)90044-2.

[40]   D. E. Gutekunst et al. "Isolation of pseudorabies virus from trigeminal ganglia of a latently infected sow." In: *American Journal of Veterinary Research* 41.8 (1980), pp. 1315–1316. ISSN: 0002-9645.

[41]   H. J. Rziha et al. "Herpesvirus (pseudorabies virus) latency in swine: Occurrence and physical state of viral DNA in neural tissues." In: *Virology* 155.2 (1986), pp. 600–613. ISSN: 0042-6822. DOI: 10.1016/0042-6822(86)90220-5.

[42]   K. J. Looker et al. "Global and Regional Estimates of Prevalent and Incident Herpes Simplex Virus Type 1 Infections in 2012." In: *PLOS ONE* 10.10 (2015), e0140765. ISSN: 1932-6203. DOI: 10.1371/JOURNAL.PONE.0140765.

[43]   M. J. Cannon, T. B. Hyde, and D. S. Schmid. "Review of cytomegalovirus shedding in bodily fluids and relevance to congenital cytomegalovirus infection." In: *Reviews in medical virology* 21.4 (2011), pp. 240–255. ISSN: 1099-1654. DOI: 10.1002/RMV.695.

[44]   M. Ihira et al. "Variation of Human Herpesvirus 7 Shedding in Saliva." In: *Journal of Infectious Diseases* 188.9 (2003), pp. 1352–1354. ISSN: 00221899. DOI: 10.1086/379040/2/188-9-1352-TAB001.GIF.

[45]   J. H. Arbuckle et al. "The latent human herpesvirus-6A genome specifically integrates in telomeres of human chromosomes in vivo and in vitro." In: *Proceedings of the National Academy of Sciences* 107.12 (2010), pp. 5563–5568. ISSN: 0027-8424. DOI: 10.1073/PNAS.0913586107.

[46]   J. Sinclair and P. Sissons. "Latency and reactivation of human cytomegalovirus." In: *Journal of General Virology* 87.7 (2006), pp. 1763–1779. ISSN: 0022-1317. DOI: 10.1099/VIR.0.81891-0.

[47]   S. M. Mbulaiteye et al. "Human Herpesvirus 8 Infection within Families in Rural Tanzania." In: *The Journal of Infectious Diseases* 187.11 (2003), pp. 1780–1785. ISSN: 0022-1899. DOI: 10.1086/374973.

[48]   R. Newton et al. "Determinants of Gammaherpesvirus Shedding in Saliva Among Ugandan Children and Their Mothers." In: *The Journal of Infectious Diseases* 218.6 (2018), p. 892. ISSN: 15376613. DOI: 10.1093/INFDIS/JIY262.

[49] M. JOHN PAUK, M.D., M.P.H., MEEI-LI HUANG, PH.D., SCOTT J. BRODIE, D.V.M., PH.D., ANNA WALD, M.D., M. DAVID M. KOELLE, M.D., TIMOTHY SCHACKER, M.D., CONNIE CELUM, M.D., M.P.H., STACY SELKE, and M. AND LAWRENCE COREY. "Mucosal Shedding of Human Herpesvirus 8 in Men." In: 343.19 (2000), pp. 1369–1377. ISSN: 0028-4793. DOI: `10.1056/NEJM200011093431904`.

[50] R. R et al. "The size and conformation of Kaposi's sarcoma-associated herpesvirus (human herpesvirus 8) DNA in infected cells and virions." In: *Journal of virology* 70.11 (1996), pp. 8151–8154. ISSN: 0022-538X. DOI: `10.1128/JVI.70.11.8151-8154.1996`.

[51] A. J. Barbera et al. "The nucleosomal surface as a docking station for Kaposi's sarcoma herpesvirus LANA." In: *Science (New York, N.Y.)* 311.5762 (2006), pp. 856–861. ISSN: 1095-9203. DOI: `10.1126/SCIENCE.1120541`.

[52] M. E. Ballestas, P. A. Chatis, and K. M. Kaye. "Efficient persistence of extrachromosomal KSHV DNA mediated by latency-associated nuclear antigen." In: *Science (New York, N.Y.)* 284.5414 (1999), pp. 641–644. ISSN: 0036-8075. DOI: `10.1126/SCIENCE.284.5414.641`.

[53] M. C. Morris et al. "Sero-epidemiological patterns of Epstein-Barr and herpes simplex (HSV-1 and HSV-2) viruses in England and Wales." In: *Journal of medical virology* 67.4 (2002), pp. 522–527. ISSN: 0146-6615. DOI: `10.1002/JMV.10132`.

[54] J. W. S. Setoh et al. "Epstein-Barr Virus Seroprevalence and Force of Infection in a Multiethnic Pediatric Cohort, Singapore." In: *The Pediatric infectious disease journal* 38.12 (2019), pp. 1173–1176. ISSN: 1532-0987. DOI: `10.1097/INF.0000000000002484`.

[55] E. T. Lennette, D. J. Blackbourn, and J. A. Levy. "Antibodies to human herpesvirus type 8 in the general population and in Kaposi's sarcoma patients." In: *Lancet (London, England)* 348.9031 (1996), pp. 858–861. ISSN: 0140-6736. DOI: `10.1016/S0140-6736(96)03240-0`.

[56] S. J. Gao et al. "KSHV antibodies among Americans, Italians and Ugandans with and without Kaposi's sarcoma." In: *Nature medicine* 2.8 (1996), pp. 925–927. ISSN: 1078-8956. DOI: `10.1038/NM0896-925`.

[57] H. H. Balfour et al. "Behavioral, Virologic, and Immunologic Factors Associated With Acquisition and Severity of Primary Epstein–Barr Virus Infection in University Students." In: *The Journal of Infectious Diseases* 207.1 (2013), pp. 80–88. ISSN: 0022-1899. DOI: `10.1093/INFDIS/JIS646`.

[58] G. Henle and W. Henle. "Immunofluorescence, interference, and complement fixation technics in the detection of the herpes-type virus in Burkitt tumor cell lines." In: *Cancer Research* 27.12 (1967), pp. 2442–2446. ISSN: 0008-5472.

[59] Z. H. Zhou et al. "Seeing the herpesvirus capsid at 8.5 Å." In: *Science* 288.5467 (2000), pp. 877–880. ISSN: 00368075. DOI: `10.1126/science.288.5467.877`.

[60] K. Grünewald et al. "Three-Dimensional Structure of Herpes Simplex Virus from Cryo-Electron Tomography." In: *Science* 302.5649 (2003), pp. 1396–1398. ISSN: 00368075. DOI: `10.1126/science.1090284`.

[61] B. Roizman. "The organization of the herpes simplex virus genomes." In: *Annual review of genetics* 13 (1979), pp. 25–57. ISSN: 0066-4197. DOI: `10.1146/ANNUREV.GE.13.120179.000325`.

[62] A. Dolan et al. "Genetic content of wild-type human cytomegalovirus." In: *The Journal of general virology* 85.Pt 5 (2004), pp. 1301–1312. ISSN: 0022-1317. DOI: `10.1099/VIR.0.79888-0`.

[63] J. J. Russo et al. "Nucleotide sequence of the Kaposi sarcoma-associated herpesvirus (HHV8)." In: *Proceedings of the National Academy of Sciences of the United States of America* 93.25 (1996), pp. 14862–14867. ISSN: 0027-8424. DOI: `10.1073/PNAS.93.25.14862`.

[64] A. Dolan et al. "The genome sequence of herpes simplex virus type 2." In: *Journal of virology* 72.3 (1998), pp. 2010–2021. ISSN: 0022-538X. DOI: `10.1128/JVI.72.3.2010-2021.1998`.

[65] G. S. Hayward et al. "Anatomy of herpes simplex virus DNA: evidence for four populations of molecules that differ in the relative orientations of their long and short components." In: *Proceedings of the National Academy of Sciences* 72.11 (1975), pp. 4243–4247. ISSN: 0027-8424. DOI: `10.1073/PNAS.72.11.4243`.

[66] K. Umene et al. "Diversity of the a sequence of herpes simplex virus type 1 developed during evolution." In: *The Journal of general virology* 89.Pt 4 (2008), pp. 841–852. ISSN: 0022-1317. DOI: `10.1099/VIR.0.83467-0`.

[67] M. Lagunoff and D. Ganem. "The structure and coding organization of the genomic termini of Kaposi's sarcoma-associated herpesvirus." In: *Virology* 236.1 (1997), pp. 147–154. ISSN: 0042-6822. DOI: `10.1006/VIRO.1997.8713`.

[68] F. P. Booy et al. "Liquid-crystalline, phage-like packing of encapsidated DNA in herpes simplex virus." In: *Cell* 64.5 (1991), pp. 1007–1015. ISSN: 0092-8674. DOI: `10.1016/0092-8674(91)90324-R`.

[69] D. J. Owen, C. M. Crump, and S. C. Graham. *Tegument assembly and secondary envelopment of alphaherpesviruses.* 2015. DOI: `10.3390/v7092861`.

[70] J. D. Heming, J. F. Conway, and F. L. Homa. "Herpesvirus capsid assembly and DNA packaging." In: *Advances in anatomy, embryology, and cell biology* 223 (2017), p. 119. ISSN: 03015556. DOI: `10.1007/978-3-319-53168-7_6`.

[71] Y. You et al. "The suppression of apoptosis by α-herpesvirus." In: *Cell Death & Disease 2017 8:4* 8.4 (2017), e2749–e2749. ISSN: 2041-4889. DOI: `10.1038/cddis.2017.139`.

[72] B. C. Herold et al. "Glycoprotein C-independent binding of herpes simplex virus to cells requires cell surface heparan sulphate and glycoprotein B." In: *The Journal of general virology* 75 (Pt 6).6 (1994), pp. 1211–1222. ISSN: 0022-1317. DOI: `10.1099/0022-1317-75-6-1211`.

[73] W. Cai, B. Gu, and S. Person. "Role of glycoprotein B of herpes simplex virus type 1 in viral entry and cell fusion." In: *Journal of Virology* 62.8 (1988), p. 2596. ISSN: 0022-538X. DOI: `10.1128/jvi.62.8.2596-2604.1988`.

[74] C. Addison et al. "Characterisation of a herpes simplex virus type 1 mutant which has a temperature-sensitive defect in penetration of cells and assembly of capsids." In: *Virology* 138.2 (1984), pp. 246–259. ISSN: 0042-6822. DOI: 10.1016/0042-6822(84)90349-0.

[75] V. C. Bond and S. Person. "Fine structure physical map locations of alterations that affect cell fusion in herpes simplex virus type 1." In: *Virology* 132.2 (1984), pp. 368–376. ISSN: 0042-6822. DOI: 10.1016/0042-6822(84)90042-4.

[76] S. M. Akula et al. "Human herpesvirus 8 envelope-associated glycoprotein B interacts with heparan sulfate-like moieties." In: *Virology* 284.2 (2001), pp. 235–249. ISSN: 0042-6822. DOI: 10.1006/VIRO.2001.0921.

[77] A. S. Hahn et al. "The ephrin receptor tyrosine kinase A2 is a cellular receptor for Kaposi's sarcoma–associated herpesvirus." In: *Nature medicine* 18.6 (2012), pp. 961–966. ISSN: 1546-170X. DOI: 10.1038/NM.2805.

[78] R. S. Cooper and E. E. Heldwein. "Herpesvirus gB: A Finely Tuned Fusion Machine." In: *Viruses* 7.12 (2015), p. 6552. ISSN: 19994915. DOI: 10.3390/V7122957.

[79] M. W. Ligas and D. C. Johnson. "A herpes simplex virus mutant in which glycoprotein D sequences are replaced by beta-galactosidase sequences binds to but is unable to penetrate into cells." In: *Journal of Virology* 62.5 (1988), pp. 1486–1494. ISSN: 0022-538X. DOI: 10.1128/JVI.62.5.1486-1494.1988.

[80] P. E. Pertel et al. "Cell fusion induced by herpes simplex virus glycoproteins gB, gD, and gH-gL requires a gD receptor but not necessarily heparan sulfate." In: *Virology* 279.1 (2001), pp. 313–324. ISSN: 0042-6822. DOI: 10.1006/VIRO.2000.0713.

[81] B. C. Herold et al. "Glycoprotein C of herpes simplex virus type 1 plays a principal role in the adsorption of virus to cells and in infectivity." In: *Journal of virology* 65.3 (1991), pp. 1090–1098. ISSN: 0022-538X. DOI: 10.1128/JVI.65.3.1090-1098.1991.

[82] S. A. Simpson et al. "Nectin-1/HveC mediates herpes simplex virus type 1 entry into primary human sensory neurons and fibroblasts." In: *Journal of NeuroVirology 2005 11:2* 11.2 (2005), pp. 208–218. ISSN: 1538-2443. DOI: 10.1080/13550280590924214.

[83] C.-F. G et al. "The multipartite system that mediates entry of herpes simplex virus into the cell." In: *Reviews in medical virology* 17.5 (2007), pp. 313–326. ISSN: 1052-9276. DOI: 10.1002/RMV.546.

[84] S. PG. "Herpes simplex virus: receptors and ligands for cell entry." In: *Cellular microbiology* 6.5 (2004), pp. 401–410. ISSN: 1462-5814. DOI: 10.1111/J.1462-5822.2004.00389.X.

[85] D. Atanasiu et al. "Bimolecular complementation reveals that glycoproteins gB and gH/gL of herpes simplex virus interact with each other during cell fusion." In: *Proceedings of the National Academy of Sciences of the United States of America* 104.47 (2007), p. 18718. DOI: 10.1073/PNAS.0707452104.

[86] E. Lycke et al. "Herpes simplex virus infection of the human sensory neuron." In: *Archives of Virology 1988 101:1* 101.1 (1988), pp. 87–104. ISSN: 1432-8798. DOI: 10.1007/BF01314654.

[87] S. B, E. MW, and H. A. "Microtubule-mediated transport of incoming herpes simplex virus 1 capsids to the nucleus." In: *The Journal of cell biology* 136.5 (1997), pp. 1007–1021. ISSN: 0021-9525. DOI: `10.1083/JCB.136.5.1007`.

[88] S. M. Akula et al. "Integrin $\alpha 3\beta 1$ (CD 49c/29) Is a Cellular Receptor for Kaposi's Sarcoma-Associated Herpesvirus (KSHV/HHV-8) Entry into the Target Cells." In: *Cell* 108.3 (2002), pp. 407–419. ISSN: 0092-8674. DOI: `10.1016/S0092-8674(02)00628-1`.

[89] J. A. Kaleeba and E. A. Berger. "Kaposi's sarcoma-associated herpesvirus fusion-entry receptor: cystine transporter xCT." In: *Science (New York, N.Y.)* 311.5769 (2006), pp. 1921–1924. ISSN: 1095-9203. DOI: `10.1126/SCIENCE.1120878`.

[90] G. Rappocciolo et al. "Human Herpesvirus 8 Infects and Replicates in Primary Cultures of Activated B Lymphocytes through DC-SIGN." In: *Journal of Virology* 82.10 (2008), pp. 4793–4806. ISSN: 0022-538X. DOI: `10.1128/JVI.01587-07/ASSET/4F20D80A-D1B3-4163-88F3-3BC84BBC803C/ASSETS/GRAPHIC/ZJV0100805600009.JPEG`.

[91] A. SM et al. "Kaposi's sarcoma-associated herpesvirus (human herpesvirus 8) infection of human fibroblast cells occurs through endocytosis." In: *Journal of virology* 77.14 (2003), pp. 7978–7990. ISSN: 0022-538X. DOI: `10.1128/JVI.77.14.7978-7990.2003`.

[92] P. P. Naranatt et al. "Kaposi's Sarcoma-Associated Herpesvirus Modulates Microtubule Dynamics via RhoA-GTP-Diaphanous 2 Signaling and Utilizes the Dynein Motors To Deliver Its DNA to the Nucleus." In: *Journal of Virology* 79.2 (2005), pp. 1191–1206. ISSN: 0022-538X. DOI: `10.1128/JVI.79.2.1191-1206.2005/ASSET/4569B3D4-A957-4A98-983E-4061E402E7CB/ASSETS/GRAPHIC/ZJV0020556790011.JPEG`.

[93] T. Günther and A. Grundhoff. "The epigenetic landscape of latent kaposi sarcoma-associated herpesvirus genomes." In: *PLoS Pathogens* 6.6 (2010). ISSN: 15537366. DOI: `10.1371/journal.ppat.1000935`.

[94] Z. Toth et al. "Epigenetic analysis of KSHV latent and lytic genomes." In: *PLoS Pathogens* 6.7 (2010), pp. 1–17. ISSN: 15537374. DOI: `10.1371/journal.ppat.1001013`.

[95] A. R. Cliffe, D. M. Coen, and D. M. Knipe. "Kinetics of facultative heterochromatin and polycomb group protein association with the herpes simplex viral genome during establishment of latent infection." In: *mBio* 4.1 (2013). ISSN: 21507511. DOI: `10.1128/mBio.00590-12`.

[96] A. R. Cliffe and D. M. Knipe. "Herpes Simplex Virus ICP0 Promotes both Histone Removal and Acetylation on Viral DNA during Lytic Infection." In: *Journal of Virology* 82.24 (2008), pp. 12030–12038. ISSN: 0022-538X. DOI: `10.1128/jvi.01575-08`.

[97] D. M. Knipe and A. Cliffe. "Chromatin control of herpes simplex virus lytic and latent infection." In: *Nature Reviews Microbiology* 6.3 (2008), pp. 211–221. ISSN: 17401526. DOI: `10.1038/nrmicro1794`.

[98] W. Hafezi et al. "Entry of Herpes Simplex Virus Type 1 (HSV-1) into the Distal Axons of Trigeminal Neurons Favors the Onset of Nonproductive, Silent Infection." In: *PLOS Pathogens* 8.5 (2012), e1002679. ISSN: 1553-7374. DOI: `10.1371/JOURNAL.PPAT.1002679`.

[99] L. W. Enquist et al. "Infection and spread of alphaherpesviruses in the nervous system." In: *Advances in virus research* 51 (1998), pp. 237–347. ISSN: 0065-3527. DOI: `10.1016/S0065-3527(08)60787-3`.

[100] B. Sodeik. "Mechanisms of viral transport in the cytoplasm." In: *Trends in microbiology* 8.10 (2000), pp. 465–472. ISSN: 0966-842X. DOI: `10.1016/S0966-842X(00)01824-2`.

[101] G. A. Smith, S. P. Gross, and L. W. Enquist. "Herpesviruses use bidirectional fast-axonal transport to spread in sensory neurons." In: *Proceedings of the National Academy of Sciences* 98.6 (2001), pp. 3466–3470. ISSN: 0027-8424. DOI: `10.1073/PNAS.061029798`.

[102] S. V. Zaichick et al. "The Herpesvirus VP1/2 Protein Is an Effector of Dynein-Mediated Capsid Transport and Neuroinvasion." In: *Cell Host & Microbe* 13.2 (2013), pp. 193–203. ISSN: 1931-3128. DOI: `10.1016/J.CHOM.2013.01.009`.

[103] B. Roizman and A. E. Sears. "An Inquiry into the Mechanisms of Herpes Simplex Virus Latency." In: *http://dx.doi.org/10.1146/annurev.mi.41.100187.002551* 41 (1987), pp. 543–571. ISSN: 00664227. DOI: `10.1146/ANNUREV.MI.41.100187.002551`.

[104] G. B. Clements and P. G. Kennedy. "Modulation of herpes simplex virus (HSV) infection of cultured neuronal cells by nerve growth factor and antibody to HSV." In: *Brain : a journal of neurology* 112 (Pt 5.5 (1989), pp. 1277–1294. ISSN: 0006-8950. DOI: `10.1093/BRAIN/112.5.1277`.

[105] S. Tanaka et al. "Analysis by RNA-PCR of latency and reactivation of herpes simplex virus in multiple neuronal tissues." In: *The Journal of general virology* 75 (Pt 10.10 (1994), pp. 2691–2698. ISSN: 0022-1317. DOI: `10.1099/0022-1317-75-10-2691`.

[106] R. J. Visalli, R. J. Courtney, and C. Meyers. "Infection and replication of herpes simplex virus type 1 in an organotypic epithelial culture system." In: *Virology* 230.2 (1997), pp. 236–243. ISSN: 0042-6822. DOI: `10.1006/VIRO.1997.8484`.

[107] I. Hogk et al. "An In Vitro HSV-1 Reactivation Model Containing Quiescently Infected PC12 Cells." In: *BioResearch Open Access* 2.4 (2013), p. 250. ISSN: 2164-7860. DOI: `10.1089/BIORES.2013.0019`.

[108] M. J. Farrell, A. T. Dobson, and L. T. Feldman. "Herpes simplex virus latency-associated transcript is a stable intron." In: *Proceedings of the National Academy of Sciences* 88.3 (1991), pp. 790–794. ISSN: 0027-8424. DOI: `10.1073/PNAS.88.3.790`.

[109] J. L. Umbach et al. "MicroRNAs expressed by herpes simplex virus 1 during latent infection regulate viral mRNAs." In: *Nature 2008 454:7205* 454.7205 (2008), pp. 780–783. ISSN: 1476-4687. DOI: `10.1038/nature07103`.

[110] J. G. Spivack and N. W. Fraser. "Detection of herpes simplex virus type 1 transcripts during latent infection in mice." In: *Journal of Virology* 61.12 (1987), pp. 3841–3847. ISSN: 0022-538X. DOI: 10.1128/JVI.61.12.3841-3847.1987.

[111] S. JG et al. "RNA complementary to a herpesvirus alpha gene mRNA is prominent in latently infected neurons." In: *Science (New York, N.Y.)* 235.4792 (1987), pp. 1056–1059. ISSN: 0036-8075. DOI: 10.1126/SCIENCE.2434993.

[112] J. L. Umbach et al. "Identification of Viral MicroRNAs Expressed in Human Sacral Ganglia Latently Infected with Herpes Simplex Virus 2." In: *Journal of Virology* 84.2 (2010), pp. 1189–1192. ISSN: 0022-538X. DOI: 10.1128/JVI.01712-09/ASSET/5BFC487F-997D-4705-A9C8-EAF3D1C0F5B4/ASSETS/GRAPHIC/ZJV0021027700004.JPEG.

[113] T. Du et al. "Patterns of accumulation of miRNAs encoded by herpes simplex virus during productive infection, latency, and on reactivation." In: *Proceedings of the National Academy of Sciences of the United States of America* 112.1 (2015), E49–E55. ISSN: 10916490. DOI: 10.1073/PNAS.1422657112.

[114] J. L. Arthur et al. "Disruption of the 5' and 3' splice sites flanking the major latency-associated transcripts of herpes simplex virus type 1: Evidence for alternate splicing in lytic and latent infections." In: *Journal of General Virology* 79.1 (1998), pp. 107–116. ISSN: 00221317. DOI: 10.1099/0022-1317-79-1-107/CITE/REFWORKS.

[115] T. Du, G. Zhou, and B. Roizman. "HSV-1 gene expression from reactivated ganglia is disordered and concurrent with suppression of latency-associated transcript and miRNAs." In: *Proceedings of the National Academy of Sciences of the United States of America* 108.46 (2011), p. 18820. ISSN: 00278424. DOI: 10.1073/PNAS.1117203108.

[116] I. Steiner. "Herpes simplex virus encephalitis: new infection or reactivation?" In: *Current opinion in neurology* 24.3 (2011), pp. 268–274. ISSN: 1473-6551. DOI: 10.1097/WCO.0B013E328346BE6F.

[117] R. L. Kodukula, Padma and Liu, Ting and Rooijen, Nico Van and Jager, Martine J. and Hendricks. *Macrophage Control of Herpes Simplex Virus Type 1 Replication in the Peripheral Nervous System.* 1999.

[118] N. De Regge et al. "Interferon Alpha Induces Establishment of Alphaherpesvirus Latency in Sensory Neurons In Vitro." In: *PLOS ONE* 5.9 (2010), e13076. ISSN: 1932-6203. DOI: 10.1371/JOURNAL.PONE.0013076.

[119] J. B. Suzich et al. "PML-Dependent Memory of Type I Interferon Treatment Results in a Restricted Form of HSV Latency." In: *bioRxiv* (2021), p. 2021.02.03.429616. DOI: 10.1101/2021.02.03.429616.

[120] R. D. Everett et al. "Herpes Simplex Virus Type 1 Genomes Are Associated with ND10 Nuclear Substructures in Quiescently Infected Human Fibroblasts." In: *Journal of Virology* 81.20 (2007), pp. 10991–11004. ISSN: 0022-538X. DOI: 10.1128/jvi.00705-07.

[121] M. Catania and G. Di Fede. "One or more β-amyloid(s)? New insights into the prion-like nature of Alzheimer's disease." In: *Progress in Molecular Biology and Translational Science* 175 (2020), pp. 213–237. ISSN: 1877-1173. DOI: `10.1016/BS.PMBTS.2020.07.003`.

[122] T. E. Allsopp et al. "Virus infection induces neuronal apoptosis: A comparison with trophic factor withdrawal." In: *Cell death and differentiation* 5.1 (1998), pp. 50–59. ISSN: 1350-9047. DOI: `10.1038/SJ.CDD.4400298`.

[123] L. E. Pomeranz, A. E. Reynolds, and C. J. Hengartner. "Molecular Biology of Pseudorabies Virus: Impact on Neurovirology and Veterinary Medicine." In: *Microbiology and Molecular Biology Reviews* 69.3 (2005), pp. 462–500. ISSN: 1092-2172. DOI: `10.1128/MMBR.69.3.462-500.2005/ASSET/89F5DA7A-672B-4395-BDCB-33D06EAEBE72/ASSETS/GRAPHIC/ZMR0030520960005.JPEG`.

[124] A. Orvedahl et al. "HSV-1 ICP34.5 Confers Neurovirulence by Targeting the Beclin 1 Autophagy Protein." In: *Cell Host & Microbe* 1.1 (2007), pp. 23–35. ISSN: 1931-3128. DOI: `10.1016/J.CHOM.2006.12.001`.

[125] K. M. Khanna et al. "Herpes simplex virus-specific memory CD8+ T cells are selectively activated and retained in latently infected sensory ganglia." In: *Immunity* 18.5 (2003), pp. 593–603. ISSN: 1074-7613. DOI: `10.1016/S1074-7613(03)00112-2`.

[126] T. Liu et al. "CD8(+) T cells can block herpes simplex virus type 1 (HSV-1) reactivation from latency in sensory neurons." In: *The Journal of experimental medicine* 191.9 (2000), pp. 1459–1466. ISSN: 0022-1007. DOI: `10.1084/JEM.191.9.1459`.

[127] D. Theil et al. "Latent herpesvirus infection in human trigeminal ganglia causes chronic immune response." In: *The American journal of pathology* 163.6 (2003), pp. 2179–2184. ISSN: 0002-9440. DOI: `10.1016/S0002-9440(10)63575-4`.

[128] J. E. Knickelbein et al. "Noncytotoxic Lytic Granule-Mediated CD8+ T Cell Inhibition of HSV-1 Reactivation from Neuronal Latency." In: *Science (New York, N.Y.)* 322.5899 (2008), p. 268. ISSN: 00368075. DOI: `10.1126/SCIENCE.1164164`.

[129] K. E. Allen and R. D. Everett. "Mutations which alter the DNA binding properties of the herpes simplex virus type 1 transactivating protein Vmw175 also affect its ability to support virus replication." In: *Journal of General Virology* 78.11 (1997), pp. 2913–2922. ISSN: 00221317. DOI: `10.1099/0022-1317-78-11-2913`.

[130] N. A. DeLuca, A. M. McCarthy, and P. A. Schaffer. "Isolation and characterization of deletion mutants of herpes simplex virus type 1 in the gene encoding immediate-early regulatory protein ICP4." In: *Journal of Virology* 56.2 (1985), pp. 558–570. ISSN: 0022-538X. DOI: `10.1128/jvi.56.2.558-570.1985`.

[131] R. J. Watson and J. B. Clements. "A herpes simplex virus type 1 function continuously required for early and late virus RNA synthesis." In: *Nature* 285.5763 (1980), pp. 329–330. ISSN: 00280836. DOI: `10.1038/285329a0`.

[132]   J. Pardo et al. "The biology of cytotoxic cell granule exocytosis pathway: granzymes have evolved to induce cell death and inflammation." In: *Microbes and Infection* 11.4 (2009), pp. 452–459. ISSN: 1286-4579. DOI: `10.1016/J.MICINF.2009.02.004`.

[133]   X. Jiang et al. "The Herpes Simplex Virus Type 1 Latency-Associated Transcript Can Protect Neuron-Derived C1300 and Neuro2A Cells from Granzyme B-Induced Apoptosis and CD8 T-Cell Killing." In: *Journal of Virology* 85.5 (2011), p. 2325. ISSN: 0022-538X. DOI: `10.1128/JVI.01791-10`.

[134]   A. R. Cliffe, D. A. Garber, and D. M. Knipe. "Transcription of the Herpes Simplex Virus Latency-Associated Transcript Promotes the Formation of Facultative Heterochromatin on Lytic Promoters." In: *Journal of Virology* 83.16 (2009), pp. 8182–8190. ISSN: 0022-538X. DOI: `10.1128/jvi.00712-09`.

[135]   C. Cohen et al. *Promyelocytic leukemia (PML) nuclear bodies (NBs) induce latent/quiescent HSV-1 genomes chromatinization through a PML NB/Histone H3.3/H3.3 Chaperone Axis.* Vol. 14. 9. 2018, pp. 1–39. ISBN: 1111111111. DOI: `10.1371/journal.ppat.1007313`.

[136]   J. M. Cabral, H. S. Oh, and D. M. Knipe. "ATRX promotes maintenance of herpes simplex virus heterochromatin during chromatin stress." In: *eLife* 7 (2018), pp. 1–32. ISSN: 2050084X. DOI: `10.7554/eLife.40228`.

[137]   A. Grundhoff and D. Ganem. "Inefficient establishment of KSHV latency suggests an additional role for continued lytic replication in Kaposi sarcoma pathogenesis." In: *The Journal of Clinical Investigation* 113.1 (2004), pp. 124–136. ISSN: 0021-9738. DOI: `10.1172/JCI17803`.

[138]   K. A. Staskus et al. "Kaposi's sarcoma-associated herpesvirus gene expression in endothelial (spindle) tumor cells." In: *Journal of virology* 71.1 (1997), pp. 715–719. ISSN: 0022-538X. DOI: `10.1128/JVI.71.1.715-719.1997`.

[139]   D. Dittmer et al. "A cluster of latently expressed genes in Kaposi's sarcoma-associated herpesvirus." In: *Journal of virology* 72.10 (1998), pp. 8309–8315. ISSN: 0022-538X. DOI: `10.1128/JVI.72.10.8309-8315.1998`.

[140]   X. Cai et al. "Kaposi's sarcoma-associated herpesvirus expresses an array of viral microRNAs in latently infected cells." In: *Proceedings of the National Academy of Sciences* 102.15 (2005), pp. 5570–5575. ISSN: 0027-8424. DOI: `10.1073/PNAS.0408192102`.

[141]   A. Grundhoff and D. Ganem. "The Latency-Associated Nuclear Antigen of Kaposi's Sarcoma-Associated Herpesvirus Permits Replication of Terminal Repeat-Containing Plasmids." In: *Journal of Virology* 77.4 (2003), p. 2779. ISSN: 0022-538X. DOI: `10.1128/JVI.77.4.2779-2783.2003`.

[142]   J. Hu, A. C. Garber, and R. Renne. "The Latency-Associated Nuclear Antigen of Kaposi's Sarcoma-Associated Herpesvirus Supports Latent DNA Replication in Dividing Cells." In: *Journal of Virology* 76.22 (2002), p. 11677. ISSN: 0022-538X. DOI: `10.1128/JVI.76.22.11677-11687.2002`.

[143] S. C. Verma et al. "Latency-Associated Nuclear Antigen (LANA) of Kaposi's Sarcoma-Associated Herpesvirus Interacts with Origin Recognition Complexes at the LANA Binding Sequence within the Terminal Repeats." In: *Journal of Virology* 80.5 (2006), p. 2243. ISSN: 0022-538X. DOI: `10.1128/JVI.80.5.2243-2256.2006`.

[144] K. Lan et al. "Kaposi's Sarcoma-Associated Herpesvirus-Encoded Latency-Associated Nuclear Antigen Inhibits Lytic Replication by Targeting Rta: a Potential Mechanism for Virus-Mediated Control of Latency." In: *Journal of Virology* 78.12 (2004), p. 6585. ISSN: 0022-538X. DOI: `10.1128/JVI.78.12.6585-6594.2004`.

[145] T. Uppal et al. "Chromatinization of the KSHV Genome During the KSHV Life Cycle." In: *Cancers* 7.1 (2015), p. 112. ISSN: 20726694. DOI: `10.3390/CANCERS7010112`.

[146] T. Günther et al. "Influence of ND10 Components on Epigenetic Determinants of Early KSHV Latency Establishment." In: *PLoS Pathogens* 10.7 (2014). ISSN: 15537374. DOI: `10.1371/journal.ppat.1004274`.

[147] I. B. Hilton et al. "The open chromatin landscape of Kaposi's sarcoma-associated herpesvirus." In: *Journal of virology* 87.21 (2013), pp. 11831–11842. ISSN: 1098-5514. DOI: `10.1128/JVI.01685-13`.

[148] R. P. Darst et al. "Epigenetic diversity of Kaposi's sarcoma–associated herpesvirus." In: *Nucleic Acids Research* 41.5 (2013), pp. 2993–3009. ISSN: 0305-1048. DOI: `10.1093/NAR/GKT033`.

[149] R. W. Honess and B. Roizman. "Regulation of Herpesvirus Macromolecular Synthesis I. Cascade Regulation of the Synthesis of Three Groups of Viral Proteins." In: *Journal of Virology* 14.1 (1974), pp. 8–19. ISSN: 0022-538X. DOI: `10.1128/JVI.14.1.8-19.1974`.

[150] J. P. Weir. "Regulation of herpes simplex virus gene expression." In: *Gene* 271.2 (2001), pp. 117–130. ISSN: 0378-1119. DOI: `10.1016/S0378-1119(01)00512-1`.

[151] B. W and R. B. "Characterization of the herpes simplex virion-associated factor responsible for the induction of alpha genes." In: *Journal of virology* 46.2 (1983), pp. 371–377. ISSN: 0022-538X. DOI: `10.1128/JVI.46.2.371-377.1983`.

[152] T. M. Kristie and P. A. Sharp. "Interactions of the Oct-1 POU subdomains with specific DNA sequences and with the HSV α-trans-activator protein." In: *Genes and Development* 4.12 B (1990), pp. 2383–2396. ISSN: 08909369. DOI: `10.1101/gad.4.12b.2383`.

[153] M. Katan et al. "Characterization of a cellular factor which interacts functionally with Oct-1 in the assembly of a multicomponent transcription complex." In: *Nucleic Acids Research* 18.23 (1990), pp. 6871–6880. ISSN: 03051048. DOI: `10.1093/nar/18.23.6871`.

[154] J. S. Lai and W Herr. "Interdigitated residues within a small region of VP16 interact with Oct-1, HCF, and DNA." In: *Molecular and Cellular Biology* 17.7 (1997), pp. 3937–3946. ISSN: 0270-7306. DOI: `10.1128/mcb.17.7.3937`.

[155]   J. Knez, P. T. Bilan, and J. P. Capone. "A Single Amino Acid Substitution in Herpes Simplex Virus Type 1 VP16 Inhibits Binding to the Virion Host Shutoff Protein and Is Incompatible with Virus Growth." In: *Journal of Virology* 77.5 (2003), pp. 2892–2902. ISSN: 0022-538X. DOI: 10.1128/jvi.77.5.2892-2902.2003.

[156]   W. Cun et al. "Transcriptional regulation of the herpes Simplex Virus 1α-gene by the viral immediate-early protein ICP22 in association with VP16." In: *Science in China, Series C: Life Sciences* 52.4 (2009), pp. 344–351. ISSN: 10069305. DOI: 10.1007/s11427-009-0051-2.

[157]   M. Miranda-Saksena et al. "Anterograde Transport of Herpes Simplex Virus Type 1 in Cultured, Dissociated Human and Rat Dorsal Root Ganglion Neurons." In: *Journal of Virology* 74.4 (2000), pp. 1827–1839. ISSN: 0022-538X. DOI: 10.1128/jvi.74.4.1827-1839.2000.

[158]   N. M. Sawtell and R. L. Thompson. "De Novo Herpes Simplex Virus VP16 Expression Gates a Dynamic Programmatic Transition and Sets the Latent/Lytic Balance during Acute Infection in Trigeminal Ganglia." In: *PLoS Pathogens* 12.9 (2016), e1005877. ISSN: 15537374. DOI: 10.1371/journal.ppat.1005877.

[159]   R. L. Thompson, C. M. Preston, and N. M. Sawtell. "De Novo Synthesis of VP16 Coordinates the Exit from HSV Latency In Vivo." In: *PLOS Pathogens* 5.3 (2009), e1000352. ISSN: 1553-7374. DOI: 10.1371/JOURNAL.PPAT.1000352.

[160]   R. L. Thompson and N. M. Sawtell. "Targeted Promoter Replacement Reveals That Herpes Simplex Virus Type-1 and 2 Specific VP16 Promoters Direct Distinct Rates of Entry Into the Lytic Program in Sensory Neurons in vivo." In: *Frontiers in Microbiology* 10 (2019), p. 1624. ISSN: 1664-302X. DOI: 10.3389/fmicb.2019.01624.

[161]   L. Frizzo da Silva et al. "Bovine Herpesvirus 1 Regulatory Proteins bICP0 and VP16 Are Readily Detected in Trigeminal Ganglionic Neurons Expressing the Glucocorticoid Receptor during the Early Stages of Reactivation from Latency." In: *Journal of Virology* 87.20 (2013), pp. 11214–11222. ISSN: 0022-538X. DOI: 10.1128/JVI.01737-13/ASSET/D9E5FE9D-A1C0-4A54-9A0F-3886DCE58BF3/ASSETS/GRAPHIC/ZJV9990981660007.JPEG.

[162]   I. Kook, A. Doster, and C. Jones. "Bovine herpesvirus 1 regulatory proteins are detected in trigeminal ganglionic neurons during the early stages of stress-induced escape from latency." In: *Journal of NeuroVirology* 21.5 (2015), pp. 585–591. ISSN: 15382443. DOI: 10.1007/S13365-015-0339-X/FIGURES/4.

[163]   L. Sawant et al. "The Cellular Coactivator HCF-1 Is Required for Glucocorticoid Receptor-Mediated Transcription of Bovine Herpesvirus 1 Immediate Early Genes." In: *Journal of Virology* 92.17 (2018), pp. 987–1005. ISSN: 0022-538X. DOI: 10.1128/JVI.00987-18/ASSET/84C6667F-7755-45E8-8E26-CDEC4EA8D6F4/ASSETS/GRAPHIC/ZJV0161837960007.JPEG.

[164] C. Boutell, S. Sadis, and R. D. Everett. "Herpes Simplex Virus Type 1 Immediate-Early Protein ICP0 and Its Isolated RING Finger Domain Act as Ubiquitin E3 Ligases In Vitro." In: *Journal of Virology* 76.2 (2002), pp. 841–850. ISSN: 0022-538X. DOI: 10.1128/jvi.76.2.841-850.2002.

[165] L. J. Perry et al. "Characterization of the IE110 gene of herpes simplex virus type 1." In: *Journal of General Virology* 67.11 (1986), pp. 2365–2380. ISSN: 00221317. DOI: 10.1099/0022-1317-67-11-2365.

[166] I. H. Gelman and S. Silverstein. "Identification of immediate early genes from herpes simplex virus that transactivate the virus thymidine kinase gene." In: *Proceedings of the National Academy of Sciences of the United States of America* 82.16 (1985), pp. 5265–5269. ISSN: 00278424. DOI: 10.1073/pnas.82.16.5265.

[167] P O'Hare and G. S. Hayward. "Three trans-acting regulatory proteins of herpes simplex virus modulate immediate-early gene expression in a pathway involving positive and negative feedback regulation." In: *Journal of Virology* 56.3 (1985), pp. 723–733. ISSN: 0022-538X. DOI: 10.1128/jvi.56.3.723-733.1985.

[168] R. D. Everett. "The products of herpes simplex virus type 1 (HSV-1) immediate early genes 1, 2, 3 can activate HSV-1 gene expression in trans." In: *Journal of General Virology* 67.11 (1986), pp. 2507–2513. ISSN: 00221317. DOI: 10.1099/0022-1317-67-11-2507.

[169] G. G. Maul, H. H. Guldner, and J. G. Spivack. "Modification of discrete nuclear domains induced by herpes simplex virus type 1 immediate early gene 1 product (ICPO)." In: *Journal of General Virology* 74.12 (1993), pp. 2679–2690. ISSN: 00221317. DOI: 10.1099/0022-1317-74-12-2679.

[170] G. G. Maul and R. D. Everett. "The nuclear location of PML, a cellular member of the C3HC4 zinc-binding domain protein family, is rearranged during herpes simplex virus infection by the C3HC4 viral protein ICP0." In: *Journal of General Virology* 75.6 (1994), pp. 1223–1233. ISSN: 00221317. DOI: 10.1099/0022-1317-75-6-1223.

[171] R. Everett and G. Maul. "HSV-1 IE protein Vmw110 causes redistribution of PML." In: *The EMBO Journal* 13.21 (1994), pp. 5062–5069. ISSN: 02614189. DOI: 10.1002/j.1460-2075.1994.tb06835.x.

[172] H. Gu and B. Roizman. "The degradation of promyelocytic leukemia and Sp100 proteins by herpes simplex virus 1 is mediated by the ubiquitin-conjugating enzyme UbcH5a." In: *Proceedings of the National Academy of Sciences of the United States of America* 100.15 (2003), pp. 8963–8968. ISSN: 00278424. DOI: 10.1073/pnas.1533420100.

[173] R Everett et al. "Point mutations in the herpes simplex virus type 1 Vmw110 RING finger helix affect activation of gene expression, viral growth, and interaction with PML-containing nuclear structures." In: *Journal of virology* 69.11 (1995), pp. 7339–7344. ISSN: 0022-538X. DOI: 10.1128/jvi.69.11.7339-7344.1995.

[174] D. O'Rourke et al. "Examination of determinants for intranuclear localization and transactivation within the RING finger of herpes simplex virus type 1 IE110k protein." In: *Journal of General Virology* 79.3 (1998), pp. 537–548. ISSN: 00221317. DOI: `10.1099/0022-1317-79-3-537`.

[175] N. D. Stow and E. C. Stow. "Isolation and characterization of a herpes simplex virus type 1 mutant containing a deletion within the gene encoding the immediate early polypeptide Vmw110." In: *Journal of General Virology* 67.12 (1986), pp. 2571–2585. ISSN: 00221317. DOI: `10.1099/0022-1317-67-12-2571`.

[176] W. R. Sacks and P. A. Schaffer. "Deletion mutants in the gene encoding the herpes simplex virus type 1 immediate-early protein ICP0 exhibit impaired growth in cell culture." In: *Journal of Virology* 61.3 (1987), pp. 829–839. ISSN: 0022-538X. DOI: `10.1128/JVI.61.3.829-839.1987`.

[177] R. D. Everett, C. Boutell, and A. Orr. "Phenotype of a Herpes Simplex Virus Type 1 Mutant That Fails To Express Immediate-Early Regulatory Protein ICP0." In: *Journal of Virology* 78.4 (2004), pp. 1763–1774. ISSN: 0022-538X. DOI: `10.1128/jvi.78.4.1763-1774.2004`.

[178] F Yao and P. A. Schaffer. "An activity specified by the osteosarcoma line U2OS can substitute functionally for ICP0, a major regulatory protein of herpes simplex virus type 1." In: *Journal of Virology* 69.10 (1995).

[179] T. Deschamps and M. Kalamvoki. "Impaired STING Pathway in Human Osteosarcoma U2OS Cells Contributes to the Growth of ICP0-Null Mutant Herpes Simplex Virus." In: *Journal of Virology* 91.9 (2017). ISSN: 0022-538X. DOI: `10.1128/jvi.00006-17`.

[180] T. Alandijany et al. "Distinct temporal roles for the promyelocytic leukaemia (PML) protein in the sequential regulation of intracellular host immunity to HSV-1 infection." In: *PLoS Pathogens* 14.1 (2018), pp. 1–36. ISSN: 15537374. DOI: `10.1371/journal.ppat.1006769`.

[181] J. S. Lee, P. Raja, and D. M. Knipe. "Herpesviral ICP0 protein promotes two waves of heterochromatin removal on an early viral promoter during lytic infection." In: *mBio* 7.1 (2016). ISSN: 21507511. DOI: `10.1128/mBio.02007-15`.

[182] J. A. Dembowski and N. A. Deluca. "Temporal viral genome-protein interactions define distinct stages of productive herpesviral infection." In: *mBio* 9.4 (2018), pp. 1–18. ISSN: 21507511. DOI: `10.1128/mBio.01182-18`.

[183] M. Kalamvoki and B. Roizman. "The Histone Acetyltransferase CLOCK Is an Essential Component of the Herpes Simplex Virus 1 Transcriptome That Includes TFIID, ICP4, ICP27, and ICP22." In: *Journal of Virology* 85.18 (2011), pp. 9472–9477. ISSN: 0022-538X. DOI: `10.1128/jvi.00876-11`.

[184] S. Tang, A. Patel, and P. R. Krause. "Herpes simplex virus ICP27 regulates alternative pre-mRNA polyadenylation and splicing in a sequence-dependent manner." In: *Proceedings of the National Academy of Sciences of the United States of America* 113.43 (2016), pp. 12256–12561. ISSN: 10916490. DOI: `10.1073/pnas.1609695113`.

[185] S. Tang, A. Patel, and P. R. Krause. "Hidden regulation of herpes simplex virus 1 pre-mRNA splicing and polyadenylation by virally encoded immediate early gene ICP27." In: *PLoS Pathogens* 15.6 (2019), pp. 1–30. ISSN: 15537374. DOI: 10.1371/journal.ppat.1007884.

[186] C. K. Lee and D. M. Knipe. "An immunoassay for the study of DNA-binding activities of herpes simplex virus protein ICP8." In: *Journal of Virology* 54.3 (1985), pp. 731–738. ISSN: 0022-538X. DOI: 10.1128/jvi.54.3.731-738.1985.

[187] W. T. Ruyechan. "The major herpes simplex virus DNA-binding protein holds single-stranded DNA in an extended configuration." In: *Journal of Virology* 46.2 (1983), pp. 661–666. ISSN: 0022-538X. DOI: 10.1128/jvi.46.2.661-666.1983.

[188] M. Olesky et al. "Evidence for a direct interaction between HSV-1 ICP27 and ICP8 proteins." In: *Virology* 331.1 (2005), pp. 94–105. ISSN: 00426822. DOI: 10.1016/j.virol.2004.10.003.

[189] K. L. Carter and B. Roizman. "The promoter and transcriptional unit of a novel herpes simplex virus 1 alpha gene are contained in, and encode a protein in frame with, the open reading frame of the alpha 22 gene." In: *Journal of Virology* 70.1 (1996), pp. 172–178. ISSN: 0022-538X. DOI: 10.1128/JVI.70.1.172-178.1996.

[190] A. E. Sears ' et al. "Herpes simplex virus 1 mutant deleted in the alpha 22 gene: growth and gene expression in permissive and restrictive cells and establishment of latency in mice." In: *Journal of Virology* 55.2 (1985), pp. 338–346. ISSN: 0022-538X. DOI: 10.1128/JVI.55.2.338-346.1985.

[191] J. S. Orlando et al. "ICP22 Is Required for Wild-Type Composition and Infectivity of Herpes Simplex Virus Type 1 Virions." In: *Journal of Virology* 80.19 (2006), pp. 9381–9390. ISSN: 0022-538X. DOI: 10.1128/JVI.01061-06/ASSET/3002A742-C17E-4461-8990-3BA85F5172E9/ASSETS/GRAPHIC/ZJV0190682210007.JPEG.

[192] T. W. Bastian et al. "Herpes Simplex Virus Type 1 Immediate-Early Protein ICP22 Is Required for VICE Domain Formation during Productive Viral Infection." In: *Journal of Virology* 84.5 (2010), pp. 2384–2394. ISSN: 0022-538X. DOI: 10.1128/jvi.01686-09.

[193] H. H. Mostafa and D. J. Davido. " Herpes Simplex Virus 1 ICP22 but Not U S 1.5 Is Required for Efficient Acute Replication in Mice and VICE Domain Formation." In: *Journal of Virology* 87.24 (2013), pp. 13510–13519. ISSN: 0022-538X. DOI: 10.1128/JVI.02424-13/ASSET/FD3EC17C-45AC-4E64-9D02-65F591DEB644/ASSETS/GRAPHIC/ZJV9990984030010.JPEG.

[194] L. Li et al. "Hsc70 focus formation at the periphery of HSV-1 transcription sites requires ICP27." In: *PLoS one* 3.1 (2008). ISSN: 1932-6203. DOI: 10.1371/JOURNAL.PONE.0001491.

[195] A. D. Burch and S. K. Weller. "Herpes Simplex Virus Type 1 DNA Polymerase Requires the Mammalian Chaperone Hsp90 for Proper Localization to the Nucleus." In: *Journal of Virology* 79.16 (2005), pp. 10740–10749. ISSN: 0022-538X. DOI: `10.1128/JVI.79.16.10740-10749.2005/ASSET/2DB00729-C6AC-44E3-99BF-8BF77E2D36B1/ASSETS/GRAPHIC/ZJV0160566420006.JPEG`.

[196] C. M. Livingston et al. "Virus-Induced Chaperone-Enriched (VICE) Domains Function as Nuclear Protein Quality Control Centers during HSV-1 Infection." In: *PLOS Pathogens* 5.10 (2009), e1000619. ISSN: 1553-7374. DOI: `10.1371/JOURNAL.PPAT.1000619`.

[197] K. Früh et al. "A viral inhibitor of peptide transporters for antigen presentation." In: *Nature* 375.6530 (1995), pp. 415–418. ISSN: 0028-0836. DOI: `10.1038/375415A0`.

[198] B. K. Goldsmith et al. "Neurovirulence by Blocking the CD8+ T Cell Response." In: *The Journal of experimental medicine* 187.3 (1998), pp. 0–7.

[199] A. K. Cheung. "DNA nucleotide sequence analysis of the immediate-early gene of pseudorabies virus." In: *Nucleic Acids Research* 17.12 (1989), pp. 4637–4646. ISSN: 0305-1048. DOI: `10.1093/NAR/17.12.4637`.

[200] N. Van Opdenbosch et al. "The IE180 protein of pseudorabies virus suppresses phosphorylation of translation initiation factor eIF2α." In: *Journal of virology* 86.13 (2012), pp. 7235–7240. ISSN: 1098-5514. DOI: `10.1128/JVI.06929-11`.

[201] S. Yamada and M. Shimizu. "Isolation and characterization of mutants of pseudorabies virus with deletion in the immediate-early regulatory gene." In: *Virology* 199.2 (1994), pp. 366–375. ISSN: 00426822. DOI: `10.1006/viro.1994.1134`.

[202] J. Parkinson and R. D. Everett. "Alphaherpesvirus proteins related to herpes simplex virus type 1 ICP0 affect cellular structures and proteins." In: *Journal of virology* 74.21 (2000), pp. 10006–10017. ISSN: 0022-538X. DOI: `10.1128/JVI.74.21.10006-10017.2000`.

[203] A. Brukman and L. W. Enquist. "Pseudorabies Virus EP0 Protein Counteracts an Interferon-Induced Antiviral State in a Species-Specific Manner." In: *Journal of Virology* 80.21 (2006), p. 10871. ISSN: 0022-538X. DOI: `10.1128/JVI.01308-06`.

[204] J. Guito and D. M. Lukac. "KSHV Rta Promoter Specification and Viral Reactivation." In: *Frontiers in microbiology* 3.FEB (2012). ISSN: 1664-302X. DOI: `10.3389/FMICB.2012.00030`.

[205] D. M. Lukac, J. R. Kirshner, and D. Ganem. "Transcriptional Activation by the Product of Open Reading Frame 50 of Kaposi's Sarcoma-Associated Herpesvirus Is Required for Lytic Viral Reactivation in B Cells." In: *Journal of Virology* 73.11 (1999), pp. 9348–9361. ISSN: 0022-538X. DOI: `10.1128/JVI.73.11.9348-9361.1999/ASSET/9E13ED7A-660F-411B-983A-B06ED44F35A3/ASSETS/GRAPHIC/JV1190851008.JPEG`.

[206] Y. Liang et al. "The lytic switch protein of KSHV activates gene expression via functional interaction with RBP-Jκ (CSL), the target of the Notch signaling pathway." In: *Genes & Development* 16.15 (2002), pp. 1977–1989. ISSN: 0890-9369. DOI: `10.1101/GAD.996502`.

[207] R. Kaul et al. "KSHV lytic proteins K-RTA and K8 bind to cellular and viral chromatin to modulate gene expression." In: *PLoS ONE* 14.4 (2019). ISSN: 19326203. DOI: `10.1371/JOURNAL.PONE.0215394`.

[208] Z. Toth et al. "Biphasic Euchromatin-to-Heterochromatin Transition on the KSHV Genome Following De Novo Infection." In: *PLOS Pathogens* 9.12 (2013), e1003813. ISSN: 1553-7374. DOI: `10.1371/JOURNAL.PPAT.1003813`.

[209] Z. Toth et al. "LANA-Mediated Recruitment of Host Polycomb Repressive Complexes onto the KSHV Genome during De Novo Infection." In: *PLOS Pathogens* 12.9 (2016), e1005878. ISSN: 1553-7374. DOI: `10.1371/JOURNAL.PPAT.1005878`.

[210] T. Günther et al. "A comparative epigenome analysis of gammaherpesviruses suggests cis-acting sequence features as critical mediators of rapid polycomb recruitment." In: *PLoS Pathogens* 15.10 (2019). ISSN: 15537374. DOI: `10.1371/journal.ppat.1007838`.

[211] C. C. Rossetto and G. Pari. "KSHV PAN RNA Associates with Demethylases UTX and JMJD3 to Activate Lytic Replication through a Physical Interaction with the Virus Genome." In: *PLOS Pathogens* 8.5 (2012), e1002680. ISSN: 1553-7374. DOI: `10.1371/JOURNAL.PPAT.1002680`.

[212] F. Y. Wu et al. "Origin-Independent Assembly of Kaposi's Sarcoma-Associated Herpesvirus DNA Replication Compartments in Transient Cotransfection Assays and Association with the ORF-K8 Protein and Cellular PML." In: *Journal of Virology* 75.3 (2001), pp. 1487–1506. ISSN: 0022-538X. DOI: `10.1128/JVI.75.3.1487-1506.2001/ASSET/20E40004-3210-48C1-9B82-C5289B60A260/ASSETS/GRAPHIC/JV0311805011.JPEG`.

[213] I. Y. C. Lai, P. J. Farrell, and P. Kellam. "X-box binding protein 1 induces the expression of the lytic cycle transactivator of Kaposi's sarcoma-associated herpesvirus but not Epstein–Barr virus in co-infected primary effusion lymphoma." In: *The Journal of General Virology* 92.Pt 2 (2011), p. 421. ISSN: 00221317. DOI: `10.1099/VIR.0.025494-0`.

[214] L. Dalton-Griffin, S. J. Wilson, and P. Kellam. "X-box binding protein 1 contributes to induction of the Kaposi's sarcoma-associated herpesvirus lytic cycle under hypoxic conditions." In: *Journal of virology* 83.14 (2009), pp. 7202–7209. ISSN: 1098-5514. DOI: `10.1128/JVI.00076-09`.

[215] S. J. Wilson et al. "X box binding protein XBP-1s transactivates the Kaposi's sarcoma-associated herpesvirus (KSHV) ORF50 promoter, linking plasma cell differentiation to KSHV reactivation from latency." In: *Journal of virology* 81.24 (2007), pp. 13578–13586. ISSN: 1098-5514. DOI: `10.1128/JVI.01663-07`.

[216] L. M. Liptak, S. L. Uprichard, and D. M. Knipe. "Functional order of assembly of herpes simplex virus DNA replication proteins into prereplicative site structures." In: *Journal of virology* 70.3 (1996), pp. 1759–1767. ISSN: 0022-538X. DOI: `10.1128/JVI.70.3.1759-1767.1996`.

[217] R. Skaliter and I. R. Lehman. "Rolling circle DNA replication in vitro by a complex of herpes simplex virus type 1-encoded enzymes." In: *Proceedings of the National Academy of Sciences of the United States of America* 91.22 (1994), p. 10665. ISSN: 00278424. DOI: `10.1073/PNAS.91.22.10665`.

[218] F. J. Rixon et al. "Multiple interactions control the intracellular localization of the herpes simplex virus type 1 capsid proteins." In: *Journal of General Virology* 77.9 (1996), pp. 2251–2260. ISSN: 00221317. DOI: `10.1099/0022-1317-77-9-2251`.

[219] A. A. Aksyuk et al. "Subassemblies and asymmetry in assembly of herpes simplex virus procapsid." In: *mBio* 6.5 (2015). ISSN: 21507511. DOI: `10.1128/MBIO.01525-15/SUPPL_FILE/MBO005152496SM1.MOV`.

[220] W. W. Newcomb, F. L. Homa, and J. C. Brown. "Involvement of the Portal at an Early Step in Herpes Simplex Virus Capsid Assembly." In: *Journal of Virology* 79.16 (2005), pp. 10540–10546. ISSN: 0022-538X. DOI: `10.1128/JVI.79.16.10540-10546.2005/ASSET/74E52616-C0F1-4612-8ABD-AAAADD7CDFB6/ASSETS/GRAPHIC/ZJV0160566860007.JPEG`.

[221] W. W. Newcomb et al. "Assembly of the Herpes Simplex Virus Procapsid from Purified Components and Identification of Small Complexes Containing the Major Capsid and Scaffolding Proteins." In: *Journal of Virology* 73.5 (1999), pp. 4239–4250. ISSN: 0022-538X. DOI: `10.1128/JVI.73.5.4239-4250.1999/ASSET/ECAEC9FC-D03B-4764-AC80-BAC58B113B7F/ASSETS/GRAPHIC/JV0591987011.JPEG`.

[222] Y. Yang et al. "Architecture of the herpesvirus genome-packaging complex and implications for DNA translocation." In: *Protein and Cell* 11.5 (2020), pp. 339–351. ISSN: 16748018. DOI: `10.1007/S13238-020-00710-0/FIGURES/4`.

[223] N. S. Taus and J. D. Baines. "Herpes Simplex Virus 1 DNA Cleavage/Packaging: The UL28 Gene Encodes a Minor Component of B Capsids." In: *Virology* 252.2 (1998), pp. 443–449. ISSN: 0042-6822. DOI: `10.1006/VIRO.1998.9475`.

[224] P. M. Beard, C. Duffy, and J. D. Baines. " Quantification of the DNA Cleavage and Packaging Proteins U L 15 and U L 28 in A and B Capsids of Herpes Simplex Virus Type 1." In: *Journal of Virology* 78.3 (2004), pp. 1367–1374. ISSN: 0022-538X. DOI: `10.1128/JVI.78.3.1367-1374.2004/ASSET/991CC0CE-5DC5-4F78-B254-E31A463DEFF6/ASSETS/GRAPHIC/ZJV0030414250006.JPEG`.

[225] R. W. Darlington and I. L. Howard Moss. "Herpesvirus Envelopment." In: *Journal of Virology* 2.1 (1968), pp. 48–55. ISSN: 0022-538X. DOI: `10.1128/JVI.2.1.48-55.1968`.

[226] P. J. Desai et al. "Reconstitution of the Kaposi's Sarcoma-Associated Herpesvirus Nuclear Egress Complex and Formation of Nuclear Membrane Vesicles by Coexpression of ORF67 and ORF69 Gene Products." In: *Journal of Virology* 86.1 (2012), pp. 594–598. ISSN: 0022-538X. DOI: `10.1128/JVI.05988-11/ASSET/BD50A6A9-9AD1-42D0-9EE8-AEBDE0FF9DFC/ASSETS/GRAPHIC/ZJV9990954150003.JPEG`.

[227] B. G. Klupp et al. "Vesicle formation from the nuclear membrane is induced by coexpression of two conserved herpesvirus proteins." In: *Proceedings of the National Academy of Sciences* 104.17 (2007), pp. 7241–7246. ISSN: 0027-8424. DOI: `10.1073/PNAS.0701757104`.

[228] P. Siminoff and M. G. Menefee. "Normal and 5-bromodeoxyuridine-inhibited development of herpes simplex virus: An electron microscope study." In: *Experimental Cell Research* 44.2-3 (1966), pp. 241–255. ISSN: 0014-4827. DOI: `10.1016/0014-4827(66)90429-0`.

[229] J. N. Skepper et al. "Herpes Simplex Virus Nucleocapsids Mature to Progeny Virions by an Envelopment → Deenvelopment → Reenvelopment Pathway." In: *Journal of Virology* 75.12 (2001), pp. 5697–5702. ISSN: 0022-538X. DOI: `10.1128/JVI.75.12.5697-5702.2001/ASSET/AA5260B3-4B67-4708-9B3E-9F342516057E/ASSETS/GRAPHIC/JV12122952DF.JPEG`.

[230] A. A. Gershon et al. "Intracellular transport of newly synthesized varicella-zoster virus: final envelopment in the trans-Golgi network." In: *Journal of Virology* 68.10 (1994), pp. 6372–6390. ISSN: 0022-538X. DOI: `10.1128/JVI.68.10.6372-6390.1994`.

[231] T. N. McMillan and D. C. Johnson. " Cytoplasmic Domain of Herpes Simplex Virus gE Causes Accumulation in the trans -Golgi Network, a Site of Virus Envelopment and Sorting of Virions to Cell Junctions." In: *Journal of Virology* 75.4 (2001), pp. 1928–1940. ISSN: 0022-538X. DOI: `10.1128/JVI.75.4.1928-1940.2001/ASSET/AAD5868C-C0BE-4891-B340-7B7580E41881/ASSETS/GRAPHIC/JV0411710010.JPEG`.

[232] E. Avitabile et al. "The herpes simplex virus UL20 protein compensates for the differential disruption of exocytosis of virions and viral membrane glycoproteins associated with fragmentation of the Golgi apparatus." In: *Journal of Virology* 68.11 (1994), pp. 7397–7405. ISSN: 0022-538X. DOI: `10.1128/JVI.68.11.7397-7405.1994`.

[233] H. Granzow et al. "Egress of Alphaherpesviruses: Comparative Ultrastructural Study." In: *Journal of Virology* 75.8 (2001), pp. 3675–3684. ISSN: 0022-538X. DOI: `10.1128/JVI.75.8.3675-3684.2001/ASSET/8C28BDED-2D38-480F-90E9-2152D97540C9/ASSETS/GRAPHIC/JV0812232006.JPEG`.

[234] T. C. Mettenleiter. "Herpesvirus Assembly and Egress." In: *Journal of Virology* 76.4 (2002), pp. 1537–1547. ISSN: 0022-538X. DOI: `10.1128/JVI.76.4.1537-1547.2002/ASSET/55DEBCB4-B7B5-42CC-8281-E9A40348BE61/ASSETS/GRAPHIC/JV0421958004.JPEG`.

[235] M. J. Tomishima and L. W. Enquist. "A conserved α-herpesvirus protein necessary for axonal localization of viral membrane proteins." In: *Journal of Cell Biology* 154.4 (2001), pp. 741–752. ISSN: 0021-9525. DOI: `10.1083/JCB.200011146`.

[236] M. E. Whealy et al. "Specific pseudorabies virus infection of the rat visual system requires both gI and gp63 glycoproteins." In: *Journal of virology* 67.7 (1993), pp. 3786–3797. ISSN: 0022-538X. DOI: `10.1128/JVI.67.7.3786-3797.1993`.

[237] K. S. Dingwell, L. C. Doering, and D. C. Johnson. "Glycoproteins E and I facilitate neuron-to-neuron spread of herpes simplex virus." In: *Journal of virology* 69.11 (1995), pp. 7087–7098. ISSN: 0022-538X. DOI: `10.1128/JVI.69.11.7087-7098.1995`.

[238]   T. Kramer et al. "Kinesin-3 Mediates Axonal Sorting and Directional Transport of Alpha-herpesvirus Particles in Neurons." In: *Cell Host & Microbe* 12.6 (2012), pp. 806–814. ISSN: 1931-3128. DOI: `10.1016/J.CHOM.2012.10.013`.

[239]   N. Siddiqui and A. Straube. "Intracellular cargo transport by kinesin-3 motors." In: *Biochemistry (Moscow) 2017 82:7* 82.7 (2017), pp. 803–815. ISSN: 1608-3040. DOI: `10.1134/S0006297917070057`.

[240]   N. Hirokawa and Y. Noda. "Intracellular transport and kinesin superfamily proteins, KIFs: Structure, function, and dynamics." In: *Physiological Reviews* 88.3 (2008), pp. 1089–1118. ISSN: 00319333. DOI: `10.1152/PHYSREV.00023.2007/ASSET/IMAGES/LARGE/Z9J0030824820007.JPEG`.

[241]   N. Hirokawa and R. Takemura. "Molecular motors and mechanisms of directional transport in neurons." In: *Nature Reviews Neuroscience 2005 6:3* 6.3 (2005), pp. 201–214. ISSN: 1471-0048. DOI: `10.1038/nrn1624`.

[242]   A. Negatsch et al. "Ultrastructural Analysis of Virion Formation and Intraaxonal Transport of Herpes Simplex Virus Type 1 in Primary Rat Neurons." In: *Journal of Virology* 84.24 (2010), pp. 13031–13035. ISSN: 0022-538X. DOI: `10.1128/JVI.01784-10/ASSET/667CEB31-3E51-436A-A2E0-AB68003E427C/ASSETS/GRAPHIC/ZJV9990940000003.JPEG`.

[243]   S. E. Antinone and G. A. Smith. "Retrograde Axon Transport of Herpes Simplex Virus and Pseudorabies Virus: a Live-Cell Comparative Analysis." In: *Journal of Virology* 84.3 (2010), pp. 1504–1512. ISSN: 0022-538X. DOI: `10.1128/JVI.02029-09/ASSET/AF9AC360-9F63-4140-9A1F-A79D42EBAFD8/ASSETS/GRAPHIC/ZJV0031028480008.JPEG`.

[244]   S. E. Antinone and G. A. Smith. "Two Modes of Herpesvirus Trafficking in Neurons: Membrane Acquisition Directs Motion." In: *Journal of Virology* 80.22 (2006), pp. 11235–11240. ISSN: 0022-538X. DOI: `10.1128/JVI.01441-06/ASSET/27D4DE53-AB18-4B7D-926E-670F71F7868E/ASSETS/GRAPHIC/ZJV0220684430004.JPEG`.

[245]   A. Snyder, T. W. Wisner, and D. C. Johnson. "Herpes Simplex Virus Capsids Are Transported in Neuronal Axons without an Envelope Containing the Viral Glycoproteins." In: *Journal of Virology* 80.22 (2006), pp. 11165–11177. ISSN: 0022-538X. DOI: `10.1128/JVI.01107-06/SUPPL_FILE/SUPPLEMENTAL_MOVIE_DESCRIPTION.DOC`.

[246]   I. Ibiricu et al. "Cryo Electron Tomography of Herpes Simplex Virus during Axonal Transport and Secondary Envelopment in Primary Neurons." In: *PLoS Pathogens* 7.12 (2011), p. 1002406. ISSN: 15537366. DOI: `10.1371/JOURNAL.PPAT.1002406`.

[247]   J. R. Kent et al. "During Lytic Infection Herpes Simplex Virus Type 1 Is Associated with Histones Bearing Modifications That Correlate with Active Transcription." In: *Journal of Virology* 78.18 (2004), pp. 10178–10186. ISSN: 0022-538X. DOI: `10.1128/jvi.78.18.10178-10186.2004`.

[248]   R. Murr. "Interplay Between Different Epigenetic Modifications and Mechanisms." In: *Advances in Genetics* 70.C (2010), pp. 101–141. ISSN: 0065-2660. DOI: `10.1016/B978-0-12-380866-0.60005-8`.

[249] R. D. Kornberg. "Structure of Chromatin." In: *Annual review of biochemistry* 46.1 (1977), pp. 931–954. ISSN: 00664154. DOI: `10.1146/annurev.bi.46.070177.004435`.

[250] J. D. McGhee and G Felsenfeld. "Nucleosome Structure." In: *Annual Review of Biochemistry* 49.1 (1980), pp. 1115–1156. ISSN: 0066-4154. DOI: `10.1146/annurev.bi.49.070180.005343`.

[251] K. Luger et al. "Crystal structure of the nucleosome core particle at 2.8 Å resolution." In: *Nature* 389.6648 (1997), pp. 251–260. ISSN: 00280836. DOI: `10.1038/38444`.

[252] K. Ahmad and S. Henikoff. "Centromeres are specialized replication domains in heterochromatin." In: *Journal of Cell Biology* 153.1 (2001), pp. 101–109. ISSN: 00219525. DOI: `10.1083/jcb.153.1.101`.

[253] C. M. Weber and S. Henikoff. *Histone variants: Dynamic punctuation in transcription.* 2014. DOI: `10.1101/gad.238873.114`.

[254] S. Smith and B. Stillman. "Purification and characterization of CAF-I, a human cell factor required for chromatin assembly during DNA replication in vitro." In: *Cell* 58.1 (1989), pp. 15–25. ISSN: 0092-8674. DOI: `10.1016/0092-8674(89)90398-X`.

[255] R. Natsume et al. "Structure and function of the histone chaperone CIA/ASF1 complexed with histones H3 and H4." In: *Nature 2006 446:7133* 446.7133 (2007), pp. 338–341. ISSN: 1476-4687. DOI: `10.1038/nature05613`.

[256] T. Tamura et al. "Inducible deposition of the histone variant H3.3 in interferon-stimulated genes." In: *The Journal of biological chemistry* 284.18 (2009), pp. 12217–12225. ISSN: 0021-9258. DOI: `10.1074/JBC.M805651200`.

[257] A. Piazzesi et al. "Replication-Independent Histone Variant H3.3 Controls Animal Lifespan through the Regulation of Pro-longevity Transcriptional Programs." In: *Cell Reports* 17.4 (2016), pp. 987–996. ISSN: 22111247. DOI: `10.1016/j.celrep.2016.09.074`.

[258] K. Ahmad and S. Henikoff. "The Histone Variant H3.3 Marks Active Chromatin by Replication-Independent Nucleosome Assembly." In: *Molecular Cell* 9.6 (2002), pp. 1191–1200. ISSN: 1097-2765. DOI: `10.1016/S1097-2765(02)00542-7`.

[259] H. Tagami et al. "Histone H3.1 and H3.3 Complexes Mediate Nucleosome Assembly Pathways Dependent or Independent of DNA Synthesis." In: *Cell* 116.1 (2004), pp. 51–61. ISSN: 00928674. DOI: `10.1016/S0092-8674(03)01064-X`.

[260] B. Loppin et al. "The histone H3.3 chaperone HIRA is essential for chromatin assembly in the male pronucleus." In: *Nature 2005 437:7063* 437.7063 (2005), pp. 1386–1390. ISSN: 1476-4687. DOI: `10.1038/nature04059`.

[261] A. D. Goldberg et al. "Distinct Factors Control Histone Variant H3.3 Localization at Specific Genomic Regions." In: *Cell* 140.5 (2010), pp. 678–691. ISSN: 00928674. DOI: `10.1016/j.cell.2010.01.003`.

[262] E. M. Green et al. "Replication-Independent Histone Deposition by the HIR Complex and Asf1." In: *Current Biology* 15.22 (2005), pp. 2044–2049. ISSN: 0960-9822. DOI: `10.1016/J.CUB.2005.10.053`.

[263] B. Horard et al. "ASF1 is required to load histones on the HIRA complex in preparation of paternal chromatin assembly at fertilization." In: *Epigenetics and Chromatin* 11.1 (2018), pp. 1–16. ISSN: 17568935. DOI: `10.1186/S13072-018-0189-X/FIGURES/6`.

[264] E. P. Rogakou and K. E. Sekeri-Pataryas. "Histone variants of H2A and H3 families are regulated during in vitro aging in the same manner as during differentiation." In: *Experimental Gerontology* 34.6 (1999), pp. 741–754. ISSN: 0531-5565. DOI: `10.1016/S0531-5565(99)00046-7`.

[265] E. Saade et al. "Molecular turnover, the H3.3 dilemma and organismal aging (hypothesis)." In: *Aging Cell* 14.3 (2015), pp. 322–333. ISSN: 1474-9726. DOI: `10.1111/ACEL.12332`.

[266] L. H. Wong et al. "ATRX interacts with H3.3 in maintaining telomere structural integrity in pluripotent embryonic stem cells." In: *Genome Research* 20.3 (2010), p. 351. ISSN: 10889051. DOI: `10.1101/GR.101477.109`.

[267] P. W. Lewis et al. "Daxx is an H3.3-specific histone chaperone and cooperates with ATRX in replication-independent chromatin assembly at telomeres." In: *Proceedings of the National Academy of Sciences of the United States of America* 107.32 (2010), pp. 14075–14080. ISSN: 00278424. DOI: `10.1073/pnas.1008850107`.

[268] C. W. Jang et al. "Histone H3.3 maintains genome integrity during mammalian development." In: *Genes & development* 29.13 (2015), pp. 1377–1393. ISSN: 1549-5477. DOI: `10.1101/GAD.264150.115`.

[269] G. Egger et al. "Epigenetics in human disease and prospects for epigenetic therapy." In: *Nature 2004 429:6990* 429.6990 (2004), pp. 457–463. ISSN: 1476-4687. DOI: `10.1038/nature02625`.

[270] P. Grippo et al. "Methylation of DNA in developing sea urchin embryos." In: *Journal of Molecular Biology* 36.2 (1968), pp. 195–208. ISSN: 0022-2836. DOI: `10.1016/0022-2836(68)90375-6`.

[271] O. M et al. "DNA methyltransferases Dnmt3a and Dnmt3b are essential for de novo methylation and mammalian development." In: *Cell* 99.3 (1999), pp. 247–257. ISSN: 0092-8674. DOI: `10.1016/S0092-8674(00)81656-6`.

[272] H. Lei et al. "De novo DNA cytosine methyltransferase activities in mouse embryonic stem cells." In: *Development* 122.10 (1996), pp. 3195–3205. ISSN: 0950-1991. DOI: `10.1242/DEV.122.10.3195`.

[273] B. T et al. "Cloning and sequencing of a cDNA encoding DNA methyltransferase of mouse cells. The carboxyl-terminal domain of the mammalian enzymes is related to bacterial restriction methyltransferases." In: *Journal of molecular biology* 203.4 (1988), pp. 971–983. ISSN: 0022-2836. DOI: `10.1016/0022-2836(88)90122-2`.

[274] C. Y. Okitsu and C.-L. Hsieh. "DNA Methylation Dictates Histone H3K4 Methylation." In: *Molecular and Cellular Biology* 27.7 (2007), pp. 2746–2757. DOI: 10.1128/MCB.02291-06.

[275] A. Riggs. "X inactivation, differentiation, and DNA methylation." In: *Cytogenetic and Genome Research* 14.1 (1975), pp. 9–25. ISSN: 1424-8581. DOI: 10.1159/000130315.

[276] J. Borgel et al. "Targets and dynamics of promoter DNA methylation during early mouse development." In: *Nature Genetics 2010 42:12* 42.12 (2010), pp. 1093–1100. ISSN: 1546-1718. DOI: 10.1038/ng.708.

[277] W Reik. "Stability and flexibility of epigenetic gene regulation in mammalian development." In: *Nature* 447.7143 (2007), pp. 425–432. DOI: 10.1038/nature05918.

[278] M. Shamay et al. "CpG methylation as a tool to characterize cell-free Kaposi sarcoma herpesvirus DNA." In: *The Journal of infectious diseases* 205.7 (2012), pp. 1095–1099. ISSN: 1537-6613. DOI: 10.1093/INFDIS/JIS032.

[279] J. Chen et al. "Activation of latent Kaposi's sarcoma-associated herpesvirus by demethylation of the promoter of the lytic transactivator." In: *Proceedings of the National Academy of Sciences of the United States of America* 98.7 (2001), pp. 4119–4124. ISSN: 0027-8424. DOI: 10.1073/PNAS.051004198.

[280] S. Jeudy et al. "The DNA methylation landscape of giant viruses." In: *Nature Communications 2020 11:1* 11.1 (2020), pp. 1–12. ISSN: 2041-1723. DOI: 10.1038/s41467-020-16414-2.

[281] A. P. Bird. "DNA methylation and the frequency of CpG in animal DNA." In: *Nucleic Acids Research* 8.7 (1980), p. 1499. DOI: 10.1093/NAR/8.7.1499.

[282] D. Takai and P. A. Jones. "Comprehensive analysis of CpG islands in human chromosomes 21 and 22." In: *Proceedings of the National Academy of Sciences* 99.6 (2002), pp. 3740–3745. ISSN: 0027-8424. DOI: 10.1073/PNAS.052410099.

[283] S. Saxonov, P. Berg, and D. L. Brutlag. "A genome-wide analysis of CpG dinucleotides in the human genome distinguishes two distinct classes of promoters." In: *Proceedings of the National Academy of Sciences* 103.5 (2006), pp. 1412–1417. ISSN: 0027-8424. DOI: 10.1073/PNAS.0510310103.

[284] T. H et al. "The presence of RNA polymerase II, active or stalled, predicts epigenetic fate of promoter CpG islands." In: *Genome research* 19.11 (2009), pp. 1974–1982. ISSN: 1549-5469. DOI: 10.1101/GR.093310.109.

[285] A. R. Krebs et al. "High-throughput engineering of a mammalian genome reveals building principles of methylation states at CG rich regions." In: *eLife* 3 (2014), e04094. ISSN: 2050084X. DOI: 10.7554/ELIFE.04094.

[286] T. M et al. "Conversion of 5-methylcytosine to 5-hydroxymethylcytosine in mammalian DNA by MLL partner TET1." In: *Science (New York, N.Y.)* 324.5929 (2009), pp. 930–935. ISSN: 0036-8075. DOI: 10.1126/SCIENCE.1170116.

[287] H. YF et al. "Tet-mediated formation of 5-carboxylcytosine and its excision by TDG in mammalian DNA." In: *Science (New York, N.Y.)* 333.6047 (2011), pp. 1303–1307. ISSN: 1095-9203. DOI: `10.1126/SCIENCE.1210944`.

[288] S. DF and G. SM. "Analysis of CpG suppression in methylated and nonmethylated species." In: *Proceedings of the National Academy of Sciences of the United States of America* 89.3 (1992), pp. 957–961. ISSN: 0027-8424. DOI: `10.1073/PNAS.89.3.957`.

[289] S.-R. H et al. "Active genes are tri-methylated at K4 of histone H3." In: *Nature* 419.6905 (2002), pp. 407–411. ISSN: 0028-0836. DOI: `10.1038/NATURE01080`.

[290] M. P. Creyghton et al. "Histone H3K27ac separates active from poised enhancers and predicts developmental state." In: *Proceedings of the National Academy of Sciences of the United States of America* 107.50 (2010), pp. 21931–21936. DOI: `10.1073/PNAS.101607110 7/-/DCSUPPLEMENTAL/ST01.XLSX`.

[291] S. Bilokapic and M. Halic. "Nucleosome and ubiquitin position Set2 to methylate H3K36." In: *Nature Communications 2019 10:1* 10.1 (2019), pp. 1–9. ISSN: 2041-1723. DOI: `10.1038/s41467-019-11726-4`.

[292] G. V. Rayasam et al. "NSD1 is essential for early post-implantation development and has a catalytically active SET domain." In: *The EMBO Journal* 22.12 (2003), pp. 3153–3163. ISSN: 1460-2075. DOI: `10.1093/EMBOJ/CDG288`.

[293] W. DN et al. "The histone mark H3K36me2 recruits DNMT3A and shapes the intergenic DNA methylation landscape." In: *Nature* 573.7773 (2019), pp. 281–286. ISSN: 1476-4687. DOI: `10.1038/S41586-019-1534-3`.

[294] K. Skvortsova, N. Iovino, and O. Bogdanović. "Functions and mechanisms of epigenetic inheritance in animals." In: *Nature Reviews Molecular Cell Biology 2018 19:12* 19.12 (2018), pp. 774–790. ISSN: 1471-0080. DOI: `10.1038/s41580-018-0074-2`.

[295] Z. Shao et al. "Stabilization of chromatin structure by PRC1, a polycomb complex." In: *Cell* 98.1 (1999), pp. 37–46. ISSN: 00928674. DOI: `10.1016/S0092-8674(00)80604-2`.

[296] A. Kuzmichev et al. "Histone methyltransferase activity associated with a human multiprotein complex containing the enhancer of zeste protein." In: *Genes and Development* 16.22 (2002), pp. 2893–2905. ISSN: 08909369. DOI: `10.1101/gad.1035902`.

[297] D. Pasini et al. "Suz12 is essential for mouse development and for EZH2 histone methyltransferase activity." In: *The EMBO Journal* 23.20 (2004), pp. 4061–4071. ISSN: 1460-2075. DOI: `10.1038/SJ.EMBOJ.7600402`.

[298] D. O'Carroll et al. " The Polycomb -Group Gene Ezh2 Is Required for Early Mouse Development." In: *Molecular and Cellular Biology* 21.13 (2001), pp. 4330–4336. ISSN: 0270-7306. DOI: `10.1128/MCB.21.13.4330-4336.2001/ASSET/083B47DF-978B-463D-8325- 24C4C190D892/ASSETS/GRAPHIC/MB1312151005.JPEG`.

[299] W. Zhou et al. "Histone H2A Monoubiquitination Represses Transcription by Inhibiting RNA Polymerase II Transcriptional Elongation." In: *Molecular Cell* 29.1 (2008), pp. 69–80. ISSN: 1097-2765. DOI: 10.1016/J.MOLCEL.2007.11.002.

[300] C. Rougeulle et al. "Differential Histone H3 Lys-9 and Lys-27 Methylation Profiles on the X Chromosome." In: *Molecular and Cellular Biology* 24.12 (2004), pp. 5475–5484. ISSN: 0270-7306. DOI: 10.1128/MCB.24.12.5475-5484.2004/SUPPL_FILE/SUPPLEMENTARY_FIGURE_S2.PDF.

[301] M. de Napoles et al. "Polycomb group proteins Ring1A/B link ubiquitylation of histone H2A to heritable gene silencing and X inactivation." In: *Developmental cell* 7.5 (2004), pp. 663–676. ISSN: 1534-5807. DOI: 10.1016/J.DEVCEL.2004.10.005.

[302] H. Wang et al. "Role of histone H2A ubiquitination in Polycomb silencing." In: *Nature* 431.7010 (2004), pp. 873–878. ISSN: 1476-4687. DOI: 10.1038/NATURE02985.

[303] N. Soshnikova and D. Duboule. "Epigenetic temporal control of mouse hox genes in vivo." In: *Science* 324.5932 (2009), pp. 1321–1323. ISSN: 00368075. DOI: 10.1126/SCIENCE.1171468/SUPPL_FILE/SOSHNIKOVA_SOM.PDF.

[304] L. A. Boyer et al. "Polycomb complexes repress developmental regulators in murine embryonic stem cells." In: *Nature 2006 441:7091* 441.7091 (2006), pp. 349–353. ISSN: 1476-4687. DOI: 10.1038/nature04733.

[305] J. Yu et al. "Reduced H3K27me3 leads to abnormal Hox gene expression in neural tube defects." In: *Epigenetics and Chromatin* 12.1 (2019), pp. 1–19. ISSN: 17568935. DOI: 10.1186/S13072-019-0318-1/TABLES/1.

[306] B. E. Bernstein et al. "A Bivalent Chromatin Structure Marks Key Developmental Genes in Embryonic Stem Cells." In: *Cell* 125.2 (2006), pp. 315–326. ISSN: 0092-8674. DOI: 10.1016/J.CELL.2006.02.041.

[307] V. Loubiere et al. "Widespread activation of developmental gene expression characterized by PRC1-dependent chromatin looping." In: *Science Advances* 6.2 (2020). ISSN: 23752548. DOI: 10.1126/SCIADV.AAX4001/SUPPL_FILE/AAX4001_TABLE_S9.XLSX.

[308] T. Kondo et al. "Polycomb Potentiates Meis2 Activation in Midbrain by Mediating Interaction of the Promoter with a Tissue-Specific Enhancer." In: *Developmental Cell* 28.1 (2014), pp. 94–101. ISSN: 1534-5807. DOI: 10.1016/J.DEVCEL.2013.11.021.

[309] S. Cruz-Molina et al. "PRC2 Facilitates the Regulatory Topology Required for Poised Enhancer Function during Pluripotent Stem Cell Differentiation." In: *Cell Stem Cell* 20.5 (2017), 689–705.e9. ISSN: 1934-5909. DOI: 10.1016/J.STEM.2017.02.004.

[310] V. Azuara et al. "Chromatin signatures of pluripotent cell lines." In: *Nature Cell Biology 2006 8:5* 8.5 (2006), pp. 532–538. ISSN: 1476-4679. DOI: 10.1038/ncb1403.

[311] M. TS et al. "Genome-wide maps of chromatin state in pluripotent and lineage-committed cells." In: *Nature* 448.7153 (2007), pp. 553–560. ISSN: 1476-4687. DOI: 10.1038/NATURE06008.

[312] G. Wei et al. "Global Mapping of H3K4me3 and H3K27me3 Reveals Specificity and Plasticity in Lineage Fate Determination of Differentiating CD4+ T Cells." In: *Immunity* 30.1 (2009), pp. 155–167. ISSN: 1074-7613. DOI: `10.1016/J.IMMUNI.2008.12.009`.

[313] S. Chen et al. "A Dimeric Structural Scaffold for PRC2-PCL Targeting to CpG Island Chromatin." In: *Molecular Cell* 77.6 (2020), 1265–1278.e7. ISSN: 1097-2765. DOI: `10.1016/J.MOLCEL.2019.12.019`.

[314] C. S et al. "Jarid2 binds mono-ubiquitylated H2A lysine 119 to mediate crosstalk between Polycomb complexes PRC1 and PRC2." In: *Nature communications* 7 (2016). ISSN: 2041-1723. DOI: `10.1038/NCOMMS13661`.

[315] A. S, M. G, and D. C. L. "Regulation of gene transcription by Polycomb proteins." In: *Science advances* 1.11 (2015). ISSN: 2375-2548. DOI: `10.1126/SCIADV.1500737`.

[316] M. K. Huseyin and R. J. Klose. "Live-cell single particle tracking of PRC1 reveals a highly dynamic system with low target site occupancy." In: *Nature Communications 2021 12:1* 12.1 (2021), pp. 1–20. ISSN: 2041-1723. DOI: `10.1038/s41467-021-21130-6`.

[317] M. J. Clague, J. M. Coulson, and S. Urbé. "Deciphering histone 2A deubiquitination." In: *Genome Biology* 9.1 (2008), p. 202. ISSN: 14656914. DOI: `10.1186/GB-2008-9-1-202`.

[318] S. S. Levine et al. "The Core of the Polycomb Repressive Complex Is Compositionally and Functionally Conserved in Flies and Humans." In: *Molecular and Cellular Biology* 22.17 (2002), pp. 6070–6078. ISSN: 0270-7306. DOI: `10.1128/mcb.22.17.6070-6078.2002`.

[319] J. Vandamme et al. "Interaction proteomics analysis of polycomb proteins defines distinct PRC1 complexes in mammalian cells." In: *Molecular and Cellular Proteomics* 10.4 (2011). ISSN: 15359484. DOI: `10.1074/mcp.M110.002642`.

[320] R. Koyama-Nasu, G. David, and N. Tanese. "The F-box protein Fbl10 is a novel transcriptional repressor of c-Jun." In: *Nature Cell Biology 2007 9:9* 9.9 (2007), pp. 1074–1080. ISSN: 1476-4679. DOI: `10.1038/ncb1628`.

[321] M. D. Gearhart et al. "Polycomb Group and SCF Ubiquitin Ligases Are Found in a Novel BCOR Complex That Is Recruited to BCL6 Targets." In: *Molecular and Cellular Biology* 26.18 (2006), pp. 6880–6889. ISSN: 0270-7306. DOI: `10.1128/MCB.00630-06/SUPPL_FILE/SUPPLEMENTARY_TABLE_1.ZIP`.

[322] M. Liu et al. "The polycomb group protein PCGF6 mediates germline gene silencing by recruiting histone-modifying proteins to target gene promoters." In: *Journal of Biological Chemistry* 295.28 (2020), pp. 9712–9724. ISSN: 1083351X. DOI: `10.1074/JBC.RA119.012121/ATTACHMENT/FDC8C4B6-3EB5-4774-B65D-075BA85FB37A/MMC1.ZIP`.

[323] P. J. Hurlin et al. "Mga, a dual-specificity transcription factor that interacts with Max and contains a T-domain DNA-binding motif." In: *The EMBO Journal* 18.24 (1999), pp. 7019–7028. ISSN: 1460-2075. DOI: `10.1093/EMBOJ/18.24.7019`.

[324] Y. Huang et al. "Combinatorial Control of Recruitment of a Variant PRC1.6 Complex in Embryonic Stem Cells." In: *Cell Reports* 22.11 (2018), pp. 3032–3043. ISSN: 2211-1247. DOI: `10.1016/J.CELREP.2018.02.072`.

[325] G. Pintacuda et al. "hnRNPK Recruits PCGF3/5-PRC1 to the Xist RNA B-Repeat to Establish Polycomb-Mediated Chromosomal Silencing." In: *Molecular Cell* 68.5 (2017), 955–969.e10. ISSN: 1097-2765. DOI: `10.1016/J.MOLCEL.2017.11.013`.

[326] M. Almeida et al. "PCGF3/5-PRC1 initiates Polycomb recruitment in X chromosome inactivation." In: *Science* 356.6342 (2017), pp. 1081–1084. ISSN: 10959203. DOI: `10.1126/SCIENCE.AAL2512/SUPPL_FILE/AAL2512S6.MP4`.

[327] L. Morey et al. "RYBP and Cbx7 Define Specific Biological Functions of Polycomb Complexes in Mouse Embryonic Stem Cells." In: *Cell Reports* 3.1 (2013), pp. 60–69. ISSN: 2211-1247. DOI: `10.1016/J.CELREP.2012.11.026`.

[328] W. Yang et al. "The histone H2A deubiquitinase Usp16 regulates embryonic stem cell gene expression and lineage commitment." In: *Nature Communications 2014 5:1* 5.1 (2014), pp. 1–15. ISSN: 2041-1723. DOI: `10.1038/ncomms4818`.

[329] H. Y. Joo et al. "Regulation of cell cycle progression and gene expression by H2A deubiquitination." In: *Nature* 449.7165 (2007), pp. 1068–1072. ISSN: 1476-4687. DOI: `10.1038/NATURE06256`.

[330] N. P. Blackledge et al. "Variant PRC1 complex-dependent H2A ubiquitylation drives PRC2 recruitment and polycomb domain formation." In: *Cell* 157.6 (2014), pp. 1445–1459. ISSN: 10974172. DOI: `10.1016/j.cell.2014.05.004`.

[331] R. Margueron et al. "Ezh1 and Ezh2 Maintain Repressive Chromatin through Different Mechanisms." In: *Molecular Cell* 32.4 (2008), pp. 503–518. ISSN: 1097-2765. DOI: `10.1016/J.MOLCEL.2008.11.004`.

[332] K. Agger et al. "UTX and JMJD3 are histone H3K27 demethylases involved in HOX gene regulation and development." In: *Nature 2007 449:7163* 449.7163 (2007), pp. 731–734. ISSN: 1476-4687. DOI: `10.1038/nature06145`.

[333] F. De Santa et al. "The Histone H3 Lysine-27 Demethylase Jmjd3 Links Inflammation to Inhibition of Polycomb-Mediated Gene Silencing." In: *Cell* 130.6 (2007), pp. 1083–1094. ISSN: 0092-8674. DOI: `10.1016/J.CELL.2007.08.019`.

[334] S. Chen et al. "The histone H3 Lys 27 demethylase JMJD3 regulates gene expression by impacting transcriptional elongation." In: *Genes & Development* 26.12 (2012), pp. 1364–1375. ISSN: 0890-9369. DOI: `10.1101/GAD.186056.111`.

[335] K. Williams et al. "The Histone Lysine Demethylase JMJD3/KDM6B Is Recruited to p53 Bound Promoters and Enhancer Elements in a p53 Dependent Manner." In: *PLOS ONE* 9.5 (2014), e96545. ISSN: 1932-6203. DOI: `10.1371/JOURNAL.PONE.0096545`.

[336] M. L. Pardue and J. G. Gall. "Chromosomal Localization of Mouse Satellite DNA." In: *Science* 168.3937 (1970), pp. 1356–1358. ISSN: 00368075. DOI: 10.1126/SCIENCE.168.3937.1356.

[337] R. H. Waterston, K. Lindblad-Toh, and E. Birney. "Initial sequencing and comparative analysis of the mouse genome." In: *Nature 2003 420:6915* 420.6915 (2002), pp. 520–562. ISSN: 1476-4687. DOI: 10.1038/nature01262.

[338] I. M. Hall et al. "Establishment and maintenance of a heterochromatin domain." In: *Science* 297.5590 (2002), pp. 2232–2237. ISSN: 00368075. DOI: 10.1126/SCIENCE.1076466/ASSET/70A57F5B-9693-40AF-B1FC-CB9C32317963/ASSETS/GRAPHIC/SE3720877005.JPEG.

[339] T. Jenuwein and C. D. Allis. "Translating the histone code." In: *Science* 293.5532 (2001), pp. 1074–1080. ISSN: 00368075. DOI: 10.1126/SCIENCE.1063127/ASSET/FCD15CEA-ECDC-41AF-AE32-FEDCEA8620CC/ASSETS/GRAPHIC/SE3119652003.JPEG.

[340] B. Lehnertz et al. "Suv39h-Mediated Histone H3 Lysine 9 Methylation Directs DNA Methylation to Major Satellite Repeats at Pericentric Heterochromatin." In: *Current Biology* 13.14 (2003), pp. 1192–1200. ISSN: 0960-9822. DOI: 10.1016/S0960-9822(03)00432-9.

[341] S. A. Jacobs et al. "Specificity of the HP1 chromo domain for the methylated N-terminus of histone H3." In: *The EMBO Journal* 20.18 (2001), pp. 5232–5241. ISSN: 1460-2075. DOI: 10.1093/EMBOJ/20.18.5232.

[342] S. J. Nielsen et al. "Rb targets histone H3 methylation and HP1 to promoters." In: *Nature* 412.6846 (2001), pp. 561–565. ISSN: 0028-0836. DOI: 10.1038/35087620.

[343] S. Epsztejn-Litman et al. "De novo DNA methylation promoted by G9a prevents reprogramming of embryonically silenced genes." In: *Nature Structural & Molecular Biology 2008 15:11* 15.11 (2008), pp. 1176–1183. ISSN: 1545-9985. DOI: 10.1038/nsmb.1476.

[344] W. Ren et al. "Direct readout of heterochromatic H3K9me3 regulates DNMT1-mediated maintenance DNA methylation." In: *Proceedings of the National Academy of Sciences of the United States of America* 117.31 (2020), pp. 18439–18447. ISSN: 10916490. DOI: 10.1073/PNAS.2009316117/-/DCSUPPLEMENTAL.

[345] A. H. Peters et al. "Loss of the Suv39h Histone Methyltransferases Impairs Mammalian Heterochromatin and Genome Stability." In: *Cell* 107.3 (2001), pp. 323–337. ISSN: 0092-8674. DOI: 10.1016/S0092-8674(01)00542-6.

[346] D. B. Marina et al. "A conserved ncRNA-binding protein recruits silencing factors to heterochromatin through an RNAi-independent mechanism." In: *Genes & Development* 27.17 (2013), pp. 1851–1856. ISSN: 0890-9369. DOI: 10.1101/GAD.226019.113.

[347] M. Bühler, A. Verdel, and D. Moazed. "Tethering RITS to a Nascent Transcript Initiates RNAi- and Heterochromatin-Dependent Gene Silencing." In: *Cell* 125.5 (2006), pp. 873–886. ISSN: 0092-8674. DOI: 10.1016/J.CELL.2006.04.025.

[348] T. A. Volpe et al. "Regulation of heterochromatic silencing and histone H3 lysine-9 methylation by RNAi." In: *Science* 297.5588 (2002), pp. 1833–1837. ISSN: 00368075. DOI: 10.1126/SCIENCE.1074973/SUPPL_FILE/VOLPESOM.PDF.

[349] A. Buscaino et al. "Distinct roles for Sir2 and RNAi in centromeric heterochromatin nucleation, spreading and maintenance." In: *The EMBO Journal* 32.9 (2013), pp. 1250–1264. ISSN: 1460-2075. DOI: 10.1038/EMBOJ.2013.72.

[350] F. Simmer et al. "Hairpin RNA induces secondary small interfering RNA synthesis and silencing in trans in fission yeast." In: *EMBO reports* 11.2 (2010), pp. 112–118. ISSN: 1469-3178. DOI: 10.1038/EMBOR.2009.273.

[351] A. Kloc et al. "RNA Interference Guides Histone Modification during the S Phase of Chromosomal Replication." In: *Current Biology* 18.7 (2008), pp. 490–495. ISSN: 0960-9822. DOI: 10.1016/J.CUB.2008.03.016.

[352] E. S. Chen et al. "Cell cycle control of centromeric repeat transcription and heterochromatin assembly." In: *Nature 2008 451:7179* 451.7179 (2008), pp. 734–737. ISSN: 1476-4687. DOI: 10.1038/nature06561.

[353] M. R. Motamedi et al. "Two RNAi Complexes, RITS and RDRC, Physically Interact and Localize to Noncoding Centromeric RNAs." In: *Cell* 119.6 (2004), pp. 789–802. ISSN: 0092-8674. DOI: 10.1016/J.CELL.2004.11.034.

[354] I. A. Tchasovnikarova et al. "Epigenetic silencing by the HUSH complex mediates position-effect variegation in human cells." In: *Science (New York, N.Y.)* 348.6242 (2015), p. 1481. ISSN: 10959203. DOI: 10.1126/SCIENCE.AAA7227.

[355] J. Li et al. "Structural Basis for Specific Binding of Human MPP8 Chromodomain to Histone H3 Methylated at Lysine 9." In: *PLOS ONE* 6.10 (2011), e25104. ISSN: 1932-6203. DOI: 10.1371/JOURNAL.PONE.0025104.

[356] D. C. Schultz et al. "SETDB1: a novel KAP-1-associated histone H3, lysine 9-specific methyltransferase that contributes to HP1-mediated silencing of euchromatic genes by KRAB zinc-finger proteins." In: *Genes & development* 16.8 (2002), pp. 919–932. ISSN: 0890-9369. DOI: 10.1101/GAD.973302.

[357] A. D. Capili et al. "Solution structure of the PHD domain from the KAP-1 corepressor: structural determinants for PHD, RING and LIM zinc-binding domains." In: *The EMBO Journal* 20.1-2 (2001), pp. 165–177. ISSN: 1460-2075. DOI: 10.1093/EMBOJ/20.1.165.

[358] D. C. Schultz, J. R. Friedman, and F. J. Rauscher. "Targeting histone deacetylase complexes via KRAB-zinc finger proteins: the PHD and bromodomains of KAP-1 form a cooperative unit that recruits a novel isoform of the Mi-2α subunit of NuRD." In: *Genes & Development* 15.4 (2001), pp. 428–443. ISSN: 0890-9369. DOI: 10.1101/GAD.869501.

[359] J. J. Luciani et al. "PML nuclear bodies are highly organised DNA-protein structures with a function in heterochromatin remodelling at the G2 phase." In: *Journal of Cell Science* 119.12 (2006), pp. 2518–2531. ISSN: 0021-9533. DOI: 10.1242/JCS.02965.

[360] E. Delbarre et al. "PML protein organizes heterochromatin domains where it regulates histone H3.3 deposition by ATRX/DAXX." In: *Genome Research* 27.6 (2017), pp. 913–921. ISSN: 1088-9051. DOI: 10.1101/GR.215830.116.

[361] S. Cho, J. S. Park, and Y. K. Kang. "Dual Functions of Histone-Lysine N-Methyltransferase Setdb1 Protein at Promyelocytic Leukemia-Nuclear Body (PML-NB): MAINTAINING PML-NB STRUCTURE AND REGULATING THE EXPRESSION OF ITS ASSOCIATED GENES*." In: *The Journal of Biological Chemistry* 286.47 (2011), p. 41115. ISSN: 00219258. DOI: 10.1074/JBC.M111.248534.

[362] R. Wu et al. "H3K9me3 demethylase Kdm4d facilitates the formation of pre-initiative complex and regulates DNA replication." In: *Nucleic Acids Research* 45.1 (2017), p. 169. ISSN: 13624962. DOI: 10.1093/NAR/GKW848.

[363] F. Meng et al. "Targeted demethylation of H3K9me3 and H3K36me3 improves somatic cell reprogramming into cloned preimplantation but not postimplantation bovine concepti." In: *bioRxiv* (2019), p. 699181. ISSN: 2692-8205. DOI: 10.1101/699181.

[364] Q. Ye et al. "Domain-specific Interactions of Human HP1-type Chromodomain Proteins and Inner Nuclear Membrane Protein LBR *." In: *Journal of Biological Chemistry* 272.23 (1997), pp. 14983–14989. ISSN: 0021-9258. DOI: 10.1074/JBC.272.23.14983.

[365] A. J. Bannister et al. "Selective recognition of methylated lysine 9 on histone H3 by the HP1 chromo domain." In: *Nature 2001 410:6824* 410.6824 (2001), pp. 120–124. ISSN: 1476-4687. DOI: 10.1038/35065138.

[366] M. Lachner et al. "Methylation of histone H3 lysine 9 creates a binding site for HP1 proteins." In: *Nature 2001 410:6824* 410.6824 (2001), pp. 116–120. ISSN: 1476-4687. DOI: 10.1038/35065132.

[367] K. Hiragami-Hamada et al. "Dynamic and flexible H3K9me3 bridging via HP1β dimerization establishes a plastic state of condensed chromatin." In: *Nature Communications 2016 7:1* 7.1 (2016), pp. 1–16. ISSN: 2041-1723. DOI: 10.1038/ncomms11310.

[368] D. Canzio et al. "A conformational switch in HP1 releases auto-inhibition to drive heterochromatin assembly." In: *Nature 2013 496:7445* 496.7445 (2013), pp. 377–381. ISSN: 1476-4687. DOI: 10.1038/nature12032.

[369] A. G. Larson et al. "Liquid droplet formation by HP1α suggests a role for phase separation in heterochromatin." In: *Nature 2017 547:7662* 547.7662 (2017), pp. 236–240. ISSN: 1476-4687. DOI: 10.1038/nature22822.

[370] A. R. Strom et al. "Phase separation drives heterochromatin domain formation." In: *Nature 2017 547:7662* 547.7662 (2017), pp. 241–245. ISSN: 1476-4687. DOI: 10.1038/nature22989.

[371] F. Erdel et al. "Mouse Heterochromatin Adopts Digital Compaction States without Showing Hallmarks of HP1-Driven Liquid-Liquid Phase Separation." In: *Molecular Cell* 78.2 (2020), 236–249.e7. ISSN: 1097-2765. DOI: 10.1016/J.MOLCEL.2020.02.005.

[372] J. Oh and N. W. Fraser. "Temporal Association of the Herpes Simplex Virus Genome with Histone Proteins during a Lytic Infection." In: *Journal of Virology* 82.7 (2008), pp. 3530–3537. ISSN: 0022-538X. DOI: `10.1128/JVI.00586-07/ASSET/48CC101B-FBDF-4AB5-8831-30453D9EBCE4/ASSETS/GRAPHIC/ZJV0070804020005.JPEG`.

[373] P. F. Pignattii and E. Cassai2. "Analysis of herpes simplex virus nucleoprotein complexes extracted from infected cells." In: *Journal of Virology* 36.3 (1980), pp. 816–828. ISSN: 0022-538X. DOI: `10.1128/JVI.36.3.816-828.1980`.

[374] G. H. Cohen et al. "Structural analysis of the capsid polypeptides of herpes simplex virus types 1 and 2." In: *Journal of Virology* 34.2 (1980), pp. 521–531. ISSN: 0022-538X. DOI: `10.1128/JVI.34.2.521-531.1980`.

[375] F. J. Herrera and S. J. Triezenberg. "VP16-Dependent Association of Chromatin-Modifying Coactivators and Underrepresentation of Histones at Immediate-Early Gene Promoters during Herpes Simplex Virus Infection." In: *Journal of Virology* 78.18 (2004), pp. 9689–9696. ISSN: 0022-538X. DOI: `10.1128/jvi.78.18.9689-9696.2004`.

[376] H. Gu et al. "Components of the REST/CoREST/histone deacetylase repressor complex are disrupted, modified, and translocated in HSV-1-infected cells." In: *Proceedings of the National Academy of Sciences* 102.21 (2005), pp. 7571–7576. ISSN: 0027-8424. DOI: `10.1073/PNAS.0502658102`.

[377] H. Gu and B. Roizman. "Herpes simplex virus-infected cell protein 0 blocks the silencing of viral DNA by dissociating histone deacetylases from the CoREST–REST complex." In: *Proceedings of the National Academy of Sciences* 104.43 (2007), pp. 17134–17139. ISSN: 0027-8424. DOI: `10.1073/PNAS.0707266104`.

[378] T. J. Taylor and D. M. Knipe. "Proteomics of Herpes Simplex Virus Replication Compartments: Association of Cellular DNA Replication, Repair, Recombination, and Chromatin Remodeling Proteinswith ICP8." In: *Journal of Virology* 78.11 (2004), pp. 5856–5866. ISSN: 0022-538X. DOI: `10.1128/JVI.78.11.5856-5866.2004/ASSET/5C08857A-5C84-419E-92D8-399F92B7A87C/ASSETS/GRAPHIC/ZJV0110446950002.JPEG`.

[379] K. Tsai and B. R. Cullen. "Epigenetic and epitranscriptomic regulation of viral replication." In: *Nature Reviews Microbiology 2020 18:10* 18.10 (2020), pp. 559–570. ISSN: 1740-1534. DOI: `10.1038/s41579-020-0382-3`.

[380] K. Jensen, C. Shiels, and P. S. Freemont. "PML protein isoforms and the RBCC/TRIM motif." In: *Oncogene 2001 20:49* 20.49 (2001), pp. 7223–7233. ISSN: 1476-5594. DOI: `10.1038/sj.onc.1204765`.

[381] S. Nisole, J. P. Stoye, and A. Saïb. "TRIM family proteins: retroviral restriction and antiviral defence." In: *Nature Reviews Microbiology 2005 3:10* 3.10 (2005), pp. 799–808. ISSN: 1740-1534. DOI: `10.1038/nrmicro1248`.

[382] P. Kastner et al. "Structure, localization and transcriptional properties of two classes of retinoic acid receptor alpha fusion proteins in acute promyelocytic leukemia (APL): structural similarities with a new family of oncoproteins." In: *The EMBO Journal* 11.2 (1992), pp. 629–642. ISSN: 1460-2075. DOI: 10.1002/J.1460-2075.1992.TB05095.X.

[383] A. J. Saurin et al. "Does this have a familiar RING?" In: *Trends in Biochemical Sciences* 21.6 (1996), pp. 208–214. ISSN: 09680004. DOI: 10.1016/S0968-0004(96)80017-X.

[384] G. Meroni and G. Diez-Roux. "TRIM/RBCC, a novel class of 'single protein RING finger' E3 ubiquitin ligases." In: *BioEssays* 27.11 (2005), pp. 1147–1157. ISSN: 1521-1878. DOI: 10.1002/BIES.20304.

[385] G. Dellaire et al. "Promyelocytic leukemia nuclear bodies behave as DNA damage sensors whose response to DNA double-strand breaks is regulated by NBS1 and the kinases ATM, Chk2, and ATR." In: *The Journal of cell biology* 175.1 (2006), pp. 55–66. ISSN: 0021-9525. DOI: 10.1083/JCB.200604009.

[386] V. Fogal et al. "Regulation of p53 activity in nuclear bodies by a specific PML isoform." In: *The EMBO Journal* 19.22 (2000), p. 6185. ISSN: 02614189. DOI: 10.1093/EMBOJ/19.22.6185.

[387] M. Pearson et al. "PML regulates p53 acetylation and premature senescence induced by oncogenic Ras." In: *Nature* 406.6792 (2000), pp. 207–210. ISSN: 0028-0836. DOI: 10.1038/35018127.

[388] Z.-G. G. Wang et al. "Pml is essential for multiple apoptotic pathways." In: *Nature Genetics 1998 20:3* 20.3 (1998), pp. 266–272. ISSN: 1546-1718. DOI: 10.1038/3073.

[389] M. T. Daniel et al. "PML protein expression in hematopoietic and acute promyelocytic leukemia cells." In: *Blood* 82.6 (1993), pp. 1858–1867. ISSN: 0006-4971. DOI: 10.1182/BLOOD.V82.6.1858.1858.

[390] J. Takahashi et al. "PML nuclear bodies and neuronal intranuclear inclusion in polyglutamine diseases." In: *Neurobiology of Disease* 13.3 (2003), pp. 230–237. ISSN: 0969-9961. DOI: 10.1016/S0969-9961(03)00080-9.

[391] A. M. Ishov et al. "Pml Is Critical for Nd10 Formation and Recruits the Pml-Interacting Protein Daxx to This Nuclear Structure When Modified by Sumo-1." In: *Journal of Cell Biology* 147.2 (1999), pp. 221–234. ISSN: 0021-9525. DOI: 10.1083/JCB.147.2.221.

[392] T. H. Shen et al. "The Mechanisms of PML-Nuclear Body Formation." In: *Molecular Cell* 24.3 (2006), pp. 331–339. ISSN: 1097-2765. DOI: 10.1016/J.MOLCEL.2006.09.013.

[393] B. R and P. PP. "Structure, dynamics and functions of promyelocytic leukaemia nuclear bodies." In: *Nature reviews. Molecular cell biology* 8.12 (2007), pp. 1006–1016. ISSN: 1471-0080. DOI: 10.1038/NRM2277.

[394] Z. S, S. P, and P. PP. "The transcriptional role of PML and the nuclear body." In: *Nature cell biology* 2.5 (2000). ISSN: 1465-7392. DOI: 10.1038/35010583.

[395] P. Xu and B. Roizman. "The SP100 component of ND10 enhances accumulation of PML and suppresses replication and the assembly of HSV replication compartments." In: *Proceedings of the National Academy of Sciences* 114.19 (2017), E3823–E3829. ISSN: 0027-8424. DOI: `10.1073/PNAS.1703395114`.

[396] E. RD and C.-A. MK. "PML and PML nuclear bodies: implications in antiviral defence." In: *Biochimie* 89.6-7 (2007), pp. 819–830. ISSN: 0300-9084. DOI: `10.1016/J.BIOCHI.2007.01.004`.

[397] G. D et al. "A conserved truncated isoform of the ATR-X syndrome protein lacking the SWI/SNF-homology domain." In: *Gene* 326.1-2 (2004), pp. 23–34. ISSN: 0378-1119. DOI: `10.1016/J.GENE.2003.10.026`.

[398] M. Han et al. "Synthetic lethality of cytolytic HSV-1 in cancer cells with ATRX and PML deficiency." In: *Journal of Cell Science* 132.5 (2019). ISSN: 14779137. DOI: `10.1242/jcs.222349`.

[399] G. Maarifi, M. K. Chelbi-Alix, and S. Nisole. "PML control of cytokine signaling." In: *Cytokine & Growth Factor Reviews* 25.5 (2014), pp. 551–561. ISSN: 1359-6101. DOI: `10.1016/J.CYTOGFR.2014.04.008`.

[400] P. I. Marcus. "Interferon induction by viruses: one molecule of dsRNA as the threshold for interferon induction." In: *Interferon* 5 (1983), pp. 115–180. ISSN: 0276-1076.

[401] J.-H. Ahn, W.-J. Jang, and G. S. Hayward. "The human cytomegalovirus IE2 and UL112-113 proteins accumulate in viral DNA replication compartments that initiate from the periphery of promyelocytic leukemia protein-associated nuclear bodies (PODs or ND10)." In: *Journal of virology* 73.12 (1999), pp. 10458–10471. ISSN: 0022-538X. DOI: `10.1128/JVI.73.12.10458-10471.1999`.

[402] T. Carvalho et al. "Targeting of adenovirus E1A and E4-ORF3 proteins to nuclear matrix-associated PML bodies." In: *The Journal of cell biology* 131.1 (1995), pp. 45–56. ISSN: 0021-9525. DOI: `10.1083/JCB.131.1.45`.

[403] M. PE, O. MH, and K. DM. "Mechanisms of Host IFI16, PML, and Daxx Protein Restriction of Herpes Simplex Virus 1 Replication." In: *Journal of virology* 92.10 (2018). ISSN: 1098-5514. DOI: `10.1128/JVI.00057-18`.

[404] D. Cuchet-Lourenco et al. "Herpes Simplex Virus 1 Ubiquitin Ligase ICP0 Interacts with PML Isoform I and Induces Its SUMO-Independent Degradation." In: *Journal of Virology* 86.20 (2012), pp. 11209–11222. ISSN: 0022-538X. DOI: `10.1128/JVI.01145-12/ASSET/9FFB2F3E-5101-40ED-B1E8-68B4F02D1B13/ASSETS/GRAPHIC/ZJV9990966650011.JPEG`.

[405] R. D. Everett. *Interactions between DNA viruses, ND10 and the DNA damage response*. 2006. DOI: `10.1111/j.1462-5822.2005.00677.x`.

[406] P. Xu, S. Mallon, and B. Roizman. "PML plays both inimical and beneficial roles in HSV-1 replication." In: *Proceedings of the National Academy of Sciences of the United States of America* 113.21 (2016), E3022–E3028. ISSN: 10916490. DOI: `10.1073/pnas.1605513113`.

[407] C. Boutell et al. "A Viral Ubiquitin Ligase Has Substrate Preferential SUMO Targeted Ubiquitin Ligase Activity that Counteracts Intrinsic Antiviral Defence." In: *PLOS Pathogens* 7.9 (2011), e1002245. ISSN: 1553-7374. DOI: 10.1371/JOURNAL.PPAT.1002245.

[408] J. M. Cabral et al. "ATRX limits the accessibility of histone H3-occupied HSV genomes during lytic infection." In: *PLOS Pathogens* 17.4 (2021), e1009567. ISSN: 1553-7374. DOI: 10.1371/JOURNAL.PPAT.1009567.

[409] V. Lukashchuk and R. D. Everett. "Regulation of ICP0-Null Mutant Herpes Simplex Virus Type 1 Infection by ND10 Components ATRX and hDaxx." In: *Journal of Virology* 84.8 (2010), pp. 4026–4040. ISSN: 0022-538X. DOI: 10.1128/JVI.02597-09/ASSET/30BFE54E-22CD-460C-BA79-13F3035B9DC5/ASSETS/GRAPHIC/ZJV9990931070013.JPEG.

[410] F. Catez et al. "HSV-1 Genome Subnuclear Positioning and Associations with Host-Cell PML-NBs and Centromeres Regulate LAT Locus Transcription during Latency in Neurons." In: *PLOS Pathogens* 8.8 (2012), e1002852. ISSN: 1553-7374. DOI: 10.1371/JOURNAL.PPAT.1002852.

[411] C. Yu et al. "Swine Promyelocytic Leukemia Isoform II Inhibits Pseudorabies Virus Infection by Suppressing Viral Gene Transcription in Promyelocytic Leukemia Nuclear Bodies." In: *Journal of Virology* 94.18 (2020). ISSN: 0022-538X. DOI: 10.1128/JVI.01197-20.

[412] O. Vladimirova et al. "Phase separation and DAXX redistribution contribute to LANA nuclear body and KSHV genome dynamics during latency and reactivation." In: *PLOS Pathogens* 17.1 (2021), e1009231. ISSN: 1553-7374. DOI: 10.1371/JOURNAL.PPAT.1009231.

[413] M. He et al. "Cancer angiogenesis induced by Kaposi's sarcoma-associated herpesvirus is mediated by EZH2." In: *Cancer research* 72.14 (2012), p. 3582. ISSN: 00085472. DOI: 10.1158/0008-5472.CAN-11-2876.

[414] D. L. Kwiatkowski, H. W. Thompson, and D. C. Bloom. "The Polycomb Group Protein Bmi1 Binds to the Herpes Simplex Virus 1 Latent Genome and Maintains Repressive Histone Marks during Latency." In: *Journal of Virology* 83.16 (2009), pp. 8173–8181. ISSN: 0022-538X. DOI: 10.1128/JVI.00686-09/ASSET/1DAC46E8-523A-4F09-8D42-C548BCEA0CE7/ASSETS/GRAPHIC/ZJV0160921780007.JPEG.

[415] H. K. Oyibo et al. "Long-term Cre-mediated retrograde tagging of neurons using a novel recombinant pseudorabies virus." In: *Frontiers in Neuroanatomy* 8.SEP (2014), pp. 1–11. ISSN: 16625129. DOI: 10.3389/fnana.2014.00086.

[416] C. M. Preston. "Control of herpes simplex virus type 1 mRNA synthesis in cells infected with wild-type virus or the temperature-sensitive mutant tsK." In: *Journal of Virology* 29.1 (1979), pp. 275–284. ISSN: 0022-538X. DOI: 10.1128/jvi.29.1.275-284.1979.

[417] C. M. Preston, R. Mabbs, and M. J. Nicholl. "Construction and characterization of herpex simplex virus type 1 mutants with conditional defects in immediate early gene expression." In: *Virology* 229.1 (1997), pp. 228–239. ISSN: 00426822. DOI: 10.1006/viro.1996.8424.

[418] A. Sarfo et al. "The UL21 Tegument Protein of Herpes Simplex Virus 1 Is Differentially Required for the Syncytial Phenotype." In: *Journal of Virology* 91.21 (2017). ISSN: 0022-538X. DOI: `10.1128/JVI.01161-17`.

[419] M. Van Zijl et al. "Identification of two genes in the unique short region of pseudorabies virus; comparison with herpes simplex virus and varicella-zoster virus." In: *Journal of General Virology* 71.8 (1990), pp. 1747–1755. ISSN: 00221317. DOI: `10.1099/0022-1317-71-8-1747/CITE/REFWORKS`.

[420] W. A. Derbigny et al. "EHV-1 EICP22 protein sequences that mediate its physical interaction with the immediate-early protein are not sufficient to enhance the trans-activation activity of the IE protein." In: *Virus Research* 84.1-2 (2002), pp. 1–15. ISSN: 0168-1702. DOI: `10.1016/S0168-1702(01)00377-X`.

[421] L. Flori et al. "Transcriptomic analysis of the dialogue between Pseudorabies virus and porcine epithelial cells during infection." In: *BMC Genomics* 9.1 (2008), pp. 1–24. ISSN: 14712164. DOI: `10.1186/1471-2164-9-123/TABLES/7`.

[422] P. J. Desai. "A Null Mutation in the UL36 Gene of Herpes Simplex Virus Type 1 Results in Accumulation of Unenveloped DNA-Filled Capsids in the Cytoplasm of Infected Cells." In: *Journal of Virology* 74.24 (2000), pp. 11608–11618. ISSN: 0022-538X. DOI: `10.1128/JVI.74.24.11608-11618.2000/ASSET/7DFF9CE9-A395-463C-AF54-CBB843A73443/ASSETS/GRAPHIC/JV2401356008.JPEG`.

[423] Y. Pollack et al. "Methylation of foreign DNA sequences in eukaryotic cells." In: *Proceedings of the National Academy of Sciences of the United States of America* 77.11 (1980), p. 6463. ISSN: 00278424. DOI: `10.1073/PNAS.77.11.6463`.

[424] M. Szyf et al. "Cellular and viral DNA hypomethylation associated with induction of Epstein-Barr virus lytic cycle." In: *Proceedings of the National Academy of Sciences* 82.23 (1985), pp. 8090–8094. ISSN: 0027-8424. DOI: `10.1073/PNAS.82.23.8090`.

[425] F. Fuks et al. "The DNA methyltransferases associate with HP1 and the SUV39H1 histone methyltransferase." In: *Nucleic Acids Research* 31.9 (2003), pp. 2305–2312. ISSN: 0305-1048. DOI: `10.1093/NAR/GKG332`.

[426] S. Gopalakrishnan et al. "DNMT3B interacts with constitutive centromere protein CENP-C to modulate DNA methylation and the histone code at centromeric regions." In: *Human Molecular Genetics* 18.17 (2009), pp. 3178–3193. ISSN: 0964-6906. DOI: `10.1093/HMG/DDP256`.

[427] S. Honda and E. U. Selker. " Direct Interaction between DNA Methyltransferase DIM-2 and HP1 Is Required for DNA Methylation in Neurospora crassa." In: *Molecular and Cellular Biology* 28.19 (2008), pp. 6044–6055. ISSN: 0270-7306. DOI: `10.1128/MCB.00823-08/SUPPL_FILE/HONDA_SELKERMCBSUP.PDF`.

[428] M. E. Tanenbaum et al. "A protein-tagging system for signal amplification in gene expression and fluorescence imaging." In: *Cell* 159.3 (2014), pp. 635–646. ISSN: 1097-4172. DOI: `10.1016/J.CELL.2014.09.039`.

[429] A. De Bruyn, K. And, and D. M. Knipe. "Preexisting nuclear architecture defines the intranuclear location of herpesvirus DNA replication structures." In: *Journal of Virology* 68.6 (1994), pp. 3512–3526. ISSN: 0022-538X. DOI: `10.1128/JVI.68.6.3512-3526.1994`.

[430] T. J. Taylor et al. "Herpes simplex virus replication compartments can form by coalescence of smaller compartments." In: *Virology* 309.2 (2003), pp. 232–247. ISSN: 0042-6822. DOI: `10.1016/S0042-6822(03)00107-7`.

[431] A. S. B. Jalal and T. B. K. Le. "Bacterial chromosome segregation by the ParABS system." In: *Open Biology* 10.6 (2020), p. 200097. DOI: `10.1098/RSOB.200097`.

[432] K. BYSTRICKY et al. "CONSTRUCTS AND METHOD FOR REGULATING GENE EXPRESSION OR FOR DETECTING AND CONTROLLING A DNA LOCUS IN EUKARYOTES." In: (2012).

[433] B. Mariamé et al. "Real-Time Visualization and Quantification of Human Cytomegalovirus Replication in Living Cells Using the ANCHOR DNA Labeling Technology." In: *Journal of virology* 92.18 (2018). ISSN: 1098-5514. DOI: `10.1128/JVI.00571-18`.

[434] T. Komatsu et al. "In Vivo Labelling of Adenovirus DNA Identifies Chromatin Anchoring and Biphasic Genome Replication." In: *Journal of Virology* 92.18 (2018), pp. 795–813. ISSN: 0022-538X. DOI: `10.1128/JVI.00795-18/SUPPL_FILE/ZJV018183871SM7.MOV`.

[435] G. Blanco-Rodriguez et al. "Remodeling of the Core Leads HIV-1 Preintegration Complex into the Nucleus of Human Lymphocytes." In: *Journal of Virology* 94.11 (2020). ISSN: 0022-538X. DOI: `10.1128/JVI.00135-20/SUPPL_FILE/JVI.00135-20-SM009.AVI`.

[436] E. Sekine et al. "Spatiotemporal dynamics of HSV genome nuclear entry and compaction state transitions using bioorthogonal chemistry and super-resolution microscopy." In: *PLOS Pathogens* 13.11 (2017), e1006721. ISSN: 1553-7374. DOI: `10.1371/JOURNAL.PPAT.1006721`.

[437] A. M. Farcas et al. "KDM2B links the polycomb repressive complex 1 (PRC1) to recognition of CpG islands." In: *eLife* 2012.1 (2012), pp. 1–26. ISSN: 2050084X. DOI: `10.7554/eLife.00205`.

[438] E. M. Cohen et al. "Abortive herpes simplex virus infection of nonneuronal cells results in quiescent viral genomes that can reactivate." In: *Proceedings of the National Academy of Sciences of the United States of America* 117.1 (2020), pp. 635–640. ISSN: 10916490. DOI: `10.1073/pnas.1910537117`.

[439] E. M. Cohen and O. Kobiler. "Gene Expression Correlates with the Number of Herpes Viral Genomes Initiating Infection in Single Cells." In: *PLOS Pathogens* 12.12 (2016), e1006082. ISSN: 1553-7374. DOI: `10.1371/JOURNAL.PPAT.1006082`.

[440] L. Shapira et al. "Histone deacetylase inhibitors reduce the number of herpes simplex virus-1 genomes initiating expression in individual cells." In: *Frontiers in Microbiology* 7.DEC (2016), p. 1970. ISSN: 1664302X. DOI: `10.3389/FMICB.2016.01970/BIBTEX`.

[441] N. J. Kubat et al. "Specific Histone Tail Modification and Not DNA Methylation Is a Determinant of Herpes Simplex Virus Type 1 Latent Gene Expression." In: *Journal of Virology* 78.3 (2004), pp. 1139–1149. ISSN: 0022-538X. DOI: `10.1128/JVI.78.3.1139-1149.2004/ASSET/2009D4B8-CEBB-4586-A238-D6B4A5DC23F6/ASSETS/GRAPHIC/ZJV0030415970005.JPEG`.

[442] P. Drané et al. "The death-associated protein DAXX is a novel histone chaperone involved in the replication-independent deposition of H3.3." In: *Genes and Development* 24.12 (2010), pp. 1253–1265. ISSN: 08909369. DOI: `10.1101/gad.566910`.

[443] A. C. Wilson and I. Mohr. "A cultured affair: HSV latency and reactivation in neurons." In: *Trends in Microbiology* 20.12 (2012), pp. 604–611. ISSN: 0966842X. DOI: `10.1016/j.tim.2012.08.005`.

[444] Q.-Y. Wang et al. "Herpesviral latency-associated transcript gene promotes assembly of heterochromatin on viral lytic-gene promoters in latent infection." In: *Proceedings of the National Academy of Sciences of the United States of America* 102.44 (2005), p. 16055. DOI: `10.1073/PNAS.0505850102`.

[445] D. A. Leib et al. "A deletion mutant of the latency-associated transcript of herpes simplex virus type 1 reactivates from the latent state with reduced frequency." In: *Journal of Virology* 63.7 (1989), p. 2893. ISSN: 0022-538X. DOI: `10.1128/jvi.63.7.2893-2900.1989`.

[446] C. Kleijwegt et al. "Interplay between PML NBs and HIRA for H3.3 deposition on transcriptionally active interferon-stimulated genes." In: *bioRxiv* (2021), p. 2021.11.30.470516. DOI: `10.1101/2021.11.30.470516`.

[447] B. J. Placek et al. "The Histone Variant H3.3 Regulates Gene Expression during Lytic Infection with Herpes Simplex Virus Type 1." In: *Journal of Virology* 83.3 (2009), pp. 1416–1421. ISSN: 0022-538X. DOI: `10.1128/jvi.01276-08`.

[448] C. Alabert et al. "Two distinct modes for propagation of histone PTMs across the cell cycle." In: *Genes and Development* 29.6 (2015), pp. 585–590. ISSN: 15495477. DOI: `10.1101/GAD.256354.114`.

[449] Y. Wang et al. "Histone variants H2A.Z and H3.3 coordinately regulate PRC2-dependent H3K27me3 deposition and gene expression regulation in mES cells." In: *BMC Biology* 16.1 (2018), pp. 1–18. ISSN: 17417007. DOI: `10.1186/S12915-018-0568-6/FIGURES/6`.

[450] P. W. Lewis et al. "Inhibition of PRC2 activity by a gain-of-function H3 mutation found in pediatric glioblastoma." In: *Science* 340.6134 (2013), pp. 857–861. ISSN: 10959203. DOI: `10.1126/SCIENCE.1232245/SUPPL_FILE/LEWIS.SM.PDF`.

[451] Y. Jacob et al. "ATXR5 and ATXR6 are H3K27 monomethyltransferases required for chromatin structure and gene silencing." In: *Nature Structural & Molecular Biology 2009 16:7* 16.7 (2009), pp. 763–768. ISSN: 1545-9985. DOI: `10.1038/nsmb.1611`.

[452] M. H. Orzalli et al. "Nuclear interferon-inducible protein 16 promotes silencing of herpesviral and transfected DNA." In: *Proceedings of the National Academy of Sciences of the United States of America* 110.47 (2013), E4492–E4501. ISSN: 00278424. DOI: `10.1073/PNAS.1316194110/-/DCSUPPLEMENTAL`.

[453] K. E. Johnson et al. "IFI16 Restricts HSV-1 Replication by Accumulating on the HSV-1 Genome, Repressing HSV-1 Gene Expression, and Directly or Indirectly Modulating Histone Modifications." In: *PLOS Pathogens* 10.11 (2014), e1004503. ISSN: 1553-7374. DOI: `10.1371/JOURNAL.PPAT.1004503`.

[454] A. G. Bodnar et al. "Extension of life-span by introduction of telomerase into normal human cells." In: *Science (New York, N.Y.)* 279.5349 (1998), pp. 349–352. ISSN: 0036-8075. DOI: `10.1126/SCIENCE.279.5349.349`.

[455] J. B. Bosse et al. "Remodeling nuclear architecture allows efficient transport of herpesvirus capsids by diffusion." In: *Proceedings of the National Academy of Sciences of the United States of America* 112.42 (2015), E5752–E5733. ISSN: 1091-6490. DOI: `10.1073/PNAS.1513876112`.

[456] M. Sandbaumhüter et al. "Cytosolic herpes simplex virus capsids not only require binding inner tegument protein pUL36 but also pUL37 for active transport prior to secondary envelopment." In: *Cellular microbiology* 15.2 (2013), pp. 248–269. ISSN: 1462-5822. DOI: `10.1111/CMI.12075`.

[457] K. Mullis et al. "Specific enzymatic amplification of DNA in vitro: The polymerase chain reaction." In: *Cold Spring Harbor Symposia on Quantitative Biology* 51.1 (1986), pp. 263–273. ISSN: 00917451. DOI: `10.1101/sqb.1986.051.01.032`.

[458] T. Günther et al. "Investigation of viral and host chromatin by ChIP-PCR or ChIP-Seq analysis." In: *Current Protocols in Microbiology* 2016 (2016), 1E.10.1–1E.10.21. ISSN: 19348533. DOI: `10.1002/9780471729259.mc01e10s40`.

[459] B. Langmead and S. L. Salzberg. "Fast gapped-read alignment with Bowtie 2." In: *Nature Methods* 9.4 (2012), pp. 357–359. ISSN: 15487091. DOI: `10.1038/nmeth.1923`.

[460] M. Lerdrup et al. "An interactive environment for agile analysis and visualization of ChIP-sequencing data." In: *Nature structural & molecular biology* 23.4 (2016), pp. 349–357. ISSN: 1545-9985. DOI: `10.1038/NSMB.3180`.

[461] M. Lerdrup and K. Hansen. "User-Friendly and Interactive Analysis of ChIP-Seq Data Using EaSeq." In: *Methods in molecular biology (Clifton, N.J.)* 2117 (2020), pp. 35–63. ISSN: 1940-6029. DOI: `10.1007/978-1-0716-0301-7_2`.

[462] A. Dobin et al. "STAR: ultrafast universal RNA-seq aligner." In: *Bioinformatics* 29.1 (2013), pp. 15–21. ISSN: 1367-4803. DOI: `10.1093/BIOINFORMATICS/BTS635`.

[463] H. Thorvaldsdóttir, J. T. Robinson, and J. P. Mesirov. "Integrative Genomics Viewer (IGV): high-performance genomics data visualization and exploration." In: *Briefings in bioinformatics* 14.2 (2013), pp. 178–192. ISSN: 1477-4054. DOI: `10.1093/BIB/BBS017`.

[464]   J. Schindelin et al. "Fiji: an open-source platform for biological-image analysis." In: *Nature Methods 2012 9:7* 9.7 (2012), pp. 676–682. ISSN: 1548-7105. DOI: 10.1038/nmeth.2019.

[465]   P. Bankhead et al. "QuPath: Open source software for digital pathology image analysis." In: *Scientific Reports 2017 7:1* 7.1 (2017), pp. 1–7. ISSN: 2045-2322. DOI: 10.1038/s41598-017-17204-5.

[466]   E. B. Stovner and P. Sætrom. "epic2 efficiently finds diffuse domains in ChIP-seq data." In: *Bioinformatics* 35.21 (2019), pp. 4392–4393. ISSN: 1367-4803. DOI: 10.1093/BIOINFORMATICS/BTZ232.

[467]   H. M. Amemiya, A. Kundaje, and A. P. Boyle. "The ENCODE Blacklist: Identification of Problematic Regions of the Genome." In: *Scientific Reports 2019 9:1* 9.1 (2019), pp. 1–5. ISSN: 2045-2322. DOI: 10.1038/s41598-019-45839-z.

[468]   Y. Liao, G. K. Smyth, and W. Shi. "featureCounts: an efficient general purpose program for assigning sequence reads to genomic features." In: *Bioinformatics* 30.7 (2014), pp. 923–930. ISSN: 1367-4803. DOI: 10.1093/BIOINFORMATICS/BTT656.

List of Toxic Chemicals

Substance	Hazard pictogram	Hazard statements	Precautionary statements
β-Mercaptoethanol		H227, H301,331, H310, H315, H317, H318, H373, H410	P261, P273, P280, P302, P350, P305, P351, P338, P310, P501
Acetic acid		H226, H314, H402	P210, P233, P240, P241, P242, P243, P260, P264, P273, P280, P301, P330, P331, P303, P361, P353
Acrylamide		H301, H312, H315, H317, H319, H332, H340, H350, H361, H372	P201, P280, P301, P310, P308, P360, P313
APS		H272, H302, H315, H317, H319, H334, H335	P280, P302, 352, P304, P340, P305, P351, P338, P342, P311
Ampicillin		H315-H317-H319-H334-H335	P261, P280, P305, P351, P338, P342, P311
Bromophenolblue		H332-H302-H319	P261, P264-P280-P304, P340, P312, P301, P312, P330, P305, P351, P338, P337, P313
Chloroform		H302, H315, H319, H331, H351, H361, H372	P202, P260, P264,P270, P201, P271, P280
DTT		H302, H315, H319, H335	P261, P302,352, P305, 351, 338, P501
DMSO		H227	P210, P280, P370, P378, P403, P235-P501

Chemical	Pictogram	Hazard	Precaution
EDTA		H302, H315, H319, H335	P261, P264, P270, P271, P280, P301,330,331, P302, P352, P311, P305, P351, P338, P332,313, P337, P313, P362, P403, P233
Ethanol		H225, H319	P210, P233, P241, P243, P280, P337,P313, P403,P235
Ethidium bromide		H302, H330, H341	P260, P280, P284, P301, P312, P405, P501
Glycerin		H315-H319-H335	P280, P302,P352, P304, P340, P305, P351, P338
Isopropanol		H225, H319, H336	P210, P261, P305 , P351, P338
Kanamycin		H360	P201, P308, P313
Formaldehyde		H226, H302, H314, H317, H318, H331, H350, H401	P201, P202, P210, P233, P240, P241, P242, P243, P260, P264, P270, P271, P272, P273, P280, P301, P330,331, P303, P361, P353, P304, P351, P338, P308, P313, P310, P333, P363, P370,378, P403, P233, P235, P405, P501
Magnesium sulfate		H302, H312, H332	P102, P202, P261, P64, P280
Methanol		H225, H301, H311, H331, H370	P210, P233, P240, P241, P242, P243, P260, P264, P270, P271, P280, P301,310, P303,361,353, P304,340, P330, P361,364, P370,378, P403,235, P404, P501
Nonidet-P40		H315-H319-H302	P264, P280, P305,P351, P338, P332, P313-P337, P313, P362,364

Chemical	Pictograms	Hazard statements	Precautionary statements
Paraformaldehyde		H228, H302, H332, H315, H317, H318, H335, H341, H350	P202, P210, P270, P280, P305, P351, P338, P308, P313
Penicillin		H317, H334	P261, P280, P342 , P311
Phenol		H301, H311, H331, H314, H341, H373, H411	P270, P280
Phenol-Chloroform - Isoamylalcohol		H301, H311, H331, H314, H341, H373, H411, H302, H315, H319, H331, H351, H361, H372	P270, P280, P201, P202, P260, P264, P271
Potassium chloride		H412	P273, P501
Potassium hydroxide		H315, H319, H335	P261, P264, P271, P280, P302 + P352, P305 + P351 + P338
Puromycin		H373	P270, P301, P312
SDS		H302, H311, H315, H319	P280, P305, P351, P338, P361, P405, P501
Sodium chloride		H314	P260, P264, P280, P301, P330, P331, P303, P361, P353, P305, P351, P338, P310, P363, P405, P501
Streptomycin		H302, H361	P281
TEMED		H225, H314, H302, H332	P210, P280, P305, P351, P338, P310
Triton X-100		H315, H319	P264, P280, P302, P352, P305, P351, P338, P332, P313, P338, P313, P362

Acknowledgment

First and foremost, I want to thank my supervisor Prof. Dr. Adam Grundhoff for giving me the opportunity to perform this interesting and challenging study in his laboratory. Furthermore, I want to thank him for the constant support and active participation during the whole project.

I would like to thank Prof. Dr. Kay Grünewald for the supervision and review of this thesis.

I would like to thank Prof. Dr. Nicole Fischer for the review of this thesis.

Furthermore, I would like to thank Assistant Prof. Dr. Jens Bosse for his supervision and constant input on the imaging part of this project.

I would like to thank my colleagues and lab mates from AG75: Thomas Günther, Simon Weißmann, Romina Vargas-Ayala, Alexis Robitaille, Marion Ziegler, Claudia Schmidt, Armin Günther, Jan Knickmann and Christine Block as well as the members from the NGS-facility: Jacqueline Nakel, Christina Herrde, Kerstin Reumann, and Sanam Virdi. Furthermore, I would like to thank the members from the Bosse Lab: Saskia Sanders, Felix Flomm, Enrico Caragliano, Timothy Soh, Linda Wedemann and Dörte Stalling. You gave me support, encouragement, fruitful discussions and a nice, welcoming and helpful working atmosphere.

Especially, I would like to thank Martin, Thomas and Jacqueline for reading parts of the manuscript; Thomas, Simon and Jacqueline for their constant input to my project and helpful discussion; Timothy Soh for reading the manuscript and correcting my English and Marion for her help in the lab.

Special thanks goes to my husband Robert, who always supported me and had my back and for reading the manuscript and giving me input from a non-biological point of view.

Last but not least I would like to thank my parents and my siblings, who always believed in me.

Declaration

Hiermit versichere ich an Eides statt, dass ich die vorliegende Dissertation selbst verfasst und keine anderen als die angegebenen Hilfsmittel benutzt habe. Die eingereichte schriftliche Fassung entspricht der auf dem elektronischen Speichermedium. Ich versichere, dass diese Dissertation nicht in einem früheren Promotionsverfahren eingereicht wurde.

Datum   Unterschrift